New Insights into the Origin and Phylogeny of Cryptodiran Turtles Based on Key Fossil Taxa from the Mesozoic of Asia

Dissertation

der Mathematisch-Naturwissenschaftlichen Fakultät
der Eberhard Karls Universität Tübingen
zur Erlangung des Grades eines
Doktors der Naturwissenschaften
(Dr. rer. nat.)

vorgelegt von
Dipl. Geol. Márton Rabi
aus Ungarn, Budapest

Tübingen
2014

Tag der mündlichen Qualifikation:	30.07.2014
Dekan:	Prof. Dr. Wolfgang Rosenstiel
1. Berichterstatter:	Prof. Dr. Hervé Bocherens
2. Berichterstatter:	Prof. Dr. Walter G. Joyce

Contents

Erklärung nach § 5 Abs. 2 Nr. 7 der Promotionsordnung der Math.-Nat. Fakultät

-Anteil an gemeinschaftlichen Veröffentlichungen-
Nur bei kumulativer Dissertation erforderlich!

Declaration according to § 5 Abs. 2 No. 7 of the PromO of the Faculty of Science

-Share in publications done in team work-

Name:

List of Publications

1. **Rabi, M.** Sukhanov, V.B., Egorova, V., Danilov, I. Joyce, W.G. 2014. Osteology, relationships, and ecology of *Annemys* (Testudines: Eucryptodira) from the Late Jurassic of Shar Teg, Mongolia and a phylogenetic definition Of Xinjiangchelyidae, Sinemydidae, and Macrobaenidae. *Journal of Vertebrate Paleontology*. 34 (2): 327–352.

2. **Rabi, M.**, Zhou, C.-F., Wings, O., Sun, G., Joyce, W.G. 2013. A new xinjiangchelyid Turtle from the Middle Jurassic of Xinjiang, China and the evolution of the basipterygoid process in Mesozoic Turtles. *BMC Evolutionary Biology*. 13 (203): 1–28.

3. Zhou, C.-F†., **Rabi, M†.** & Joyce, W.G. 2014. A new specimen of *Manchurochelys manchoukuoensis* from the Early Cretaceous Jehol Biota of Chifeng, Inner Mongolia, China and the phylogeny of Cretaceous basal eucryptodiran turtles. *BMC Evolutionary Biology*. 14 (77): 1–16.

† = equal contributors

Nr.	**Accepted for publication yes/no**	**Number of all authors**	Position of the candidate in list of authors	Scientific ideas of candidate (%)	Data generation by candidate (%)	Analysis and Interpretation by candidate (%)	Paper writing by candidate (%)
			Optional, the declaration of the own share can also be done in words, please add an extra sheet.				
1	published	5	1	80 %	65 %	80 %	80 %
2	published	5	1	90 %	85 %	80 %	85 %
3	published	3	equal with 1st author	60 %	50 %	80 %	60 %

I certify that the above statement is correct.

_____

EBERHARD KARLS
UNIVERSITÄT
TÜBINGEN

Mathematisch-Naturwissenschaftliche Fakultät

Date, Signature of the candidate

I/We certify that the above statement is correct.

Date, Signature of the

List of publications not included but relevant to the topic of the thesis

Delfino, M., Scheyer, T. M., Chesi, F., Fletcher, T., Gemel, R., **Rabi, M.** & Salisbury, S. W. 2013. Gross morphology and microstructure of type locality ossicles of *Psephophorus polygonus* Meyer, 1847 (Testudines, Dermochelyidae). *Geological Magazine* 150 (5): 767–782.

Ősi, A., **Rabi, M.**, Makádi, L., Szentesi, Z., Botfalvai, G. & Gulyás, P. 2012. The Late Cretaceous continental vertebrate fauna from Iharkút (Western Hungary, Central Europe): a review, pp. 533–570 *In* "Tribute to Charles Darwin and the Bernissart Iguanodons: new perspectives of vertebrate evolution and Early Cretaceous ecosystems" (ed. Pascal Godfroit), Indiana University Press, Bloomington.

Rabi, M., Vremir, M. & Tong, H. 2012. Preliminary overview of Late Cretaceous turtle diversity in eastern Central Europe (Austria, Hungary, and Romania), pp. 307–336 *In* "Morphology and Evolution of Turtles: Origin and Early Diversification" (eds: D. B. Brinkman, P. A. Holroyd, and J. D. Gardner), Springer, Dordrecht.

Rabi, M., Tong, H. & Botfalvai, G. 2012. A new species of the side-necked turtle *Foxemys* (Pelomedusoides: Bothremydidae) from the Late Cretaceous of Hungary and the historical biogeography of the Bothremydini. *Geological Magazine* 149: 662–674.

Wings, O., **Rabi, M.,** Schneider, J. W., Schwermann L., Sun G., Zhou, C.-F., & Joyce, W.G. 2012. An enormous Jurassic turtle bone bed from the Turpan basin of Xinjiang, China. Naturwissenschaften 99: 925–935.

Rabi, M., Joyce, W.G., & Wings, O. 2010. A review of the mesozoic turtles of the Junggar Basin (Xinjiang, Northwest China) and the paleobiogeography of Jurassic to Early Cretaceous Asian testudinates. *Paleobiodiversity and paleoenvironments* 90: 259–273.

Summary

Most turtles from the Jurassic to Early Cretaceous of Asia are referred to the poorly circumscribed taxa Xinjiangchelyidae, Sinemydidae, and Macrobaenidae, groups that mostly include shell-based, generalized, small to mid-sized aquatic forms that are widely considered to represent the stem lineage of Cryptodira. These groups are critical for reconstructing the plesiomorphic anatomy of crown-cryptodires, the most diverse group of living turtles, and they are therefore particularly relevant for understanding the origin and early divergence of the primary clades of extant turtles.

The complete description of excellent xinjiangchelyid and sinemydid material from the Upper Jurassic of Mongolia and the Middle Jurassic and Early Cretaceous of China (referable to *Annemys levensis*, *A. latiens*, *Xinjiangchelys wusu* nov. sp. and *Manchurochelys manchoukuoensis*) provides new insights into the anatomy of these otherwise poorly known groups. The overall similarity of the shells of the two *Annemys* species combined with significant differences in the skull indicate that these turtles probably partitioned the aquatic niche by exploring different feeding strategies. Among xinjiangchelyids, at least three different skull morphotypes can be differentiated, which implies a moderate level of ecological diversification among Late Jurassic Asian turtles. Phylogenetic definitions of Xinjiangchelyidae, Sinemydidae, and Macrobaenidae are provided for nomenclatural clarity and precision.

Phylogenetic analysis weakly supports the inclusion of *Xinjiangchelys wusu* n. sp., *A. levensis*, and *A. latiens* in a monophyletic polytomy with other xinjiangchelyids, including *Xinjiangchelys junggarensis* and *X. radiplicatoides*. However, the analysis supports the unorthodox, though tentative placement of xinjiangchelyids and sinemydids outside of crown-group Testudines. A particularly interesting new observation is that the skull of xinjiangchelyids retains such primitive features as a reduced interpterygoid vacuity and basipterygoid processes. The homology of the basipterygoid processes is confidently demonstrated based on a comprehensive review of the basicranial anatomy of Mesozoic turtles and a new nomenclatural system is introduced for the carotid canal system of turtles. The loss of the basipterygoid process and the bony enclosure of the carotid circulation system occurred a number of times independently during turtle evolution suggesting that the reinforcement of the basicranial region was essential for developing a rigid skull, thus paralleling the evolution of other amniote groups with massive skulls.

A thorough revision of the phylogeny of Macrobaenidae, Sinemydidae, and closely allied forms yielded two main competing hypotheses: in the first, these taxa form a paraphyletic grade, whereas in the second they form a monophyletic clade. The inclusion of problematic tree changing taxa, such as Panpleurodires (stem + crown side-neck turtles) has a major influence on the phylogenetic relationships of Sinemydidae and closely allied forms. *Manchurochelys manchoukuoensis* nests within Sinemydidae together with *Sinemys* spp. and *Dracochelys bicuspis* in the majority of the analyses.

Zusammenfassung

Die meisten asiatischen Schildkröten aus der Jurazeit bis frühen Kreidezeit werden den schlecht definierte Taxa Xinjiangchelyidae, Sinemydidae und Macrobaenidae zugeordnet, Gruppen die meist auf Panzer basierte, generalisierte, kleine bis mittelgroße aquatische Formen beinhalten und die generell als Stammlinienvertreter der Cryptodira dargestellt werden. Diese Gruppen sind entscheidend für das Verständnis der plesiomorphe Anatomie der Kronengruppe der Cryptodira, der diversesten Gruppe der lebenden Schildkröten, und sind deshalb auch für das Verständnis der Entstehung und frühen Divergenz der primären Subtypen der modernen Schildkröten von besonderer Relevanz.

Die systematische Beschreibung von ausgezeichnetem xinjiangchelyiden und sinemyden Material aus dem Oberjura der Mongolei und aus dem Mittleljura und der frühen Kreidezeit von China (*Annemys levensis*, *A. latiens*, *Xinjiangchelys wusu* nov. sp. *Manchurochelys manchoukuoensis*) bietet neue Einblicke in die Anatomie dieser sonst nur unvollständig bekannten Gruppen. Die generelle Ähnlichkeit der Schalen der beiden *Annemys* Arten, kombiniert mit erheblichen Unterschieden im Schädel, zeigen, dass diese Schildkröten wahrscheinlich die aquatische Nische durch verschiedenen Nahrungsstrategien geteilt haben. Bei den Xinjiangchelyidae können mindestens drei verschiedene Schädel Morphotypen unterschieden werden, was eine moderate ökologische Diversifizierung bei diesen spätjurassischen Schildkröten impliziert. Phylogenetische Definitionen werden für Xinjiangchelyidae, Sinemydidae und Macrobaenidae vorgeschlagen, um Klarheit und Genauigkeit in der taxonomischen Nomenklatur zu sichern.

Eine phylogenetische Analyse vereinigt *Xinjiangchelys wusu* n. sp., *A. levensis* und *A. latiens* nur schwach mit anderen Xinjiangchelyidae, einschließlich *Xinjiangchelys junggarensis* und *X*. *radiplicatoides*. Allerdings unterstützt die Analyse die unorthodoxe, wenn auch vorläufige Plazierung von Xinjiangchelyidae und Sinemydidae außerhalb der Kronengruppe Testudines. Eine besonders interessante Beobachtung ist, dass der Schädel von Xinjiangchelyidae primitive Merkmale wie zum Beispiel ein reduziertes Fossa mesopterygoidea und Basipterygoidfortsätze aufweisst. Die Homologie der Basipterygoidfortsätze wird nach einer umfassenden Revision der basikranialen Anatomie der mesozoischen Schildkröten neu aufgestellt und eine neue Nomenklatur für das Karotidkanalsystem der Schildkröten vorgeschlagen. Der Verlust der Basipterygoidfortsatzes und die knöcherne Einfassung des Karotidkanalsystems tritt mehrmals unabhängig voneinander während Schildkröte Evolution auf, was darauf hindeutet, dass die Verstärkung der Basikranialregion für die Entwicklung eines akinetischen Schädels wichtig war und parallel zu ähnlichen Entwicklung bei anderen Gruppen der Amnioten verlief.

Eine gründliche Überarbeitung der Stammesgeschichte von Macrobaenidae, Sinemydidae und anderen, eng verwandten Formen, ergab zwei konkurrierende Hypothesen. In der ersten Hypothese bilden diese Taxa ein Paraphylum, während sie in der zweiten eine Monophylum bilden. Die Einbeziehung von problematischen Taxa, wie zum Beispiel die Stamliniengruppe Panpleurodira, hat einen großen Einfluß auf die Verwandtschaftsverhältnisse von Sinemydidae und eng verwandter Formen. *Manchurochelys manchoukuoensis* liegt innerhalb von Sinemydidae zusammen mit *Sinemys* spp. und *Dracochelys bicuspis* in der Mehrzahl der Analysen.

1. Introduction

Present day turtle diversity (Testudines) is largely constituted by a single monophyletic clade, the crown-group of Cryptodira, including 250 species distributed on all continents and countless islands except Antarctica. The remaining 81 species form the second monophyletic clade, Pleurodira, or side-neck turtles, which are restricted to former Gondwana continents, including South America, Africa, Madagascar, and Australia-Papua-New Guinea (Turtle Taxonomy Workgroup 2012). Cryptodires show a wide range of habitat preference from terrestrial forms to aquatic bottom dwellers, freshwater swimmers and fully marine forms, and they are important elements of both aquatic and terrestrial modern-day vertebrate faunas (Ernst and Barbour 1989). They show a high tolerance for climate and live in both humid and arid environments from tropical to cold temperate zones. Some of them are characterized by heavily built or spiny shells whereas others have reduced armor, often regardless of habitat. Body size disparity in Cryptodires is great and ranges from > 10 cm to ~2 m total length (Moen 2006). Feeding preference vary from herbivory to omnivory and carnivory (Ernst and Barbour 1989) with corresponding suction-snapper, durophagous, and shearing ecomorphs (Claude et al. 2004, Parham and Pyenson 2010). Fossils reveal that past pancryptodiran eco-morphological diversity was even higher, including bizarre shapes with no modern analogues (e.g. Wieland 1900, Ye 1966, Gaffney 1975a, Brinkman and Peng 1993a, Meylan et al. 2000, Bardet et al. 2013). Osteological correlates of ecology are often apparent in cryptodires (Claude et al. 2003, 2004) and with their long evolutionary history and excellent fossil record they therefore serve as ideal model organisms for investigating relationships between environment, morphological evolution, paleogeography, and diversification though deep time.

A deeper understanding of evolutionary patterns within cryptodiran turtles is currently hampered by contradictory hypotheses regarding the interrelationships and divergence timing of the major clades of extant cryptodires and the placement of fossil taxa. For instance, morphological phylogenies consistently recover a musk turtle (Kinosternoidea) and softshell turtle (Trionychia) clade and position chelonioid sea turtles or snapping turtles (Chelydridae) at the base of crown-cryptodires (Gaffney 1975b, Meylan 1987, Meylan and Gaffney 1989, Gaffney and Meylan 1988,

Gaffney 1996, Shaffer et al. 1997, Hirayama et al. 2000, Parham and Hutchison 2003, Brinkman et al. 2006, Gaffney et al. 2007, Joyce 2007, Anquetin 2012, Brinkman et al. 2013a, Sterli and de la Fuente 2011, Sterli et al. 2013; Figure 1). In contrast, most molecular analyses argue for a basal placement of Trionychia and sea turtles are retrieved either as closest to chelydrids or kinosternoids (Shaffer et al. 1997, Fujita et al. 2004, Near et al. 2005, Krenz et al. 2005, Chandler and Janzen 2009, Thomson and Shaffer 2010, Barley et al. 2010; Figure 1) or to testudinoids (Parham et al. 2006).

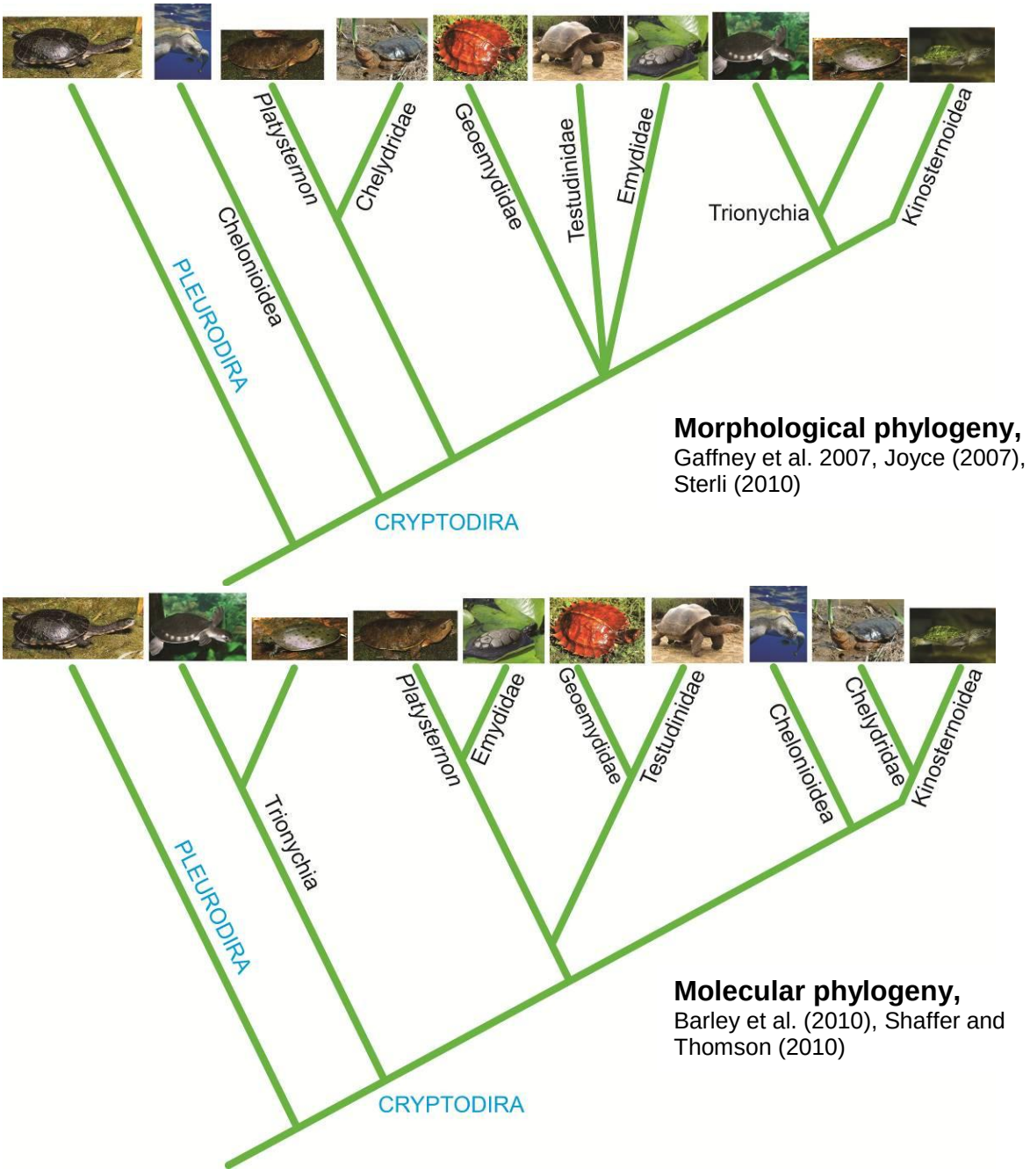

Figure 1. Examples of competing hypotheses of crown-cryptodiran relationships. Image source: wikipedia.org

Another conflict involves the affinity of the enigmatic, highly specialized big-headed turtle, *Platysternon megacephalum* Gray 1831, which has been considered to be a chelydrid based on morphological evidence (Gaffney 1975c, Gaffney and Meylan 1988, Brinkman and Wu 1999) but several recent molecular studies demonstrated its close relationship to emydids (Euramerican pond turtles; Parham et al. 2006, Chandler and Janzen 2009, Thomson and Shaffer 2010, Barley et al. 2010) or to the more inclusive clade of testudinoids (Krenz et al. 2005, Near et al. 2005; Figure 1). Similarly, Geoemydidae, a diverse clade of predominantly aquatic and Asian cryptodires (Turtle Taxonomy Workgroup 2012), are considered to be most closely related to the terrestrial Testudinidae by molecular analyses (Shaffer et al. 1997, Krenz et al. 2005, Thomson and Shaffer 2010, Barley et al. 2010), but this result that has not been reproduced by most recent morphological studies (Joyce and Bell 2004, Joyce 2007, Sterli 2010, Sterli and de la Fuente 2011, 2013), except for Anquetin (2012).

One reason that complicates phylogenetic reconstruction within Cryptodira is the limited knowledge of the composition of its stem-linage that in turn strongly influences our interpretation of character polarity. The obscure relationships along the stem is most likely due to the high degree of homoplasy in the skeletal evolution of turtles as well as to the low number of fossils from the rapid initial divergence period of the major crown-cryptodiran clades during the second half of the Jurassic and the Early Cretaceous (Shaffer et al. 1997, Danilov and Parham 2006, Sterli et al. 2013, Joyce et al. 2013).

A first step towards the solution is the anatomical revision of Mesozoic stem-cryptodire turtles. The origin of Cryptodira is considered to take place in Asia (Sukhanov 2000, Danilov and Parham 2008) and therefore the focus should be directed on the turtle faunas from this continent. The time interval between the Middle Jurassic and the Early Cretaceous was critical for turtle diversification (Sukhanov 2000, Danilov and Parham 2006, Gaffney et al. 2007, Joyce 2007, Sterli 2010, Sterli et al. 2013, Joyce et al. 2013) and taxa should therefore be selected from these periods to address issues pertaining to the early diversification of the group. New anatomical insights gained from the study of stem- and early cryptodires have to be analyzed in a phylogenetic framework and hopefully provide the basis for better-

resolved phylogenetic relationships and divergence time estimate within and around the crown.

The most relevant taxa for cryptodiran origins undoubtedly include three groups from the Mesozoic of Asia: the Jurassic Xinjiangchelyidae and the Early Cretaceous Sinemydidae and Macrobaenidae (Sukhanov and Narmandakh 1974, Gaffney 1996, Peng and Brinkman 1993). The fact that Xinjiangchelyidae, Sinemydidae, and Macrobaenidae form successively internested paraphyletic groups, coupled with the fact that the vast majority of taxa attributable to these grades are Asian, strongly confirms the notion that the stem evolution of crown Cryptodira occurred in Asia.

Xinjiangchelyidae Nessov in Kaznyshkin et al. 1990

Xinjiangchelyids are medium sized (carapace length up to 375 mm) aquatic turtles known from the Middle Jurassic to Early Cretaceous of Asia (Sukhanov 2000, Danilov and Parham 2007, Rabi et al. 2010, Tong et al. 2012a,b). The skull, which has only been described for *Annemys* spp. (*Xinjiangchelys*) and Xinjiangchelys radiplicatoides Brinkman et al. 2013a in a preliminary way, is characterized by deep upper and lower temporal emarginations, prefrontals that contact one another along the midline, and the absence of an interpterygoid vacuity (Sukhanov 2000, Brinkman et al. 2013a). Well preserved xinjiangchelyid skulls from the Late Jurassic Qigu Formation of the nearby Turpan Basin (Wings et al. 2012) reveal that the internal carotid arteries entered at the back of the skull at the pterygoid/basisphenoid suture, but an open ventral groove formed by the basisphenoid reveals that the internal carotid canal was incompletely floored. The poor preservation of the *Annemys* (*Xinjiangchelys*) *levensis* type skull might have obscured this morphology. The shell of xinjiangchelyids is low and wide, posteriorly rounded, a nuchal emargination is present, the carapace has a ligamentous contact with the plastron, the axillary and inguinal buttresses laterally contact the peripherals along grooves, the second to seventh peripherals are thickened and bent upwards to form a gutter, and a pair of reduced epiplastral processes is present (Sukhanov 2000).

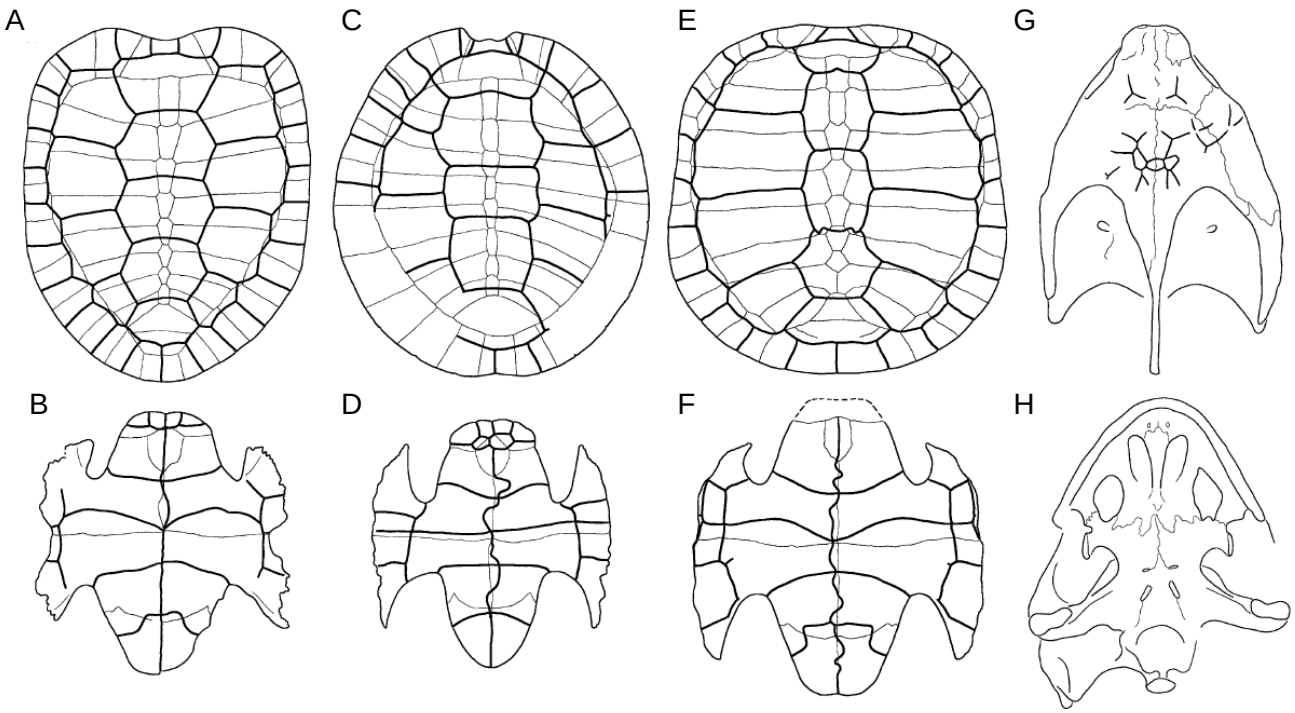

Figure 2. **Examples of "xinjiangchelyid" turtles recovered from Jurassic sediments in China and Mongolia.** A-B: ***Xinjiangchelys junggarensis* Ye 1986 carapace and plastron redrawn from Peng and Brinkman (1993).** C-D: ***Xinjiangchelys qiguensis* Matzke et al., 2004a carapace and plastron redrawn from Matzke et al. (2004a).** E-F: ***Annemys* (*Xinjiangchelys*) *latiens* Sukhanov and Narmandakh 2006 carapace and plastron redrawn from Sukhanov (2000).** G-H: ***Annemys* (*Xinjiangchelys*) sp., skull in dorsal and ventral view (Brinkman et al. 2013a). Specimens not drawn to scale. After Rabi et al. (2010).**

Xinjiangchelyids are typical elements of Middle to Late Jurassic vertebrate faunas of inland Asia, including China, Russia, Kyrgyzstan, and Mongolia and perhaps South-East Asia (Rabi et al. 2010). Their stratigraphic range is thought to extend into the Early Cretaceous largely based on a single plastron found in a slab together with several individuals of *Ordosemys brinkmania* Danilov and Parham 2007 from the Aptian-Albian of the Junggar Basin, Xinjiang, China. After personal observation I doubt that this specimen (IVPP V4074) is a xinjiangchelyid and based on my experience with a growth series of a new species of *Xinjiangchelys* I rather consider it as a simply more ossified individual of *O*. *brinkmania*. Similarly, the xinjiangchelyid affinity of *Brodiechelys brodiei* (Lydekker 1889) from the Early Cretaceous of Europe (Hirayama et al. 2000, Pérez-García 2012) remains to be tested in a rigorous and more comprehensive global phylogenetic framework. Either way, such questions are fairly pointless while the application of the name Xinjiangchelyidae remains unresolved. The monophyly of this group is at best poorly supported (Anquetin 2012, Tong et al. 2012a,b) and the vast majority of characters that diagnose this group under a Linnéan-type classification (e.g., Sukhanov 2000)

are symplesiomorphies when mapped onto global trees (e.g., Gaffney et al. 2007, Hirayama et al. 2000, Joyce 2007). As currently circumscribed (e.g., Matzke et al. 2004a), “Xinjiangchelyidae” is therefore likely paraphyletic relative to “Sinemydidae”/“Macrobaenidae.” The interpretation of “Xinjiangchelyidae” as basal eucryptodires is widely accepted in the literature and most authors consider this clade to be more closely related to modern cryptodires than Paracryptodira or Plesiochelyidae (Gaffney 1996, Hirayama et al. 2000, Joyce 2007, Parham and Hutchison 2003) and, with the exception of Danilov and Parham (2008), basal to “Sinemydidae”/“Macrobaenidae”. Hirayama et al. (2000) concluded that the European taxon *Brodiechelys brodiei* may be a close relative of “Xinjiangchelyidae,” whereas Danilov and Parham (2008) noted close relationships with Asian *Chengyuchelys* spp. As it stands, most global analyses hand pick a select number of one or two “xinjiangchelyids” (e.g., Danilov and Parham 2008, Gaffney 1996, Hirayama et al. 2000, Joyce 2007, Parham and Hutchison 2003) or find low support for monophyly when taxon sample is increased (Anquetin 2012). “Xinjiangchelyid” analyses (e.g., Matzke et al. 2004a, Peng and Brinkman 1993, Tong et al. 2012a,b) maybe either limited for sample or simply irrelevant for the question given the lack of a sufficient number of outgroup-taxa and characters.

The name Xinjiangchelyidae was originally coined by Nessov (in Kaznyshkin et al. 1990) along with Xinjiangchelydia, but subsequent workers did not adapted the latter term. Nessov (in Kaznyshkin et al. 1990) provided a diagnosis for Xinjiangchelyidae and synonymized *X*. *junggarensis* and ‘*Plesiochelys*’ *radiplicatus* Young and Chow 1953 with the type species of the family, *Xinjiangchelys latimarginalis* (Young and Chow 1953) (= *Chengyuchelys latimarginalis* sensu Tong et al. 2012b), but it is unclear if he believed this taxon to be more inclusive than *Xinjiangchelys latimarginalis*. Sukhanov (2000) subsequently provided an emended diagnosis for Xinjiangchelyidae and explicitly circumscribed this taxon to include *Xinjiangchelys* spp., *Annemys* (*Xinjiangchelys*) from Shar Teg, and the poorly known turtles *Shartegemys laticentralis*, *Undjulemys platensis* Sukhanov and Narmandakh 2006, and *Tienfuchelys tzuyangensis* Young and Chow 1953. Although this circumscription was followed by Matzke et al. (2004a), their phylogenetic analysis did not rigorously test the monophyly of the group. Tong et al. (2012a) circumscribed Xinjiangchelyidae as including *X. latimarginalis*, *X*. *tianshanensis* Nessov 1995, and *Protoxinjiangchelys salis* Tong et al. 2012a, but their phylogenetic analysis revealed

this grouping to be paraphyletic relative to the clade formed by *Bashuchelys zigongensis* (Ye 1982), *Bashuchelys youngi* Tong et al. 2012a, and *Chuannanchelys dashanpuensis* (Fang, 1987). Tong et al. (2012b) circumscribed Xinjiangchelyidae as consisting of *Brodiechelys* spp., *Chengyuchelys* spp., *Protoxinjiangchelys salis*, *Tienfuchelys* spp., *Xinjiangchelys* spp. (including *Annemys* and *Shartegemys* Sukhanov and Narmandakh 2006), and *Yanduchelys delicatus* Peng et al. 2005, and provided some support for the monophyly of this group of turtles with a phylogenetic analysis. By contrast, Anquetin (2012) circumscribed Xinjiangchelyidae as consisting of *Xinjiangchelys qiguensis* Matzke et al. 2004a, *X. latimarginalis* (sensu Peng and Brinkman 1993), *X*. *tianshanensis*, *Annemys (Xinjiangchelys) levensis*, and *Siamochelys peninsularis* Tong et al. 2002. Various other authors discussed the phylogenetic relationship of *Xinjiangchelys latimarginalis*, but refrained from using the name Xinjiangchelyidae because of the lack of a clear definition for the name (Gaffney et al. 2007, Joyce 2007, Danilov and Parham 2008, Sterli 2010).

Sinemydidae Ye 1963 and **Macrobaenidae** Sukhanov 1964

Most Early Cretaceous eucryptodiran turtles more derived than "xinjiangchelyids" are referred to sinemydids and/or macrobaenids. These forms are generally known from the Cretaceous and Paleogene of Asia and North America (Brinkman 2001, Brinkman and Peng 1993a, Gaffney and Ye 1992, Parham and Hutchison 2003, Sukhanov 2000). Two main skull morphologies are apparent within this group. *Sinemys lens* Wiman 1930 and *Sinemys gamera* Brinkman and Peng 1993a are characterized by very deep upper temporal and cheek, prefrontals that do not meet one another along in the midline, an elongated basisphenoid, and an enclosed incisura columella auris (Brinkman and Peng 1993a). On the other hand, *Ordosemys* spp., *Dracochelys bicuspis*, and *Kirgizemys* spp. possess only a moderate upper temporal emargination, but deep cheek emarginations, medially meeting prefrontals (except for *Ordosemys* spp.), an open incisura columellae auris, and a short basisphenoid (Brinkman and Peng 1993a, Danilov et al. 2006, Gaffney and Ye 1992, Sukhanov 2000, Tong et al. 2004). The shell of *Sinemys* spp. is highly aberrant: the pygal bone is absent, the twelfth peripherals are reduced, a ninth neural is present, and the seventh peripherals are developed into laterally protruding spines (Brinkman and Peng 1993a).

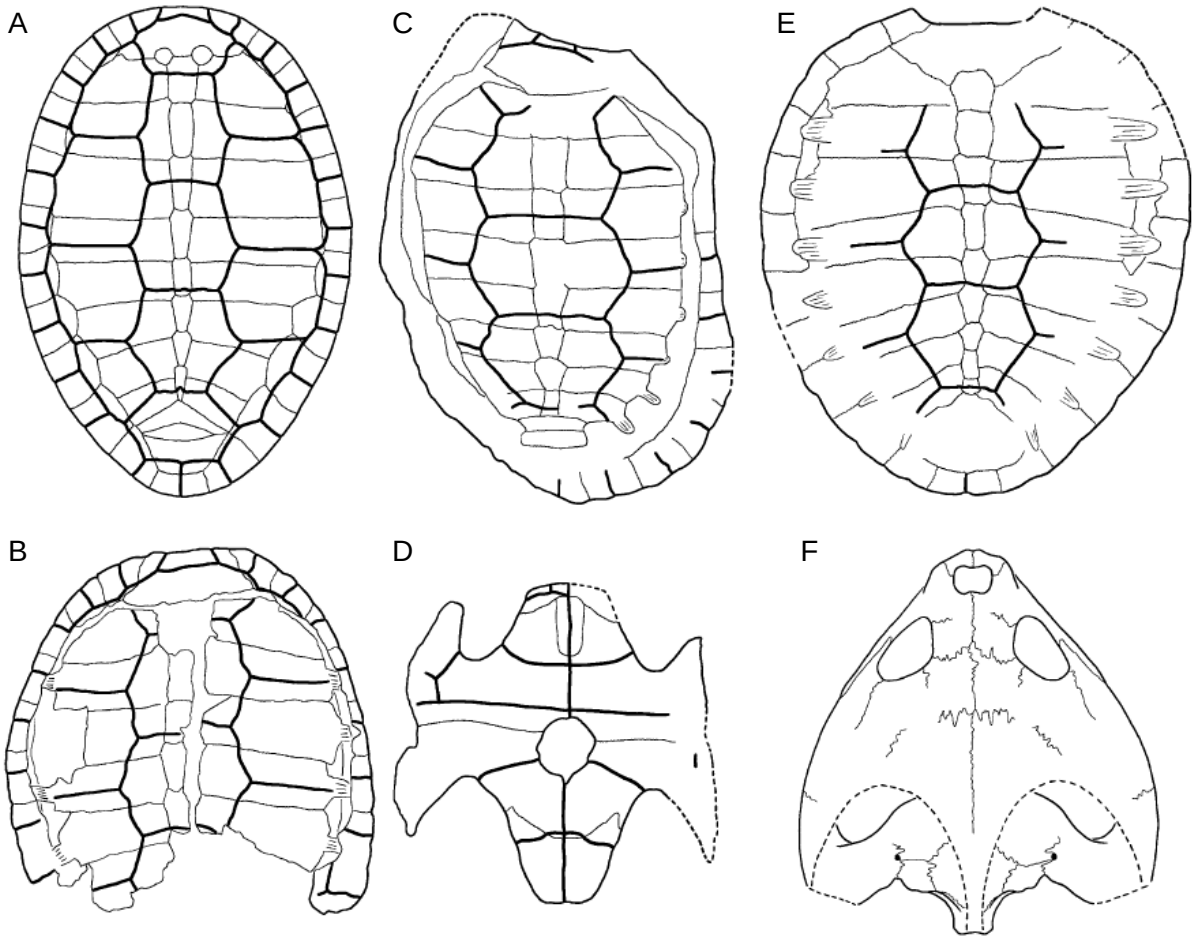

Figure 3. **Examples of "sinemydid/macrobaenid" fossil turtles from the Early Cretaceous of China (Junggar Basin, Tugulu Group).** A: ***Wuguia hutubeiensis*** **Matzke et al. 2004b carapace redrawn from Matzke et al. (2004b).** B: ***Wuguia efremovi*** **(Khosatzky 1996) carapace redrawn from Maisch et al. (2003).** C-D: ***Ordosemys brinkmania*** **Danilov and Parham 2007 carapace and plastron redrawn from Danilov and Parham (2007).** E-F: ***Dracochelys bicuspis*** **Gaffney and Ye 1992 carapace redrawn from Brinkman (2001), skull redrawn from Gaffney and Ye (1992). Specimens not drawn to scale. After Rabi et al. (2010).**

The paraphyly of „sinemydids/"macrobaenids" has been recently suggested by the phylogenetic analyses of Gaffney et al. (2007) and Joyce (2007). Among others, the topology of Gaffney et al. (2007) differs from that of Joyce (2007) in that *Ordosemys leios* is not sister to *Sinemys lens* and primitive to *Dracochelys bicuspis.*

The term Sinemydidae has been widely used as a collective name for many Early Cretaceous turtles from Asia (Ye 1963, Chkhikvadze 1975, 1977, 1987; Khosatzky and Nessov 1979, Hutchison and Archibald 1986, Brinkman & Peng 1993ab, Hirayama et al. 2000, Sukhanov 2000, Brinkman 2001, Maisch et al. 2003, Matzke et al. 2004b, Tong et al. 2009) and represents another group of questionable utility without an explicit definition (Parham and Hutchison 2003, Gaffney 1996, Gaffney et al. 1998, 2007; Joyce 2007, Danilov and Parham 2008, Rabi et al., 2010).

Sinemydidae was established by Ye (1963) for *Sinemys lens* and *Manchurochelys manchoukuoensis* Endo and Shikama 1942. Subsequent workers has since proposed a disparate set of circumscriptions for Sinemydidae, including *S*. *lens*, *Man*. *manchoukuoensis*, *Macrobaena mongolica*, *Hangaiemys* (*Kirgizemys*) *hoburensis*, *Kirgizemys exaratus* Nessov and Khosatzky 1973, and *Yaxartemys longicauda* Ryabinin 1948 (Chkhikvadze 1975, 1977, 1987); *Man. manchoukuoensis* and *Sinemys* spp. (Brinkman and Peng 1993a); *Dracochelys bicuspis*, *Ordosemys* spp., and *Sinemys* spp. (Gaffney 1996); *Sinemys* spp., *D*. *bicuspis*, *H*. *hoburensis* (Brinkman and Wu 1999); *D. bicuspis*, *Hongkongochelys yehi* Ye 1999, *Man. manchoukuoensis*, *Ordosemys* spp., *Sinemys* spp., *Wuguia* spp., and *Yumenemys inflatus* Bohlin 1953 (Brinkman et al. 2008); *D. bicuspis*, *Man. manchoukuoensis*, and *Sinemys* spp. (Zhou 2010a,b), or only *Sinemys* spp. (Sukhanov 2000, Tong and Brinkman 2013). Only the circumscriptions of Gaffney (1996) and Zhou (2010a,b) were based on a phylogenetic analysis and therefore unite monophyletic clades.

Macrobaenidae is another name traditionally used for uniting various Asian and North American Cretaceous and Tertiary fossil eucryptodires that are more derived than xinjiangchelyids. Macrobaenidae was established by Sukhanov (1964) for *Mac*. *mongolica*. Several other taxa were at one or the other time referred to this group, including *Hangaiemys* (*Kirgizemys*) *hoburensis*, *Ordosemys* spp., *Kirgizemys exaratus*, *Asiachelys perforata* Sukhanov and Narmandakh 2006, and *Anatolemys maximus* Khosatzky and Nessov 1979 (see Sukhanov 2000 for a more complete review and references). Some of the listed taxa were variously referred to Sinemydidae by other authors (see above) and the names Sinemydidae and Macrobaenidae therefore often had overlapping circumscription. However, *Xinjiangchelys junggarensis* and *Sinemys lens* were consistently excluded from the group. Interestingly, even though various circumscription of Macrobaenidae are universally agreed to be paraphyletic (e.g., Parham and Hutchison 2003, Joyce 2007, Gaffney et al. 2007, Danilov and Parham 2008, Zhou 2010b, Sterli and Fuente 2011, Anquetin 2012), the name giving taxon *Mac*. *mongolica* was never included in a phylogenetic analysis. There is therefore no precedence of applying the name Macrobaenidae to a monophyletic clade.

2. Objectives

The objectives of this doctoral research project are to resolve controversial phylogenetic relationships of the major clades along the stem and within Cryptodira including Xinjiangchelyidae, Sinemydidae, Macrobaenidae, Trionychia, Kinosternoidea, Chelydridae, and Chelonioidea. This is to be achieved by developing a revised taxon-character matrix with increased morphological and taxon sampling. I aim to add new data to existing matrices by understanding and documenting the anatomy of key stem-cryptodire taxa from the Mesozoic of Asia including the xinjiangchelyid *Annemys (Xinjiangchelys) levensis*, *Annemys (Xinjiangchelys) latiens*, and a new species of *Xinjiangchelys*, the sinemydid *Manchurochelys manchoukuoensis*, and the potential macrobaenid *Hangaiemys* (*Kirgizemys*) *hoburensis*. I intend to review and rescore other relevant taxa based on my direct observations of museum specimens.

In order to stabilize the nomenclature and definition of the stem-cryptodire taxa Xinjiangchelyidae, Sinemydidae and Macrobaenidae, a phylogenetic classification is developed here which would stabilize the meaning of these names for future workers.

Given that the carotid circulation system of turtles has long been considered to be an important anatomical region for assessing the relationships of the major groups of turtles. The evolution of this system is still poorly understood because the carotid pattern of most Jurassic and Cretaceous taxa is unknown. A related issue is the evolution of basicranial akinesis and the reinforcement of the skull to allow greater bite performance (e.g., Sterli and de la Fuente 2010). Using a broad sample of fossil specimens I aim to review the osteological correlates and associated structures of these systems, to provide a new nomenclatural scheme and to analyze character evolution in a novel phylogenetic framework.

It is expected that new insights in the anatomy and ecology of stem-cryptodires will help resolving the phylogeny and origins of Cryptodira. Such work will undoubtedly serve as a basis for future research on morphological and biogeographical evolution on Cryptodires and will be critical for understanding the physical/environmental drivers of these processes. It will also yield an improved

framework for molecular divergence dating analyses and provide an independent test of the phylogeny.

3. Methods

Fossil specimens were accessed in collections and were rescored in the taxon-character matrix of Sterli and de la Fuente (2011). Precise anatomical documentation and description was produced for *Annemys (Xinjiangchelys) levensis* Sukhanov and Narmandakh 2006 (PIN 4636-4-2), *Annemys* (*Xinjiangchelys) latiens* Sukhanov and Narmandakh 2006 (PIN 4636-6-2), *Manchurochelys manchoukuoensis* Endo and Shikama, 1942 (PMOL-AR00180), and *Hangaiemys hoburensis* Sukhanov and Narmandakh 1974 (not included in the thesis; PIN 3334-4, PIN 3334-34, PIN 3334-35, PIN 3334-36, PIN 3334-37).

The following fossil taxa were furthermore studied first hand: *Allopleuron hoffmanni* (Gray, 1831) (NHMUK R42913), *Chubutemys copelloi* Gaffney et al. 2007 (MPEF-PV1236), *Dracochelys bicuspis* Gaffney and Ye 1992 (IVPP V4075), *Hangaiemys hoburensis* Sukhanov and Narmandakh 1974 (PIN 3334-4, PIN 3334-34, PIN 3334-35, PIN 3334-36, PIN 3334-37), *Heckerochelys romani* Sukhanov 2006 (PIN 4561-2 and PIN 4719-34), *Kallokibotion bajazidi* Nopcsa 1923 (NHMUK R4921 and NHMUK R4925), *Kayentachelys aprix* Gaffney et al. 1987 (MNA V1558, MCZ 8917), *Liaochelys jianchangensis* (PMOL-AR00140 holotype, PMOL-AR00160), *Macrobaena mongolica* Tatarinov 1959 (PIN 533-4), *Manchurochelys manchoukuoensis* (PMOL AR00008), *Meiolania platyceps* Owen 1886 (NHMUK R682), *Mongolemys elegans* Khosatzky and Mlynarski 1971 (five uncatalogued skulls at the collections of PIN), *Mongolochelys efremovi* Khozatsky 1997 (PIN 552-459 and two uncatalogued skulls), *Naomichelys speciosa* Hay 1908 (FMNH PR 273), *Niolamia argentina* Ameghino 1899, *Notoemys laticentralis* Cattoi and Freiberg 1961 (cast of MOZP 2487), *Odontochelys semitestacea* Li et al. 2008 (IVPP V13240), *Ordosemys leios* Brinkman and Peng 1993b (IVPP V9534-1 and material listed in), *Peligrochelys walshae* Sterli and de la Fuente 2013 (MACN PV CH 2017, MACN PV CH 2017), *Portlandemys mcdowelli* Gaffney 1975b (NHMUK R2914, NHMUK R3163, NHMUK R3164), *Proganochelys quenstedti* Baur 1887 (SMNS 16980), *Rhinochelys*

elegans Lydekker 1889 (NHMUK R27), *Sandownia harrisi* Meylan et al. 2000 (MIWG 3480), *Sinemys gamera* Brinkman and Peng 1993a (IVPP V9532-11), *Sinemys brevispinus* Tong and Brinkman 2013, (IVPP V9538-1, IVPP V9532-11), *Solnhofia parsonsi* Gaffney 1975a (TM 4023), *Toxochelys latiremis* Cope 1873 (NHMUK R4530 and NHMUK R3902) and *Xinjiangchelys radiplicatoides* Brinkman et al. 2013 (IVPP V18104).

The following taxa were studied on the basis of photographs: *Adocus lineolatus* Cope 1874 (CCM 60-15), *Basilochelys macrobios* Tong et al. 2009 (MD 8-2), *Bouliachelys suteri* Kear and Lee 2006 (SAM P41106), *Meiolania platyceps* (AM F: 18671), *Plesiochelys etalloni* Pictet and Humbert 1857 (MH 435), and *Pleurosternon bullockii* Owen 1842 (UMZC T1041).

Fieldwork was performed in Middle-Upper Jurassic formations of the Turpan Basin, Xinjiang Autonomous Province, China as part of a Sino-German co-operation between the University of Tübingen and the Shenyang Normal University, Liaoning in the fall of 2011. Several turtle specimens were collected from at least three sites. Mechanical preparation and subsequent study took place in the Paleontological Laboratory in Shenyang. In the present work, I included material from the 'Turtle Cliff' site.

Institutional abbreviations

AM: Australian Museum, Sydney, Australia; CCM: Carter County Museum, Montana USA; FMNH: Field Museum of Natural History, Chicago, USA; IVPP: Institute of Vertebrate Paleontology and Paleoanthropology, Beijing, China; IWCMS: Dinosaur Isle Museum, see MIWG; MACN: Museo Argentino de Ciencias Naturales "Bernardino Rivadavia", Buenos Aires, Argentina; MCCM: Museo de las Ciencias de Castilla−La Mancha, Cuenca, Spain; MCZ: Museum of Comparative Zoology, Harvard University, Cambridge, USA; MD: Sirindhorn Museum, Phu Kum Khao, Sahatsakhan, Kalasin Province, Thailand; MH: Naturhistorisches Museum, Basel, Switzerland; MIWG: Museum of Isle of Wight Geology, Sandown, United Kingdom; MNA: Museum of Northern Arizona, Flagstaff, USA; MOZP: Museo "Prof. Dr. Juan A. Olsacher", Zapala, Argentina; MPEF: Museo Paleontológico Egidio Feruglio, Trelew, Argentina; MRF: Marmarth Research Foundation, Marmarth, North Dakota, USA; NHMUK: Natural History Museum of London, United Kingdom; PIN: Paleontological Institute, Russian Academy of Sciences, Moscow, Russia; PMOL: Paleontological

Museum of Liaoning, Shenyang Normal University, Shenyang, China; SAM: South Australian Museum, Adelaide, Australia; SGP: Sino-German Cooperation Project; SMNS: Staatliches Museum für Naturkunde, Stuttgart, Germany; UMZC: University Museum of Zoology, Cambridge, United Kingdom; TM: Teylers Museum, Haarlem, The Netherlands; TMP: Royal Tyrrell Museum of Palaeontology, Drumheller, Canada.

3.1. Phylogenetic analysis

Four separate phylogenetic analyses were run in order to test the relationships of stem-cryptdoires from the Mesozoic of Asia and North America. All analyses used a revised version of the latest global turtle character-taxon matrix by Sterli and de la Fuente (2013) which in turn is based on Gaffney (1996), Gaffney et al. (2007), Joyce (2007), Sterli (2010) and Sterli and de la Fuentre (2011). In addition to the taxa sampled in Sterli and de la Fuente (2013), the matrix was expanded by adding *Xinjiangchelys radiplicatoides*, *X. junggarensis* (sensu Brinkman et al. 2008), *Annemys* (*Xinjiangchelys*) *levensis*, *A*. *latiens*, *Basilochelys macrobios* Tong et al. 2009, *Liaochelys jianchangensis*, *Changmachelys bohlini* Brinkman et al. 2013b, *Sinemys gamera*, *Sinemys lens*, *Sinemys brevispinus*, and the skull of *Ordosemys* sp. (Brinkman and Wu 1999). The taxon *Ordosemys leios* is only considered to consist of material described in Brinkman and Peng (1993b). *Manchurochelys manchoukuoensis* was scored on the basis of three specimens: the specimen described herein (PMOL-AR00180), the one described by Zhou (2010b; PMOL-AR00008), and the lost holotype (Endo and Shikama 1942). It has to be noted that the scorings for *Xinjiangchelys latimarginalis* sensu Peng and Brinkman (1993) [= *X*. *junggarensis* sensu Brinkman et al. 2008] are likely based on a chimera taxon. Brinkman and Wu (1999) used *X*. *latimarginalis* as a terminal taxon, but their scorings were based on material from two distantly placed localities: the shell characters were based on material from the Pingfengshan locality of the Junggar Basin, Xinjiang, China (Peng and Brinkman 1993) whereas the skull characters were scored for material from Kyrgyzstan (Fergana Basin, Sarykamyshsay locality) after Kaznyshkin et al. (1990). However, Nessov (1995) separated the Fergana *X*. *latimarginalis* from the Junggar *X*. *latimarginalis* and included the former into a new species, *X*. *tianshanensis*. Joyce (2007) and all subsequent phylogenetic workers adopted the

scorings of Brinkman and Wu (1999) for *X*. *latimarginalis*. For the present analyses I considered *X*. *latimarginalis* synonymous with *X*. *junggarensis* as suggested by Brinkman et al. (2008) and rescored this taxon based on Pingfengshan material only as observed directly or described in Peng and Brinkman (1993). All skull characters for this taxon were therefore scored as '?' as no skull material is available from this locality. Several scorings were changed for *Hangaiemys (Kirgizemys) hoburensis*, *Sinemys lens*, *Dracochelys bicuspis*, and *Ordosemys leios*, among others, based on personal observations of the relevant material (see 'Appendix 1' of Publication #3 and 'Phylogenetic analysis' section of Publication #2 for list of changes). The following characters were treated as ordered: 7 (Nasal A), 19 (Parietal H), 27 (Squamosal C), 40 (Maxilla D), 42 (Vomer A), 50 (Quadrate B + C), 52 (Antrum Postoticum A), 59 (Pterygoid B), 81 (Opisthotic C), 82 (Opisthotic D), 89 (Stapedial Artery B), 98 (Canalis Caroticum F), 120 (Carapace A), 121 (Carapace B), 130 (Peripheral A), 133 (Costal B), 138 (Supramarginal A), 158 (Hyoplastron B), 159 (Mesoplastron A), 161 (Hyoplastron B), 176 (Abdominal A), 213 (Cleithrum A), 214 (Scapula A), 232 (Manus B), 233 (Manus C). *Sphenodon punctatus*, *Owenetta kitchingorum*, *Simosaurus gaillardoti*, and *Anthodon serrarius* were designated as outgroups. In each analysis I omitted the following characters: Maxilla B, Basioccipital B, Pterygoid M, and Cervical Vertebra D and K. Maxilla B was omitted because the meaning or scoring of this character as provided in Sterli and de la Fuente (2013) could not be reproduced. As scored, this character does not show any variation within Cretaceous basal eucryptodires and I therefore do not expect any impact from its omission. Basioccipital B is omitted for similar reasons: the definition of a deep, C-shaped concavity on the basioccipital is quite vague since almost all turtles with basioccipital tubera have some sort of C-shaped concavity, but were scored as absent by Sterli and de la Fuente. Pterygoid M is omitted because, unlike as stated (Sterli and de la Fuente 2013), the derived state of this character (basisphenoid and pterygoid in different levels) is present in many basal taxa (actually being the ancestral state for turtles, e.g. *Proganochelys quenstedti*) and therefore the character should be rescored in the future. Cervical D is omitted once again because the meaning of 'triangular diapophysis' could not be reproduced and because the current distribution of this character does not help us either (scored as present for panpleurodires, *Chubutemys copelloi*, *Glyptops plicatulus* and baenids). Finally,

Cervical vertebra K is omitted because it is redundant with Cervical vertebra B (both characters pertain to the depth of the ventral keel on posterior cervicals).

Analysis A

For this analysis, a simple heuristic search was performed in TNT (Goloboff et al. 2008a,b) using the tree-bisection-reconnection swapping algorithm with thousands of random addition sequence replicates and 10 trees saved per replicate. Wildcard taxa were removed following the search to improve resolution within the strict consensus tree.

Analysis B

The protocol from 'Analysis A' was repeated, but this time the relationship of the major crown-cryptodire clades following the current molecular consensus (Krenz et al. 2005): (Trionychia (Emydidae (Geoemydidae + Testudinidae)) + (Chelonioidea (Chelydridae + Kinosternoidea)))). The internal relationships of these clades were left unconstrained and *Platysternon megacephalum* was considered a stem-emydid. Heuristic searches were repeated until the most parsimonious trees (MPT) were found 30 times during each replicate (using the command "xmult = hits 30").

Analysis C

The protocol from 'Analysis B' was repeated, but nine new characters that are thought to be relevant for the interrelationships of Cretaceous basal eucryptodires were added (see 'Appendix 2' of Publication #3 for character definitions). Heuristic searches were repeated until the most parsimonious trees (MPT) were found 30 times during each replicate.

Analysis D

This analysis differs from 'C' in that *Basilochelys macrobios* and most pan-pleurodires except for *Podocnemis expansa* and *Pelomedusa subrufa* were excluded a priori before running the heuristic search. This experimental approach is justified by the work of Sterli (2010) in which the position of pan-pleurodires proved to be problematic in that xinjiangchelyids, sinemydids, and other, widely recognized Mesozoic stem-cryptodires were unorthodoxly placed outside of Testudines and in that Cryptodira was not found to be monophyletic relative to Pleurodira. As such, it is

interesting to test how the removal of most pan-pleurodires affects tree topology, especially in the case of Mesozoic basal eucryptodires. The search was again repeated until the most parsimonious trees (MPT) were found 30 times during each replicate.

3.2. Osteological terminology

The cranial nomenclature presented by Gaffney (1972, 1979a) has been highly influential, because all anatomical systems of the cranium were clearly described and illustrated in these publications and because a broad audience was thereby enabled to apply these names consistently to the skulls of fossil and recent turtles. Only in the last few years have some shortcomings become apparent, however, particularly in regards to the nomenclature of the carotid system. It is here attempted to rectify this situation by providing an internally consistent nomenclatural system for this anatomical region (Fig. 4).

The internal carotid artery of most turtles, like most amniotes, splits into a cerebral and a palatine (lateral) branch. Although these structures are interrelated, they can be thought of as three different vessels, which are herein terms the internal carotid artery, the cerebral artery, and the palatine artery. New insights into the cranial anatomy of basal turtles (Brinkman et al. 2013a, Sterli et al. 2010, Müller et al. 2011) has revealed that these three blood vessels can enter the skull through three non-homologous foramina and that they can also exit the skull through three non-homologous foramina, for a total of six non-homologous foramina. The nomenclatural system of Gaffney (1972, 1979a) proved to be confusing, because it only provides three names for these six foramina (i.e., foramen *anterior* [italics added for emphasis] canalis carotici interni, foramen *posterior* canalis carotici interni, and foramen caroticum laterale) and because these names were defined as applying to inappropriate portions of the carotid system. Sterli et al. (2010) were the first to realize these deficiencies in the nomenclatural system of Gaffney (1972, 1979a) and proposed new terms, but these new terms are not sufficient to name all six potential foramina. Moreover they break with the tradition set by Gaffney (1972, 1979a) in their grammatical construction. These inconsistencies were partially addressed recently (Brinkman et al. 2013a) but some parts of the system still remain unnamed and the palatine artery is still defined as sitting in the lateral canal.

A new nomenclatural system is proposed here that attempts to follow the grammatical precedence set forth by Gaffney (1972, 1979a), but that breaks tradition by providing names for all potential foramina and by renaming the lateral canal the palatine canal. This nomenclatural system consists of a total of 10 new terms (Fig. 4):

Canalis caroticus internus: The bony canal that holds any portion of the internal carotid artery, absent, among others, in basal turtles and paracryptodires.

Foramen posterius canalis carotici interni (fpcci): The posterior entry of the internal carotid artery, absent, among others, in basal turtles and paracryptodires.

Foramen anterius canalis carotici interni (facci): The anterior exit of the internal carotid artery, only present in turtles with a fenestra caroticus.

Canalis caroticus cerebralis: The bony canal that holds any portion of the cerebral artery, present in all turtles.

Foramen posterius canalis carotici cerebralis (fpccc): The posterior entry of the cerebral artery, not developed in turtles where the split of the internal carotid artery into the cerebral and palatine branches is covered by bone.

Foramen anterius canalis carotici cerebralis (faccc): The anterior exit of the cerebral artery, present in all turtles, typically located near the dorsum sellae.

Canalis caroticus palatinum: The bony canal that holds any portion of the palatine artery, generally absent in turtles with an open interpterygoid vacuity.

Foramen posterius canalis carotici palatinum (fpccp): The posterior entry of the palatine artery, generally developed in turtles with a closed interpterygoid vacuity, but not in those where the split of the internal carotid artery into the cerebral and palatine branches is covered by bone.

Foramen anterius canalis carotici palatinum (faccp): The anterior exit of the palatine artery, generally present in turtles with a close interpterygoid vacuity.

Fenestra caroticus (fca): A figurative bony window into the otherwise closed carotid system, which exposes the split of the internal carotid artery into the cerebral and palatine branches. The window is posteriorly defined by the foramen anterius canalis carotici interni and anteriorly defined by the foramen posterius canalis carotici cerebralis and the foramen posterius canalis carotici palatinum or the interpterygoid vacuity.

I here otherwise follow the nomenclature of the skull used in Gaffney (1972) and Hutchison and Bramble (1981) for the shell.

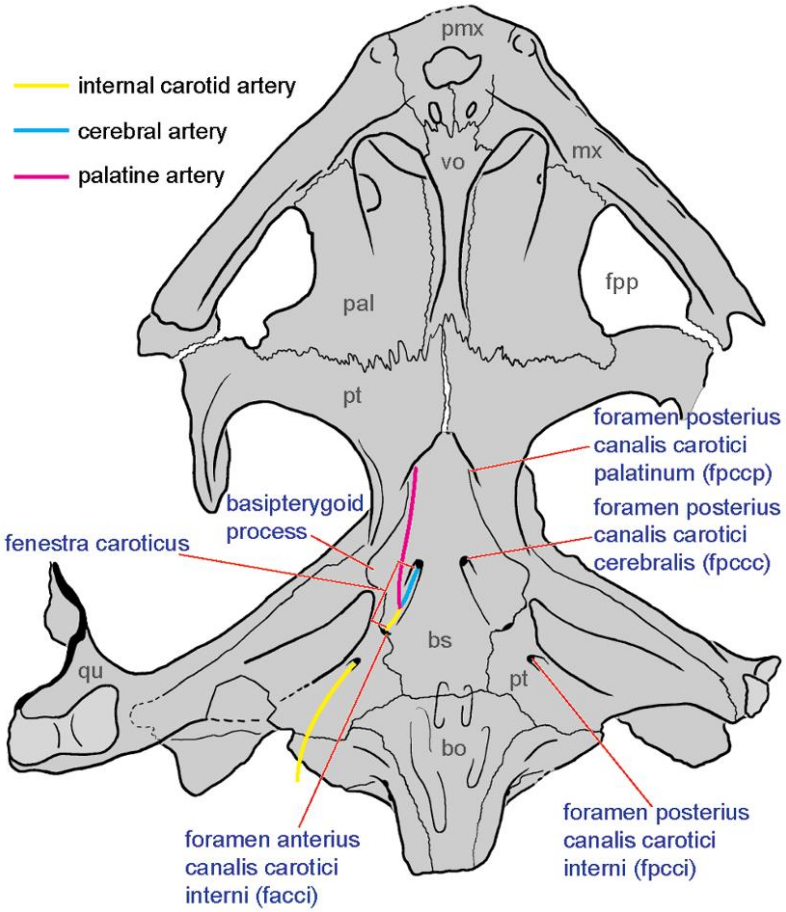

Figure 4. **Proposed internally consistent nomenclature for the osseous portion of the carotid circulation system of turtles as exemplified on the skull of *Dracochelys bicuspis* (IVPP V4075). Abbreviations:** bo: **basioccipital,** bs: **basisphenoid,** fpp: **foramen palatinum posterius,** mx: **maxilla,** pal: **palatine,** pmx: **premaxilla,** pt: **pterygoid,** qu: **quadrate,** vo: **vomer.**

3.3. Geological settings

The *Xinjiangchelys wusu* nov. sp. material comes from the “Turtle Cliff Fossil Site” located within the Flaming Mountains about 26 km ENE of the city of Shanshan

in the Turpan Basin, Xinjiang Autonomous Province, China. The Flaming Mountains consist of Triassic to Paleogene sediments that were uplifted during the Neogene (Dong 1992, Wings et al. 2007). Published reports on the geology and stratigraphy of the Flaming Mountains in particular and the Turpan Basin in general are rare (e.g., Shao et al. 1999 and references therein) and many uncertainties therefore exist regarding the absolute age of formations and their correlation with similar units in other Central Asian basins. Jurassic clastic strata in the Flaming Mountains were preliminarily divided into the Early Jurassic Sangonghe Formation, the Middle Jurassic Xishanyao, Sanjianfang, Qiketai, and Qigu Formations (the latter was recently dated in the Junggar Basin with 164.6 Ma ± 1.4 Ma, Wang and Gao 2012), and the Late Jurassic Karaza Formation Dong (1997). Future stratigraphic research needs to clarify whether Late Jurassic strata are indeed mostly absent in the area. Piedmont-fluvial deposits dominate the upper parts of the Jurassic sequence (Wings et al. 2012). The total thickness of the supposed Qigu Formation is about 850 m in the area of the Turtle Cliff Fossil Site. The formation is rich in vertebrate fossils, dominated by dinosaurs and turtles. Finds of the latter include the spectacular turtle taphocoenosis at Mesa Chelonia (Wings et al. 2012) near the lower border of the formation and the herein introduced Turtle Cliff Fossil Site near the base of the upper third of the formation. The Turtle Cliff Fossil Site is situated geographically 1 km to the ENE and stratigraphically 500 m above the Mesa Chelonia site. The deposits that allegedly represent the Qigu Formation in the Turpan Basin are characterized by alternating coarse and fine-grained sediments that often contain unionid freshwater bivalves, reflecting changing depositional conditions typical of river systems (Shao et al. 1999). The turtle skeletons at the Turtle Cliff Fossil Site were found on the top of a low hill in a steeply inclined (65°), fine-grained and strongly cemented sandstone layer rich in lithoclasts. Above and below the turtle-bearing sandstone horizon follows a succession of predominately red silt-and mudstones.

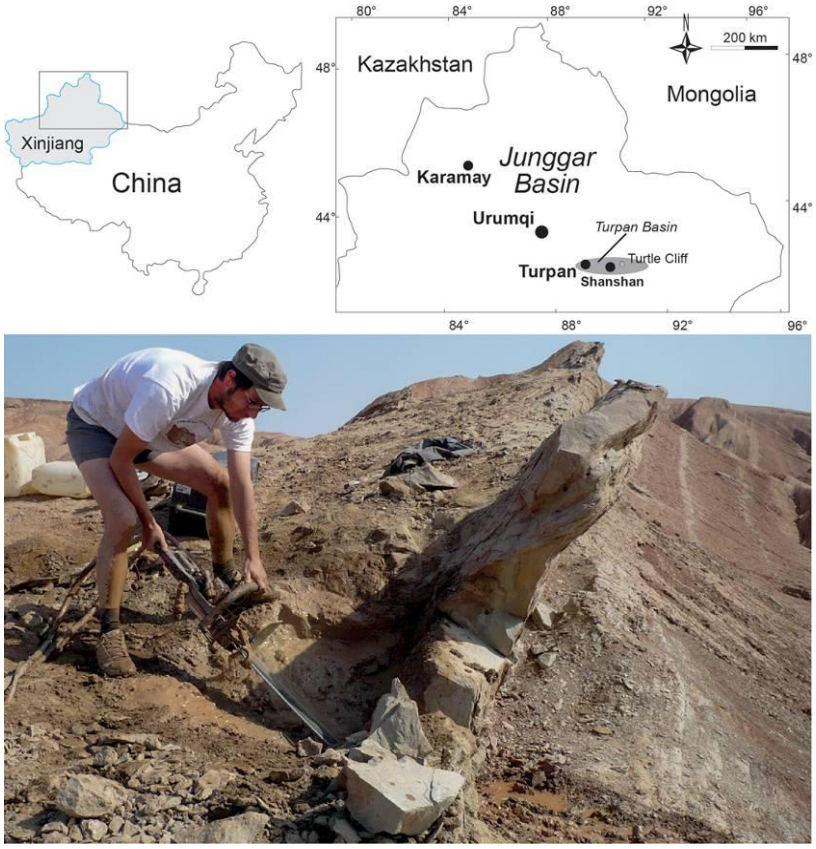

Figure 5. **The geographic location of the "Turtle Cliff" site in the Turpan Basin of Xinjiang Autonomous Province, China (above) and a photograph of the cliff where the turtles were found and cut out with the help of a rock saw (below).**

The material of *Annemys (Xinjiangchelys) levensis*, *Annemys latiens*, and *Annemys* sp. described and documented in detail as part of the doctorate research (the description is included in Publication #1) originate from the Ulan Malgait beds cropping out at the locality of Shar Teg, which is situated in the Transaltai Gobi approximately 100 km east-southeast from the town of Altai, within Altai Somon District in the southern part of Govi Altai Aimag Province of Mongolia (Gubin and Sinitza 1996). The Ulan Malgait beds form a mostly siliciclastic unit composed of red, grey, brown, or yellow siltstones with interbedded coarse and fine sandstones. The turtle remains were found in four different sandstone horizons together with gastropods, bivalves, fishes, crocodilians, and sauropod dinosaurs (Gubin and Sinitza 1996, Watabe et al. 2004). The depositional environment is considered to represent an extensive fluvial system and the vertebrate bearing sandstone lenses are interpreted as crevasse splay (flood) deposits (Gubin and Sinitza 1996, Watabe et al. 2004). The age of the Ulan Malgait beds is poorly resolved. Biostratigraphic data retrieved from stoneflies from the underlying Shar Teg beds indicated a Middle

Jurassic age, whereas a more recent study of mayflies argued for a Late Jurassic age (Sinitshenkova 1995, 2002). No biostratigraphic data is available from the Ulan Malgait beds themselves (Watabe et al. 2004).

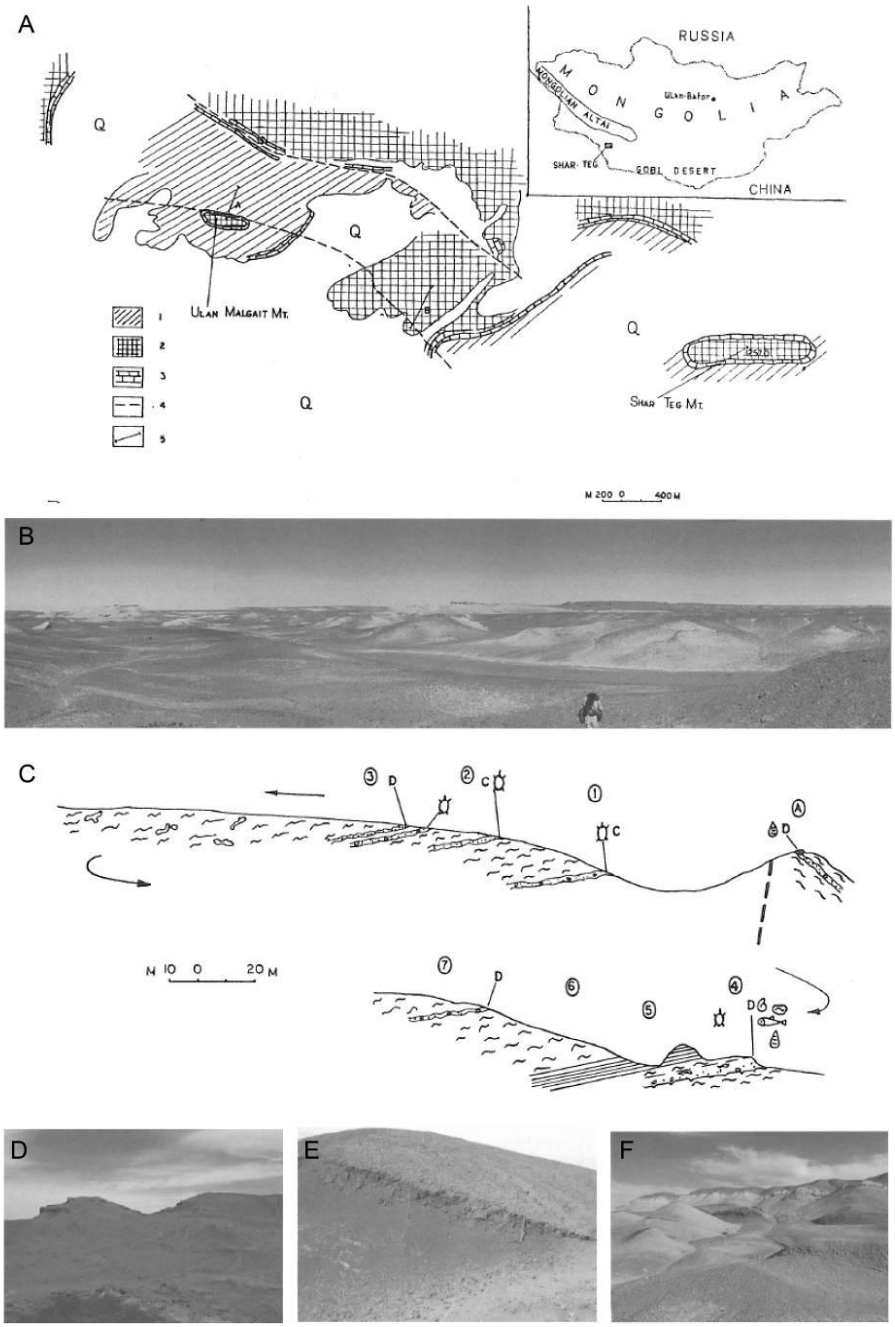

Figure 6. **Geographic location, stratigraphy and outcrops of the Upper Jurassic Shar Teg locality within Transaltai Gobi, Altai Somon District in the southern part of Govi Altai Aimag Province of Mongolia.** A: **geologic sketch of the Shar Teg locality showing the Shar Teg Beds (1), the Ulan Malgait Beds (2), caliche layers (3), tectonic structures (4), and the position of the Shar Teg and Ulan Malgait sections documented by the joint Soviet-Mongolian expedition in 1984, 1987 and 1989 (5).** B: **panorama view of Shar Teg area with the Ulan Malgait hill in the middle right portion.** C: **cross-section of an outcrop of the Ulan Malgait beds showing the turtle sites.** D: **the Ulan Malgait beds in the Ulan Malgait hill (southwest to the left and northwest to the right).** E: **paleosol layer in the Ulan Malgait beds.** F: **Southern Hills area with the Ulan Malgait Beds red beds on the top of the hills. The *Annemys* material comes from the Ulan Malgait beds. Taken from Gubin and Sinitza (1996) and Watabe et al. (2004).**

The *Manchurochelys manchoukuoensis* specimen (PMOL-AR00180) comes from the Early Cretaceous Jiufotang Formation of northeastern China, near Chifeng city, Inner Mongolia. The Yixian and Jiufotang Formations are well-known for their lagerstätten-type fossil preservation of the Early Cretaceous Jehol Biota that consisted of plants, various invertebrates, amphibians, squamate reptiles, turtles, non-avian dinosaurs (including the much-publicized feathered theropods), birds and mammals (Benton et al. 2008). The two formations are widespread in Liaoning, Hebei and Inner Mongolia provinces (Manchuria) and the Jehol Biota itself is considered to have extended as far as Korea to the east, Mongolia and southern Siberia to the north and the Yangtze River to the south (Chang et al. 2012). The Jiufotang Formation is overlying the Yixian Formation and is mainly built up by mudstone, siltstone, shale, sandstone and tuff deposited in a lacustrine environment. $^{40}Ar/^{39}Ar$ age determination of tuff layers from the lower part of the Jiufotang yielded an absolute age of 122 Ma, corresponding to the beginning of the Aptian (Chang et al. 2009).

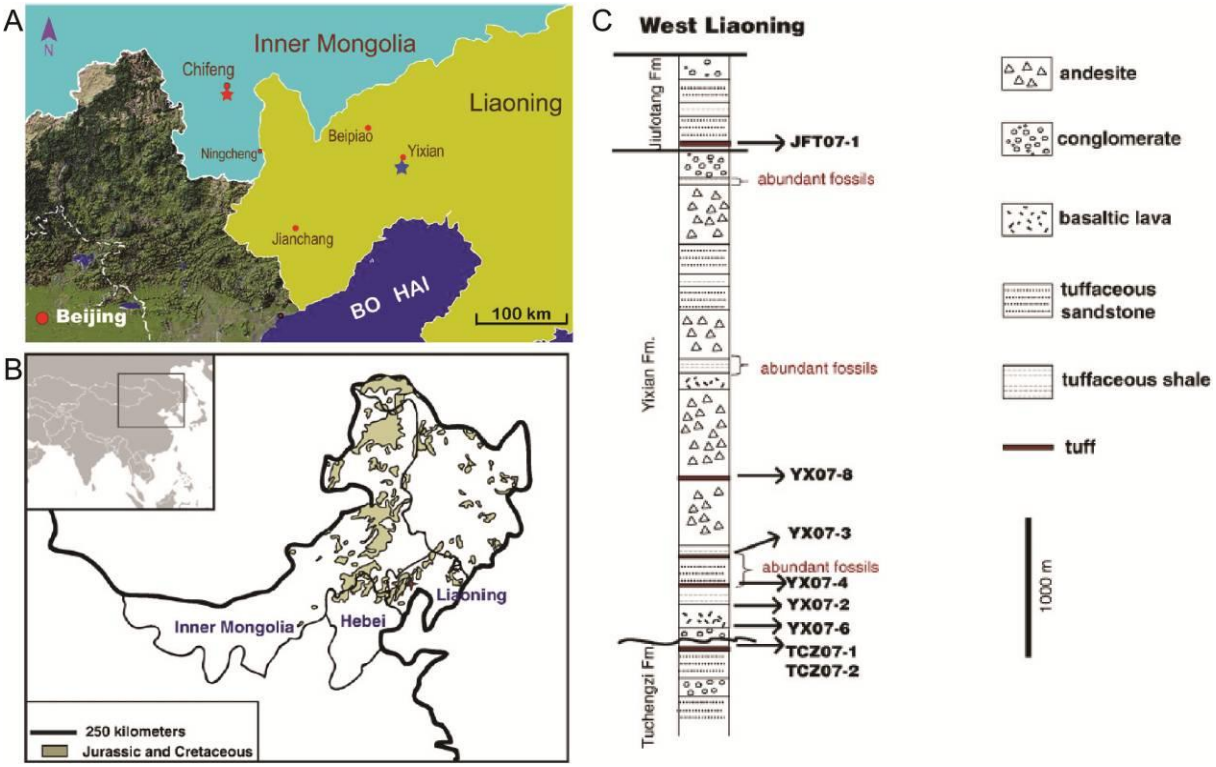

Figure 7. **Geography and geology of the Early Cretaceous Jehol Biota bearing Yixian and Jiufotang formations in Northeast China or Manchuria (Liaoning, Hebei and Inner Mongolia provinces).** A: **Map showing the known localities of *Manchurochelys manchoukuoensis*, in Qilinshan (=Heishangou; marked by a red asterisk; E118°50′46.4″, N42°08′33.3″), Chifeng City, Inner Mongolia; and in Yixian (marked by a blue asterisk), Jinzhou City, Liaoning Province.** B: **distribution of the Jehol Biota bearing rocks in Manchuria.** C: **section of Yixian and Jiufotang formations in Liaoning Province. B and C taken from Chang et al. (2009).**

3.4. Phylogenetic nomenclature

The description of phylogenetic results within Eucryptodira has been greatly hampered by a nomenclatural system that is universally agreed to be confusing. The suprageneric names Sinemydidae Ye 1963, Macrobaenidae Sukhanov 1964, and Xinjiangchelyidae Nessov in Kaznyshkin et al. 1990 were introduced by taxonomists to group various fossil eucryptodires. However, given that most characters that were used to diagnose these groups have since been shown to represent plesiomorphies (e.g., Sukhanov 2000, Rabi et al. 2010) and given that changing phylogenies have not allowed well-diagnosed clades worth naming to be identified (e.g., Gaffney 1996, Brinkman and Wu 1999, Gaffney et al. 2007, Gaffney and Ye 1992, Joyce 2007, Parham and Hutchison 2003, Anquetin 2012, Tong et al. 2012a,b), most authors have resorted to placing these names in quotation marks to indicate their likely paraphyly while tolerating the resulting taxonomic imprecision. This situation is herein attempted to be resolved by providing phylogenetic definitions of these names and to thereby stabilize their taxonomic meanings. Sinemydidae, Macrobaenidae, and Xinjiangchelyidae refer to monophyletic clades throughout this contribution (see Phylogenetic Definitions below) and are therefore not placed in quotation marks anymore. All other higher taxonomic names are clade names as defined by Joyce et al. (2004).

XINJIANGCHELYIDAE Nessov in Kaznyshkin et al. 1990, converted clade name

Definition—Xinjiangchelyidae refers to the most inclusive clade containing *Xinjiangchelys junggarensis* Ye 1986, but not *Sinemys lens* Wiman 1930, *Macrobaena mongolica* Tatarinov 1959, or any species of Recent turtle.

SINEMYDIDAE Ye 1963, converted clade name

Definition—Sinemydidae refers to the most inclusive clade containing *Sinemys lens* but not *Xinjiangchelys junggarensis, Macrobaena mongolica*, or any species of Recent turtle.

MACROBAENIDAE Sukhanov 1964, converted clade name

Definition—Macrobaenidae refers to the most inclusive clade containing *Macrobaena mongolica* but not *Xinjiangchelys junggarensis*, *Sinemys lens*, or any species of Recent turtle.

4. Systematic paleontology

TESTUDINATA Klein 1760

TESTUDINES Batsch 1788

XINJIANGCHELYIDAE Nessov in Kaznyshkin et al. 1990

Xinjiangchelys Ye 1986

Remark: A number of genera other than *Xinjiangchelys* have been referred to Xinjiangchelyidae in recent years, including *Chengyuchelys* Young and Chow 1953; *Tienfuchelys* Young and Chow 1953; *Annemys* Sukhanov and Narmandakh 2006; *Shartegemys* Sukhanov and Narmandakh 2006; *Yanduchelys* Peng et al. 2005; *Protoxinjiangchelys* Tong et al. 2012a (Sukhanov 2000, Sukhanov and Narmandakh 2006, Brinkman et al. 2008, 2013a; Tong et al. 2012a,b). The majority of these genera are sufficiently diagnosed relative to *Xinjiangchelys*, but there is no up-dated diagnosis available for *Xinjiangchelys*. This taxon has therefore been rendered a waste-backed taxon defined by what it is *not*. To avoid further complications the using of a more inclusive definition is suggested for *Xinjiangchelys* that includes all species of Xinjiangchelyidae (sensu the herein proposed phylogenetic definition) until the phylogenetic relationships of the included taxa can be determined more confidently.

Xinjiangchelys wusu sp. nov.

(Fig. 8)

Holotype—PMOL-SGP A0100-1, a partial skeleton, including the skull exposed in dorsal view.

Referred material—PMOL-SGP A0100-3, partial skeleton (Figures 8); PMOL-SGP A0100-2, partial skeleton without skull, plastron not exposed.

Locality and horizon—Turtle Cliff Fossil Locality (see Geological Settings), Shanshan, Turpan Basin, Xinjiang Autonomous Province, People's Republic of China (Figure 5); ?Qigu Formation, Upper Jurassic.

Etymology—*wusu* refers to a small town in Xinjiang Autonomous Province.

Diagnosis—A species of *Xinjiangchelys*; skull differing from *Annemys (Xinjiangchelys) levensis* in the prefrontals being fully separated by the frontals; from *Annemys (Xinjiangchelys) latiens* by the broader skull and the extensive jugal and frontal contribution to the orbit, from *X. radiplicatoides* by the flattened skull and the presence of a remnant of the interpterygoid vacuity. Shell differing from *X*. *chowi* Matzke et al. 2005 *X*. *qiguensis* Matzke et al. 2004a, *X*. *tianshanensis* Kaznyshkin et al. 1990 and *X*. *junggarensis* (sensu Brinkman et al. 2008) by the narrow vertebral scales. See Publication #2 for a comprehensive description.

Taxonomic comments—Following the herein proposed phylogenetic definition, *Xinjiangchelys wusu* is assigned to Xinjiangchelyidae because it is recovered in a monophyletic group together with *Xinjiangchelys junggarensis* (Figure 19). Other members of Xinjiangchelyidae include *X*. *radiplicatoides*, *Annemys (Xinjiangchelys) latiens* and *Annemys levensis* and this clade is only supported by one unambiguous synapomorphy (Anal A:1, extension of anal scale onto hypoplastron).

Among taxa traditionally referred to Xinjiangchelyidae, the morphology of *Xinjiangchelys. wusu* is most similar to that of *Annemys levensis*, *Annemys latiens* and *X. radiplicatoides*, however, a number of differences justify its recognition as a separate taxon. In contrast to *A*. *levensis*, the prefrontals do not meet in the midline in *X*. *wusu*, the basioccipital tubera are better developed, there are two foramina nervi hypoglossi instead of three, the vertebral 3-4 sulcus extends onto neural 5 not neural 6, and the midline plastral sulcus is straight instead of sinusoidal. *Annemys latiens* has a proportionally more elongated skull, reduced frontal and jugal contribution to the orbit and sinusoidal midline plastral sulcus, whereas *X*. *radiplicatoides* has a more inflated skull, a slit-like interpterygoid vacuity instead of a round opening with very indistinct foramen caroticus palatinum, a strongly plicated carapace, and a sinusoidal midline plastral sulcus.

Since the interrelationships of xinjiangchelyids are unresolved in the consensus tree and pruning the rouge taxon *Xinjiangchelys junggarensis* reveals that *Annemys* (i.e., *A. levensis* and *A. latiens*) is paraphyletic (*levensis* forms the sister taxon of a *latiens*, *X*. *wusu* and *X*. *radiplicatoides* trichotomy), I suggest referring *wusu* to the genus *Xinjiangchelys* Ye 1986 as this taxon has priority over *Annemys* Sukhanov and Narmandakh 2006. However, until the phylogenetic relationships of xinjiangchelyid taxa have been resolved with greater assurance, I suggest keeping the name *Annemys* as well.

Recently, abundant remains of xinjiangchelyids were reported from the Mesa Chelonia turtle bone bed, which is stratigraphically situated 500 m below and spatially located 1 km away from the Turtle Cliff site (Wings et al. 2012). These Mesa Chelonia turtles are represented by several partial skeletons and were all referred to an indeterminate species of *Annemys*. The Mesa Chelonia form is very similar to *X. wusu* but a few differences are present and therefore it is considered as a separate taxon. *Xinjiangchelys wusu* is about 15 % larger, the foramen posterius canalis carotici interni is located along the posterior surface of the pterygoid, not in a notch at the back of the skull, the vertebral 3-4 sulcus extends onto neural 5 (extends onto neural 6 in eleven specimens out of twelve in the Mesa Chelonia form) and the plastral pegs are visible even when the plastron is articulated with the carapace, whereas the pegs are mostly covered by the peripheral ring in the fully ossified specimens of the Mesa Chelonia forms. A further difference might be that *X*. *wusu* lacks any types of fontanelles in the carapace or the plastron whereas they are present in more than half of the specimens from Mesa Chelonia that appear to be adult-sized individuals.

Another closely related form, mostly known by the skull, has been reported from the Junggar Basin (Brinkman et al. 2013a) and was referred to *Annemys* sp. The foramen posterius canalis carotici interni of this skull is located in a notch between the basisphenoid and the pterygoid (unlike *X*. *wusu*) and the lateral plate of the jugal lacks a posterodorsal process extending ventral to the postorbital. On the other hand, the skull from the Junggar Basin is very similar to the Mesa Chelonia form and I tentatively refer them to the same, yet unnamed taxon.

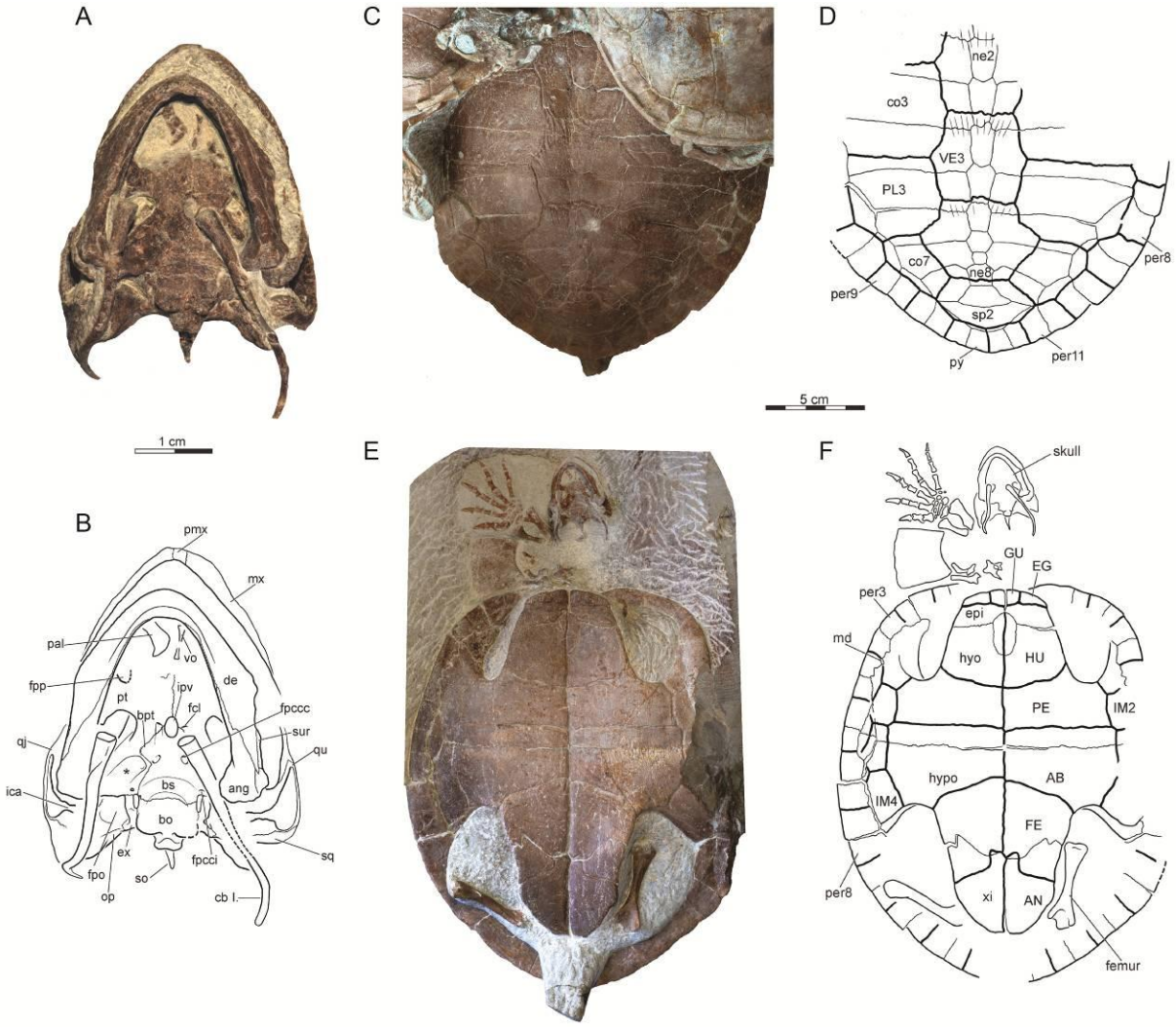

Figure 8. **Skeletal remains of *Xinjiangchelys wusu* Rabi et al. 2013, (PMOL-SGP A0100-3), Middle Jurassic, ?Qigu Formation, "Turtle Cliff", Shanshan area, Turpan Basin, Xinjiang Autonomous Province, China.** A-B: **photograph and line drawing of skull, mandible and hyoid apparatus in ventral view. Abbreviations:** ang, **angular;** bo, **basioccipital;** bpt, **basipterygoid process;** bs, **basisphenoid;** cb I., **cornu branchiale I;** cor, **coronoid;** de, **dentary;** ex, **exoccipital;** fcl, **foramen caroticum laterale,** fpccc: **foramen posterius canalis carotici cerebralis,** fpcci: **foramen posterius canalis carotici interni;** fpo, **fenestra postotica;** fpp, **foramen palatinum posterius;** ica, **incisura columella auris;** ipv, **interpterygoid vacuity;** mx, **maxilla;** op, **opisthotic;** pal, **palatine;** pmx, **premaxilla;** pt, **pterygoid;** qj, **quadratojugal;** qu, **quadrate;** so, **supraoccipital;** sq, **squamosal;** sur, **surangular;** vo, **vomer;** * **refers to fossa pterygoidea.**
C-D: **photograph and line drawing of posterior two third of carapace.** E-F: **photograph and line drawing of plastron. The right forelimb in 'e-f' does not belong to PMOL-SGP A0100-3 but to PMOL-SGP A0100-1. Abbreviations:** AB, **abdominal;** AN, **anal;** co, **costal;** EG, **extra gular;** epi, **epiplastron;** FE, **femoral;** GU, **gular;** HU, **humeral;** hyo, **hyoplastron;** hypo, **hypoplastron;** IM, **inframarginals;** md, **musk duct foramen;** ne, **neural;** per, **peripheral;** PE, **pectoral;** PL, **pleural;** py, **pygal;** sp, **suprapygal;** VE, **vertebral;** xi, **xiphiplastron.**

Annemys Sukhanov and Narmandakh 2006

Types Species—*Annemys latiens* Sukhanov and Narmandakh 2006.

Included Species—*Annemys levensis* Sukhanov and Narmandakh 2006.

Distribution—Late Jurassic of Shar Teg locality, Govi Altai Aimag, Mongolia (Sukhanov 2000, Sukhanov and Narmandakh 2006) and late Middle Jurassic to early Late Jurassic of Wucaiwan area, Junggar Basin, Xinjiang Autonomous Uyghur Province, China (Brinkman et al. 2013a).

Diagnosis—See Sukhanov and Narmandakh (2006) for a non-differential diagnosis. The skull of *Annemys (Xinjiangchelys)* differs from *Xinjiangchelys radiplicatoides* Brinkman et al. 2013a in being flattened, having a deeper upper temporal emargination, a longer supraoccipital crest, and reduced basioccipital tubera; from *Hangaiemys* (*Kirgizemys*) *hoburensis* Sukhanov and Narmandakh 1974 and *Kirgizemys dmitrievi* Nessov and Khosatzky 1981 in the presence of a laterally widely open foramen jugulare posterius, and the absence of paired pits on the basisphenoid. The latter also differentiates *Annemys* from Shar Teg from *Sinemys* spp. (sensu Brinkman and Peng 1993a), *Dracochelys bicuspis* Gaffney and Ye 1992, and *Ordosemys* spp. (sensu Danilov and Parham 2007 and Tong et al. 2004). The shell of *Annemys* differs from *Xinjiangchelys* spp. (sensu Brinkman et al. 2008 and Brinkman et al. 2013a) in the vertebral 2 and 3 being almost as long as wide, vertebral 4 being wider than vertebral 2 and 3, the placement of vertebral 3/4 sulcus on neural 6, and an interrupted neural row that allows a midline contact of costals 7; differs from *Shartegemys laticentralis* in the square epiplastra; differs from *Chengyuchelys* spp. (sensu Tong et al. 2012b), *Protoxinjiangchelys salis* Tong et al. 2012a, and *Yanduchelys delicatus* Peng et al., 2005 (sensu Tong et al. 2012b) in the presence of a ligamentous carapace-plastron attachment; further differs from *Chengyuchelys* spp. in the vertebral 5 not overlapping onto peripheral 10; differs from *Tienfuchelys* spp. (sensu Tong et al. 2012b) in having four pairs of inframarginals; differs from *Kirgizemys* (*Hangaiemys*) *hoburensis*, *Sinemys lens* and *Ordosemys* spp. in the relatively shorter dorsal rib 1, extension of marginals 4 to 8 on to costals, square-shaped epiplastron that is tightly sutured to the ento- and hyoplastron, reduced epiplastral process present, extragulars present, femoro-anal sulcus omega shaped and extending onto hypoplastron, and sinuous midline sulcus.

Annemys (Xinjiangchelys) levensis Sukhanov and Narmandakh 2006

(Fig. 9)

Annemys levensis Sukhanov and Narmandakh, In Press in Sukhanov, 2000:314, fig. 17.2 (unavailable under articles 13.1.1 and 16.1 ICZN [1999]).
Annemys levensis Sukhanov and Narmandakh, 2006:120, fig. 1a, b (original description).
Xinjiangchelys levensis (Sukhanov and Narmandakh 2006), Tong et al. 2012a: p. 107 (new combination).

Holotype—PIN 4636-4, associated skull and mandible (PIN 4636-4-2), shell, right femur, right humerus, right scapula and fragment of coracoid and incomplete right pelvic girdle (PIN 4636-4-1).

Locality and Horizon—Shar Teg locality, Govi Altai Aimag, Mongolia, Upper Jurassic, Ulan Malgait beds.

Revised Diagnosis—A species of *Annemys (Xinjiangchelys)* differing from *Annemys latiens* in the presence of a broader and shorter skull, partially separated prefrontals, more extensive contributions of the frontal and the jugal to the orbital rim, quadrangular neural 1, longer and narrower posterior plastral lobe, and relatively narrower anterior projection of the anal scales. See Publication #1 for a comprehensive description.

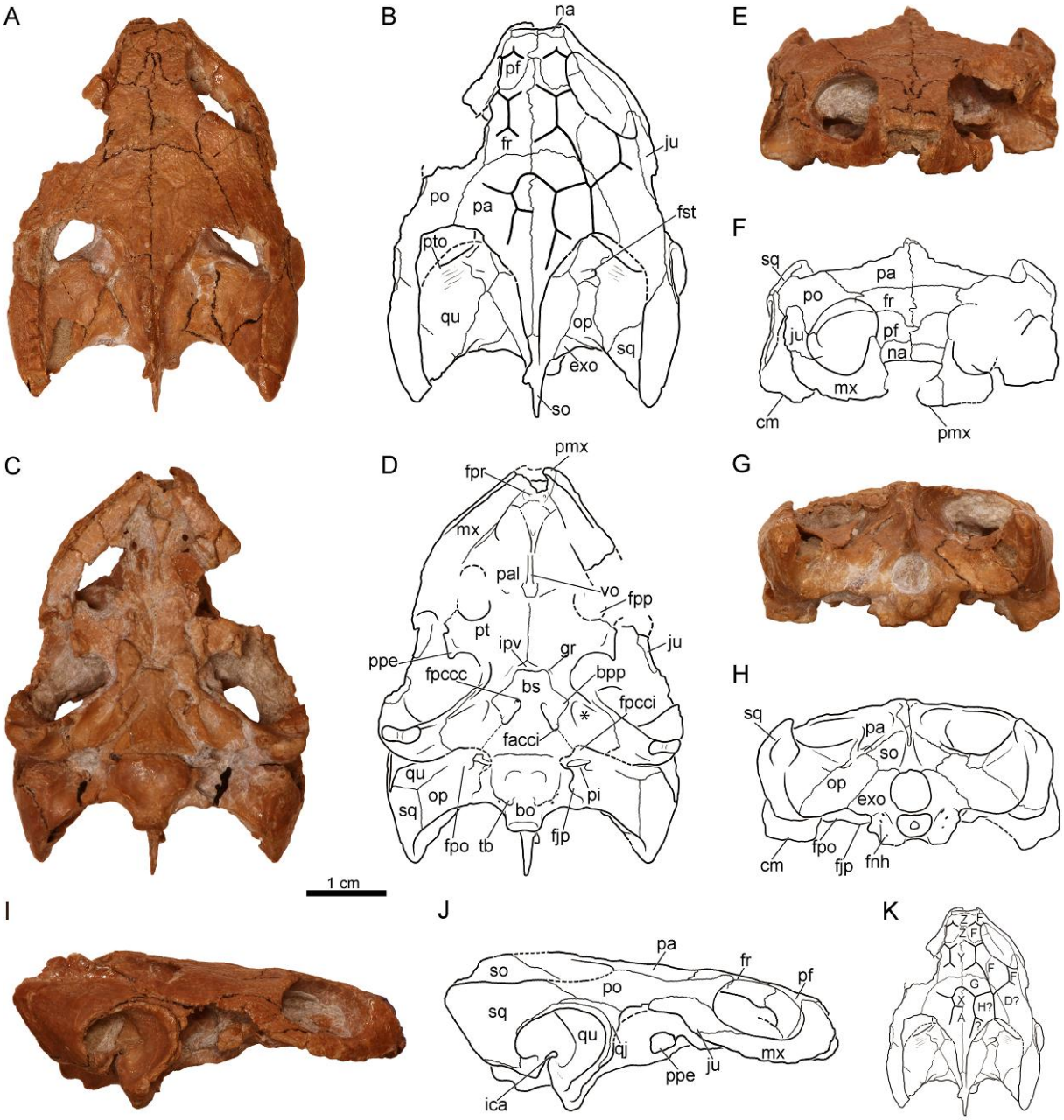

Figure 9. **PIN 4636-4-2 (holotype), *Annemys (Xinjiangchelys) levensis*, skull, Late Jurassic, Shar Teg, Ulan Malgait beds, Govi Altai Aimag, Mongolia.** A-B, **photograph and line drawing in dorsal view;** C-D, **photograph and line drawing in ventral view;** E-F, **photograph and line drawing in anterior view;** G-H, **photograph and line drawing in posterior view;** I-J, **photograph and line drawing in right lateral view;** K, **line drawing of skull roof scales. Abbreviations:** bo, **basioccipital;** bpp, **basipterygoid process;** bs, **basisphenoid;** cm, **condylus mandibularis;** exo, **exoccipital;** facci, **foramen anterius canalis caroticus internus**; fjp, **foramen jugulare posterius;** fnh, **foramen nervi hypoglossi;** fpccc, **foramen posterius canalis caroticus cerebralis;** fpcci, **foramen posterius canalis carotici interni;** fpo, **fenestra postotica;** fpp, **foramen palatinum posterius;** fpr, **foramen praepalatinum;** fr, **frontal;** fst, **foramen stapedio-temporale;** gr, **groove for palatine branch of the carotid;** ica, **incisura columella auris;** ipv, **interpterygoid vacuity;** ju, **jugal;** mx, **maxilla;** na, **nasal;** op, **opisthotic;** pa, **parietal;** pal, **palatine;** pf, **prefrontal;** pi, **processus interfenestralis;** pmx, **premaxilla;** po, **postorbital;** ppe, **processus pterygoideus externus;** pt, **pterygoid;** pto, **processus trochlearis oticum;** qj, **quadratojugal;** qu, **quadrate;** so, **supraoccipital;** sq, **squamosal;** tb, **tubera basioccipitalis;** vo, **vomer;** A, D, F, H, G, X, Y, Z, **cranial scales (following the terminology of Sterli and de la Fuente, 2013); *, pterygoid pit.**

Annemys (Xinjiangchelys) latiens Sukhanov and Narmandakh 2006

(Fig. 10)

Annemys latiens Sukhanov and Narmandakh, In Press in Sukhanov, 2000:317, fig. 17.4 (unavailable under articles 13.1.1 and 16.1 of the ICZN [1999]).
Xinjiangchelys latiens (Sukhanov and Narmandakh, In Press): Matzke et al., 2004a:1295 (new combination of unavailable name).
Annemys latiens Sukhanov and Narmandakh 2006:120 (original description).
Xinjiangchelys latiens (Sukhanov and Narmandakh 2006), Tong et al. 2012a: p. 107 (new combination).

Holotype—PIN 4636-5, an almost complete shell (PIN 4636-5-1), a partial basicranium and lower jaw ramus (PIN 4636-5-2), and other poorly preserved disarticulated cranial elements.

Referred Material—PIN 4636-6-1, an incomplete shell lacking most of the carapace; PIN 4636-6-2, a partial skull associated with PIN 4636-6-1; PIN 4636-7, an almost complete shell and a humerus. All referred material is from the type locality.

Locality and Horizon—Shar Teg locality, Govi Altai Aimag, Mongolia, Upper Jurassic, Ulan Malgait beds.

Revised Diagnosis—A species of *Annemys* (*Xinjiangchelys*) differing from *Annemys levensis* in the presence of a narrower and longer skull, frontals that fully separate the prefrontals, a minor contribution of the frontal and the jugal to the orbital rim, hexagonal neural 1, a shorter and broader posterior plastral lobe, and relatively wider anterior projection of the anal scales. See Publication #1 for a comprehensive description.

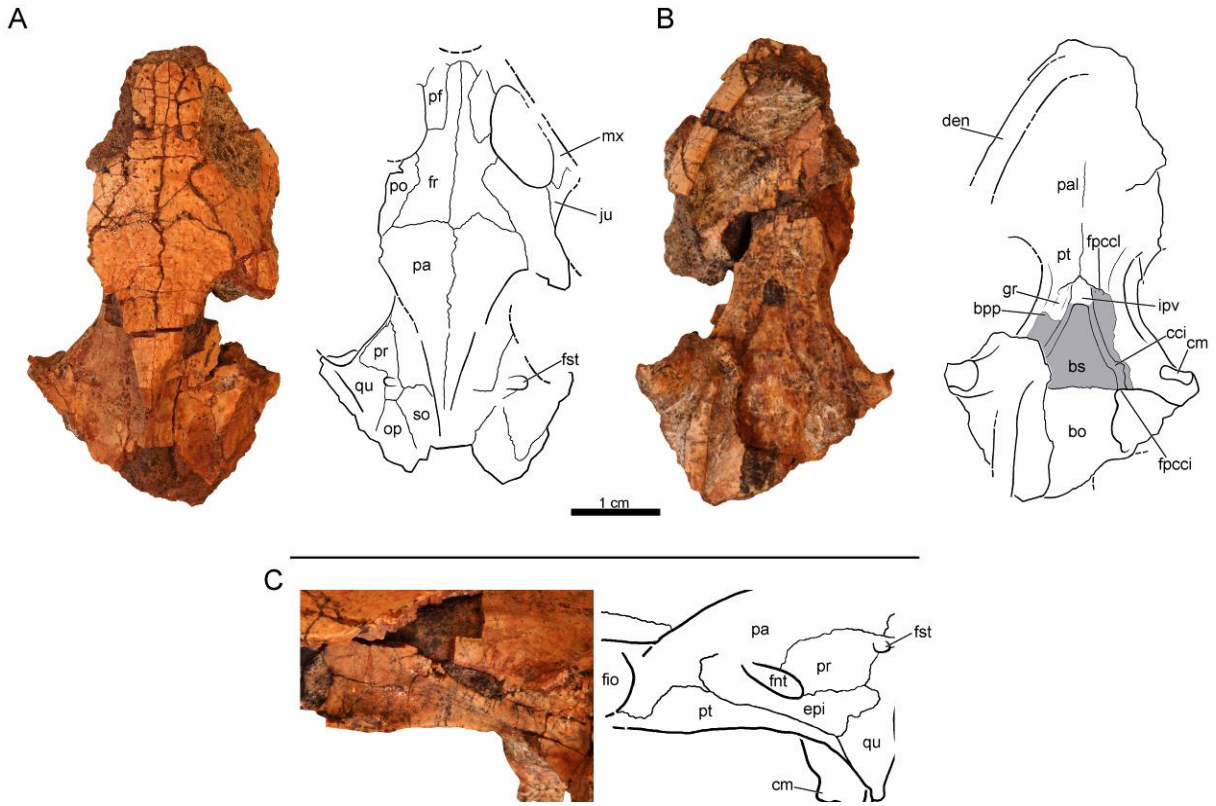

Figure 10. **PIN 4636-6-1, *Annemys (Xinjiangchelys) latiens*, skull, Late Jurassic, Shar Teg, Ulan Malgait beds, Govi Altai Aimag, Mongolia.** A, **photograph and line drawing in dorsal view;** B, **photograph and line drawing in ventral view;** C, **left trigeminal region in lateral view. Abbreviations:** bo, **basioccipital;** bpp, **basipterygoid process;** bs, **basisphenoid;** cci, **canalis caroticus internus;** cm, **condylus mandibularis;** den, **dentary;** epi, **epipterygoid;** fio, **foramen interorbitale;** fnt, **foramen nervi trigemini;** fpcci, **foramen posterius canalis carotici interni;** fpccl, **foramen posterius canalis carotici lateralis;** fr, **frontal;** fst, **foramen stapedio-temporale;** gr, **groove for palatine branch of carotid artery;** ipv, **interpterygoid vacuity;** ju, **jugal;** mx, **maxilla;** op, **opisthotic;** pa, **parietal;** pal, **palatine;** pf, **prefrontal;** po, **postorbital;** pr, **prootic;** pt, **pterygoid;** qu, **quadrate;** so, **supraoccipital. Gray color indicates eroded surfaces.**

Taxonomic comments—The taxa *Annemys levensis* and *Annemys latiens* were used informally in Sukhanov (2000) for material from the Upper Jurassic of Shar Teg, Mongolia, and the names were only made available following the rules of the ICZN in a subsequent paper by Sukhanov and Narmandakh (2006). *Annemys latiens* is based on an almost complete shell (PIN 4635-5-1) associated with a poorly preserved lower jaw ramus and multiple skull fragments, of which the partial basicranium (PIN 4635-5-2) is the most informative. This damaged skull was not reported in Sukhanov (2000) or Sukhanov and Narmandakh (2006) and *A. latiens* was diagnosed relative to *A. levensis* on the basis of shell characters only (Sukhanov and Narmandakh 2006). Another, previously unreported *A. latiens* skull-shell association from Shar Teg (PIN 4636-6) reveals distinct cranial differences relative to the skull of *A. levensis* (see above) and thereby supports the presence of two separate taxa at Shar Teg using cranial characters. The carapace (PIN 4636-6) of

the associated skull is very incomplete, but its wide posterior plastral lobe is consistent with the morphology seen in the holotype of *A. latiens*. The small amount of information that is possible to extract from the badly preserved holotype skull of *A. latiens* (PIN 4636-5-2) agrees with PIN 4636-6-2 in being narrow and elongated, unlike *A. levensis* (see the description of PIN 4636-6-2 above). Another shell (PIN 4636-7) is tentatively also refered to *A. latiens* based on the proportions of the posterior plastral lobe (see the description of this shell above). *Annemys levensis* is therefore only known from a single specimen, the type specimen (PIN 4636-4), which consists of an associated skull, lower jaw, shell, and some other appendicular elements. Additional material from Shar Teg may allow a better understanding of the intra- and interspecific variation in *Annemys* and at present it seems difficult to distinguish the two species on the basis of discrete shell characters. The lack of characters that allow distinguishing the postcranial of *A. levensis* and *A. latiens* force us to refer all fragmentary remains to *Annemys* sp.

Matzke et al. (2004a) and Tong et al. (2012a) both synonymized *Annemys* with *Xinjiangchelys* because their phylogenetic analysis of 'xinjiangchelyids' revealed *A. levensis* and *A. latiens* to be situated within a clade formed by taxa typically attributed to *Xinjiangchelys*. However, neither analysis included any member of the 'sinemydid-macrobaenid' grade or other more advanced Pancryptodires but instead extensively sampled 'xinjiangchelyid' taxa – to an extent that it seems the authors *a priori* inferred that *Annemys* belong to the latter group. My (global) analyses found *Annemys levensis* in a monophyletic clade with *X*. *latimarginalis* (sensu Peng and Brinkman 1993) but the inclusion of more xinjiangchelyid taxa are required to test the monophyly of this group and the relationship of *Annemys* to *Xinjiangchelys* spp. This study found no evidence for the exclusive monophyly of *Annemys* (Fig. 19) but I do not consider my analysis to be a highly rigorous test of the relationships of this taxon within xinjiangchelyids since the taxonomic sample is limited for this group. Until the phylogenetic relationships of xinjiangchelyid taxa have been resolved with greater assurance, I suggest keeping the name *Annemys*.

Brinkman et al. (2013a) recently described and figured a skull with associated shell elements from the Upper Jurassic of the Junggar Basin (Wucaiwan area, Xinjiang, China) that they referred to *Annemys* sp. (also figured in Rabi et al. (2010:fig. 1g-h; Fig. 2 g-h of present work). As in A. *latiens* and A. *levensis* this skull has an unossified gap anterior to the basisphenoid between the pterygoids and

therefore I agree that it is morphologically closer to *Annemys* spp. than to *Xinjiangchelys radiplicatoides*. I also agree that this skull is clearly different from that of *A*. *levensis* (see Brinkman et al., 2013a for a list of differences). The *Annemys* sp. skull is furthermore different from *A. latiens* in its proportions, by being less elongated and by having a distinctly more extensive frontal and jugal contribution to the orbit compared to *A*. *latiens*. It is therefore suggested that this fossil represents a taxon different from both *A. levensis* and *A. latiens* but likely closely related to them.

PANCRYPTODIRA Joyce, Parham, and Gauthier 2004

Manchurochelys manchoukuoensis Endo and Shikama 1942

(Fig. 11)

Holotype—"Registration No. 3898 (former Central National Museum of Manchoukuo) from Tsaotzushan, approximately 21km southwest of Yixian, western Liaoning, China. The whereabouts of the holotype are currently unknown, and it was probably lost during World War II." (Zhou 2010b).

Referred specimen—PMOL-AR00180 (Fig. 11), a partial articulated skeleton, including the skull, the first six cervical vertebrae, the anterior part of the carapace, two fragmentary scapulae, and a proximal end of the right humerus.

Locality and Horizons—The fossil is from a site near Qilinshan (Heishangou), Chifeng City, Inner Mongolia (E118°50′46.4″, N42°08′33.3″; Figure 1); the Early Cretaceous Jiufotang Formation (Chang et al. 2009). Given the novelty of this site, detailed information is not yet available regarding its precise age or accompanying fauna.

Revised diagnosis—*Manchurochelys manchoukuoensis* is diagnosed as a primitive pancryptodire by the presence of a low domed shell and a ligamentous connection between the plastron and carapace. It is distinguished from other basal pancryptodires by the following unique combination of characters: prefrontals contact one another along the midline, postorbital-squamosal contact absent, parietal and squamosal separated, crista supraoccipitalis relatively long, foramen palatinum posterius large, nuchal emargination shallow, cervical scale present, vertebral scales 2-4 longer than wide, first vertebral wider than nuchal, preneural absent, eight neurals present, peripheral 1 - costal contact present, costal 3 with parallel anterior

and posterior sides, process or spine on peripheral 7 absent, two suprapygals present of which the posterior one is much larger than the anterior one, pygal present, central and posterior fontanelles absent, posterior lobe of plastron long and narrow. See Publication #3 for a comprehensive description.

Taxonomic comments—PMOL-AR00180 is assigned to *Manchurochelys manchoukuoensis* because no major differences are apparent in the proportions and contacts in the skull and the shell with those of the holotype (Endo and Shikama 1942) or the referred specimen PMOL-AR00008 (Zhou 2010b). A striking similarity of PMOL-AR00180 with PMOL-AR00008 is the presence of a long supraoccipital crest that extends markedly more posteriorly than in *Liaochelys jianchangensis*, *Ordosemys liaoxiensis*, *Kirgizemys hoburensis*, and *Sinemys lens* (unknown for other species of *Sinemys*). Although differences appear to be present, at first sight, between the neck of PMOL-AR00008 and PMOL-AR00180, particularly in the degree of separation of the postzygapophyses, these are only because different sections of the neck are exposed in the two specimens. As in modern cryptodires, the postzygapophyses of the anterior cervicals in *M. manchoukuoensis* (as well as in *Sinemys brevispinus*, *Kirgizemys hoburensis*) are more fused than the posterior ones. In addition, the foramen posterius canalis carotici cerebralis was illustrated in the pterygoid in PMOL-AR00008 (labeled as foramen basisphenoidale; Zhou 2010b) but a revision of the specimen reveals that the position of this foramen is unclear and preservation makes comparison difficult with PMOL-AR00180 where it is on the pterygoid-basisphenoid suture.

With the discovery of the new specimen, the number of described *M. manchoukuoensis* fossils has increased to three. Two of these originate from the Yixian Formation of Liaoning Province (including the lost holotype, Endo and Shikama 1942, Zhou 2010b) whereas PMOL-AR00180 was recovered from the Jiufotang Formation of Inner Mongolia. Both formations are considered to be Lower Cretaceous, with the Yixian being Barremian to Upper Aptian (129-122 Ma) and the younger Jiufotang Formation being Aptian to Upper Albian (122-110 Ma) in age. (Chang et al. 2009). Thus, the range of *M. manchoukuoensis* is extended geographically and, less unequivocally, temporally by the new fossil from Chifeng. However, given this difference in geography and perhaps in age it is not excluded that more complete findings may reveal distinct morphological features not preserved in the specimen from Chifeng and arguing for a separate species of *Manchurochelys*.

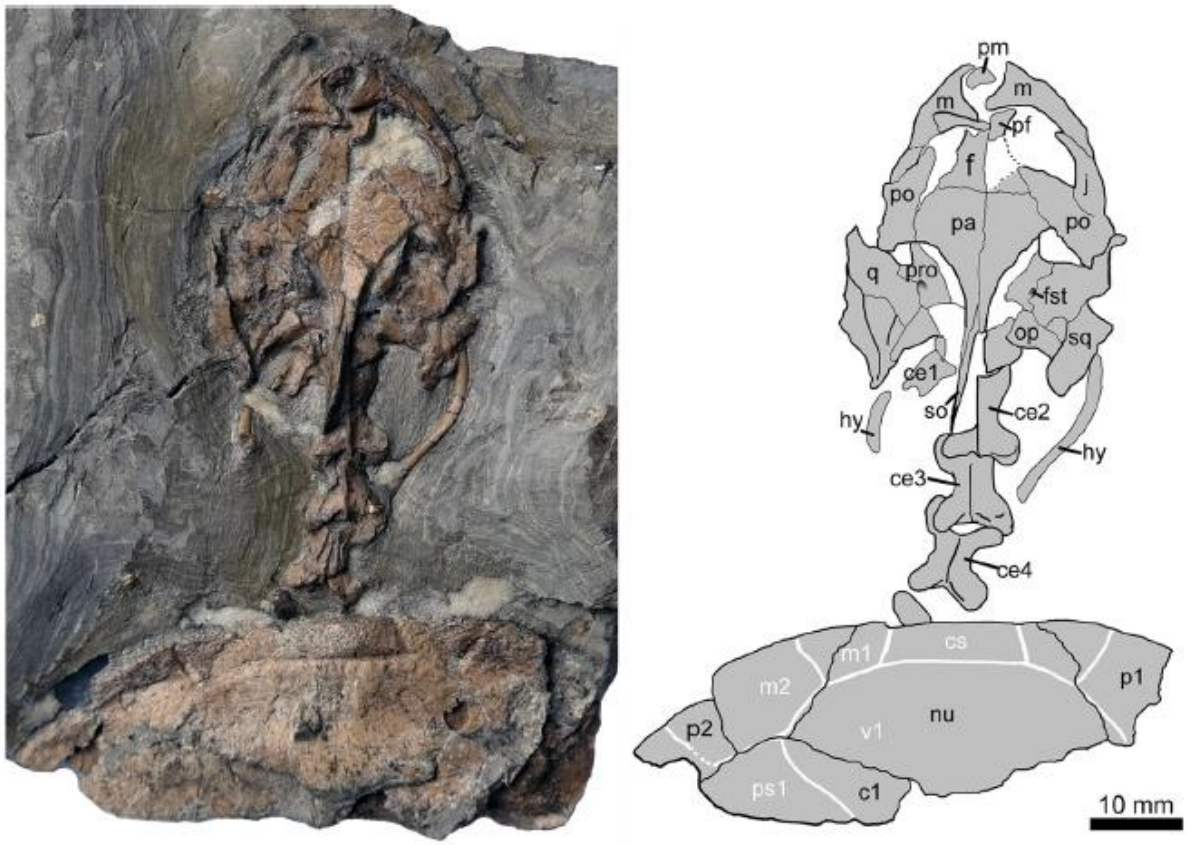

Figure 11. **New material of *Manchurochelys manchoukuoensis* (PMOL-AR00180) from the Early Cretaceous Jiufotang Formation of Qilinshan, Chifeng, Inner Mongolia, China. Anterior part of the skeleton in dorsal view. Abbreviations:** c1, **costal Plate 1;** cs, **cervical scale;** ce1-4, **cervical vertebrae 1-4;** f, **frontal;** fst, **foramen stapedio-temporale;** hy, **hyoid;** m, **maxilla;** m1-2, **marginal scales 1–2;** nu, **nuchal;** op, **opisthotic;** p1-2, **peripheral Plates 1–2;** pa, **parietal;** pf, **prefrontal;** pm, **premaxilla;** po, **postorbital;** pro, **prootic;** ps1, **pleural scale 1;** q, **quadrate;** so, **supraoccipital;** sq, **squamosal;** v1, **vertebral scale 1.**

5. Discussion

5.1. Presence of a reduced interpterygoid vacuity in Xinjiangchelyidae

One of the most interesting observations regarding the cranial morphology of *Annemys levensis*, *A*. *latiens*, and Xinjiangchelys *wusu* is the presence of a small gap between the pterygoid and the basisphenoid. In basal turtles, such as *Proganochelys quenstedti* Baur 1887, *Kayentachelys aprix* Gaffney et al. 1987, and *Condorchelys antiqua* Sterli 2008 the palatine artery entered the skull via a wide gap between the pterygoids, the interpterygoid vacuity. The vacuity is absent in all more derived fossil turtles and the palatine artery therefore entered the skull through a pair of distinct foramina, the foramina posterius canalis carotici lateralis (fpccl). *Annemys latiens* clearly displays an intermediate morphology by displaying both a pair of fpccl and remnants of the pterygoid vacuity. The corresponding region in *A. levensis* is somewhat damaged, but a pair of grooves that lead to the lateral edge of the gap and that evidently held the palatine arteries is indicative of the former presence of paired fpccl. Slit-like fpccl have otherwise been reported for *X. radiplicatoides* (Brinkman et al. 2013a), but this taxon shows no sign of a gap anterior to the basisphenoid and therefore represents the derived condition. The slit-like shape of the palatine foramina implies that the anterior contact of the basisphenoid with the pterygoid was at best poorly ossified in this xinjiangchelyid. An unossified area between the pterygoids coupled with fpccl is also present in *Annemys* sp. from Wucaiwan, Junggar Basin (Brinkman et al. 2013a) and is therefore consistent with the morphology of *A*. *latiens* and *Xinjinagchelys wusu* and what is inferred for *A*. *levensis*. A larger sample of xinjiangchelyid skulls may eventually reveal that the gap between the pterygoids closes during ontogeny and abundant material from the Turpan Basin (Wings et al. 2012) is particularly promising.

The palatine arteries probably entered via the fpccl in these taxa and the xinjiangchelyid condition may represent an evolutionary stage when the interpterygoid vacuity was not yet closed completely but already lost its function.

5.2. Paleoecology of Xinjiangchelyidae

The overall shell morphology and the size of *Annemys latiens*, *A. levensis*, and *Xinjiangchelys wusu* are highly similar and these taxa are therefore only poorly diagnosed by the shells. On the other hand, the skulls of *A*. *latiens* and *A*. *levensis* are greatly different in the arrangement of the dermal roofing elements and in their relative proportions: *A. latiens* has an elongated and narrow skull compared to relatively broad skull of *A. levensis*.

Both species originate from a single larger horizon at Shar Teg (i.e. the Ulan Malgait beds) and therefore they may have been sympatric taxa, although no clear record exists of their co-occurrence in identical layers. However, whereas the absence of size difference may have allowed both taxa to share the same aquatic habitat, the distinct skull shapes suggest niche partition in terms of feeding strategies.

It is apparent from the depositional environment in which they were found that *Annemys latiens* and *A. levensis* were freshwater turtles. This conclusion is furthermore supported by their overall anatomy: low, suboval shell, flat skull, and relatively straight humeral and femoral shafts. However, these two taxa were probably not as adapted to the aquatic realm as *Hangaiemys* (*Kirgizemys*) *hoburensis*, *Ordosemys leios*, or *Sinemys lens*, all of which exhibit more reduced shells. The flat, triangular skull with narrow and sharp triturating surfaces in *Annemys* spp. is consistent with a predatory lifestyle. In being elongated and flat *A. latiens* had an even more streamlined skull compared to *A. levensis,* which may have been of great help while striking at small agile prey such as fish. Future collecting at Shar Teg should focus on finding the cervical vertebrae of *Annemys* in order to clarify whether they were short- or long-necked forms. *Xinjiangchelys wusu* was a short-necked form and was highly reminiscent to *levensis* in its skull proportions. On the other hand, *X. qiguensis* was a long-necked form (Matzke et al. 2004a; skull unknown) suggesting a striking-and-snapping predatory strategy as today seen in chelid snake-necked turtles (Pleurodira).

5.2.1. Ecological Diversity of Xinjiangchelyidae during the Late Jurassic

Xinjiangchelyids have so far been mostly known from their shells, which are surprisingly uniform and conservative in their morphology, although size differences of some taxa with uncertain affinities are apparent (e.g., Matzke et al. 2005). However, new data (Brinkman et al. 2013a and the present work) indicate that the skull shape of xinjiangchelyids was more variable than their shells. At present, only

few xinjiangchelyids are known from their skulls, but these can nevertheless be clearly classified into three morphotypes. The first morphotype is represented by an inflated and relatively high skull shape with shallow upper temporal emargination, as seen in *Xinjiangchelys radiplicatoides* (Brinkman et al. 2013a). The second morphotype is small, flat, and triangular with deeper temporal emargination, as seen in *Annemys levensis*, *Annemys* sp. from the Junggar Basin (Brinkman et al., 2013a) and possibly *X. wusu*. The third morphotype is an elongated and narrow variant of the second type and seen in *A. latiens*. These morphotypes probably correspond to different feeding niches and strategies and indicate that by the Late Jurassic the dominant turtle clade of Asia achieved only a moderate level of ecological diversity relative to what is present in later (e.g., Cretaceous) Pancryptodires. However, it must be noted that the lack of skull material for most Jurassic Asian turtles may result in a significant underestimate of their actual ecological diversity.

5.2.2. Functional aspects of the trochlear system in Xinjiangchelyidae

The skulls of *Annemys latiens* and *A. levensis* reveal that the processus trochlearis oticum is very poorly developed in these taxa and may not even qualify as a real process. The trochlear structure is best preserved in the skull of *A. levensis*. It consists of a rugose area on the anterodorsal wall of the otic chamber (Fig. 9A-B) and lacks the protrusion seen in many crown cryptodires (e.g. Gaffney 1979, Joyce 2007, Sterli and de la Fuente 2010, Joyce and Sterli 2012). It is likely that this surface held the cartilage that redirected the temporal musculature (the cartilago transiliens) over the otic capsule before reaching the coronoid process of the lower jaw (Schumacher 1973). The undeveloped bony base of the synovial capsule suggests that the trochlear system of *Annemys* was not as advanced as in crown cryptodires. This would be consistent with the thickened laterally protruding lip of the epipterygoid present in *A. levensis* that could have served as a barrier that hindered the adductor musculature from crossing the path of the trigeminal nerve. The primitive trochlear system of *Annemys* spp. could result in lower bite performance relative to most crown cryptodires. This is probably correlated with the short supraoccipital process (at least present in *A. levensis*) that only allows for a reduced amount of muscle mass, but also does not require an advanced and well-developed trochlear system (Herrel et al. 2002, Sterli and de la Fuente 2010).

5.3. The homology of the basipterygoid process in Mesozoic turtles

Basal tetrapods and basal amniotes have no sutural relationship between their basicranium and the palatoquadrate region (Romer 1956). Instead, the basicranium articulates anteriorly with the pterygoid via the basipterygoid process of the basisphenoid (also termed the basitrabecular process) and posteriorly with the quadrate and the squamosal via the paroccipital process of the opisthotic.

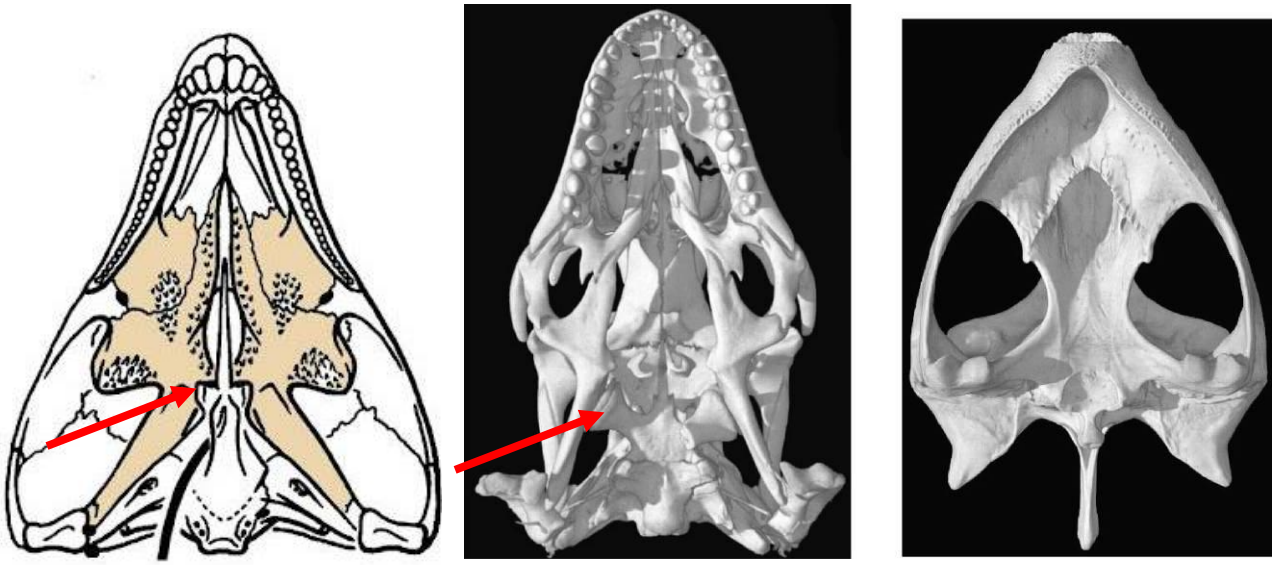

Figure 12. **The basipterygoid process of a Permian parareptile, *Captorhinus* sp. (after Heaton 1979), a recent squamate reptile (*Varanus exanthematicus*) and a cryptodiran (kinosternoid) turtle (*Staurotypus salvinii*; digimorph.org). The process is sent by the basisphenoid and serves as an articulation between the basicranium and the pterygoid.**

A basipterygoid process has been identified in a number of basal turtles and proto-turtles (Fig. 13, 16), including *Odontochelys semitestacea* (Li et al. 2008), *Proganochelys quenstedti* (Gaffney 1990), *Palaeochersis talampayensis* Rougier et al., 1995 (Sterli et al. 2007), *Australochelys africanus* Gaffney et al., 1994 (Gaffney et al. 1995), *Kayentachelys aprix* (Sterli and Joyce 2007, Gaffney and Jenkins 2010), *Heckerochelys romani* (Sukhanov 2006), and *Condorchelys antiqua* Sterli, 2008 (Sterli and de la Fuente 2010). Among this group of taxa, the more primitive ones, such as *O. semitestacea* and *Pr. quenstedti*, retain a movable basipterygoid articulation in the form of a ventrolaterally directed, blunt basipterygoid process that articulates with the corresponding facet in the pterygoid (Fig. 13). All more derived basal turtles with an unambiguous basipterygoid process are interpreted as having a fused articulation (Gaffney 1979a,c; Sukhanov 2006, Sterli and Joyce 2007, Sterli

and de la Fuente 2010, Sterli et al. 2010, Gaffney and Jenkins 2010) whereas all more advanced stem-testudine taxa and all crown turtles are universally considered to have lost their basipterygoid process completely (e.g., Gaffney 1979a,b). Some derived taxa have nevertheless been hypothesized to retain a reduced basipterygoid process, but the homology of this structure has been a controversial issue.

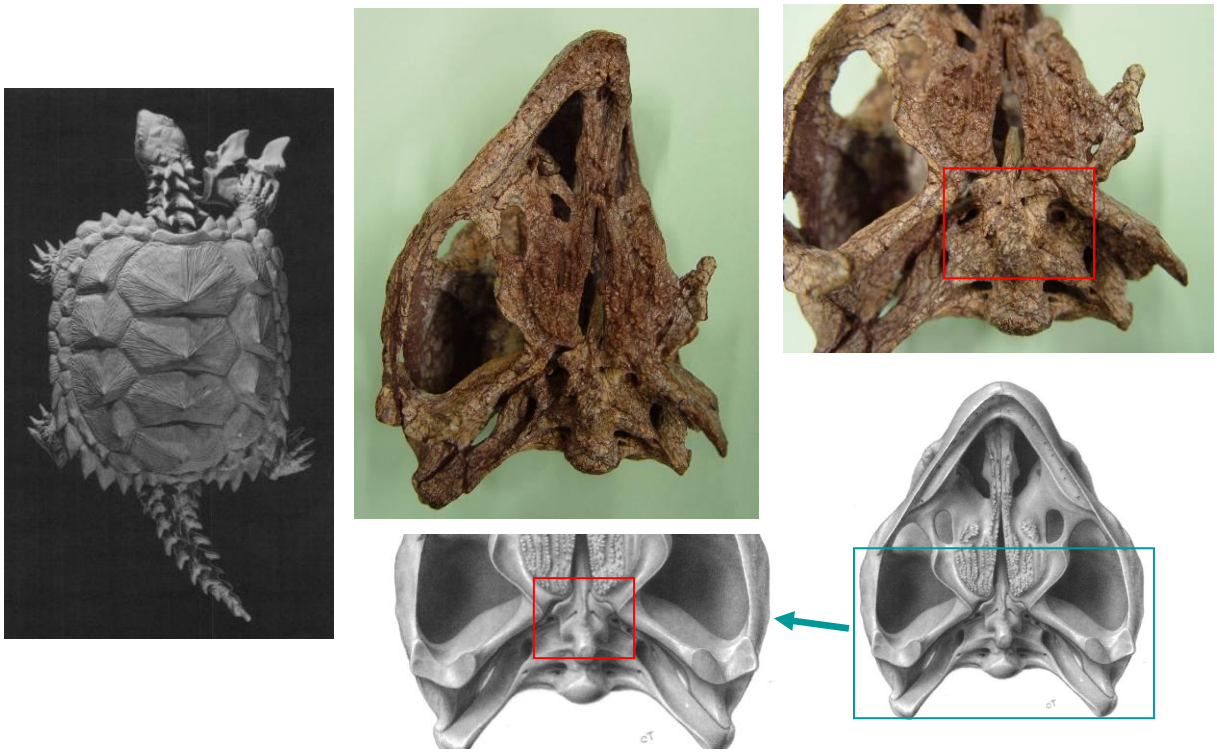

Figure 13. **The basipterygoid process in the Late Triassic stem-turtle, *Proganochelys quenstedti* (SMNS 16980). Reconstructions after Gaffney (1990).**

The presence of a basipterygoid process was first reported in the Late Jurassic turtle *Mesochelys durlstonensis* Evans and Kemp 1975 (Figs. 14, 17H), a taxon that was subsequently synonymized with *Pleurosternon bullockii* (Gaffney and Meylan 1988). A similar structure was noticed by Gaffney (1979b) in *Glyptops plicatulus* Cope 1877 (Fig. 15) and he concluded that it is not homologous with the unambiguous basipterygoid process of basal turtles based on topological considerations, a concept subsequently confirmed by Sterli et al. (2010). More recently, Brinkman et al. (2013a) identified a paired process of the basisphenoid similar to that seen in *Pleurosternon bullockii* (Figure 17H) in a broad selection of Jurassic and Early Cretaceous Asian eucryptodires and interpreted it as being homologous with the basipterygoid process of the earliest turtles, thereby contradicting the homology assessment of Gaffney (1979b) and Sterli et al. (2010).

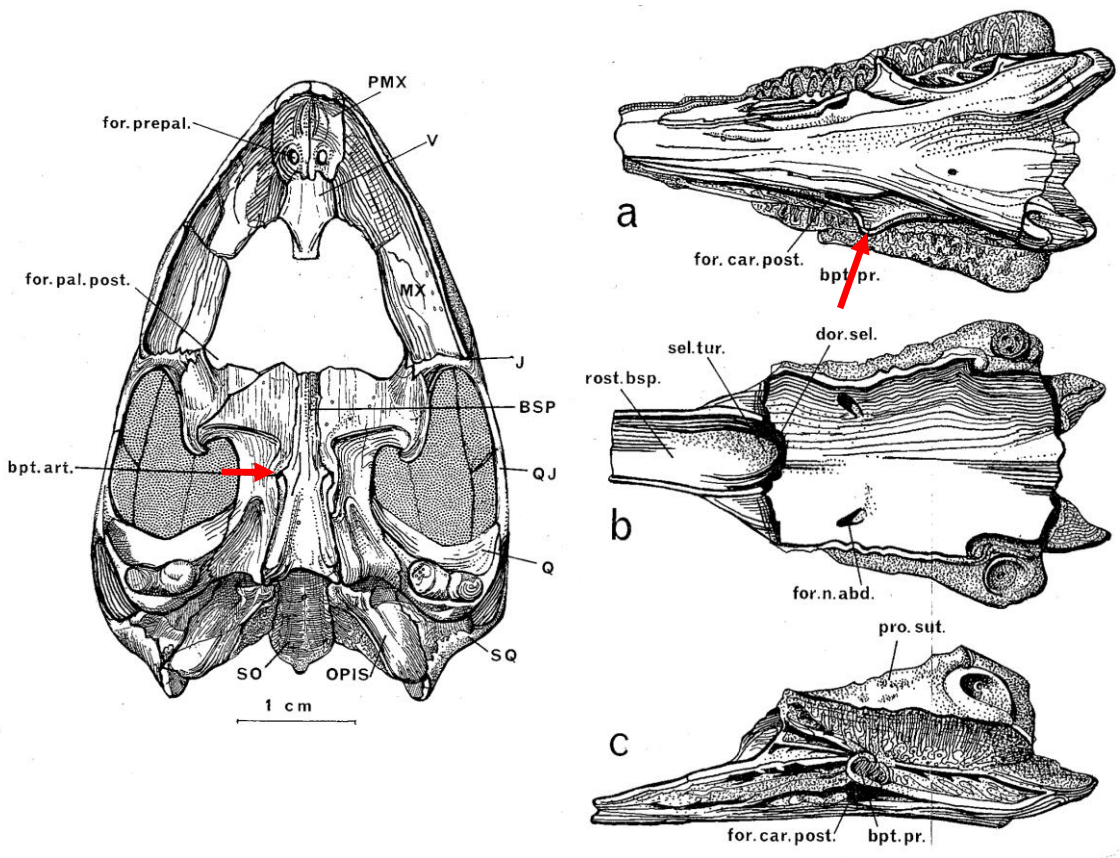

Figure 14. **The skull and basisphenoid of *Pleurosternon bullockii* showing the basipterygoid process (red arrow). After Evans and Kemp (1975). Abbreviations:** bpt. art., **basipterygoid articulation;** bpt. pr., **basipterygoid process;** BSP, **basisphenoid;** dor. sel., **dorsum sellae;** for. car. post., **foramen posterius canalis carotici cerebralis;** for. n. abd, **foramen nervi abducentis;** for. pal. post, **foramen palatinum posterius;** for. prepal., **foramen praepalatinum;** J, **jugal;** OPIS, **opisthotic;** PMX, **premaxilla;** Q, **quadrate;** QJ, **quadratojugal;** rost. bsp., **rostrum basisphenoid;** sel. tur., **sella turcica;** SO, **supraoccipital;** SQ, **squamosal;** V, **vomer.**

According to the homology concept of Gaffney (1979b) and Sterli et al. (2010), the paired lateral processes of the basisphenoid that fit into corresponding pockets in the pterygoids in *G. plicatulus* and *Pl. bullockii* cannot be interpreted as the basipterygoid process because: a) they are placed posterior to the dorsum sellae and therefore have different topological relationships compared to the true basipterygoid processes seen in captorhinomorphs (e.g., the purported basal amniote condition) and b) because the processes in question do not ascend, as in basal turtles, but are instead aligned in the same horizontal plane as the pterygoids. Indeed, the basipterygoid process of captorhinomorphs is situated anterior to the dorsum sellae, the foramen posterius canalis carotici cerebralis and the foramen nervi abducentis, whereas in *G. plicatulus* and *Pl. bullockii* the process in question is found posteriorly

to these structures (Fig. 15), note that the foramen posterius canalis carotici cerebralis is labeled foramen posterius canalis carotici interni). However, as already noted by others (Brinkman et al. 2013a) when the condition seen in *Pr. quenstedti* (Figure 13, 16A; unknown for Gaffney 1979b) is compared to that of captorhinomorphs, it is evident that the dorsum sellae is in a derived position similar to that seen in *G. plicatulus* and *Pl. bullockii* (Figs. 14-15, 17H) in that it extends more anteriorly over the foramen anterius canalis carotici cerebralis (see also Gaffney 1990, figures 42-44). This anterior movement of the dorsum sellae likely resulted in the anterior migration of the foramen nervi abducentis and the foramen posterius caroticus cerebralis (the latter being erroneously named the foramen posterius canalis carotici interni in previous studies (Evans and Kemp 1975, Gaffney 1990) for *G. plicatulus*, *Pl. bullockii*, and *Captorhinus* sp., as recently demonstrated (Sterli 2010, Müller et al. 2011). The apparent morphocline shows that the basipterygoid process of *Pr. quenstedti,* whose homology relative to captorhinomorphs had never been questioned (e.g., Gaffney 1990), is derived relative to the basal amniote condition (Fig. 15) and that it is in the same relative position as that seen in basal paracryptodires, except that in *G. plicatulus* and *Pl. bullockii* the cerebral foramen is positioned slightly more to the anterior (Figs. 14-15, 16H). In addition, there is no reason to consider the foramina of the carotid circulation system to be stable landmarks that cannot shift from their position during evolution: in *K. aprix* the cerebral foramen is positioned just posteriorly to the basipterygoid process (Fig. 16B) whereas in *H. romani* it is placed close to the anterior termination of the process (Figure 16C).

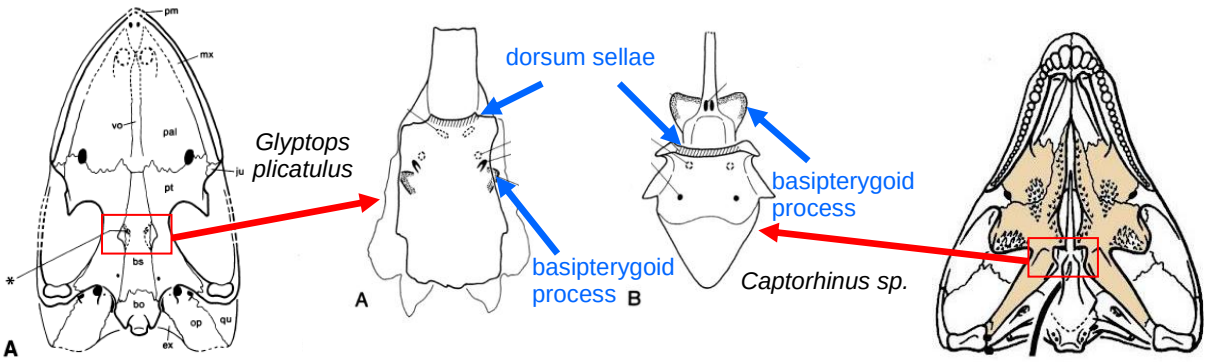

Figure 15. **Relative position of the basipterygoid process in the basisphenoid of *Glyptops plicatulus* (left) and *Captorhinus* sp. (right). After Gaffney (1979b) and Heaton (1979).**

Sterli et al. (2010) furthermore argued that the basisphenoid process of *G. plicatulus* and *Pl. bullockii* is not homologous with the basipterygoid process of basal amniotes, because it is directed laterally and found in the same plane as the pterygoid, unlike in *Pr. quenstedti*, where the basipterygoid process is directed ventrolaterally and situated ventral to the pterygoid. However, not all basal turtles have their basipterygoid process projecting ventrally. In *H. romani* the basipterygoid process is clearly present (Sukhanov 2006) but it projects laterally with a very minor ventral component and it is in the same plane as the pterygoid (Fig. 16C). Thus, this taxon demonstrates that there was a phase in the evolution of the basicranium when the basipterygoid articulation was already sutured and was in the same level as the rest of the palate. The morphology of the basipterygoid in *H. romani* is close to that of xinjiangchelyids and "sinemydids/macrobaenids" (Figs. 17A-E). A flat, triangular process projects laterally and slightly ventrally in these taxa to fit into the corresponding pit of the pterygoid in the same plane. There is no basis for interpreting this process as a neomorphic structure and given the identical topological position and the highly comparable shape the lateral basisphenoid process in basal paracryptodires (Figs. 14-15, 16H), xinjiangchelyids and "sinemydids/macrobaenids" can be confidently interpreted as being homologous with the basipterygoid process of basal turtles and basal amniotes.

5.3.1. Distribution of the basipterygoid process in Mesozoic turtles

Since the basipterygoid process is generally interpreted to be a primitive character absent in derived turtles, many published descriptions of Mesozoic turtle skulls fail to report and illustrate the basipterygoid process. This is especially true for various Jurassic and Early Cretaceous Asian forms (i.e., xinjiangchelyids, sinemydids, and macrobaenids, Figs. 17A-E). In addition to the taxa listed in a previous study (Brinkman et al. 2013a) a laterally facing basipterygoid process is further identified in *Kallokibotion bajazidi* (Fig. 16F), *Dracochelys bicuspis* (Fig. 17D), *Manchurochelys manchoukuoensis*, *Sinemys brevispinus* (as also reported elsewhere; Tong and Brinkman 2013), *Ordosemys leios*, *Xinjiangchelys levensis* (Fig. 17B), and *Xinjiangchelys latiens*, the alleged stem-adocusian *Basilochelys macrobios* (Fig. 17F) and the basal eucryptodire *Hoyasemys jimenezi*. In *Sandownia harrisi* the basipterygoid process is reduced and only visible in the floor of an opening formed by the pterygoids. A similar morphology may be present in the macrobaenid *Judithemys*

sukhanovi (Figure 17C) and *Macrobaena mongolica* and in the adocid *Adocus lineolatus* but the corresponding opening is so tight that the basipterygoid process (if any) is not visible. Consequently, I suggest scoring these taxa, including *S*. *harrisi*, as lacking the basipterygoid process, since the ventral surface of the basicranium lacks this structure. Various early marine turtles, including *Solnhofia parsonsi*, *Portlandemys mcdowelli*, *Plesiochelys etalloni*, and the early protostegid *Bouliachelys suteri* also lack basipterygoid processes. All other members of Testudines, including *Mongolemys elegans* lack a basipterygoid process as well.

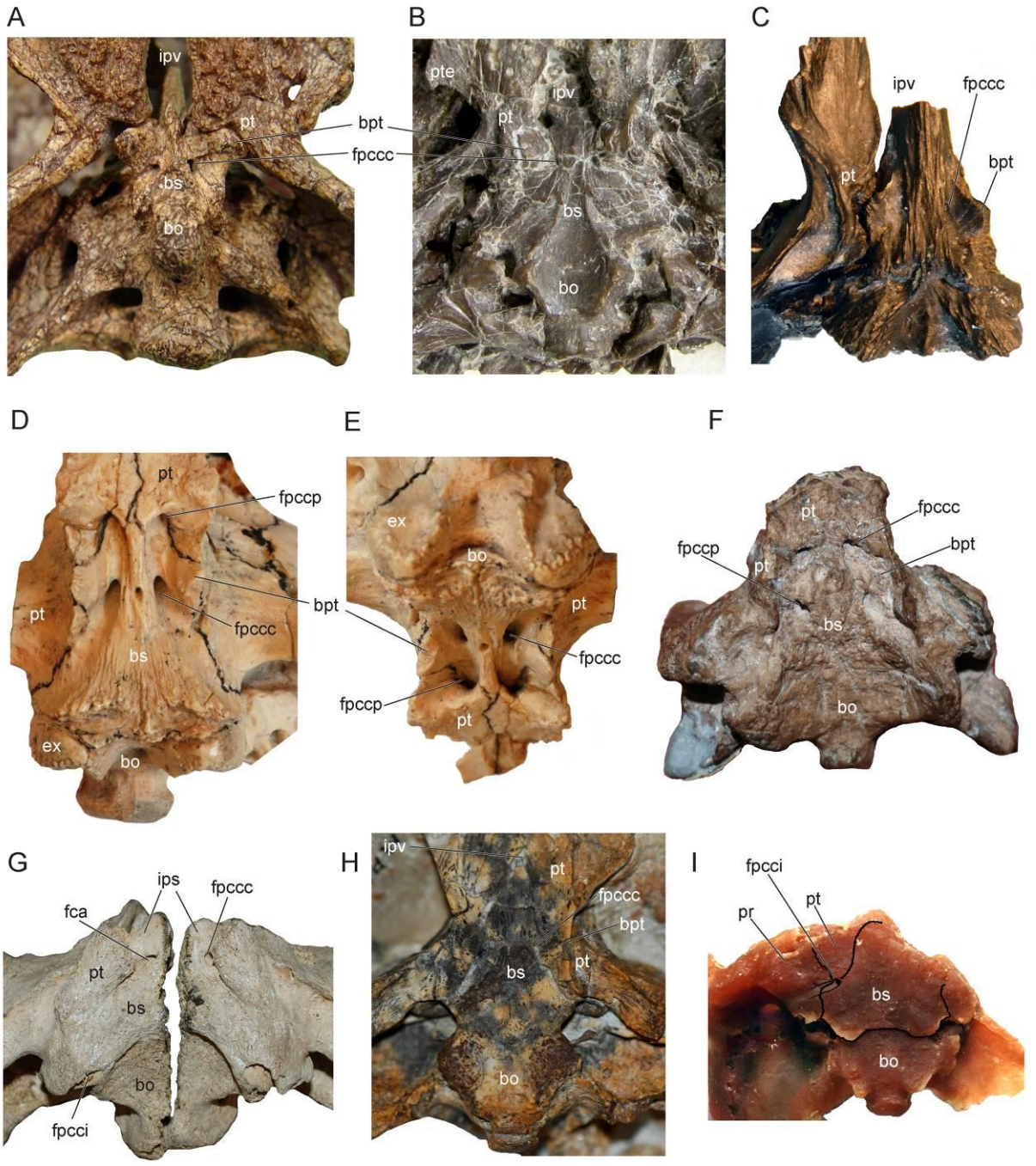

← Figure 16. **Braincase and palatoquadrate of select basal turtles and a pan-pleurodire showing the presence or absence of a basipterygoid process.** A, ***Proganochelys quenstedti*** **(SMNS 16980);** B, ***Kayentachelys aprix*** **(MCZ 8917);** C, ***Heckerochelys romani*** **(PIN 4561–2);** D-E, ***Mongolochelys efremovi*** **(PIN, uncatalogued) in ventral and oblique posterior view;** F, ***Kallokibotion bajazidi*** **(NHMUK R4925);** G, ***Meiolania platyceps*** **(NHMUK R682);** H, ***Chubutemys copelloi*** **(MPEF-PV1236);** I, ***Notoemys laticentralis*** **(cast of MOZP 2487). Abbreviations:** bo: **basioccipital,** bpt: **basipterygoid process,** bs: **basisphenoid,** ex: **exoccipital,** fca: **fenestra caroticus,** fpccc: **foramen posterius canalis carotici cerebralis,** fpcci: **foramen posterius canalis carotici interni,** fpccp: **foramen posterius canalis carotici palatinum,** ips: **intrapterygoid slit,** ipv: **interpterygoid vacuity,** pr: **prootic,** pt: **pterygoid,** pte: **processus pterygoideus externus.**

The basipterygoid process is present and ventrolaterally directed in several representatives of the Meiolaniformes, a recently recognized Mesozoic to Pleistocene clade of basal turtles (Sterli and de la Fuente 2013), including *Mongolochelys efremovi* (Fig. 16D-E) and *Chubutemys copelloi* (Figure 16H). Another putative member of this clade, *Kallokibotion bajazidi* (Figure 16F) also retains the downward facing basipterygoid process (contrary to a previous report, Gaffney and Meylan 1992). On the other hand, in *Meiolania platyceps* it is not the basisphenoid that extends ventrally to contact the pterygoid but rather it is the pterygoid that sends a process dorsally to contact the basisphenoid and to form the lateral wall of the intrapterygoid-slit (Gaffney 1983, figure 58). This is apparent since the suture between the basisphenoid and the pterygoid extends inside the fenestra caroticus, indicating that the basipterygoid process is lost (Fig. 16G). A similar morphology can be observed in the Eocene meiolaniid *Niolamia argentina* as well. In the solemydid *Helochelydra nopcsai* the basipterygoid process is clearly absent given the complete loss of basisphenoid exposure whereas the condition in *Naomichelys speciosa* is clearly more derived than in more basal turtles (e.g. *Kayentachelys aprix*, Fig. 16B) but a clear interpretation is difficult at the moment.

The oldest known panpleurodire skull is that of *Notoemys laticentralis* (Figure 16I) from the Late Jurassic of Argentina. The basisphenoid of this species shows a much reduced lateral protrusion just anterior to the foramen posterius canalis carotici interni (Fernandez and Fuente 1994, Lapparent de Broin et al. 2007). Since the split of the cerebral and palatine branches of the carotid artery is always situating ventral to the basipterygoid process in turtles known to retain this structure, I do not consider the protrusion of *Notoemys laticentralis* to be homologous with the basipterygoid process, given that it is situated dorsal to the split of the arterial branches, not ventral. The same rationale is applied for the interpretation of a lateral protrusion in the

basisphenoid of several chelids and in *Araripemys barretoi* Price 1973 (Gaffney 1977, Gaffney et al. 2006).

Given that this structure has been notoriously overlooked in many Mesozoic taxa, it is suggested that future workers should always explicitly note the presence or absence of the basipterygoid process while describing and/or scoring extinct turtles and also illustrate the basisphenoid accordingly. I suggest using the term “basipterygoid process” or “processus basipterygoideus” instead of “basitrabecular process” since the latter is less widely used in the fossil turtle literature. The term “fused basipterygoid articulation” (Gaffney 1979a) is not very precise since the basipterygoid process and the pterygoid are never fused per se, but rather connected by a suture.

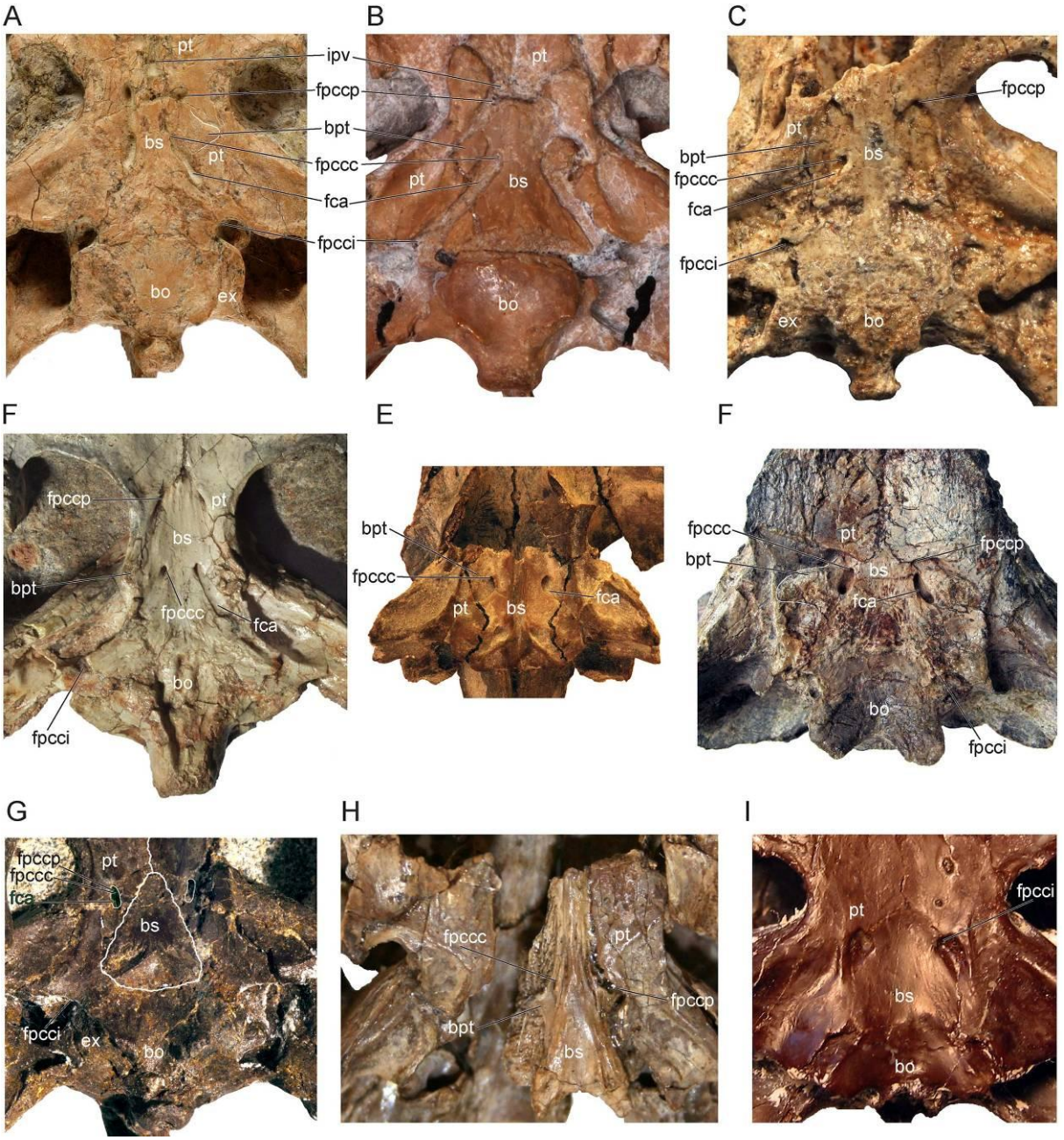

Figure 17. **Braincase and palatoquadrate of select Asian and North American Mesozoic turtles.** A, **"*Annemys*" sp. from Turpan Basin, Mesa Chelonia, (SGP 2009/18, see Wings et al. 2012);** B, ***Xinjiangchelys levensis* (PIN 4636-4-2);** C, ***Sinemys gamera* (IVPP V9532-11);** D, ***Dracochelys bicuspis* (IVPP V4075);** E, ***Hangaiemys hoburensis* (PIN 3334-36);** F, ***Basilochelys macrobios* (MD8-2);** G, ***Judithemys sukhanovi* (TMP 87.2.1);** H, ***Pleurosternon bullockii* (UMZC 1041);** I, ***Eubaena cephalica* (MRF 571). Abbreviations:** bo: **basioccipital,** bpt: **basipterygoid process,** bs: **basisphenoid,** ex: **exoccipital,** fca: **fenestra caroticus,** fpccc: **foramen posterius canalis carotici cerebralis,** fpcci: **foramen posterius canalis carotici interni,** fpccp: **foramen posterius canalis carotici palatinum,** ipv: **interpterygoid vacuity,** pt: **pterygoid.** ***Judithemys sukhanovi* (G) has a reduced fenestra caroticus (**fca, **highlighted in green). The** fpccp **and the** fpccc **in this species are situated close to one another inside the fenestra caroticus and are therefore not visible in ventral view.**

5.3.2. The evolution of the basipterygoid process in turtles

In the basal most known Triassic turtles and proto-turtles, such as *Proganochelys quenstedti* and *Odontochelys semitestacea*, the basipterygoid process is a robust and relatively thick structure that is directed ventrolaterally to articulate with a facet in the pterygoid. The pterygoid of these turtles is situated ventrally to the plane of the basisphenoid (Fig. 16A). In spite of the presence of a kinetic joint in these taxa, their skull was not kinetic in the sense of others Holliday and Witmer (2008). In more derived turtles, such as *Palaeochersis talampayensis* and *Australochelys africanus*, the basipterygoid process is still prominent and faces ventrolaterally, but the articulation with the ventrally positioned pterygoid is transformed into a sutural contact. The Early and Middle Jurassic turtles *Kayentachelys aprix* (Fig. 16B) and *Condorchelys antiqua* together with Cretaceous *Mongolochelys efremovi*, *Kallokibotion bajazidi* and *Chubutemys copelloi* (Figs. 16D-F,G) represent a more advanced phase in that the process is more reduced and compressed, but the basisphenoid is still situated dorsal to the pterygoid. The next phase is exemplified by *Heckerochelys romani* (Fig. 16C), and various members of Xinjiangchelyidae, Sinemydidae, and Macrobaenidae (Figs. 17A-E) where the process is compressed and mainly laterally oriented and the basisphenoid is aligned with the pterygoid.

According to the present phylogenetic hypothesis, the complete reduction and reorientation of the basipterygoid process happened independently in a number of turtle clades. The basipterygoid process was lost once within paracryptodires since basal members, such as *Glyptops plicatulus* and *Pleurosternon bullockii* (Figure 17H), still retain a process, whereas it is absent in *Compsemys victa* and all baenids (Figure 17I) (Lyson and Joyce 2009a,b, 2010, 2011). The basipterygoid process is furthermore lost in derived members of Meiolaniformes (i.e., *Niolamia argentina*, *Peligrochelys walshae* and *Meiolania platyceps*, Figure 16G). At least one more independent loss occurred within crown Testudines (i.e., along the stem of Pleurodira and Cryptodira) as indicated by the presence of the basipterygoid process in most xinjiangchelyids, sinemydids, and *Hangaiemys hoburensis*. Furthermore, the basal position of *Judithemys sukhanovi* implies an additional independent loss in this species (Fig. 17G).

Considering the more traditional phylogenetic hypotheses that place xinjiangchelyids on the stem of Cryptodira (e.g., Joyce 2007), these either infer two additional independent losses of the basipterygoid process (in Panpleurodires and

early marine turtles including *Solnhofia parsonsi*) or alternatively (and less likely) the basipterygoid process was reacquired in basal paracryptodires (pleurosternids), xinjiangchelyids and sinemydids (Figure 9). Since the current results themselves demonstrate that the loss of the basipterygoid process is quite homoplastic in turtles, two additional losses do not render considerably lower support for the traditional phylogenetic hypothesis (Joyce 2007) relative to the hypothesis presented here.

The reduction of the basipterygoid process in paracryptodires and crown-group Testudines was associated with the expansion of the parasphenoid ventral to the basisphenoid that eventually resulted in the complete enclosure of the arteries of the carotid circulation system in bone (Sterli et al 2010). In the case of Cryptodires the pterygoid was involved as well (Brinkman et al. 2013a, Gaffney 1979a). In all groups the synchronous loss of the basipterygoid process led to the final reinforcement of the basicranial region (Gaffney 1990, Sterli and de la Fuente 2008).

The multiple parallel losses of the basipterygoid process suggest that several clades of turtles gained an advantage by reinforcing the contact between the basicranium and the palatoquadrate. Interestingly, the loss of the basipterygoid process is often associated with another derived trait, the presence of a well-developed trochlear system. Many pancryptodires, including all crown-group members, and all pleurodires have an advanced jaw closure mechanism where the jaw adductor muscle is redirected by the otic trochlea in the former and the pterygoid trochlea in the latter, in both cases acting like a pulley system (Gaffney 1972). As already pointed out previously (Gaffney and Jenkins 2010, Joyce and Sterli 2012), many basal taxa do not possess, or do not clearly possess the advanced otic trochlear process found in most crown-group cryptodires. A review of taxa that retain a basipterygoid process, including basal turtles, most meiolaniforms, xinjiangchelyids, sinemydids, and macrobaenids reveals that these taxa possess poorly developed otic trochlea (if any) in form of a rugose surface or a low ridge that only barely protrudes anteriorly, unlike in taxa where the basipterygoid process is absent, including plesiochelyids, eurysternids, baenids, and most crown-group cryptodires, where the otic trochlea is robust and protrudes significantly (Fig. 18). The condition in pleurodires is also consistent with this correlation as they have an advanced trochlear process formed by the pterygoid and the basipterygoid process is absent even in the earliest known extinct species, *Notoemys laticentralis* (Figs. 16I, 18) (Lapparent de Broin et al. 2007).

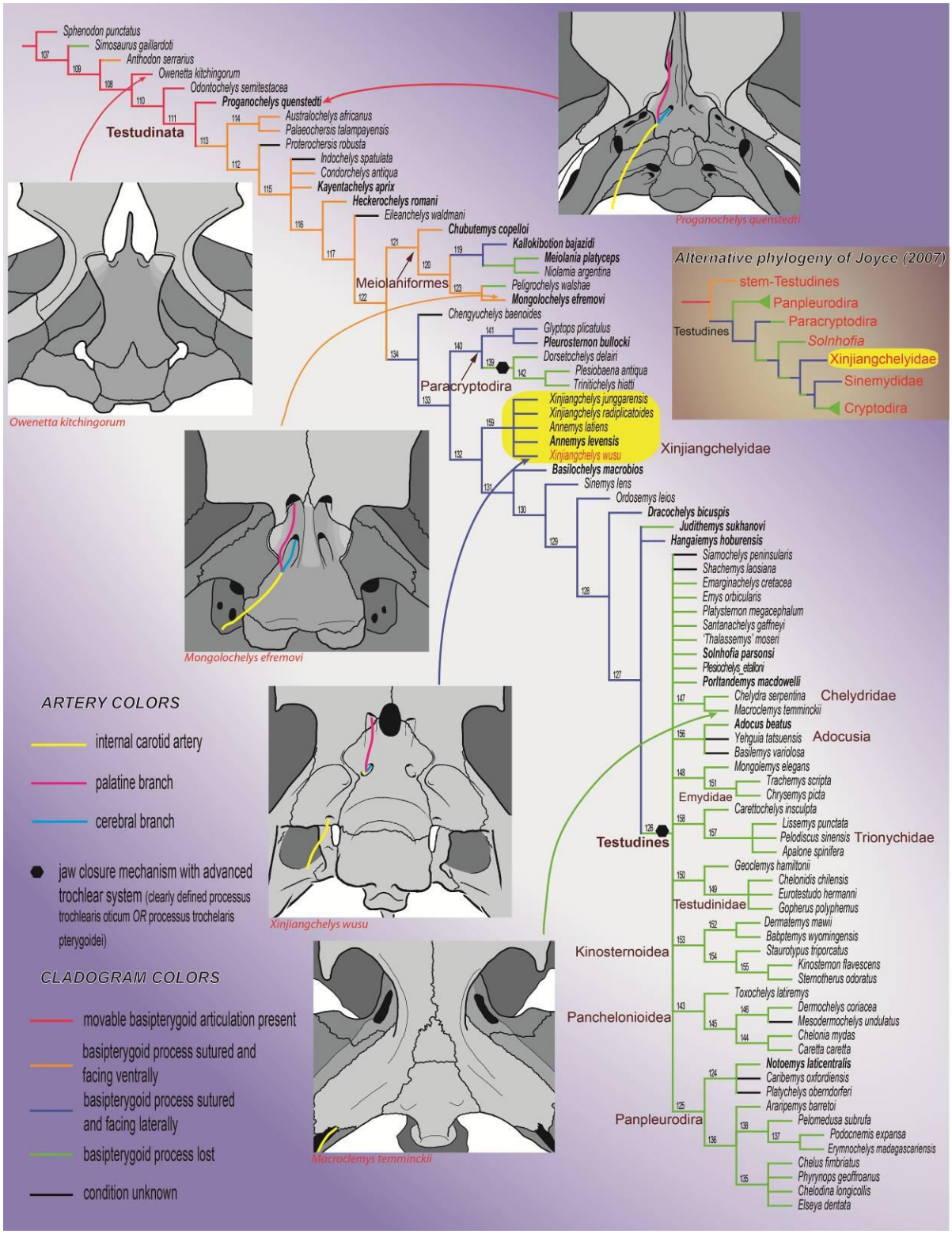

Figure 18. **Hypothetical relationships of the major clades of turtles and the evolution of the basipterygoid process and the carotid artery circulation system. The cladogram is the strict consensus tree of 9261 trees of 870 steps obtained after a parsimony analysis of 237 morphological characters and 84 extinct and extant turtle taxa. The relationships of Durocryptodira were constrained after the molecular phylogeny of Barley et al. (2010). Note the unorthodox position of Xinjiangchelyidae outside of Testudines. The more traditional phylogenetic placement of Xinjiangchelyidae is presented on the right for comparison. Numbers correspond to nodes.**

The loss of the basipterygoid process and the enclosure of the carotid circulation system in bone probably results in a reinforced connection between the basicranium and the palatoquadrate and therefore in a more rigid skull. As previous works pointed out (Gaffney 1979a, Sterli and de la Fuente 2010, Herrel et al. 2002) the development of advanced jaw closure mechanisms during turtle evolution likely required a more rigid skull that is compliant with higher bite performance and the loss of the basipterygoid process in association with the formation of an advanced trochlear system is therefore consistent with this pattern. In this regard the evolution of turtles parallels other amniote groups with rigid skulls including, therapsids, sauropterygians, and crocodyliformes which also lost their basipterygoid processes and enclosed the carotid system during the reinforcement of the basicranium (Romer 1956).

5.4. Phylogenetic Implications

None of the four phylogenetic analyses placed xinjiangchelyids, sinemydids, or other Cretaceous basal eucryptodires within Testudines, the crown-group of turtles. However, the relationships of Cretaceous forms vary among three of the analyses. All four analyses agree in that all Cretaceous taxa are consistently placed in a derived position relative to Xinjiangchelyidae.

Analysis A (220 equally parsimonious trees, tree length = 887): This analysis with no topological constraint and no new characters resulted in a largely paraphyletic arrangement of basal eucryptodires with a basally placed Sinemydidae that is only composed of *Sinemys* spp., an (*Ordosemys leios* + *Liaochelys jianchangensis*) clade and a successively more derived clade including *Judithemys sukhanovi*, *Kirgizemys hoburensis* and *Changmachelys bohlini* (the latter group roughly corresponds to the traditional circumscription of Macrobaenidae). *Manchurochelys manchoukuoensis* is found in the next less inclusive node to Sinemydidae. *Dracochelys bicuspis* occupies the most derived position among these taxa. The skull of *Ordosemys* sp. proved to be a wildcard taxon (Fig. 19).

Analysis B (136 equally parsimonious trees, tree length = 909): The constrained analysis obtained poor resolution for Cretaceous basal eucryptodires. However, a monophyletic Sinemydidae composed only of *Sinemys* spp. as well as a *Judithemys sukhanovi* – *Kirgizemys hoburensis* - *Changmachelys bohlini* clade was

again recovered. Removal of wildcard taxa, including *Ordosemys* sp. and *Basilochelys macrobios* does not improve resolution.

Analysis C (151 equally parsimonious trees, tree length = 925): Inclusion of new characters into the constrained analysis further decreases resolution. However, after pruning several Cretaceous taxa, a monophyletic Sinemydidae was obtained including *Sinemys* spp., *Manchurochelys manchoukuoensis*, and *Dracochelys bicuspis*. Removal of the constraint results in the basal placement of *M. manchoukuoensis* within Sinemydidae and in a (*Liaochelys jianchangensis* + *Ordosemys leios*) clade that in turn forms a polytomy with other Cretaceous basal eucryptodires (Additional file 3).

Analysis D (143 equally parsimonious trees, tree length = 819): When most pleurodires and *Basilochelys macrobios* are *a priori* excluded from the analysis a monophyletic Sinemydidae is recovered containing all Cretaceous forms. *Manchurochelys manchoukuoensis* is sister to a (*Dracochelys bicuspis* + *Sinemys* spp.) clade and combined they are sister to an (*Ordosemys leios* + *Liaochelys jianchangensis*) clade. *Judithemys sukhanovi* + *Kirgizemys hoburensis* are the most basal sinemydids in the context of this analysis. *Ordosemys* sp. and *Changmachelys bohlini* turned to be acting as wildcards and the inclusion of any of them sinks the *J. sukhanovi* + *K. hoburensis* clade into a polytomy. Another notable feature of these results that *Xinjiangchelys* (= *Annemys*) *levensis* is no longer recovered as a xinjiangchelyid but in the next less inclusive node to them (Figure 5). Exclusion of new characters does not influence tree topology but decrease bootstrap support for the *Sinemys* spp. clade by 47%. Other changes in support are insignificant. A search without constraints results in a basal polytomy of Cretaceous basal eucryptodires with *Manchurochelys manchoukuoensis* placed as sister to *Sinemys* spp. when most other Cretaceous target taxa are pruned.

5.4.1. Phylogenetic Relationships of Xinjiangchelyidae

The current analyses clearly recovered a monophyletic clade that partially recreates the “traditional” concept of Xinjiangchelyidae of some authors (e.g., Sukhanov 2000) and to which the phylogenetic definition of the name Xinjiangchelyidae applies. The position of Xinjiangchelyidae outside of Testudines is on the other side a rather unorthodox result (Fig. 18). Xinjiangchelyids are known to

possess several primitive characters, including the presence of nasals, amphicoelous cervical vertebrae, chevrons and dorsal process of epiplastron, yet previous analyses hypothesized a more derived position within Pancryptodira (Brinkman and Wu 1999; Joyce, 2007; Gaffney et al., 2007; Danilov and Parham, 2008; Tong et al., 2009; Anquetin, 2012; Tong et al., 2012b) or near the base of crown Testudines (Sterli, 2010; Sterli and de la Fuente 2011). The basal position in the present analysis is likely caused by numerous changes I undertook to the scoring of *Xinjiangchelys junggarensis*, *Siamochelys peninsularis*, and of *Annemys* from Shar Teg, which almost universally resulted in the recognition of primitive character states in these taxa (e.g. presence of interpterygoid vacuity, presence of basipterygoid process, open foramen jugulare posterius, long dorsal rib 1, position of the transverse process of the cervical in the middle of the centrum).

Two characters are responsible for the basal position of Xinjiangchelyidae in the current analyses. In contrast to the current analysis, the presence of a basipterygoid process was previously scored as unknown whereas the first dorsal rib was scored as short for *Xinjiangchelys junggarensis* (formerly *X*. *latimarginalis*), the only xinjiangchelyid in the original matrix (Sterli and de la Fuente 2013). However, as demonstrated above and in accordance with a recent study (Brinkman et al. 2013a), a basipterygoid process is present in the basicranium of *X*. *radiplicatoides*, *X*. *wusu*, *X. levensis* and *X*. *latiens*. The first dorsal rib of *X*. *junggarensis* was previously identified as short (reaching about half way to the axillary buttress; Peng and Brinkman 1993), but revision of the specimen in question (IVPP V9537-1) reveals that the rib was long. In fact, the rib is incompletely preserved, but the corresponding scar extends along the entire anterior edge of the second dorsal rib. A long first dorsal rib is furthermore present in *X. levensis* (unknown for *X*. *latiens* and *X*. *wusu*) and a long scar is described and figured for *X*. *radiplicatoides* (Brinkman et al 2013). I therefore scored *X*. *junggarensis*, *X*. *radiplicatoides* and *X*. *levensis* as having a long first dorsal rib.

It was previously unknown that the junction of the palatine and cerebral branches of the carotid artery was not floored in xinjiangchelyids (see also [59]), but this can not be responsible for their basal position since sinemydids had been scored with this primitive condition (Sterli and de la Fuente 2013), but were placed on the stem of crown Cryptodira.

On the other hand, I realized that the original matrix (Sterli and de la Fuente 2013) contains a good number of inconsistently scored characters and fixing these errors would likely alter the current results. A comprehensive revision and expansion of this matrix is therefore in progress as part of a larger scale project.

The results of my analyses are partially consistent with the only previous global analysis that included *Annemys levensis* (Anquetin, 2012), who scored this taxon on the basis of the preliminary reports of Sukhanov (2000) and Sukhanov and Narmandakh (2006). The analysis of Anquetin (2012) recovered Xinjiangchelyidae within Testudines and revealed that it consists of five taxa, including *Xinjiangchelys qiguensis*, *X. latimarginalis* sensu Peng and Brinkman, 1993 (= *X*. *junggarensis*), *X*. *tianshanensis*, *Annemys levensis*, and *Siamochelys peninsularis*. Although the present analyses differs in the position of Xinjiangchelyidae and *Siamochelys peninsularis*, this study agrees with Anquetin (2012) in that *A*. *levensis* and *X*. *junggarensis* (=*X*. *latimarginalis*) are members of the group in question.

5.4.2. Phylogenetic relationships of early marine turtles

Most previous analyses that included various Late Jurassic marine European taxa (e.g., *Plesiochelys solodurensis*, *Portlandemys mcdowelli*, "*Thalassemys*" *moseri* Bräm 1965 and the Early Cretaceous South American *Santanachelys gaffneyi* variously united them into clades and/or paraphyletic grades somewhere along the stem of crown Cryptodira in a more basal position than xinjiangchelyids (Hirayama et al. 2000, Gaffney et al. 2007, Joyce 2007, Tong et al. 2009, Sterli 2010, Sterli and de la Fuente 2011, Anquetin 2012). A recent exception is the analysis of Sterli and de la Fuente (2013) which found a (*Ples*. *solodurensis* + *Port*. *mcdowelli*) clade sister to Testudines and a (*Sol*. *parsonsi* (*Sant*. *gaffneyi* + "*T*." *moseri*)) clade in a polytomy with members of "sinemydids/macrobaenids" on the stem of Cryptodira. In the present analyses these taxa were found in an even more derived position as part of the crown group Testudines (Figure 18). One of the reasons for the more derived position of these taxa is likely the recognition of the basipterygoid process in xinjiangchelyids and "sinemydids/macrobaenids" that is clearly lost in all the European taxa and *Santanachelys gaffneyi*. Again, these results must be viewed with caution given the necessity of a comprehensive revision of the current matrix (see above).

5.4.2. Relationships and character evolution in Cretaceous basal eucryptodire turtles

A broad range of phylogenetic hypotheses of Cretaceous basal eucryptodires has been proposed over the course of the last decade. Some studies consider these turtles to be a predominantly monophyletic clade (Joyce 2007, Sterli 2008, 2010; Sterli and de la Fuente 2011) whereas others interpret them as being a predominantly paraphyletic assemblage (Zhou 2010a,b; Brinkman and Wu 1999, Gaffney et al. 2007, Danilov and Parham 2006, 2008; Vandermark et al. 2009). Two analyses (Sterli and de la Fuente 2013, Anquetin 2012) obtained a monophyletic Sinemydidae to the exclusion of *Judithemys sukhanovi* and *Kirgizemys hoburensis*. A more crown-ward position for *J. sukhanovi* and *K. hoburensis* has been suggested in other studies as well (Zhou 2010a,b; Parham and Hutchison 2003, Gaffney et al. 2007, Danilov and Parham 2008, Vandermark et al. 2009, Brinkman et al. 2013b). All of these analyses build either on Gaffney (1996) or Joyce (2007). The studies expanding the matrix of Gaffney (1996) are problematic in assuming monophyly for many higher groups of turtles and for using a small number of characters only (max. 45), but they have the advantage of including many Cretaceous basal eucryptodiran taxa. The matrices expanding the work of (Joyce 2007) are improved in using single species as terminals and a large number of characters, but they are limited in taxon sampling, as least for the group in question. Other downsides of all of these analyses are the dominantly literature-based character scorings and the lack of specific, phylogenetically relevant characters for sinemydids, macrobaenids, and closely allied taxa.

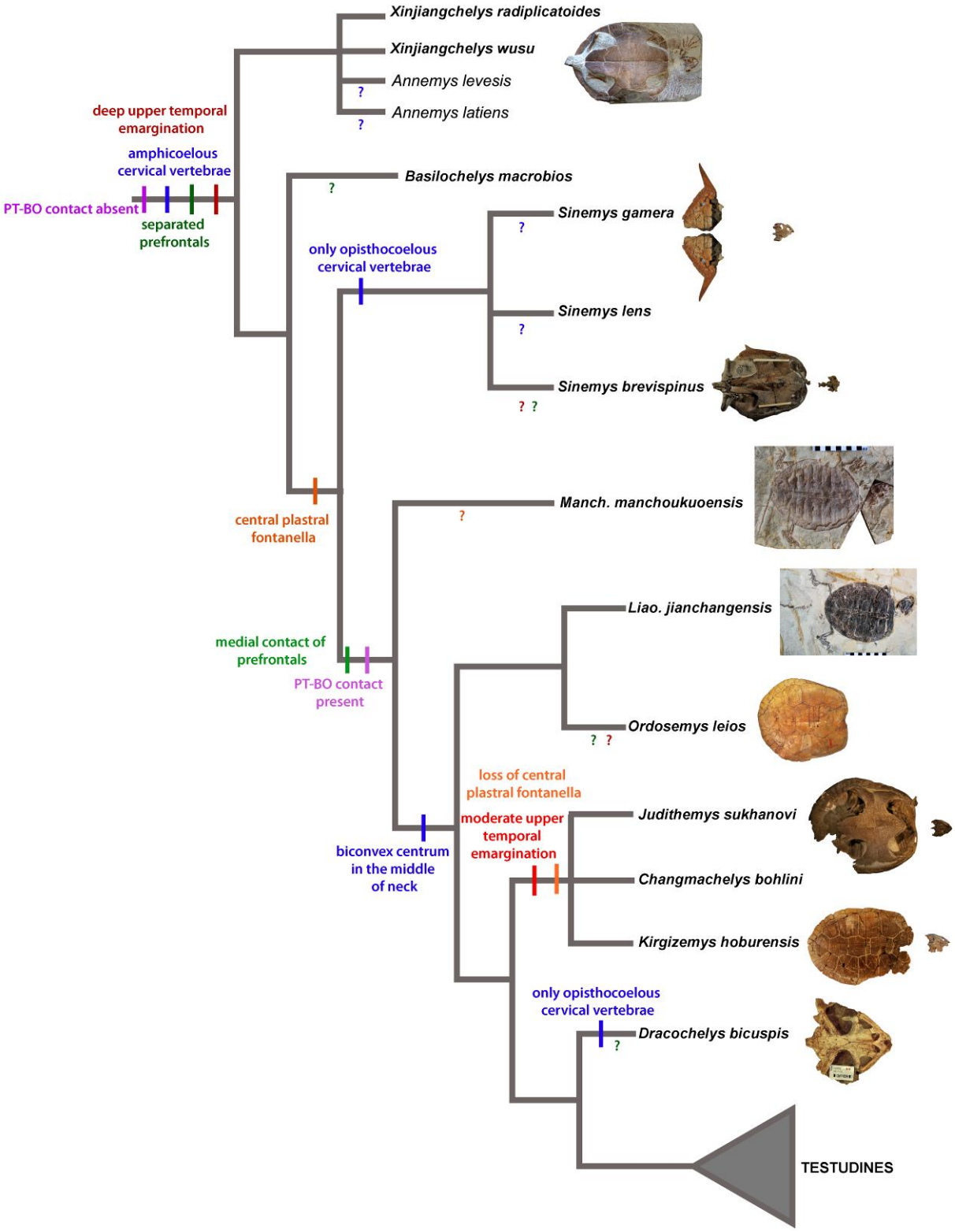

Figure 19. **Simplified strict consensus tree of Cretaceous basal eucryptodires retrieved from Analysis A (with no constraints and no new characters added) showing a paraphyletic arrangement for the taxa in question. The inferred evolution of selected characters varying among these taxa is shown on the tree. Ambiguous character states for a given taxon are indicated with '?' in a color that is corresponding to the color of that character.**

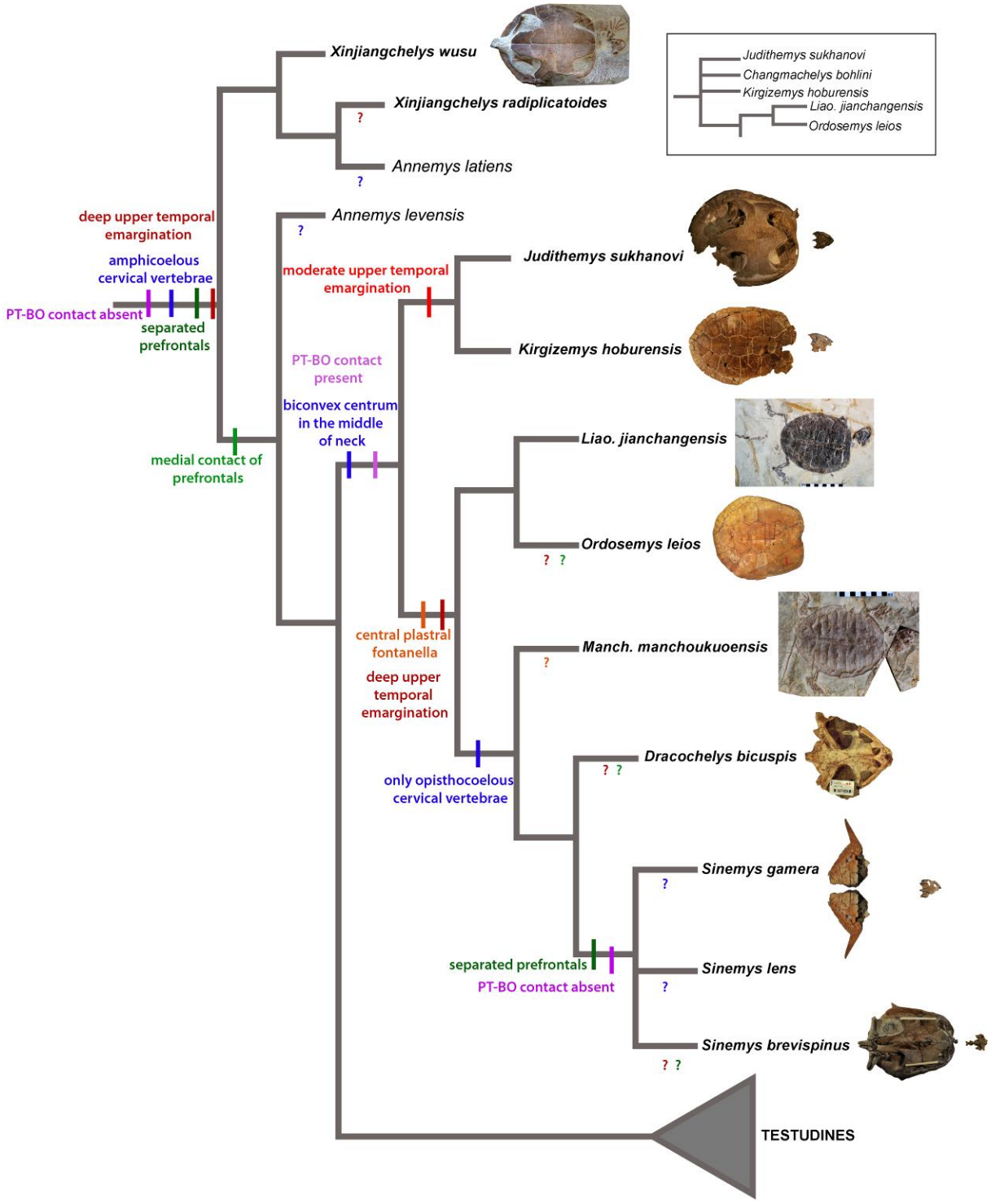

Figure 20. **Simplified strict consensus tree of Cretaceous basal eucryptodires retrieved from Analysis D. In this analysis most pan-pleurodires and *Basilochelys macrobios* was a priori removed, nine new characters were added and the relationships of cryptodires were constrained according to molecular phylogenetic results. The inferred evolution of selected characters varying among these taxa is shown on the tree. Ambiguous character states for a given taxon are indicated with '?' in a color that is corresponding to the color of that character. An alternative topology with *Changmachelys bohlini* not pruned from the strict consensus is shown in a box at the upper right corner.**

I sought progress relative to previous analysis by significantly expanding the sample of Cretaceous basal eucryptodires, by utilizing a large, global matrix, by correcting several errors that are apparent in the scorings of previous matrices, through the addition of new characters relevant to this group, and by directly studying all relevant specimens. Therefore, the present analyses are the most comprehensive and the most exhaustive attempt to resolve the phylogeny of Cretaceous basal eucryptodires to date.

The results of the unconstrained phylogenetic analysis (Analysis A, Fig. 19) agree in its primary aspects with the “paraphyletic hypothesis” of earlier global studies. However, the molecular backbone constraint of crown-cryptodire clades (Analysis B) collapses most of the nodes containing Cretaceous basal eucryptodires. Addition of new morphological characters places *Manchurochelys manchoukuoensis* and *Dracochelys bicuspis* within Sinemydidae together with *Sinemys* spp. while leaving other taxa largely unresolved. Interestingly, *a priori* exclusion of most panpleurodires and *Basilochelys macrobios* (Analysis D, Fig. 20), results in the monophyly of all Cretaceous basal eucryptodires.

The question remains unanswered whether the monophyletic or the paraphyletic hypothesis of basal eucryptodires is a better estimate of the phylogeny of sinemydid and macrobaenid turtles. From a parsimony point of view, the monophyletic arrangement is better supported since it requires five (or at least four, as two characters seem to be correlated) steps less than the paraphyletic topology as optimized within this part of the consensus trees of analysis A and D. However, most of these differences in the number of steps correspond either to the loss of traits, retention of juvenile characters (i.e. plastral fontanelles), or the acquisitions of highly variable and homoplastic characters (i.e. number of neurals). When only the acquisitions of more complex characters are taken into account, the differences are far less obvious and the monophyletic hypothesis appears to have less support. In this case, the monophyletic hypothesis requires a reversal to separated prefrontals (from medially contacting prefrontals) and the absence of pterygoid-basioccipital (and exoccipital) contact. On the other hand, the paraphyletic hypothesis requires that opisthocoely in the neck evolved twice within this group (Figs. 19-21).

There are some other noteworthy results of the present contribution. The Mongolian *Kirgizemys hoburensis* and the North American *Judithemys sukhanovi* form a clade in all of our analyses (in agreement with some previous works; Gaffney

et al. 2007, Danilov and Parham 2008, Anquetin 2012) and the Chinese *Changmachelys bohlini* is part of the same clade in three of the analyses, though their exact relationships are unresolved. In addition, *Liaochelys jianchangensis* is found as the sister taxon of *Ordosemys leios* in three of the analyses. A particular focus of this work, *Manchurochelys manchoukuoensis*, is placed within Sinemydidae together with *Sinemys* spp. and *Dracochelys bicuspis* in the majority of the analyses or alternatively, it is more derived than Sinemydidae and retained some typical characters of this group.

6. Conclusions

Xinjiangchelyid turtles have previously been known on the basis of shells, but new material from China together with the revised material from Mongolia provide new insights into the anatomy of the rest of the skeleton and greatly improve our knowledge of the plesiomorphic morphology of Cryptodira. Of particular interest is that xinjiangchelyids, together with sinemydids and macrobaenids, retained a generalized skull shape, a reduced basipterygoid process, a poorly developed otic trochlear system, and a relatively short supraoccipital process.

Mesozoic stem-cryptodires mostly lacked the morphological and ecological specializations of crown-cryptodires, instead they all seem to be mid-sized aquatic (freshwater) predators. However, some level of ecological diversification is apparent by the Late Jurassic, because three relatively distinct skull morphotypes are apparent at that time, including an analog to modern piscivorous turtles.

The study of the skulls of Asian stem-cryptodires demanded a review of the basicranial morphology of Mesozoic turtles, which revealed that the basipterygoid process has been overlooked in a broad range of extinct taxa. The repeated independent loss of the basipterygoid process together with the enclosure of the carotid circulation system in bone during turtle evolution argues for strong selective pressures towards reinforcing the basicranial region and developing a more rigid skull in association with an advanced trochlear system and an elongated supraoccipital process for a more forceful bite. The evolution of the turtle cranium parallels other amniote groups with rigid skulls, including therapsids, sauropterygians, and crocodyliformes in the loss of the basipterygoid processes and the enclosure of the carotid system during the reinforcement of the basicranium.

Testing the phylogenetic implications of these novel anatomical data in a global context resulted in the unorthodox basal placement of xinjiangchelyids, sinemydids, and macrobaenids. This topology needs further testing since it would infer unexpected reversals in Pan-Pleurodires, including the reacquisition of a “reduced” mesoplastron and the reorganization of the entry of the carotid artery into the skull among others and therefore a thorough revision of the matrix is of primary importance. I anticipate that these results will be adjusted by anatomical insights gained in the future. Nevertheless, this analysis raises the issue that certain widely

recognized Pan-Cryptodiran synapomorphies, including the complete flooring of the cranioquadrate space by the pterygoid and the presence of at least a poorly developed otic trochlea, might be symplesiomorphies of Testudines.

The question remains unanswered whether the monophyletic or the paraphyletic hypothesis of basal eucryptodires is a better estimate of the phylogeny of sinemydid and macrobaenid turtles. However, I here revealed that the instable position of panpleurodires in the turtle tree is primarily responsible for the ambiguous phylogeny of sinemydids and macrobaenids. Future work therefore should focus on the "pleurodire problem" to allow a better understanding of character evolution on the stem of Cryptodira.

Future Outlook

What is the best current estimate of crown-cryptodiran relationships? While this study failed to resolve the controversy between morphological and molecular hypotheses of turtle phylogeny, an unpublished phylogenetic hypothesis by the author, W.G Joyce, and J. Sterli has greater implications regarding this question. This new hypothesis is a result of an ambitious project that aimed to extensively expand on previous morphological datasets by increasing both taxon and character sample and by completely rescoring the matrix of Sterli and de la Fuente (2013). Under this hypothesis *Platysternon megacephalum* acts as a wild-card taxon and there is little morphological signal left to ally it with chelydrids. Geoemydids were found closer to testudinids than to emydids, in accordance with molecular studies (Shaffer et al. 1997, Krenz et al. 2005, Parham et al. 2006, Thomson and Shaffer 2010, Barley et al. 2010). Trionychoidea (Trionychia + Kinosternoidea) is still recovered but only with low statistical support. Chelonioid sea turtles remain basally placed and the position of chelydrids is instable. Therefore, the morphological results are beginning to converge upon the molecular studies and, remarkably, the persisting controversies involve those clades that proved to be the most problematic in molecular phylogenetic reconstruction: chelonioids, kinosternoids and chelydrids (Shaffer et al. 1997, Parham et al. 2006, Chandler and Janzen 2010, Thomson and Shaffer 2010, Barley et al. 2010). Molecular divergence dating analyses demonstrated the unusually rapid split and evolution of these clades (Joyce et al. 2013) therefore one

should not be surprised that their relationships can not be resolved using morphology, especially given that their fossil record is incomplete. Pantrionychians are likewise problematic because their initial evolution is only documented by a few fragmentary fossils (Danilov and Parham 2006) and their early split from the rest of the cryptodires in the Middle to Late Jurassic (Joyce et al. 2013) complicates the interpretation of their molecular signal as well (Sterli 2010). A close relationship of Trionychia with Kinosternoidea (as the morphology weakly suggests) is nevertheless unlikely given that the former is an Asian group with Jurassic origins whereas the latter diversified in North America during the late Early Cretaceous (Joyce et al. 2013).

A further notable advancement of the new project is the placement of sinemydids, macrobaenids, and xinjiangchelyids on the stem of Cryptodira in agreement with most previous works. Moreover, our new study confirms the recently questioned panchelonioid affinities of protostegid sea turtles (Joyce 2007 and all subsequently works building on it) and predates the divergence between extant hardshelled sea turtles (Cheloniidae) and leatherbacks (Dermochelyidae) by at least 30 million years relative to molecular clock estimates (Joyce et al. 2013) into the Albian.

The Late Jurassic to Early Cretaceous was a key period for rapid cryptodire diversification and this accelerated radiation, together with a discontinuous fossil record and high level of homoplasy obscure the relationships when morphology is used for phylogenetic reconstruction.

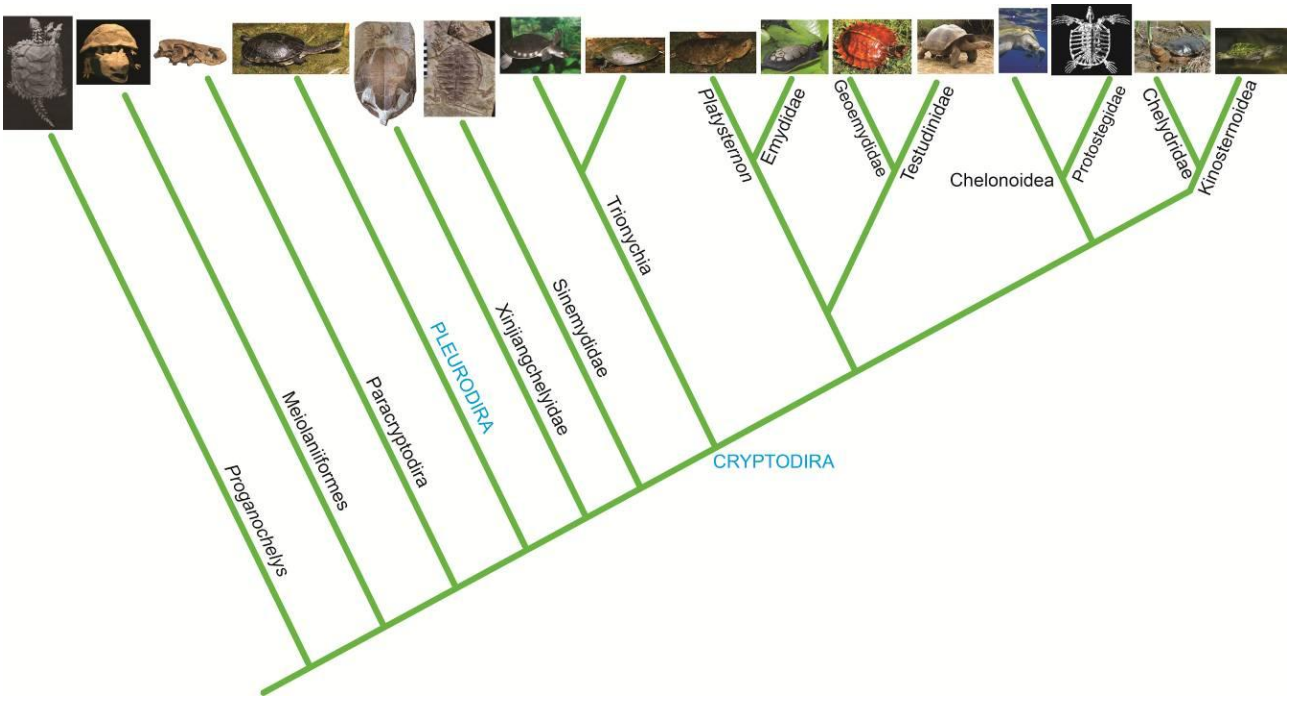

Figure 22. **Preferred phylogenetic hypothesis of turtles based on an unpublished cladogram by the author and his co-workers. The relationships of cryptodires were constrained after the molecular phylogeny of Barley et al. (2010). Image source: Gaffney (1990), Wieland (1909), wikipedia.org, and own photographs.**

Acknowledgements

First of all I thank my supervisor, Walter G. Joyce, for the opportunity to work on amazing fossil turtles in numerous places in the world and for sharing all his knowledge, trying to answer all my questions (and I had a lot of them), supporting me, and for always treating me as a colleague.

My other supervisors, Prof. Hervé Bocherens and András Galácz encouraged me with all my plans and gave very useful instructions in cases when I needed professional insights.

I am grateful to my wonderful fossil turtle colleagues for exciting and highly inspiring discussions and valuable suggestions: Juliana Sterli, Chang-Fu Zhou, Haiyan Tong, Julien Claude, Peter C. Pritchard, Igor Danilov, Ingmar Werneburg, Benjamin Kear, Tyler Lyson, Mátyás Vremir, Joe Corsini, Vladimir Sukhanov, Elena Syromyatnikova, Adán Pérez-García, Torsten Scheyer, Jeremy Anquetin, James Parham, Donald Brinkman, Marcello de la Fuente, Evangelos Vlachos, and Sandra Chapman. Other colleagues in vertebrate paleontology furthermore had a great influence on me: Attila Ősi, Massimo Delfino, Zoltán Csiki, Oliver Wings, Ursula

Göhlich, Edina Prondvai, László Makádi, Gábor Botfalvai, Miklós Kázmér, Ágnes Görög, Jeremy Martin, Eric Buffetaut, Davit Vasylian, Diego Pol, Paul Barrett, and Madelaine Böhme, among others.

The following people kindly provided access to fossil specimens under their care: Vladimir Sukhanov (PIN), Xu Xing, Liu Jun, Corwin Sullivan (IVPP), Bert Sliggers and Wouter Meyboom (TM), Sandra Chapman (NHMUK), Chang-Fu Zhou (PMOL), Eduardo Ruigómez (MPEF), and Rainer Schoch (SMNS).

I would particularly like to thank Juliana Sterli for her valuable assistance with the TNT software. The Willi Hennig Society is thanked for providing free access to the program TNT. The 2009 field season in Xinjiang was funded by a grant to Hans-Ulrich Pfretzschner (PF 219/21) of the Deutsche Forschungsgemeinschaft (DFG). The 2011 field season, was funded by a DFG grant to Walter G. Joyce (JO 928/2). Prof. Sun Ge (PMOL) is particularly thanked for organizing the fieldwork in China. This project was also funded by SYNTHESYS grant GB-TAF-1882 to M. Rabi. The University of Tübingen funded the open access publication of two of the papers resulting from this thesis. My research was also funded by the Eötvös Loránd University, the Hungarian Academy of Science and the University of Fribourg.

I am very grateful to the staff of the Department of Paleontology at the Eötvös Loránd University where it all started as well as the members of the Brocherens lab in Tübingen where I finished my PhD. Christoph Wissing and Davit Vasylian are particularly thanked for making the Tübingen years memorable, inspiring, and functioning.

This thesis would have never been produced without the encouragement, trust support and advice of my family and I am incredibly grateful to them.

Finally, I thank Emese Kövesdi, my wife, without even trying to express in words what her support, patience, and advices mean to me. To my greatest recognition, she also proved to be an excellent partner in countless discussions on turtle evolution during the years.

References

Ameghino F (1899) Sinopsis geológica-paleontológica. Suplemento (adiciones y correcciones). La Plata, Julio de 1899, 1-13.

Anquetin J (2012) Reassessment of the phylogenetic interrelationships of basal turtles (Testudinata). J Syst Palaeontol 10: 3-45.

Anquetin J, Barrett PM, Jones MEH, Moore-Fay S, Evans S (2009) A new stem turtle from the Middle Jurassic of Scotland: new insights into the evolution and palaeoecology of basal turtles. Proc R Soc B 276: 879-886.

Bardet N, Jalil N-E, Lapparent de Broin F, Germain D, Lambert O, Amaghzaz M (2013) A giant chelonioid turtle from the Late Cretaceous of Morocco with a suction feeding apparatus unique among tetrapods. Plos One 8(7): 1-10.

Barley AJ, Spinks PQ, Thomson RC, Shaffer HB (2010) Fourteen nuclear genes provide phylogenetic resolution for difficult nodes in the turtle tree of life. Mol Phylogenet Evol 55: 1189-1194.

Batsch, AJGC (1788) Versuch einer Anleitung, zur Kenntniß und Geschichte der Thiere und Mineralien. Jena: Akademische Buchhandlung. 528 p.

Baur G (1887) Osteologische Notizen über Reptilien (Fortsetzung II). Zool Anz 10: 241-268.

Benton M.J, Zhonghe Z, Orr PJ, Fucheng Z, Kearns SL (2008) The remarkable fossils from the Early Cretaceous Jehol Biota of China and how they have changed our knowledge of Mesozoic life: Presidential Address, delivered 2nd May 2008. Proceedings of the Geologists' Association, 119(3): 209-228.

Brinkman DB (2001) New material of *Dracochelys* (Eucryptodira: Sinemydidae) from the Junggar Basin, Xinjiang, People's Republic of China. Can J Earth Sci 38:1645-1651.

Brinkman DB, Peng J-H (1993a) New material of *Sinemys* (Testudines, Sinemydidae) from the Early Cretaceous of China. Can J Earth Sci 30: 2139-2152.

Brinkman DB, Peng J-H (1993b) *Ordosemys leios*, n.gen., n.sp., a new turtle from the Early Cretaceous of the Ordos Basin, Inner Mongolia. Can J Earth Sci 30: 2128-2138.

Brinkman DB, Wu X-C (1999) The skull of *Ordosemys*, an Early Cretaceous turtle from Inner Mongolia, People's Republic of China, and the interrelationships of Eucryptodira (Chelonia, Cryptodira). Paludicola 2: 134-147.

Brinkman DB, Eberth D, Clark J, Xing X, Wu XC (2013a) Turtles from the Jurassic Shishugou Formation of the Junggar Basin, People's Republic of China, and the basicranial region of basal eucryptodires. In: Brinkman DB, Gardner JD, Holroyd PA, editors. Morphology and Evolution of Turtles. Dordrecht: Springer. pp. 147-172.

Brinkman DB, Hart M, Jamniczky H, Colbert M (2006) *Nichollsemys baieri* gen. et sp. nov, a primitive chelonioid turtle from the Late Campanian of North America. Plaudicola 5(4): 111-124.

Brinkman DB, Li J-L, Ye X-K (2008) Order Testudines. In: Li J-L, Wu X-C, Zhang F-C, editors. The Chinese Fossil Reptiles and Their Kin. Beijing: Science Press. pp. 35-102.

Brinkman DB, Yuan C-X, Ji Q, Li D-Q, You H-L (2013b) A new turtle from the Xiagou Formation (Early Cretaceous) of Changma Basin, Gansu Province, P. R. China. Palaeobio Palaeoenv 93: 367-382.

Cattoi N, Freiberg MA (1961) Nuevo hallazgo de Chelonia extinguidos en la Republica Argentina. Physis 22: 202.

Chandler CH, Janzen FJ (2009) The phylogenetic position of the snapping turtles (Chelydridae) based on nucleotide sequence data. Copeia 2: 209-213.

Chang SC, Zhang H, Renne PR, Fang Y (2009) High-precision 40Ar/39Ar age for the Jehol Biota. Palaeogeogr Palaeoclimatol Palaeoecol 280: 94-104.

Chang SC, Zhang H, Hemming SR, Mesko GT and Fang Y (2012) Chronological evidence for extension of the Jehol Biota into southern China. Palaeogeogr. Palaeoclimatol. Palaeoecol. 344: 1-5.

Chkhikvadze VM (1975) [Volume and systematic position of turtles of the suborder Amphichelydia Lydekker, 1899]. Soobscheniya AN Gruzinskoy SSRR 78: 745-748. [Russian]

Chkhikvadze VM (1977) Fossil turtles of the family Sinemydidae [In Russian] Izvestiya AN Gruzinskoy SSR. Seriya Biologicheskaya 3: 265-270.

Chkhikvadze VM (1987) Sur la classification et les charactéres de certaines tortues fossiles d'Asie, rares et peu etudiees. Studia Geologica Salmaticensia, Studia Palaeocheloniologica 2: 55-85.

Cope ED (1873) [Description of *Toxochelys latiremis*]. Proc Acad Nat Sci Philadelphia 1873: 10.

Cope ED (1874) [Description of *Adocus lineolatus*] Bull US Geol and Geogr Surv Terrs 1(2): 30.

Cope ED (1877) On reptilian remains from the Dakota beds of Colorado. Proc Amer Phil Soc 17: 193-196.

Claude J, Paradis E, Tong H, Auffray J-C (2003) A geometric morphometric assessment of the effects of environment and cladogenesis on the evolution of the turtle shell. Biol J Linn Soc 79(3): 485-501.

Claude J, Pritchard PCH, Tong H, Paradis H, Auffray J-C (2004) Ecological correlates and evolutionary divergence in the skull of turtles: a geometric morphometric assessment. Syst Biol 53(6): 933-948.

Danilov IG, Parham JF (2006) A redescription of '*Plesiochelys tatsuensis'* from the Late Jurassic of China, with comments on the antiquity of the crown clade Cryptodira. J Vertebr Paleontol 26: 573-580

Danilov IG, Parham JF (2007) The type series of '*Sinemys*' *wuerhoensis*, a problematic turtle from the Lower Cretaceous of China, includes at least three taxa. Palaeontology 50: 431-444.

Danilov IG, Parham JF (2008) A reassessment of some poorly known turtles from the Middle Jurassic of China, with comments on the antiquity of extant turtles. J Vertebr Paleontol 28: 306-318.

Danilov IG, Sukhanov VB (2006) A basal eucryptodiran turtle "*Sinemys*" *efremovi* (= Wuguia efremovi) from the Early Cretaceous of China. Acta Paleontol Pol 51:105-110.

Danilov IG, Averianov AO, Skutchas PP, Rezvyi AS (2006) *Kirgizemys* (Testudines, Macrobaenidae): new material from the Lower Cretaceous of Buryatia (Russia) and taxonomic revision. Fossil Turtle Res 1: 46-62.

Dong Z-M (1992) Dinosaurian faunas of China. Beijing: China Ocean Press. 188 p.

Dong Z-M (1997) Vertebrates of the Turpan Basin, the Xinjiang Uygur Autonomous Region, China. In: Dong Z-M, editor. Sino-Japanese Silk Road Dinosaur Expedition. Beijing: China Ocean Press. pp. 96-101.

Eberth DA, Brinkman DB, Chen P, Yuan F, Wu S, Li G, Cheng X (2001) Sequence stratigraphy, paleoclimate patterns, and vertebrate fossil preservations in Jurassic-Cretaceous strata of the Junggar Basin, Xinjiang autonomous region, People's Republic of China. Can J Earth Sci 38: 1627-1644.

Endo R, Shikama T (1942) Mesozoic reptilian fauna in the Jehol mountainland, Manchoukuo. Bull Centr Nat Mus Manchoukuo 3: 1-19.

Ernst CH, Barbour RW (1989) Turtles of the World. Smithsonian Inst. Press, Washington, D. C. 313 pp.

Evans J, Kemp TS (1975) The cranial morphology of a new Lower Cretaceous turtle from southern England. Palaeontol 18: 25-40.

Fang QR (1987) A new species of Middle Jurassic turtle from Sichuan. Acta Herpetol Sin 6: 65-9.

Fernandez MS, de la Fuente M (1994) Redescription and phylogenetic position of Notoemys: the oldest Gondwanian pleurodiran turtle. N Jb Geol und Paläont Abh 193: 81-105.

Fujita MK, Engstrom TN, Starkey DE, Shaffer HB (2004) Turtle phylogeny: Insights from a novel nuclear intron. Mol Phylogenet Evol 31: 1031-1040.

Gaffney ES (1972) An illustrated glossary of turtle skull nomenclature. Am Mus Novit 2486: 1-33.

Gaffney ES (1975a) *Solnhofia parsonsi*, a new cryptodiran turtle from the Late Jurassic of Europe. Am Mus Novit 2576: 1-25.

Gaffney ES (1975b) A phylogeny and classification of the higher categories of turtles. Bull Am Mus Nat Hist 155: 389-436.

Gaffney ES (1975c) A taxonomic revision of the Jurassic turtles *Portlandemys* and Plesiochelys. Am Mus Novit 2574: 1-19.

Gaffney ES (1977) The side-necked turtle family Chelidae: a theory of relationships using shared derived characters. Am Mus Novit 2620: 1-28.

Gaffney ES (1979a) Comparative cranial morphology of Recent and fossil turtles. Bull Am Mus Nat Hist 164: 69-376.

Gaffney ES (1979b) The Jurassic turtles of North America. Bull Am Mus Nat Hist 162: 91-136.

Gaffney ES (1983) The cranial morphology of the extinct horned turtle *Meiolania platyceps*, from the Pleistocene of Lord Howe Island, Australia. Bull Am Mus Nat Hist 175: 361-480.

Gaffney ES (1990) The comparative osteology of the Triassic turtle *Proganochelys*. Bull Am Mus Nat Hist 194: 1-263.

Gaffney ES (1996) The postcranial morphology of *Meiolania platyceps* and a review of the Meiolaniidae. Bull Am Mus Nat Hist 229:1-165.

Gaffney ES, Jenkins FA Jr (2010) The cranial morphology of *Kayentachelys*, an Early Jurassic cryptodire, and the early history of turtles. Acta Zool-Stockholm 91: 335-368.

Gaffney ES, Kitching JW (1994) The most ancient African turtle. Nature 369: 55-58.

Gaffney ES, Kitching JW (1995) The morphology and relationships of *Australochelys*, an Early Jurassic turtle from South Africa. Am Mus Novit 3130: 1-29.

Gaffney ES, Meylan PA (1988) A phylogeny of turtles. In: Benton MJ, editor. The Phylogeny and Classification of the Tetrapods, Vol. 1, Amphibians, Reptiles, Birds. Systematics Association Special Volume 35A: 157-219.

Gaffney ES, Meylan PA (1992) The Transylvanian turtle *Kallokibotion*, a primitive cryptodire of Cretaceous age. Am Mus Novit 3040: 1-37.

Gaffney ES, Ye X (1992) *Dracochelys*, a new cryptodiran turtle from the Early Cretaceous of China. Am Mus Novit 3048: 1-13.

Gaffney ES, Hutchison JH, Jenkins FA Jr, Meeker, LJ (1987) Modern turtle origins: the oldest known cryptodire. Science 237: 289-291.

Gaffney ES, Kool L, Brinkman DB, Rich TH, Vickers-Rich P (1998) *Otwayemys*, a new cryptodiran turtle from the Early Cretaceous of Australia. Am Mus Novit 3233: 1-28.

Gaffney ES, Rich TH, Vickers-Rich P, Constantine A, Vacca R, Kool L (2007) Chubutemys, a new eucryptodiran turtle from the Early Cretaceous of Argentina, and the relationships of Meiolaniidae. Am Mus Novit 3599: 1-35.

Gaffney ES, Tong H, Meylan PA (2006) Evolution of the side-necked turtles: The families Bothremydidae, Euraxemydidae, and Araripemydidae. Bull Am Mus Nat Hist 300: 1-698.

Goloboff PA, Farris J, Nixon K (2008a) TNT: tree search using new technology, vers. 1.1 (Willy Hennig Society Edition). Program and documentation available at http://www.zmuc.dk/public/phylogeny/tnt.

Goloboff PA, Mattoni CI, Quinteros AS (2008b) TNT, a free program for phylogenetic analysis. Cladistics 24: 774-786.

Gray JE (1831) Synopsis Reptilium, Part 1: Tortoises, Crocodiles and Enaliosaurians. London. 85 pp.

Gubin YM, Sinitza SM (1996) Shar Teg: a unique Mesozoic locality of Asia. Museum of Northern Arizona Bulletin 60: 311-318.

Hay OP (1908) The fossil turtles of North America. Pub Carnegie Inst Washington, 75: 1-568.

Hendrix MS, Graham SA, Carroll AR, Sobel ER, McKnight CL, Schulein BJ, Wang Z (1992) Sedimentary record and climatic implications of recurrent deformation in the Tian Shan; evidence from Mesozoic strata of the north Tarim, south Junggar, and Turpan basins, Northwest China. Geol Soc Am Bull 104: 53-79.

Herrel AJ, O'Reilly C, Richmond AM (2002) Evolution of bite performance in turtles. J Evolution Biol 15: 1083-1094.

Hirayama R, Brinkman DB, Danilov IG (2000) Distribution and biogeography of non-marine Cretaceous turtles. Russ J Herpetol 7: 181-198.

Holliday CM, Witmer LM (2008) Cranial kinesis in dinosaurs: intracranial joints, protractor muscles and their significance for cranial evolution and function in diapsids. J Vertebr Paleontol 28: 1073-1088.

Hutchison, JH, Archibald JD (1986) Diversity of turtles across the Cretaceous/Tertiary Boundary in northeastern Montana. Palaeogeogr. Palaeoclimatol. Palaeoecol. 55: 1-22.

Hutchison JH, Bramble DM (1981) Homology of the plastral scales of the Kinosternidae and related turtles. Herpetologica, 73-85.

Ji S-A (1995) Reptiles. In Fauna and Stratigraphy of Jurassic-Cretaceous in Beijing and the Adjacent Areas. Edited by Ren D, Lu L-W, Guo Z-G, Ji S-A. Beijing: Seismic Press; 140-146.

Joyce WG (2007) Phylogenetic relationships of Mesozoic turtles. Bull Peabody Mus Nat Hist 48: 3-102.

Joyce WG, Bell CJ (2004) A review of the comparative morphology of extant testudinoid turtles (Reptilia: Testudines). Asiat Herpetol Res 10: 53-109.

Joyce WG, Gauthier JA (2004) Paleoecology of Triassic stem turtles sheds new light on turtle origins. Proc R Soc B 271: 1-5.

Joyce WG, Sterli J (2012) Congruence, non-homology, and the phylogeny of basal turtles. Acta Zool-Stockholm 93: 149-159.

Joyce WG, Parham JF, Gauthier JA (2004) Developing a protocol for the conversion of rank -based taxon names to phylogenetically defined clade names, as exemplified by turtles. J Paleontol 78: 989-1013.

Joyce WG, Parham JF, Lyson TR, Warnock RCM, Donoghue PCJ (2013) Fossil calibrations for molecular rate studies of turtle evolution: an example of best practice. J Paleontol 87: 612-634.

Kaznyshkin MN, Nalbandyan LA, Nessov LA (1990) Middle and Late Jurassic turtles of Fergana (Kirghiz SSR) [in Russian]. Yezhegodnik Vsesoyuznogo Paleontologicheskogo Obshchestva (Annu All-union Palaeontol Soc) 33: 185-204.

Kear BP, Lee MSY (2006) A primitive protostegid from Australia and early sea turtle evolution. Biol Lett 2: 116-119.

Khosatzky LI (1996) New turtle from the Early Cretaceous of Central Asia. Russ J Herpetol 3: 89-94.

Khozatsky LI (1997) Large turtles from the Late Cretaceous of Mongolia. Russ J Herpetol 4: 148-154.

Khosatzky LI, Młynarski M (1971) Chelonians from the Upper Cretaceous of Gobi Desert, Mongolia. Palaeontol Pol 25: 131-144.

Khosatzky LI, Nessov LA (1979) [Large turtles of the Late Cretaceous of Middle Asia]. Trudy Zoologicheskogo Instituta AN SSSR 89: 98-108. [Russian].

Klein IT (1760) Klassification und kurze Geschichte der vierfüßigen Thiere (translated by F. D. Behn). Lübeck: Jonas Schmidt.

Krenz JG, Naylor GJP, Shaffer HB, Janzen FJ (2005) Molecular phylogenetics and evolution of turtles. Mol Phylogenet Evol 37: 178-191.

Lapparent de Broin F, Murelega X (1999) Turtles from the Upper Cretaceous of Laño (Iberian peninsula). Estud Mus Cienc Nat Alava 14: 135-211.

Lapparent de Broin F, de la Fuente MS, Fernandez MS (2007) *Notoemys laticentralis* (Chelonii, Pleurodira), Late Jurassic of Argentina: new examination of the anatomical structures and comparisons. Rev Paléobiol 26: 99-136.

Li C, Wu X-C, Rieppel O, Wang L-T, Zhao J (2008) Ancestral turtle from the Late Triassic of southwestern China. Nature 456: 497-501.

Liu LY, Di SX (1997) Characteristics of Middle Jurassic sedimentation and reservoir pore evolution in Turpan Depression [in Chinese with English abstract]. Oil Gas Geol 3: 247-260.

Lourenço JM, Claude J, Galtier N, Chiari Y (2012) Dating cryptodiran nodes: Origin and diversification of the turtle superfamily Testudinoidea. Mol Phylogenet Evol 62: 496-07.

Lydekker RA (1889) On remains of Eocene and Mesozoic Chelonia and a tooth of (?) Ornithopsis. J Geol Soc London 45: 227-246.

Lyson TR, Joyce WG (2009) A new species of *Palatobaena* (Testudines: Baenidae) and a maximum parsimony and Bayesian phylogenetic analysis of Baenidae. J Paleontol 83: 457-470.

Lyson TR, Joyce WG (2009) A revision of *Plesiobaena* (Testudines: Baenidae) and an assessment of baenid ecology across the K/T boundary. J Paleontol 83: 833-853.

Lyson TR, Joyce WG (2010) A new baenid turtle from the Late Cretaceous (Maastrichtian) Hell Creek Formation of North Dakota and a preliminary taxonomic revision of Cretaceous Baenidae. J Vert Paleontol 30: 394-402.

Lyson TR, Joyce WG (2011) Cranial anatomy and phylogenetic placement of the enigmatic turtle *Compsemys victa*. J Paleontol 85: 789-801.

Maisch M, Matzke A, Sun G (2003) A new sinemydid turtle (Reptilia: Testudines) from the Lower Cretaceous of the Junggar Basin (NW-China). N Jb Geol Paläont, Mh 12: 705-722.

Matzke AT, Maisch MW, Sun G, Pfretzschner H-U, Stöhr H (2004a) A new xinjiangchelyid turtle (Testudines, Eucryptodira) from the Jurassic Qigu Formation of the southern Jungar Basin, Xinjiang, North-West China. Palaeontology 47: 1267-1299.

Matzke AT, Maisch MW, Pfretzschner H-U, Ge S, Stöhr H (2004b) A new basal sinemydid turtle (Reptilia: Testudines) from the Lower Cretaceous Tugulu Group of the Junggar Basin (NW China). N Jb Geol Paläont, Mh 2004: 151-167

Matzke AT, Maisch MW, Sun G, Pfretzschner HU, Stöhr H (2005) A new Middle Jurassic xinjiangchelyid turtle (Testudines; Eucryptodira) from China (Xinjiang, Junggar Basin). J Vert Paleontol 25: 63-70.

Meylan PA (1987) The phylogenetic relationships of soft-shelled turtles (Family Trionychidae). Bull Am Mus Nat Hist 186: 1-101.

Meylan PA (1996) Skeletal morphology and relationships of the Early Cretaceous side-necked turtle, *Araripemys barretoi* (Testudines:Pelomedusoides: Araripemydidae), from the Santana Formation of Brazil. J Vertebr Paleontol 16: 20-33.

Meylan PA, Gaffney ES (1989) The skeletal morphology of the Cretaceous cryptodiran turtle *Adocus*, and the relationships of the Trionychoidea. Am Mus Nov 2941: 1-60.

Meylan PA, Moody RTJ, Walker CA, Chapman SD (2000) *Sandownia harrisi*, a highly derived trionychoid turtle (Testudines: Cryptodira) from the Early Cretaceous of the Isle of Wight, England. J Vert Paleontol 20: 522-532.

Moen DS (2006) Cope's rule in cryptodiran turtles: do the body sizes of extant species reflect a trend of phyletic size increase? J Evol Biol 19 (4) 1210-1221.

Müller J, Sterli J, Anquetin J (2011) Carotid circulation in amniotes and its implications for turtle relationships. N Jb Geol Paläont Abh 261: 289-297.

Near TJ, Meylan PA, Shaffer HB (2005) Assessing concordance of fossil calibration points in molecular clock studies: an example using turtles. Am Nat 165(2): 137-146.

Nessov LA (1984) Data on late Mesozoic turtles from the USSR. Studia Geologica Salmaticensia. Stud Palaeocheloniol 1:215-223.

Nessov LA (1995) On some Mesozoic turtles of the Fergana Depression (Kyrgyzstan) and Dzhungar Alatau Ridge (Kazakhstan). Russian Journal of Herpetology 2: 134-141.

Nessov LA, Khosatzky LI (1973) Early Cretaceous turtles from southeastern Fergana (in Russian). In Problems in herpetology: Proc 3rd All-union Herpetological Conf. Zoological Institute of the Academy of Sciences USSR, Leningrad: 132-133.

Nessov LA, Khosatzky LI (1981) [Turtles of the Early Cretaceous of Transbaikalia]; pp. 74-78 in L. J. Borkin (ed.), [Herpetological Investigations in Siberia and the Far East]. Academy of Sciences of the USSR, Leningrad. [Russian]

Nopcsa F (1923) On the geological importance of the primitive reptilian fauna of the uppermost Cretaceous; with a description of a new tortoise (Kallokibotion). J Geol Soc London 79: 100-116.

Owen R (1842) Report on British fossil reptiles. Part II. Rep Brit Assoc Adv Sci 11: 60-204.

Owen R (1886) Description of some fossil remains of two species of a Megalanian genus (Meiolania) from “Lord Howe’s Island”. Philos T Roy Soc B 179: 181-191.

Parham JF, Hutchison JH (2003) A new eucryptodiran turtle from the Late Cretaceous of North America (Dinosaur Provincial Park, Alberta, Canada). J Vertebr Paleontol 23: 783-798.

Parham JF, Pyenson ND (2010) New sea turtle from the Miocene of Peru and the iterative evolution of feeding ecomorphologies since the Cretaceous. J Paleontol 84(2): 231-247.

Parham JF, Feldman CR, Boore JL (2006) The complete mitochondrial genome of the enigmatic bigheaded turtle (*Platysternon*): description of unusual genomic

features and the reconciliation of phylogenetic hypotheses based on mitochondrial and nuclear DNA. BMC Evol Biol 6(1): 1-11.

Peng GY, Ye Y, Gao CS, Jiang S (2005) Jurassic Dinosaur Faunas in Zigong. Zigong: Zigong Dinosaur Museum. 236 p. [in Chinese with English translation]

Peng J-H, Brinkman DB (1993) New material of *Xinjiangchelys* (Reptilia: Testudines) from the Late Jurassic Qigu Formation (Shishugou Group) of the Pingfengshan locality, Junggar Basin, Xinjiang. Can J Earth Sci 30: 2013-2026.

Pérez-García A, de la Fuente MS, Ortega F. 2012. A new freshwater basal eucryptodiran turtle from the Early Cretaceous of Spain. Acta Paleontol Pol 57:285-298.

Pictet FJ, Humbert A (1857) Description d'une emyde nouvelle (*Emys etalloni*) du terrain jurassique supérieur des environs de Saint-Claude. Mat Paléontol Suisse 1: 1-10.

Price LI (1973) Quelônio Amphichelydia no Cretáceo Inferior do Nordeste do Brasil. Rev Brasil Geociênc 3: 84-95.

Rabi M, Joyce WG, Wings O (2010) A review of the Mesozoic turtles of the Junggar Basin (Xinjiang, Northwest China) and the paleobiogeography of Jurassic to Early Cretaceous Asian Testudinates. Paleobiodiv. Paleoenv. 90: 259-273.

Romer AS (1956) Osteology of Reptiles. Chicago: University of Chicago Press. 772 p.

Rougier GW, de la Fuente MS, Arcucci AB (1995) Late Triassic turtles from South America. Science 268: 855-858.

Ryabinin AN (1948) [Turtles from the Jurassic of Kara-Tau]. Trudy Paleontologiicheskogo Instituta AN SSSR 15: 94-98. [Russian]

Schumacher GH (1973) The head muscles and hyolaryngeal skeleton of turtles and crocodilians; pp. 101-199 in C. Gans and T. Parsons (eds.), Biology of the Reptilia, Volume 4. Academic Press, London and New York.

Shaffer HB, Meylan PA, McKnight ML (1997) Tests of turtle phylogeny: molecular, morphological, and paleontological approaches. Syst Biol 46: 235–268.

Shao L, Stattegger K, Li W, Haupt BJ (1999) Depositional style and subsidence history of the Turpan Basin (NW China). Sed Geol 128:155-169.

Sinitshenkova ND (1995) New Late Mesozoic stoneflies from Shar Teg, Mongolia (Insecta: Perlida = Plecoptera). Paleontological Journal 29: 93-104.

Sinitshenkova ND (2002) New Late Mesozoic mayflies from the Shar Teg locality, Mongolia (Insecta, Ephemerida = Ephemeroptera). Paleontological Journal 36: 43-48.

Sterli J (2008) A new, nearly complete stem turtle from the Jurassic of South America with implications for turtle evolution. Biol Lett 4: 286-289.

Sterli J (2010) Phylogenetic relationships among extinct and extant turtles: the position of Pleurodira and the effects of the fossils on rooting crown-group turtles. Contrib Zool 79: 93-106.

Sterli J, de la Fuente MS, Rougier GW (2007) Anatomy and relationships of *Palaeochersis talampayensis*, a Late Triassic turtle from Argentina. Palaeontogr Abt A 281:1-61.

Sterli J, de la Fuente MS (2013) New evidence from the Palaeocene of Patagonia (Argentina) on the evolution and palaeobiogeography of meiolaniid-like turtles (Testudinata) J Syst Paleontol 11: 835-852.

Sterli J, Joyce WG (2007) The cranial anatomy of the Early Jurassic turtle *Kayentachelys aprix*. Acta Palaeontol Pol 52: 675-694.

Sterli J, MS de la Fuente (2010) Anatomy of *Condorchelys antiqua* Sterli, 2008, and the origin of the modern jaw closure mechanism in turtles. J Vertebr Paleontol 30: 351-366.

Sterli J, MS de la Fuente (2011) A new turtle from the La Colonia Formation (Campanian – Maastrichtian), Patagonia, Argentina, with remarks on the evolution of the vertebral column in turtles. Paleontology 54: 63-78.

Sterli J, Müller J, Anquetin J, Hilger A (2010) The parabasisphenoid complex in Mesozoic turtles and the evolution of the testudinate basicranium. Can J Earth Sci 47: 1337-1346.

Sterli J, Pol D, Laurin M (2013) Incorporating phylogenetic uncertainty on phylogeny-based palaeontological dating and the timing of turtle diversification. Cladistics 29: 233-246.

Sukhanov VB (1964) Subclass Testudinata, Testudinates (In Russian). In Fundamentals of Palaeontology Amphibians, Reptiles and Birds. Edited by Orlov JA. Moscow: Nauka; pp. 354-438.

Sukhanov VB (2000) Mesozoic turtles of Middle and Central Asia. In: Benton MJ, Shishkin MA, Unwin DM, Kurochkin, EN, editors. The Age of Dinosaurs in Russia and Mongolia. Cambridge: Cambridge University Press. pp. 309-367.

Sukhanov VB (2006) An archaic turtle, *Heckerochelys romani* gen. et sp. nov., from the Middle Jurassic of Moscow region, Russia. In: Danilov IG, Parham JF, editors. Fossil Turtle Research, Volume 1. St. Petersburg: Zoological Institute, Russian Academy of Sciences. pp. 112-118.

Sukhanov VB, Narmandakh P (1974) [A New Early Cretaceous turtle from the continental deposits of the Northern Gobi]. Trans Joint Soviet-Mongolian Paleontol Exped 1: 192-220. [in Russian]

Sukhanov VB, Narmandakh P (2006) New taxa of Mesozoic turtles from Mongolia. In: Danilov IG, Parham JF, editors. Fossil Turtle Research Volume 1. St. Petersburg: Zoological Institute, Russian Academy of Sciences. pp. 119-127.

Tatarinov LP (1959) [A new turtle of the family Baenidae from the Lower Eocene of Mongolia]. Paleontologicheskiy Zhurnal 1: 100-113. [in Russian]

Tong H, Brinkman D (2013) A new species of *Sinemys* (Testudines: Cryptodira: Sinemydidae) from the Early Cretaceous of Inner Mongolia, China. Palaeobiodiversity and Palaeoenvironments. 93: 355-366.

Tong H, Buffetaut E, Suteethorn V (2002) Middle Jurassic turtles from southern Thailand. Geol Mag 139: 687-697.

Tong H, Claude J, Naksri W, Suteethorn V, Buffetaut E, Khansubha S, Wongko K, Yuangdetkla P (2009) *Basilochelys macrobios* n. gen. and n. sp., a large cryptodiran turtle from the Phu Kradung Formation (latest Jurassic–earliest Cretaceous) of the Khorat Plateau, NE Thailand. Geol Soc London Spec Pub 315: 153-173.

Tong H, Danilov IG, Ye Y, Ouyang H, Peng G (2012a) Middle Jurassic turtles from Sichuan Basin, China: a review. Geol Mag 149: 675-695.

Tong H, Danilov IG, Ye Y, Ouyang H, Peng G, Li K (2012b) A revision of xinjiangchelyid turtles from the Late Jurassic of Sichuan Basin, China. Ann Paleontol 98: 73-114.

Tong H, Ji S-A, Ji Q (2004) *Ordosemys* (Testudines: Cryptodira) from the Yixian Formation of Liaoning Province, northeastern China: new specimens and systematic revision. Am Mus Novit 3438: 1-20.

Turtle Taxonomy Work Group [van Dijk PP, Iverson JB, Shaffer HB, Bour R, Rhodin AGJ] (2012) Turtles of the world, 2012 Update: annotated checklist of taxonomy, synonymy, distribution, and conservation status. In: Rhodin AGJ, Pritchard PCH, van Dijk PP, Saumure RA, Buhlmann KA, Iverson JB, Mittermeier RA (Eds.) Conservation biology of freshwater turtles and tortoises: a compilation project of the IUCN/SSC Tortoise and Freshwater Turtle Specialist Group. Chelonian Research Monographs 5: 243-328.

Vandermark D, Tarduno JA, Brinkman DB, Cottrell RD, Mason S (2009) New Late Cretaceous macrobaenid turtle with Asian affinities from the High Canadian Arctic: dispersal via ice-free polar routes. Geology 37: 183-186.

Wang SE, Gao LZ (2012) SHRIMP U-Pb dating of zircons from tuff of Jurassic Qigu Formation in Junggar Basin, Xinjiang. Geol Bull China 31: 503-509.

Watabe M, Tsogtbaatar K, Uranbileg L, Gereltsetseg L (2004) Report on the Japan-Mongolia Joint Paleontological Expedition to the Gobi desert (2002). Hayashibara Museum of Natural Sciences Research Bulletin 2: 97-122.

Wieland GR (1900) The skull, pelvis, and probable relations hips of the huge turtles of the genus *Archelon* from the Fort Pierre Cretaceous of South Dakota. Am J Sci 4(9): 237-251.

Wieland GR (1909) Revision of the Protostegidae. Am J Sci 4(158): 101-109.

Wiman C (1930) Fossile Schildkröten aus China. Paleontol Sin C 6: 1-56.

Wings O, Rabi M, Schneider JW, Schwermann L, Sun G, Zhou C-F, Joyce WG (2012) An enormous Jurassic turtle bone bed from the Turpan Basin of Xinjiang, China. Naturwissenschaften 99: 925-935.

Wings O, Schellhorn R, Mallison H, Thuy B, Sun G (2007) The first dinosaur tracksite from Xinjiang, NW China (Middle Jurassic Sanjianfang Formation, Turpan Basin)—a preliminary report. Global Geol 10: 113-129.

Ye X (1963) Fossil turtles of China. Palaeontol Sin 150: 1-112.

Ye X (1966) A new Cretaceous turtle of Nanhsiung, northern Kwangtung. Vert PalAsiat 10: 191-200.

Ye X (1982) Middle Jurassic turtles from Sichuan, SW China. Vert PalAsiat 20: 282-290.

Ye X (1986) A Jurassic turtle from Junggar, Xinjiang. Vert PalAsiat 24: 171-181.

Ye X (1999) A new genus of Sinemydidae from the Late Jurassic of Neijiang, Sichuan. Vert PalAsiat 37: 81-87.

Young C-C, Chow MC (1953) New fossil reptiles from Szechuan, China. Acta Sci Sin 2: 216-229.

Zhao XJ (1980) Mesozoic vertebrate-bearing beds and stratigraphy of northern Xinjiang. Mem Inst Vert Paleontol Paleoanthropol 16: 1-120. [in Chinese]

Zhou C-F (2010a) A new eucryptodiran turtle from the Early Cretaceous Jiufotang Formation of western Liaoning, China. Zootaxa 2676: 45-56.

Zhou C-F (2010b) A second specimen of *Manchurochelys manchoukuoensis* Endo & Shikama, 1942 (Testudines: Eucryptodira) from the Early Cretaceous Yixian Formation of western Liaoning, China. Zootaxa 2534: 57-66.

Appendix

1. **Rabi, M.** Sukhanov, V.B., Egorova, V., Danilov, I. Joyce, W.G. 2014. Osteology, relationships, and ecology of *Annemys* (Testudines: Eucryptodira) from the Late Jurassic of Shar Teg, Mongolia and a phylogenetic definition Of Xinjiangchelyidae, Sinemydidae, and Macrobaenidae. *Journal of Vertebrate Paleontology*. 34 (2): 327–352.

2. **Rabi, M.**, Zhou, C.-F., Wings, O., Sun, G., Joyce, W.G. 2013. A new xinjiangchelyid Turtle from the Middle Jurassic of Xinjiang, China and the evolution of the basipterygoid process in Mesozoic Turtles. *BMC Evolutionary Biology*. 13 (203): 1–28.

3. Zhou, C.-F†., **Rabi, M†.** & Joyce, W.G. 2014. A new specimen of *Manchurochelys manchoukuoensis* from the Early Cretaceous Jehol Biota of Chifeng, Inner Mongolia, China and the phylogeny of Cretaceous basal eucryptodiran turtles. *BMC Evolutionary Biology*. 14 (77): 1–16.

† = equal contributors

Publication #1

Rabi, M. Sukhanov, V.B., Egorova, V., Danilov, I. Joyce, W.G. 2014. Osteology, relationships, and ecology of *Annemys* (Testudines: Eucryptodira) from the Late Jurassic of Shar Teg, Mongolia and a phylogenetic definition Of Xinjiangchelyidae, Sinemydidae, and Macrobaenidae. *Journal of Vertebrate Paleontology*. 34 (2): 327–352.

Scientific ideas of candidate: 80 %

Data generation by candidate: 65 %

Analysis and Interpretation by candidate: 80 %

Paper writing by the candidate: 80 %

Journal of Vertebrate Paleontology 34(2):327–352, March 2014
© 2014 by the Society of Vertebrate Paleontology

ARTICLE

OSTEOLOGY, RELATIONSHIPS, AND ECOLOGY OF *ANNEMYS* (TESTUDINES, EUCRYPTODIRA) FROM THE LATE JURASSIC OF SHAR TEG, MONGOLIA, AND PHYLOGENETIC DEFINITIONS FOR XINJIANGCHELYIDAE, SINEMYDIDAE, AND MACROBAENIDAE

MÁRTON RABI,[*,1,2,3] VLADIMIR B. SUKHANOV,[4] VERA N. EGOROVA,[4] IGOR DANILOV,[5] and WALTER G. JOYCE[1,6]
[1]Institut für Geowissenschaften, University of Tübingen, Hölderlinstraße 12, 72074 Tübingen, Germany, iszkenderun@gmail.com;
[2]Department of Paleontology, Eötvös Loránd University, Pázmány Péter sétány 1/C, 1117 Budapest, Hungary;
[3]MTA–ELTE Lendület Dinosaur Research Group, Budapest, Hungary;
[4]Paleontological Institute of the Russian Academy of Sciences, Profsoyuznaya Str. 123, Moscow, 117997, Russia;
[5]Zoological Institute of the Russian Academy of Sciences, Universitetskaya Emb. 1, 199034 Saint Petersburg, Russia;
[6]Institute for Geosciences, University of Fribourg, Chemin du Musée 6, 1700 Fribourg, Switzerland

ABSTRACT—A complete description of the xinjiangchelyid turtles *Annemys levensis* and *A. latiens* is provided, based on all available material from the Upper Jurassic type locality of Shar Teg, Mongolia. *Annemys latiens* was previously known almost exclusively from shell material, but an undescribed skull from Shar Teg is referable to this species and its distinct morphology confirms the presence of two taxa at this locality. *Annemys latiens* has an elongated skull that markedly differs in proportions from those of *A. levensis* and resembles the shape of some recent, piscivorous turtles. The overall similarity of the shells of the two *Annemys* species combined with significant differences in the skull indicate that these turtles probably partitioned the aquatic niche by exploring different feeding strategies. Among xinjiangchelyids, at least three different skull morphotypes can be differentiated, which implies a moderate level of ecological diversification among Late Jurassic Asian turtles. Phylogenetic analysis weakly supports the inclusion of *Annemys* spp. into Xinjiangchelyidae and places xinjiangchelyids at the stem of Testudines, but the latter result is considered tentative. Phylogenetic definitions of Xinjiangchelyidae, Sinemydidae, and Macrobaenidae are provided for nomenclatural clarity and precision.

SUPPLEMENTAL DATA—Supplemental materials are available for this article for free at www.tandfonline.com/UJVP

INTRODUCTION

The fossil turtles *Annemys latiens* Sukhanov and Narmandakh, 2006, and *Annemys levensis* Sukhanov and Narmandakh, 2006, are represented by several well-preserved specimens from the Upper Jurassic locality of Shar Teg, Mongolia, and are among the most important representatives of the early eucryptodiran radiation (Sukhanov, 2000; Danilov and Parham, 2006, 2008; Rabi et al., 2010). In particular, *A. levensis* is one of the most complete and best-preserved Jurassic turtles known worldwide and therefore represents a key taxon in our understanding of the early evolution of Asian eucryptodires.

Abundant remains of *Annemys* were collected from Shar Teg by the Joint Soviet-Mongolian Paleontological Expedition during the field seasons of 1984, 1987, and 1989 and a Mongolian team led by R. Barsbold in 1985. Sukhanov (2000) provided an initial description and reconstructions of the more complete cranial and shell material, but only used the names *A. levensis* and *A. latiens* to informally refer to the two species that he recognized. These names therefore remained unavailable according to the rules of the International Commission on Zoological Nomenclature (ICZN; 1999). In a subsequent paper, Sukhanov and Narmandakh (2006) formally named and diagnosed *A. levensis* and *A. latiens,* provided a photograph of the holotype shell of *A. levensis*, but otherwise referred to the preliminary description of Sukhanov (2000). Previously, *A. latiens* had been known only from shells and undescribed skull fragments, but we here demonstrate that a fairly complete skull can be also referred to this species. The vast majority of fragmentary shell, girdle, and appendicular material, by contrast, are referable to *Annemys* sp. only. In spite of the importance of these taxa, a detailed description is still lacking. With this contribution, we intend to rectify this situation by describing and illustrating in detail the bulk of the *A. latiens* and *A. levensis* material from Shar Teg.

Previous phylogenetic studies (i.e., Anquetin, 2012; Tong et al., 2012b) that incorporated *A. levensis* utilized the available literature (Sukhanov, 2000; Sukhanov and Narmandakh, 2006) when scoring this taxon. The resulting phylogenies are in conflict with each another, in part likely because this taxon received different character scorings. Our detailed description of this taxon provides an opportunity to rigorously test the phylogenetic position of this important taxon within a global, cladistic context based on all available material and may therefore provide a more accurate phylogenetic hypothesis.

The description of phylogenetic results within Eucryptodira has been greatly hampered by a nomenclatural system that is universally agreed to be confusing. The suprageneric names Sinemydidae Ye, 1963, Macrobaenidae Sukhanov, 1964, and Xinjiangchelyidae Nessov in Kaznyshkin, Nalbandyan, and Nessov, 1990, were introduced by taxonomists to group various fossil eucryptodires. However, given that most characters that were used to diagnose these groups have since been shown to represent plesiomorphies (e.g., Sukhanov, 2000; Rabi et al., 2010) and given that changing phylogenies have not allowed some well-diagnosed clades worth naming to be identified (e.g., Gaffney and Ye, 1992; Gaffney, 1996; Brinkman and Wu, 1999; Parham

*Corresponding author.
Color versions of one or more of the figures in the article can be found online at www.tandfonline.com/ujvp.

and Hutchison, 2003; Gaffney et al., 2007; Joyce, 2007; Anquetin, 2012; Tong et al., 2012a, 2012b), most authors have resorted to placing these names in quotation marks to indicate their likely paraphyly while tolerating the resulting taxonomic imprecision. We herein attempt to resolve this situation by providing phylogenetic definitions of these names and to thereby stabilize their taxonomic meanings. Sinemydidae, Macrobaenidae, and Xinjiangchelyidae refer to monophyletic clades throughout this contribution (see Phylogenetic Definitions below) and are therefore not placed in quotation marks. Finally, in light of new data on the skull morphology of *Annemys*, we discuss the ecological diversity of xinjiangchelyids during the Late Jurassic.

Institutional Abbreviation—**PIN**, Paleontological Institute of the Russian Academy of Sciences, Moscow.

Nomenclature—The nomenclature of the skull used herein follows Gaffney (1972), that of the shell follows Hutchison and Bramble (1981). All higher taxonomic names are clade names as defined by Joyce et al. (2004) or in the section Phylogenetic Definitions.

GEOLOGIC SETTINGS

The material of *Annemys levensis*, *A. latiens*, and *A.* sp. described herein all originates from the locality of Shar Teg, which is situated in the Transaltai Gobi, approximately 100 km east-southeast of the town of Altai, within Altai Somon District in the southern part of Govi Altai Aimag Province, Mongolia. The locality is surrounded by the Az Bogdo, the Edrengiin Nuru, and the Atas Bogdo mountains from the north, northeast, and south, respectively. The Shar Teg locality spreads across several mesas and was named after one of these, Shar Teg, after it was discovered by V. Yu. Reshetov of the Joint Soviet-Mongolian Expedition in 1984 (Gubin and Sinitza, 1996). The type specimen of *Annemys levensis*, including other material of *Annemys*, were discovered in the same year, approximately halfway between the Shar Teg and Ulan Malgait hills, and 4–5 km west of the former.

The expeditions of 1987 and 1989 led by Y. M. Gubin worked on the stratigraphy of Shar Teg and recognized two units separated by a distinct limestone-caliche horizon. The lower Shar Teg beds are more widely distributed in the southwestern part of the locality, whereas the overlaying Ulan Malgait beds are more common in the northeastern part. Both beds are present along the Ulan Malgait and the Shar Teg hills. The *Annemys latiens, A. levensis*, and indeterminate *Annemys* material described herein originate from the Ulan Malgait beds. A Mongolian team collected the type material of *A. latiens* in 1985 and the remaining specimens described herein were collected in 1989. All *A. latiens* material, however, lacks more precise stratigraphic and locality data. In 2002, a joint Japanese-Mongolian Expedition collected a shell with articulated neck and skull in sandstones in the lower part of the Ulan Malgait beds (Watabe et al., 2004:pl. 4, fig. 6), but this specimen was not available to us and was therefore not included in our study.

The Ulan Malgait beds form a mostly siliciclastic unit composed of red, gray, brown, or yellow siltstones with interbedded coarse and fine sandstones. The turtle remains were found in four different sandstone horizons together with gastropods, bivalves, fishes, crocodilians, and sauropod dinosaurs (Gubin and Sinitza, 1996; Watabe et al., 2004).

The 'Shar Teg' beds are characterized by the alternation of sandstones with red, yellow, gray, brown, and green siltstones with limestone interbeddings in the lower part. A single layer of gray argillites and clays yielded a notably different vertebrate fauna relative to the Ulan Malgait beds, including the turtle *Shartegemys laticentralis* Sukhanov and Narmandakh, 2006, and isolated elements of insects, fishes, brachyopoid temnospondyls, theropod dinosaurs, tritylodontid cynodonts, and mammals (Gubin and Sinitza, 1996; Watabe et al., 2004).

The depositional environment of the Shar Teg beds is interpreted as a 20–40-km-long lake that episodically dried up during arid phases with a gradual transition from lacustrine to fluvial sedimentation. Conversely, the Ulan Malgait beds are considered to represent an extensive fluvial system and the vertebrate-bearing sandstone lenses are interpreted as crevasse splay (flood) deposits (Gubin and Sinitza, 1996; Watabe et al., 2004).

The ages of the Shar Teg and Ulan Malgait beds are poorly resolved. Biostratigraphic data based on stoneflies from the Shar Teg beds indicate a Middle Jurassic age, whereas a more recent study of mayflies argued for a Late Jurassic age (Sinitshenkova, 1995, 2002). No biostratigraphic data are available from the overlying Ulan Malgait beds (Watabe et al., 2004).

SYSTEMATIC PALEONTOLOGY

TESTUDINATA Klein, 1760
TESTUDINES Batsch, 1788
PANCRYPTODIRA Joyce, Parham, and Gauthier, 2004
XINJIANGCHELYIDAE Nessov in Kaznyshkin, Nalbandyan, and Nessov, 1990
ANNEMYS Sukhanov and Narmandakh, 2006

Types Species—*Annemys latiens* Sukhanov and Narmandakh, 2006.

Included Species—*Annemys levensis* Sukhanov and Narmandakh, 2006.

Distribution—Late Jurassic of Shar Teg locality, Govi Altai Aimag, Mongolia (Sukhanov, 2000; Sukhanov and Narmandakh, 2006) and late Middle Jurassic to early Late Jurassic of Wucaiwan area, Junggar Basin, Xinjiang Autonomous Uyghur Province, China (Brinkman et al., 2013).

Diagnosis—See Sukhanov and Narmandakh (2006) for a nondifferential diagnosis. The skull of *Annemys* differs from *Xinjiangchelys radiplicatoides* Brinkman, Eberth, Clark, Xing, and Wu, 2013, in being flattened, having a deeper upper temporal emargination, a longer supraoccipital crest, and reduced basioccipital tubera; from *Hangaiemys* (*Kirgizemys*) *hoburensis* Sukhanov and Narmandakh, 1974, and *Kirgizemys dmitrievi* Nessov and Khosatzky, 1981, in the presence of a laterally widely open foramen jugulare posterius, and the absence of paired pits on the basisphenoid. The latter also differentiates *Annemys* from Shar Teg from *Sinemys* spp. (sensu Brinkman and Peng, 1993a), *Dracochelys bicuspis* Gaffney and Ye, 1992, and *Ordosemys* spp. (sensu Danilov and Parham, 2007, and Tong et al., 2004). The shell of *Annemys* differs from *Xinjiangchelys* spp. (sensu Brinkman et al., 2008, and Brinkman et al., 2013) in the vertebrals 2 and 3 being almost as long as wide, vertebral 4 being wider than vertebrals 2 and 3, the placement of the vertebral 3/4 sulcus on neural 6, and an interrupted neural row that allows a midline contact between costal 7s; differs from *Shartegemys laticentralis* in the square epiplastra; differs from *Chengyuchelys* spp. (sensu Tong et al., 2012b), *Protoxinjiangchelys salis* Tong, Danilov, Ye, Ouyang, and Peng, 2012a, and *Yanduchelys delicatus* Peng, Ye, Gao, Shu, and Jiang, 2005 (sensu Tong et al., 2012b) in the presence of a ligamentous carapace-plastron attachment; further differs from *Chengyuchelys* spp. in the vertebral 5 not overlapping onto peripheral 10; differs from *Tienfuchelys* spp. (sensu Tong et al., 2012b) in having four pairs of inframarginals; and differs from *Hangaiemys* (*Kirgizemys*) *hoburensis*, *Sinemys lens* Wiman, 1930, and *Ordosemys* spp. in the relatively shorter dorsal rib 1, extension of marginals 4–8 onto costals, square-shaped epiplastron that is tightly sutured to the ento- and hyoplastron, reduced epiplastral process present, extragulars present, femoro-anal sulcus omega-shaped and extending onto hypoplastron, and sinuous midline sulcus.

ANNEMYS LEVENSIS Sukhanov and Narmandakh, 2006 (Figs. 1–5)

Annemys levensis Sukhanov and Narmandakh, in press, in Sukhanov, 2000:314, fig. 17.2 (unavailable under articles 13.1.1 and 16.1 of the International Commission on Zoological Nomenclature [1999]).

Annemys levensis Sukhanov and Narmandakh, 2006:120, fig. 1a, b (original description).

Xinjiangchelys levensis (Sukhanov and Narmandakh, 2006), Tong et al., 2012b:107 (new combination).

Holotype—PIN 4636-4, associated skull and mandible (PIN 4636-4-2), shell, right femur, right humerus, right scapula and fragment of coracoid, and incomplete right pelvic girdle (PIN 4636-4-1).

Locality and Horizon—Shar Teg locality, Govi Altai Aimag, Mongolia, Upper Jurassic, Ulan Malgait beds.

Revised Diagnosis—A species of *Annemys* differing from *A. latiens* in the presence of a broader and shorter skull, partially separated prefrontals, more extensive contributions of the frontal and the jugal to the orbital rim, quadrangular neural 1, longer and narrower posterior plastral lobe, and relatively narrower anterior projection of the anal scales.

ANNEMYS LATIENS Sukhanov and Narmandakh, 2006 (Figs. 6–10)

Annemys latiens Sukhanov and Narmandakh, in press, in Sukhanov, 2000:317, fig. 17.4 (unavailable under articles 13.1.1 and 16.1 of the International Commission on Zoological Nomenclature [1999]).

Xinjiangchelys latiens (Sukhanov and Narmandakh, in press): Matzke et al., 2004b:1295 (new combination of unavailable name).

Annemys latiens Sukhanov and Narmandakh, 2006:120 (original description).

Xinjiangchelys latiens (Sukhanov and Narmandakh, 2006), Tong et al., 2012b:107 (new combination).

Holotype—PIN 4636-5, an almost complete shell (PIN 4636-5-1), a partial basicranium and lower jaw ramus (PIN 4636-5-2), and other poorly preserved disarticulated cranial elements.

Referred Material—PIN 4636-6-1, an incomplete shell lacking most of the carapace; PIN 4636-6-2, a partial skull associated with PIN 4636-6-1; PIN 4636-7, an almost complete shell and a humerus. All referred material is from the type locality.

Locality and Horizon—Shar Teg locality, Govi Altai Aimag, Mongolia, Upper Jurassic, Ulan Malgait beds.

Revised Diagnosis—A species of *Annemys* differing from *A. levensis* in the presence of a narrower and longer skull, frontals that fully separate the prefrontals, a minor contribution of the frontal and the jugal to the orbital rim, hexagonal neural 1, a shorter and broader posterior plastral lobe, and relatively wider anterior projection of the anal scales.

ANNEMYS SP. (Figs. 11, 12)

Referred Material—PIN 4636-10, pelvis; PIN 4636-11, scapula; PIN 4636-12, femur; PIN 4636-13, hyoplastron buttress; PIN 4636-14, hypoplastron buttress; PIN 4636-15, peripheral 2; PIN 4636-16, articulated peripheral 6 and peripheral 7; PIN 4636-17, associated peripheral 3; PIN 4636-18, peripheral 5; PIN 4636-19, peripheral 6; PIN 4636-20, peripheral 7; PIN 4636-21, peripheral 8; PIN 4636-22, peripheral 2; PIN 4636-23, peripheral 4.

Remarks—Hundreds of further uncataloged isolated shell and appendicular elements are present in the collection of PIN from Shar Teg. Together with the material listed above, these cannot be identified to the species level and we therefore refer them to *Annemys* sp.

Locality and Horizon—Shar Teg locality, Govi Altai Aimag, Mongolia, Upper Jurassic, Ulan Malgait beds.

PHYLOGENETIC NOMENCLATURE

XINJIANGCHELYIDAE Nessov in Kaznyshkin, Nalbandyan, and Nessov, 1990, converted clade name

Definition—Xinjiangchelyidae refers to the most inclusive clade containing *Xinjiangchelys junggarensis* Ye, 1986, but not *Sinemys lens*, *Macrobaena mongolica* Tatarinov, 1959, or any species of Recent turtle.

Discussion—The name Xinjiangchelyidae was widely used to refer to a poorly defined group of basal eucryptodire taxa from the Jurassic of Asia (see Rabi et al., 2010, for a literature review). Nessov (in Kaznyshkin et al., 1990) originally coined the name along with Xinjiangchelydia, but subsequent workers did not adopt the latter term. Nessov (in Kaznyshkin et al., 1990) provided a diagnosis for Xinjiangchelyidae and synonymized *X. junggarensis* and '*Plesiochelys*' *radiplicatus* Young and Chow, 1953, with the type species of the family, *Xinjiangchelys latimarginalis* (Young and Chow, 1953) (= *Chengyuchelys latimarginalis* sensu Tong et al., 2012b), but it is unclear if he believed this taxon to be more inclusive than *Xinjiangchelys latimarginalis*. Sukhanov (2000) subsequently provided an emended diagnosis for Xinjiangchelyidae and explicitly circumscribed this taxon to include *Xinjiangchelys* spp., *Annemys* from Shar Teg, and the poorly known turtles *Shartegemys laticentralis*, *Undjulemys platensis* Sukhanov and Narmandakh, 2006, and *Tienfuchelys tzuyangensis* Young and Chow, 1953. Although this circumscription was followed by Matzke et al. (2004b), their phylogenetic analysis did not rigorously test the monophyly of the group. Tong et al. (2012a) circumscribed Xinjiangchelyidae as including *X. latimarginalis*, *X. tianshanensis* Nessov, 1995, and *Protoxinjiangchelys salis*, but their phylogenetic analysis revealed this grouping to be paraphyletic relative to the clade formed by *Bashuchelys zigongensis* (Ye, 1982), *Bashuchelys youngi* Tong, Danilov, Ye, Ouyang, and Peng, 2012a, and *Chuannanchelys dashanpuensis* (Fang, 1987). Tong et al. (2012b) circumscribed Xinjiangchelyidae as consisting of *Brodiechelys* spp., *Chengyuchelys* spp., *Protoxinjiangchelys salis*, *Tienfuchelys* spp., *Xinjiangchelys* spp. (including *Annemys* and *Shartegemys* Sukhanov and Narmandakh, 2006), and *Yanduchelys delicatus* Peng, Ye, Gao, Shu, and Jiang, 2005, and provided some support for the monophyly of this group of turtles with a phylogenetic analysis. By contrast, Anquetin (2012) circumscribed Xinjiangchelyidae as consisting of *Xinjiangchelys qiguensis* Matzke, Maisch, Sun, Pfretzschener, and Stöhr, 2004b, *X. latimarginalis* (sensu Peng and Brinkman, 1993), *X. tianshanensis*, *Annemys levensis*, and *Siamochelys peninsularis* Tong, Buffetaut, and Suteethorn, 2002. Various other authors discussed the phylogenetic relationships of *Xinjiangchelys latimarginalis*, but refrained from using the name Xinjiangchelyidae because of the lack of a clear definition for the name (Gaffney et al., 2007; Joyce, 2007; Danilov and Parham, 2008; Sterli, 2010).

Herein, we decided to phylogenetically define the taxon name Xinjiangchelyidae as referring to the most inclusive clade that includes *X. junggarensis*, but no living turtle or the 'essential' members of Sinemydidae or Macrobaenidae (i.e., *Sinemys lens* and *Macrobaena mongolica*). This captures the application of the name as undertaken by Anquetin (2012) and therefore results in the same grouping of turtles for that phylogenetic hypothesis (see above). If this definition is applied to the analysis of Tong et al. (2012a), Xinjiangchelyidae is hypothesized to consist of *X. latimarginalis*, *X. tianshanensis*, *P. salis*, *B. zigongensis*, *B. youngi*, and *C. dashanpuensis*. Our definition of Xinjiangchelyidae cannot be applied to the cladogram of Tong et al. (2012b), because

it includes no extant taxon, *Sinemys lens*, or *Macrobaena mongolica*. In the context of the phylogenetic hypothesis we present herein, *A. levensis*, *X. junggarensis*, and *X. radiplicatoides* are revealed to be part of Xinjiangchelyidae (Fig. 13).

SINEMYDIDAE Ye, 1963, converted clade name

Definition—Sinemydidae refers to the most inclusive clade containing *Sinemys lens* but not *Xinjiangchelys junggarensis, Macrobaena mongolica*, or any species of Recent turtle.

Discussion—The term Sinemydidae has been widely used as a collective name for many Early Cretaceous turtles from Asia (Ye, 1963; Chkhikvadze, 1975, 1977, 1987; Khosatzky and Nessov, 1979; Hutchison and Archibald, 1986; Brinkman and Peng, 1993a, 1993b; Hirayama et al., 2000; Sukhanov, 2000; Brinkman, 2001; Maisch et al., 2003; Matzke et al., 2004a; Tong et al., 2009) and represents another group of questionable utility without an explicit definition (Gaffney, 1996; Gaffney et al., 1998, 2007; Parham and Hutchison, 2003; Joyce, 2007; Danilov and Parham, 2008; Rabi et al., 2010). Sinemydidae was established by Ye (1963) for *Sinemys lens* and *Manchurochelys manchoukuoensis* Endo and Shikama, 1942. Subsequent workers has since proposed a disparate set of circumscriptions for Sinemydidae, including *S. lens*, *Man.* manchoukuoensis*, Macrobaena mongolica, Hangaiemys* (*Kirgizemys*) *hoburensis*, *Kirgizemys exaratus* Nessov and Khosatzky, 1973, and *Yaxartemys longicauda* Ryabinin, 1948 (Chkhikvadze, 1975, 1977, 1987); *Man. manchoukuoensis* and *Sinemys* spp. (Brinkman and Peng, 1993a); *Dracochelys bicuspis*, *Ordosemys* spp., and *Sinemys* spp. (Gaffney, 1996); *Sinemys* spp., *D. bicuspis*, and *H. hoburensis* (Brinkman and Wu, 1999); *D. bicuspis*, *Hongkongochelys yehi* Ye, 1999, *Man. manchoukuoensis*, *Ordosemys* spp., *Sinemys* spp., *Wuguia* spp., and *Yumenemys inflatus* Bohlin, 1953 (Brinkman et al., 2008); and *D. bicuspis*, *Man. manchoukuoensis,* and *Sinemys* spp. (Zhou, 2010a, 2010b), or only *Sinemys* spp. (Sukhanov, 2000; Tong and Brinkman, 2013). Only the circumscriptions of Gaffney (1996) and Zhou (2010a, 2010b) were based on a phylogenetic analysis and therefore unite monophyletic clades.

The summary above amply demonstrates that there is no consensus as to the application of the name Sinemydidae beyond the inclusion of *Sinemys* spp. and the exclusion of extant species of turtles and *Xinjiangchelys junggarensis*. The 'essential' macrobaenid *Macrobaena mongolica* was only included by Chkhikvadze (1975, 1977, 1987). We therefore capture the current consensus by restricting the term Sinemydidae to all turtles more closely related to *S. lens* than to any living turtle or the 'essential' representatives of Xinjiangchelyidae and Macrobaenidae, as already undertaken by Gaffney (1996) and Zhou (2010a, 2010b). If this definition is applied to the topology of Joyce (2007), Sinemydidae is hypothesized to include *S. lens*, *Ordosemys leios* Brinkman and Peng, 1993b, *D. bicuspis*, and *Judithemys sukhanovi* Parham and Hutchison, 2003. According to the topology of Anquetin (2012), this clade consists of *S. lens* and *O. leios*. By contrast, the topologies of Parham and Hutchison (2003), Gaffney et al. (2007), Danilov and Parham (2008), and our proposed phylogeny imply that Sinemydidae only consists of *S. lens*.

MACROBAENIDAE Sukhanov, 1964, converted clade name

Definition—Macrobaenidae refers to the most inclusive clade containing *Macrobaena mongolica* but not *Xinjiangchelys junggarensis*, *Sinemys lens*, or any species of Recent turtle.

Discussion—Macrobaenidae is another name traditionally used for uniting various Asian and North American Cretaceous and Tertiary fossil eucryptodires that are more derived than xinjiangchelyids. Macrobaenidae was established by Sukhanov (1964) for *Mac. mongolica*. Several other taxa were at one or the other time referred to this group, including *Hangaiemys* (*Kirgizemys*) *hoburensis*, *Ordosemys* spp., *Kirgizemys exaratus*, *Asiachelys perforata* Sukhanov and Narmandakh, 2006, and *Anatolemys maximus* Khosatzky and Nessov, 1979 (see Sukhanov, 2000, for a more complete review and references). Some of the listed taxa were variously referred to Sinemydidae by other authors (see above) and the names Sinemydidae and Macrobaenidae therefore often had overlapping circumscription. However, *Xinjiangchelys junggarensis* and *Sinemys lens* were consistently excluded from the group. Interestingly, even though various circumscription of Macrobaenidae are universally agreed to by paraphyletic (e.g., Parham and Hutchison, 2003; Gaffney et al., 2007; Joyce, 2007; Danilov and Parham, 2008; Zhou, 2010b; Sterli and de la Fuente, 2011; Anquetin, 2012), the name giving taxon *Mac. mongolica* was never included in a phylogenetic analysis. There is therefore no precedence of applying the name Macrobaenidae to a monophyletic clade. We decided to restrict the name to the most inclusive clade that includes *Mac. mongolica*, but no living turtle or *X. junggarensis* and *S. lens*. We are not able to apply this name to our cladogram, however, because *Mac. mongolica* is not included as a terminal taxon (Fig. 13).

DESCRIPTION OF *ANNEMYS LEVENSIS*

Based on the available material, there are relatively few differences in the anatomy of *Annemys levensis* and *A. latiens*. We therefore chose to describe the better-preserved *A. levensis* first and to only highlight differences in the section on *A. latiens*.

Skull

The holotype and only known partial skeleton of *Annemys levensis* (PIN 4636-4) has an excellent, almost complete skull (PIN 4636-4-2; Fig. 1). It only lacks parts of the premaxillae, most of the quadratojugals, and the posterodorsal margin of the supraoccipital crest. Much of the left cheek is present as an isolated element.

In general, the skull is characterized by a triangular outline that is roughly 28% longer than wide, well-developed cheek and upper temporal emarginations, dorsolaterally facing, relatively large orbits with shallow lower rim, and a short preorbital region. When viewed laterally, the skull is flat and gradually slopes from the supraoccipital towards the nasals. The skull roof is decorated with very fine grooves and ridges, whereas the otic chamber and the lateral surface of the squamosals are smooth.

Cranial Scales—Scale sulci are well defined in PIN 4634-6-2 (Fig. 1A, B, K). We adopt the system of Gaffney (1996) and Sterli and de la Fuente (2013) developed for cranial scales of basal turtles. Scale Z is subdivided into two smaller scales arranged along the midline (following Sterli and de la Fuente, 2013), a broader, anterior that covers the prefrontals and the nasals, and a narrower, posterior one that covers the frontal processes and the medial margins of the prefrontals. Scale Y is unpaired, covers the middle of the frontal bones, and has a regular hexagonal shape. Scale G was most probably paired and its anterior half extends onto the frontals and the posterior half onto the parietals. Its posterior margin is deeply emarginated. The unpaired scale X has a regular pentagonal shape and is slightly smaller in size than scale Y. Scale A is unpaired and extends along the medial rim of the upper temporal emargination formed by the parietals. Its posterior limit is unclear. Posterolaterally, scale A meets a small and triangular paired scale that borders the anteromedial rim of the upper temporal emargination. We are unable to find the homolog for this scale using the system of Sterli and de la Fuente (2013) and it could be a neomorph. Anterolaterally, scale A contacts a paired trapezoidal scale that is restricted to the parietals and we tentatively interpret it as scale H. Lateral to this scale lies another paired scale extending onto the postorbital and slightly onto the parietals. We tentatively interpret it as scale D. Scale F is interpreted to be subdivided into at least four smaller scales following Sterli and de la Fuente (2013). They extend along the dorsal margin of the orbit from the posterodorsal to

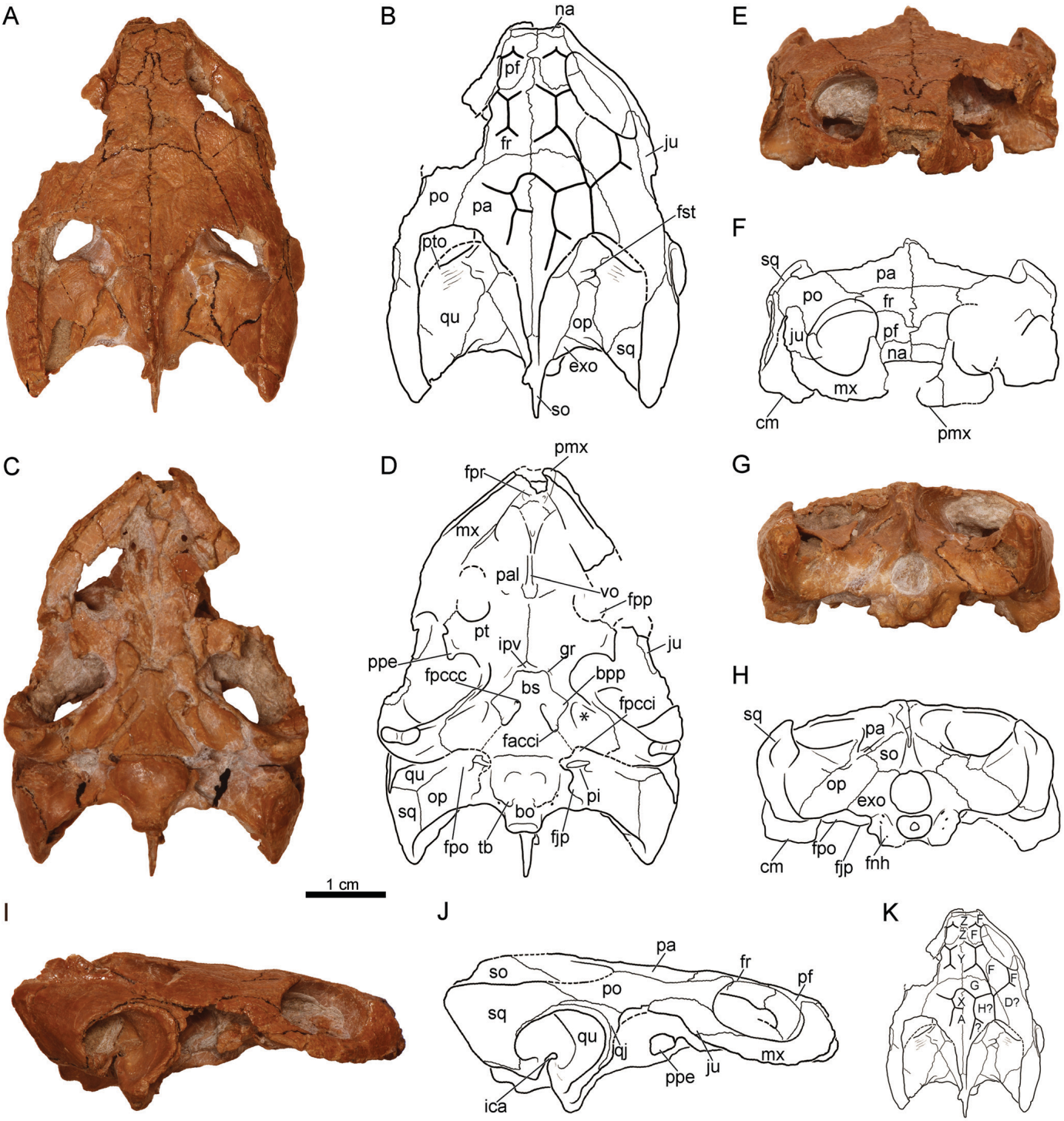

FIGURE 1. PIN 4636-4-2 (holotype), *Annemys levensis*, skull, Late Jurassic, Shar Teg, Ulan Malgait beds, Govi Altai Aimag, Mongolia. **A**, **B**, photograph and line drawing in dorsal view; **C**, **D**, photograph and line drawing in ventral view; **E**, **F**, photograph and line drawing in anterior view; **G**, **H**, photograph and line drawing in posterior view; **I**, **J**, photograph and line drawing in right lateral view; **K**, line drawing of skull roof scales. **Abbreviations**: **bo**, basioccipital; **bpp**, basipterygoid process; **bs**, basisphenoid; **cm**, condylus mandibularis; **exo**, exoccipital; **facci**, foramen anterius canalis caroticus internus; **fjp**, foramen jugulare posterius; **fnh**, foramen nervi hypoglossi; **fpccc**, foramen posterius canalis caroticus cerebralis; **fpcci**, foramen posterius canalis carotici interni; **fpo**, fenestra postotica; **fpp**, foramen palatinum posterius; **fpr**, foramen praepalatinum; **fr**, frontal; **fst**, foramen stapedio-temporale; **gr**, groove for palatine branch of the carotid; **ica**, incisura columella auris; **ipv**, interpterygoid vacuity; **ju**, jugal; **mx**, maxilla; **na**, nasal; **op**, opisthotic; **pa**, parietal; **pal**, palatine; **pf**, prefrontal; **pi**, processus interfenestralis; **pmx**, premaxilla; **po**, postorbital; **ppe**, processus pterygoideus externus; **pt**, pterygoid; **pto**, processus trochlearis oticum; **qj**, quadratojugal; **qu**, quadrate; **so**, supraoccipital; **sq**, squamosal; **tb**, tubera basioccipitalis; **vo**, vomer; **A**, **D**, **F**, **H**, **G**, **X**, **Y**, **Z**, cranial scales (following the terminology of Sterli and de la Fuente, 2013); *, pterygoid pit.

the anterodorsal corner. The largest is the third counting from the front and it contacts scales G and Y medially. The precise extent of the most posterior scale F remains unclear. Of the two anterior F scales, the second from the front is the larger and both form the lateral borders of the subdivided scale Z.

Nasals—A pair of small nasals is present that forms the dorsal margin of the apertura narium externa (Fig. 1A, B, E, F). The nasals have the shape of wide rectangles and their midline contact with one another is not interrupted by the frontals. The nasals contact the prefrontals posteriorly and the maxillae ventrolaterally.

Prefrontals—The dorsal plates of the prefrontals are subrectangular and roughly twice as long as wide (Fig. 1A, B, E, F). A clear medial contact of the prefrontals with one another is present along the anterior halves of these elements, but the anterior process of the frontals divides their posterior halves. The prefrontals form the anterior third of the dorsal rim of the orbits, meet the nasals anteriorly, the maxillae anterolaterally, and the frontals posteromedially. The descending process of the prefrontals defines the anterior wall of the orbit and the extensive development of the palatines along the floor of the orbit indicates that a distal contact of the descending process with the palatines must have been present, although it is currently not preserved. The great size of the descending process of the prefrontals furthermore evinces that a vomer-prefrontal contact is very likely present, but damage to this region obscures this contact as well. The foramen orbito-nasale is small, but badly preserved due to damage along the flooring of the fossa orbitalis, and it is therefore unclear if the prefrontals contribute to its margins.

Frontals—In dorsal view, the frontals have relatively short anteromedial processes that are about half of the length of the remaining part of these bones and only partially separate the prefrontals (Fig. 1A, B, E, F). The frontals form about one-third of the length of the dorsal orbital rim. In dorsal view, the frontals contact the prefrontals anterolaterally, the postorbital posterolaterally, and the parietals posteriorly. The olfactory region of the frontals is not visible, because the interorbital fossa is not prepared, but it is apparent that the prefrontals and frontals form a distinct sulcus olfactorius. It is unclear if the frontals contact the nasals within the roofing of the nasal capsule.

Parietals—The right parietal is preserved almost completely, including the rim of the upper temporal emargination, but excluding the posterior process along the supraoccipital crest (Fig. 1A, B, E, F). The left parietal, by contrast, is mostly damaged along the upper temporal emargination. The parietals are relatively broad elements that show long contacts with the postorbitals laterally and short, transverse contacts with the frontals anteriorly. Posteriorly, the parietals cover the anterior half of the supraoccipital crest but do not reach the level of the occipital condyle. The deepest point of the extensive upper temporal emargination is preserved by the right parietal and is located slightly anterior to the anterior border of the cavum tympani in lateral view, and anterior to the anterior wall of the otic chamber in dorsal view. Possible contacts with the squamosals cannot be verified due to the incompleteness of these elements, but if any were present, they must have been point-like contacts along the margin of the upper temporal emargination. The processus parietalis inferior broadly contacts the prootic within the upper temporal fossa and contacts the pterygoids and epipterygoids anterior to the foramen nervi trigemini to form a broad anterior braincase wall. The right side of PIN 4636-4-2 best demonstrates that the parietals form the anterodorsal margin of the foramen nervi trigemini (Fig. 2).

Jugals—Only the right jugal is completely preserved (Fig. 1A, B, E, F, I, J). The main body of the jugals forms much of the posteroventral margin of the orbit and contacts the maxilla anteriorly. The plate-like dorsal process, also preserved on the left side of the skull, contacts the postorbital dorsomedially. It appears

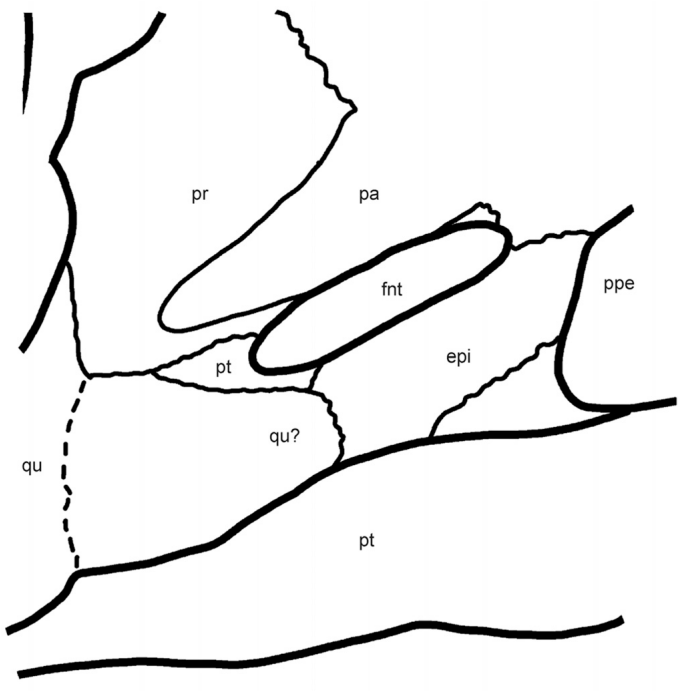

FIGURE 2. PIN 4636-4-2 (holotype), *Annemys levensis*, Late Jurassic, Shar Teg, Ulan Malgait beds, Govi Altai Aimag, Mongolia. Line drawing of the right trigeminal region of skull in lateral view, anterior is to the right. **Abbreviations**: **epi**, epipterygoid; **fnt**, foramen nervi trigemini; **pa**, parietal; **ppe**, processus pterygoideus externus; **pr**, prootic; **pt**, pterygoid; **qu**, quadrate.

that the jugal had a posterior point contact with the quadratojugal on the left side of the skull (not figured), but this is not certain, given that this region of the skull is badly damaged. A relatively deep lower temporal emargination is present, which reaches the midlevel of the orbit in lateral view. It is unclear whether the ventral plate contacted the posterior end of the triturating surface and the anterolateral tip of the external pterygoid process.

Quadratojugals—Only the dorsal portions of the quadratojugals are preserved on both sides of the skull, the right one being more complete (Fig. 1I, J). These remnants are wedged between the postorbital dorsally and the dorsal rim of the cavum tympani ventrally and narrowly contact the squamosal posteriorly. It appears that a small fragment of the left quadratojugal contacts the dorsal process of the jugal anteriorly, but damage to this region of the skull makes this contact all but certain. The articular surface for the quadratojugal along the anterior rim of the cavum tympani (i.e., the quadrate) is nicely preserved on the right side of the skull and reveals that the ventral aspect of the quadratojugals almost reaches the level of the articular condyles ventrally.

Squamosals—The squamosals are cone-shaped elements that form the roof of the inflated antrum postoticum and the posterolateral margins of the upper temporal fossa (Fig. 1). In lateral view, the squamosals have an extensive contact with the quadrates dorsally and posteriorly to the cavum tympani. It sits on the cavum tympani of the quadrate but does not contribute to the actual rim of the cavum tympani. The squamosals furthermore have a short anterior contact with the quadratojugals and a broader contact with the postorbital. Within the upper temporal fossa, the squamosal contacts the paroccipital process of the opisthotic ventromedially and laps onto the quadrates anteromedially. Anterior point contacts with the parietals may have been present along the anterior margin of the upper temporal

emargination, but an actual contact is not preserved on either side of the skull. The posterior tips of the squamosals are rounded and reach posteriorly beyond the level of the occipital condyle but not as far as that of the supraoccipital crest. The lateral surface is smooth and lacks clear muscle attachment sites.

Postorbitals—The postorbitals are anteroposteriorly elongated elements that cover much of the midlateral aspects of the skull and form the posterior margin of the orbits (Fig. 1A, B, I, J). The width of the postorbitals is slightly greater than that of the frontals. Posteromedially, the postorbitals contact the parietals along sutures that are about twice as long as the anteromedial contacts with the frontals. The postorbitals are perhaps excluded from the lower temporal emargination by a jugal-quadratojugal contact and from the upper temporal emargination by a squamosal-parietal contact, but damage to all relevant regions of the skull prohibit confident assessment of this morphology. The postorbital has no contact with the palatine.

Premaxillae—Only fragments of both premaxillae are preserved, the left one being more complete (Fig. 1F). The premaxillae form the ventral border of the external narial opening and the anterior portion of the labial ridge. They contact the maxilla posterolaterally and the vomer posteriorly, but the latter contact is partially obscured by compression. The foramina praepalatinum are located on the ventral surface of the premaxilla and do not appear to have a contribution from the vomer. A distinct premaxillary hook is absent.

Maxillae—The maxillae, as preserved on the right side of the skull, and disarticulated on the left side, form narrow, slightly curved, and parallel-sided triturating surfaces (Fig. 1A–D). A sharp labial ridge is present, whereas only hints of a lingual ridge are apparent near the palatine contacts. The palatines, jugals, and vomer are not involved in the triturating surfaces. In palatal view, the maxillae contact the premaxillae anteriorly, the vomer anteromedially, and the palatines medially. Ventrally, the posterior parts of the maxillae are not well preserved and potential posterior contacts with the pterygoids are therefore uncertain. A secondary palate is not developed.

The margins of the foramen palatinum posterius are uncertain because of rather extensive damage to this region of the skull. The distribution of palatine fragments along the middle third of the maxillae only, however, reveals that the foramen palatinum posterius was large in size. The foramen was defined by the maxillae laterally, the palatines medially, and the pterygoids posteriorly.

Lateral to the anterior wall of the orbits, the dorsal process of the maxillae overlap the descending process of the prefrontals and contact the nasals and the prefrontals medially. The maxillae form the anterior margins of the orbits, but their contribution to the anterior orbit walls is only minor. The foramen orbito-nasale is too poorly preserved to allow discerning whether the maxillae contribute to it. The lateral plate of the maxilla forms the lower rim of the orbit and is posterodorsally overlapped by the jugal.

Vomer—The vomer is damaged in PIN 4636-4-2 but enough is preserved to describe the most important features (Fig. 1C, D). This element is narrow and crest-like, has widened anterior and posterior ends, and separates the choanae. The anterior part of the vomer is broken and displaced dorsally relative to the main body of the bone together with the crushed premaxillary region. This portion nevertheless shows a clear anterior contact with the premaxillae and anterolateral contacts with the maxillae. Posteriorly, the vomer separates the palatines in ventral view and likely contacted the pterygoids as well. Although not visible directly, a contact with the prefrontal must have been present, as can be deduced from the extensive descending process of the prefrontal.

Palatines—The palate is compressed and the palatines are better preserved on the left side of the skull (Fig. 1C, D). Anterolaterally, the palatines touch the maxillae along the low lingual ridge of the triturating surface. The palatines form the medial and anterior margins of the damaged foramen palatinum posterius and medially contact the vomer. It is difficult to discern if the palatines contact one another in ventral view posterior to the vomer because this region is only poorly prepared, but the vomer likely separates the palatines from one another by contacting the pterygoid. It is also unclear if the palatines perhaps contacted one another dorsally within the interorbital foramen. The posterior suture between the palatines and the pterygoids is concave posteriorly and the posterolateral edge of the palatine is at the level of the foramen palatinum posterius.

Quadrates—The quadrates contact within the otic region the squamosals posterolaterally, the opisthotics posteromedially, and the prootics anteromedially (Fig. 1). The stapedial foramen, better preserved on the right side of the skull, is well developed and located in the anteromedial region of the roof of the otic chamber. The lateral margin of the foramen is defined by the quadrate, whereas the medial margin and a shallow, exiting groove are formed by the prootic. The presence of an unambiguous processus trochlearis oticum cannot be identified confidently because there is no prominent protrusion. The anterodorsal margin of the quadrate along the anterior margin the otic chamber nevertheless exhibits a slightly raised rugose area that probably held a cartilage that helped redirect the adductor musculature. The prootic does not participate in this structure.

The tympanic region of the quadrate is in clear contact with the quadratojugal anterodorsally and the squamosal posterodorsally. The ventral portions of the quadratojugals are damaged, but an additional anterior quadratojugal contact is evidenced by sutural margins. The antrum postoticum is well developed and the cavum tympani is deep and has a kidney-shaped outline in lateral view. No precolumellar fossa is present within the cavum tympani, but a shallow, oval-shaped embayment is apparent just dorsal to the quadrate condyle. The posterior margin of the cavum tympani is formed by the quadrates, not the squamosal. The full outline of the cavum tympani would therefore be preserved if the squamosals were removed. The incisura columella auris is very narrow, but not posteriorly enclosed, and a small fragment of the elegant stapes is preserved within the incisura on the left side of the skull.

The ventral portions of the quadrates contact the pterygoids medially and the epipterygoid anteriorly and form condyli mandibularis that are situated well anteriorly to the condylus occipitalis. The articular processes are rather low and the entire skull therefore has only a low height. The mandibular condyles are anteroposteriorly short and oriented slightly to the anterior.

Epipterygoids and Trigeminal Area—The epipterygoids are laminar elements best preserved on the right side of the skull (Fig. 2). They contact the pterygoids ventrally and form the ventral and the anterior margins of the trigeminal foramen. The posterior margin of the trigeminal foramen is formed by the pterygoid and the dorsal margin by the prootic, but here an elegant and laminar posterior process of the parietal overlaps the prootic. However, the internal dorsal margin is clearly formed by the prootic. Posteriorly, the epipterygoid is bordered by an element that is possibly a thin lamina of the quadrate overlapping the pterygoid. Along the ventral edge of the bone there is a thickened laterally protruding lip.

Pterygoids—The pterygoids send long processes posterolaterally that surround the basisphenoid laterally, reach the back of the skull without contacting the basioccipital, and lap onto the quadrate rami (Figs. 1B, 2). The cavum acustico-jugulare is fully floored by these elements and the prootics are therefore not visible in ventral view. At the back of the skull, part of the floor of the canalis carotici interni is eroded away (contra Sukhanov [2000], who interpreted the canals are being primarily exposed). However, this erosion makes it apparent that the canal extends from the foramen posterius canalis carotici interni to the unfloored carotid sulcus of the basisphenoid and is formed along

the contact of the pterygoids and the basisphenoid. The exact position of the foramen posterius canalis carotici interni is unclear, but it must have been placed at the posterior end of the pterygoid (now eroded) in line with the carotid canal. The basisphenoid might have been excluded from the formation of this foramen. Medially to the quadrate ramus the pterygoids have large, shallow, oval depressions, the fossae pterygoidei. At the anteromedial margin of the depression, the pterygoids articulate with the basipterygoid processes of the basisphenoid. Anteriorly, the pterygoid rami form flat, rectangular plates that meet each other along the midline to form part of the primary palate. The posterior margin of these plates together with the anterior portion of the pterygoid rami and the anterior margin of the basisphenoid define a small rectangular space. Even though the pterygoids are compressed in this region and the anterior portion of the right ramus of the pterygoid is slightly displaced, the intact margins of all bones involved indicate that this space is bordered by natural, bony margins and we therefore identify it as a narrow remnant of the interpterygoid vacuity. More specimens of *A. levensis* or similar species may reveal in the future that this gap closes completely in later ontogenetic stages (e.g., as in *Xinjiangchelys radiplicatoides* where the entry of the palatine artery is represented by a pair of slit-like openings; Brinkman et al., 2013). A pair of grooves is formed by the quadrate ramus of the pterygoids that lead to the posterolateral corners of the remnant of the interpterygoid vacuity and it is evident that these held the palatine arteries. The area of the interpterygoid vacuity is too poorly preserved, however, to reveal if incipient foramina posterius canalis caroticus lateralis for the palatine arteries were present laterally; therefore, it remains unclear whether the palatine branch entered the skull via the vacuity or an adjacent foramen. If the latter case were true, the vacuity had already lost its function at this evolutionary stage of transmitting the palatine branch, but had not yet closed completely.

Anterolaterally, the pterygoids form the processus pterygoideus externus. The processus has a clearly developed vertical plate and a posterior process that protrudes into the lower temporal fossa. Anterolaterally to the processus pterygoideus externus, the pterygoids contact the maxillae and form the posterior rim of the foramen palatinum posterius. The pterygoids meet the palatines anteriorly, but it is uncertain if midline contacts of the palatines prohibit an anterior contact with the vomer.

In the trigeminal area, the dorsal plate of the pterygoid contacts the epipterygoid dorsally, the quadrate posterodorsally, and forms the posterior margin of the trigeminal foramen (Fig. 2).

Supraoccipital—The supraoccipital only lacks the posterodorsal portions of the supraoccipital crest (Fig. 1A, B). It contacts the parietals anterodorsally, the prootics anterolaterally, the opisthotics posterolaterally, and the exoccipitals posteriorly along the dorsolateral margin of the foramen magnum. The supraoccipital does not contribute to the foramen stapediotemporale. The posterodorsal portion of the supraoccipital crest is slightly damaged, but the posterior tip is intact and the crest extends slightly beyond the tips of the squamosals and occipital condyle. The preserved portion of the supraoccipital crest is laminar and lacks ridges.

Exoccipitals—The exoccipitals form the lateral and ventral margins of the foramen magnum (Fig. 1G, H). Dorsally, they contact the supraoccipital, laterally the opisthotic, and ventrally the basioccipital. Anteroventrally, the exoccipitals are incomplete on both sides and a contact with the pterygoid might have been present accordingly. The exoccipitals form the posterior wall of the recessus scalae tympani, but are not developed extensively enough to separate the foramen jugulare posterius from the fenestra postotica. Three pairs of small foramina nervi hypoglossi are present that are arranged in a roughly dorsoventrally directed curve and that decrease in diameter ventrally. The exoccipitals are fully fused with the basioccipital.

Basioccipital—The basioccipital is fused with the exoccipitals dorsally and most probably forms the occipital condyle with these bones (Fig. 1C, D). An anterior, transverse contact is present with the basisphenoid. A deep groove is apparent between these two bones, and although this area is eroded, its rugose surface is indicative of being a true anatomical structure. Ventrally, the basioccipital and/or exoccipital form a pair of tubercula basioccipitale. A shallow heart-shaped depression dominates the ventral surface of the basioccipital that does not extend onto the basisphenoid.

Prootic—In dorsal view, the prootics are in contact with the parietal anteromedially, the supraoccipital posteromedially, the opisthotic posteriorly, and the quadrate laterally (Figs. 1A, 2). The prootics form the medial portion of the large foramen stapedio-temporale and the anteromedial wall of the otic chamber. They lack a rugose surface along the anterodorsal side of the otic wall and are therefore inferred to not have participated in the formation of a processus trochlearis oticum. The prootics form the inner dorsal margin of the trigeminal foramen, but the external margin is overlapped by a posterior narrow lamina of the parietal.

Opisthotic—The opisthotics contact the quadrates anterolaterally, the squamosals posterolaterally, the exoccipitals posteromedially, the supraoccipital medially, and the prootics anteriorly (Fig. 1A, B, C, D, G, H). A ventral process of the opisthotic, the processus interfenestralis, separates the recessus scalae tympani from the cavum acustico-jugulare and the cavum labyrinthicum. The distal portion of the processus interfenestralis expands to form a small horizontal plate that does not completely reach the ventral surface of the basicranium but narrowly contacts the dorsal surface of the posterior tip of the pterygoid and the basisphenoid and even the anterolateral edge of the basioccipital. The processus interfenestralis remains fully visible in ventral view, at least as preserved. However, this area is damaged and the exoccipital possibly covered it ventrally to an extent that the process may not have been visible at all. At the dorsal base of the right processus, a small foramen is present, the foramen internum nervi glossopharyngei. The fenestra perilymphatica is large and allows communication between the recessus scalae tympani and the cavum labyrinthicum. The cavum acustico-jugulare posteriorly opens into the large fenestra postotica that is defined by the opisthotics dorsally and dorsolaterally, the quadrates anterolaterally, the pterygoids and the basisphenoid anteriorly, and the basi- and exoccipitals medially.

Basisphenoid—The basisphenoid is slightly damaged posteriorly and lacks the flooring of the internal carotid canals (Fig. 1C, D). The basisphenoid is longer than wide and tapers and widens anterior and posterior to the basipterygoid processes, respectively. The basisphenoid meets the basioccipital posteriorly via a transverse suture, contacts the pterygoids laterally, and contributes to the fenestra postotica. Well-developed basipterygoid processes are present that project laterally from the anterior half of the basisphenoid to fit into the corresponding pockets of the pterygoids. The processes are flat, triangular in outline, and roughly as long as they are wide. The basisphenoid has a transverse, anterior free margin that defines the posterior border of the reduced interpterygoid vacuity. The foramen posterius canalis carotici interni is damaged but opened at the back of the skull either between the basisphenoid and the pterygoid or within the pterygoid only. The flooring of the canalis carotici interni and the posterior entry of the canal was formed by the pterygoids and basisphenoid, but is now eroded. It former presence, however, is indicated by residual fragments and broken margins. Intact margins at the level of the basipterygoid process combined with exposed posterior foramina of the cerebral artery reveal that the split of the carotid artery into cerebral and palatine branches was not floored, as in sinemydids and other xinjiangchelyids. The anterior foramen of the internal carotid artery and the posterior

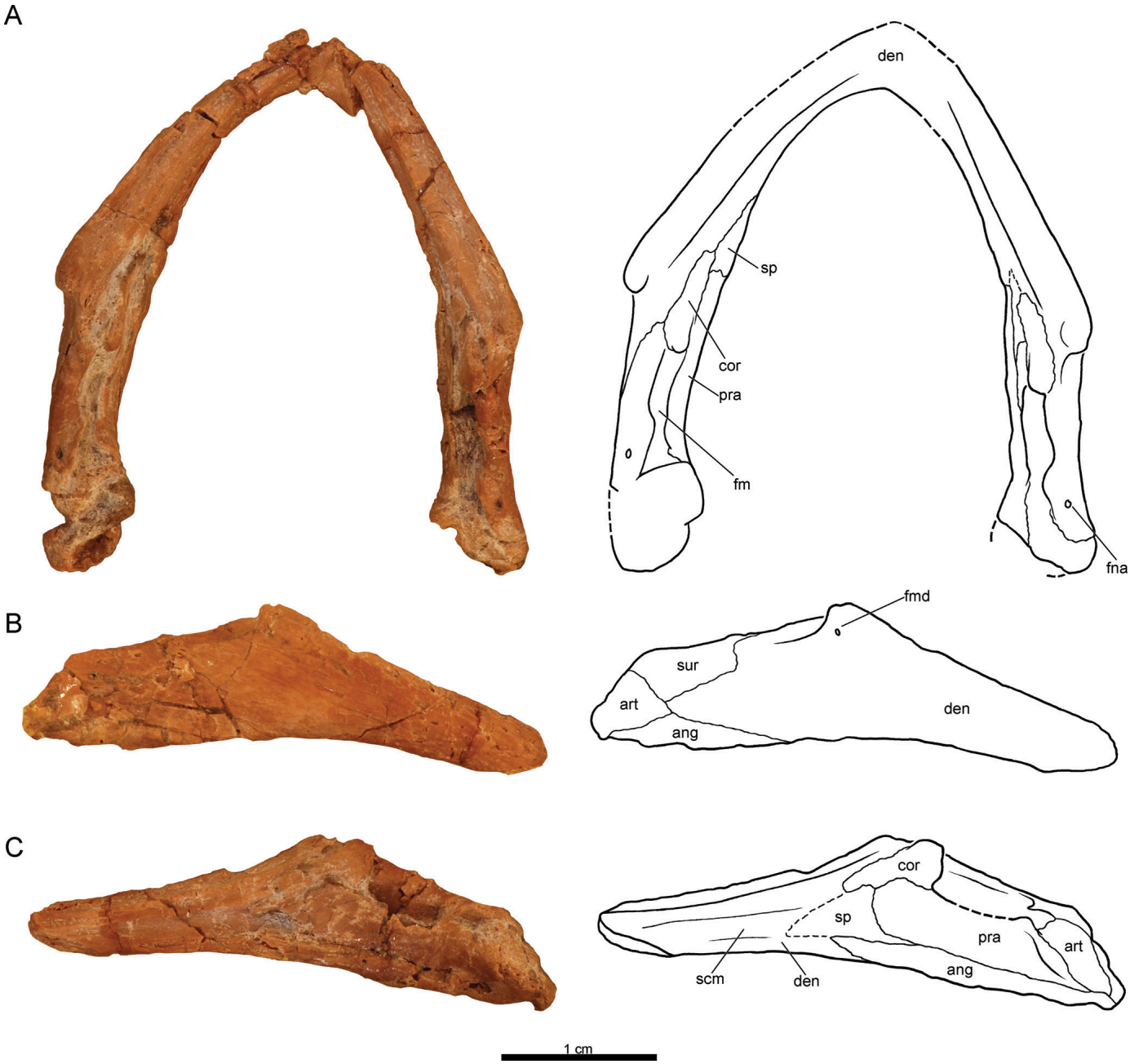

FIGURE 3. PIN 4636-4-2 (holotype), *Annemys levensis*, mandible, Late Jurassic, Shar Teg, Ulan Malgait beds, Govi Altai Aimag, Mongolia. **A**, photograph and line drawing in dorsal view; **B**, photograph and line drawing of right ramus in lateral view; **C**, photograph and line drawing of right ramus in medial view. **Abbreviations**: **ang**, angular; **art**, articular; **cor**, coronoid; **den**, dentary; **fm**, fossa Meckelii; **fmd**, foramen dentofaciale majus; **fna**, foramen nervi auriculotemporalis; **pra**, prearticular; **scm**, sulcus cartilaginis Meckelii; **sp**, splenial; **sur**, surangular.

foramen of the cerebral artery are connected by a marked sulcus. A pair of incipient foramina posterius canalis carotici lateralis may have been present along the suture with the pterygoid just lateral to the interpterygoid vacuity. Paired pits on the ventral surface of the basisphenoid are absent.

Mandible

An almost complete, delicate lower jaw is associated with the skull (Fig. 3). It is characterized by a narrow and relatively elongate triturating surface with sharp labial and lingual ridges, a low coronoid process, and a short retroarticular process. The symphysis is damaged and the presence of a midline hook therefore remains unclear, but enough is preserved to tell that the dentaries were fused. On the right side, the posterior fragment of the splenial is visible wedged between the coronoid, prearticular, and angular. The foramen dentofaciale majus is situated just below the posterodorsal corner of the triturating surface on the lateral wall of the dentary. A small foramen nervi auriculotemporalis is present on the posterior region of the surangular.

Shell

PIN 4636-4-1 is a shell found associated with the PIN 4636-4-2 skull (Figs. 4, 5). It only lacks the right peripherals 9–11, the left peripherals 7–9, and the pygal.

Carapace—The carapace is 325 mm long, low, and suboval and reaches its greatest width at the level of peripheral 8 (Fig. 4). The surface texture of the shell is generally smooth, with the exception of poorly defined outward radiating low plications on the anterior halves of the vertebrals. The nuchal is trapezoidal, about twice as wide as long, and has a distinct emargination that involves peripheral 1. Costiform processes are clearly absent. There are eight neurals, of which most are hexagonal with short sides facing anterolaterally, with the exceptions of neurals 1 (elongated, quadrangular), 7 (short oval), and 8 (short, hexagonal). The neural series is interrupted posterior to neural 6, allowing for a midline contact of costal 7 and resulting in a reduced neural 7. There are eight pairs of costal bones. Costal 1 is subtrapezoidal in shape and tapers laterally. Its anteroposterior length is not greater than that of the other costals. Costals 1–3 slightly bend anteriorly and costals 1 and 2 show a slight anterior concavity. Costal 4 is oriented perpendicular to the midline, costals 5 and 6 are slightly bent to the posterior, and costals 7 and 8 are strongly bent to the posterior (Fig. 4A). Dorsal ribs 2–9 have flat and triangular distal free ends that fit into corresponding sockets in the peripherals. The rib ends of dorsal ribs 1–8 are neither visible on the dorsal or visceral side of the carapace due to the lack of carapacial fontanelles, but those of dorsal ribs 9 and 10 are visible in ventral view. On the right side of PIN 4636-4-1, dorsal rib 1 is preserved and anteriorly overlaps the margin of dorsal rib 2, whereas laterally it extends roughly to the distal fifth of costal 1. Although dorsal rib 1 is shorter than that of *Hangaiemys* (*Kirgizemys*) *hoburensis* and *Sinemys lens*, the character definition of Joyce (2007) nevertheless requires that we score this taxon as having a 'long' dorsal rib 1, because it spans more than half the length of the costal. The second dorsal rib inserts only into the posterior third of peripheral 3. Dorsal rib 10 inserts into a groove in peripheral 11 on the visceral side of the carapace. The ilial articulation surface is visible on the visceral side of costal 8 (Fig. 4B).

Although the specimen is incomplete, we are confident that 11 pairs of peripherals were present and we number the posterior peripherals accordingly. A distinct gutter extends along the dorsolateral perimeter of the peripheral ring from the posterior half of peripheral 1 to at least peripheral 7 (Fig. 4A). Peripherals 7–11 are laterally expanded compared with the more anterior ones and peripherals 10 and 11 are slightly longer than wide (see a more detailed description of isolated peripherals of *Annemys* sp. from Shar Teg below).

Dorsal vertebrae 1–3, 5, 7, and 8 are preserved in situ in the specimen; they are narrow and bear a low ventral keel along their centra. Dorsal vertebra 1 is about half as long as dorsal vertebra 2. The anterior articulation of the centrum faces anteriorly and slightly ventrally and there are no signs of ventrally curving zygapophyses. The space between the distal portion of the dorsal ribs and the carapace is reduced (Fig. 4B).

Two suprapygals are present, the anterior one being trapezoidal and slightly wider than long and the posterior being very wide and short with biconvex lateral corners. Together with costal 8, suprapygal 2 excludes suprapygal 1 from contacting the peripherals (Fig. 4A).

Carapacial Scales—A wide cervical scale is present that covers the anterior half of the nuchal. There are five narrow vertebrals, the widest being vertebral 1, which is trapezoidal in shape, wider than long, and does not extend onto the peripherals. Vertebral 2 is hexagonal and longer than wide, vertebral 3 is hexagonal and as long as wide, and vertebral 4 is hexagonal and slightly wider than long with angular lateral corners. The sulcus between vertebrals 3 and 4 crosses the anterior third of neural 6. Vertebral 5 is wider than long, covers both suprapygals, slightly extends onto peripheral 11, and probably also onto the pygal, although this portion of the shell is not preserved.

The pleurals are about twice as wide as long and they cover much of the costals. Pleural 1 barely overlaps onto peripherals 1–3 and pleurals 2 and 3 extend onto peripherals 8–11.

There were 12 marginal scales, of which marginals 4–7 extend onto the costals, whereas the rest is restricted to the peripherals. The condition is unclear for marginal 8, because the relevant bones are not preserved. From the posterior half of peripheral 5 to peripheral 7, the sulcus between the marginals and the pleurals extends parallel to the border between the peripherals and the costals (Fig. 4A).

Plastron—The plastron is completely preserved and was found in association with the PIN 4636-4-1 carapace (Fig. 5). It is well ossified, relatively thick, and moderately extensive with a slightly short, wide, anteriorly tapering anterior lobe and a more elongated, narrow, posteriorly tapering posterior lobe. The plastron is thickened at the level of the base of the axillary and inguinal buttresses and along the lateral margin of the posterior lobe. The epiplastra meet one another on the midline, are pentagonal in outline, have rounded anterolateral margins, and almost parallel and transverse anterior and posterior borders. The anterior margin of the plastron is therefore nearly transverse. On the dorsal side of the epiplastra, remnants of the paired dorsally directed epiplastral processes (not cleithra sensu Joyce et al., 2006) are visible in the posteromedial corners of the elements, close to the suture with the entoplastron. In ventral view, the entoplastron is pentagonal, nearly twice as long as wide and its convex anterior margin partially separates the epiplastra from contacting one another. It is tightly sutured with the epiplastra and the hyoplastra via vertical, finely serrated sutures (Fig. 5A). In dorsal view, the entoplastron is more elongated and narrow than in ventral view, tapers posteriorly, and laterally extends a pair of finger-like processes to contact the hyoplastra. It contacts the epiplastra via an inverted 'V'-shaped suture. The interclavicular portion of the entoplastron extends in the form of a low median ridge along the slightly concave surface of the dorsal side of the entoplastron (Fig. 5B). The hyoplastron forms the relatively wide base of the anterior lobe and contributes to the anterior half of the bridge. The plastron contacted the carapace via pegs and ligaments that insert into pits on the peripherals that are aligned into a ventromedially oriented row. The contacts of the axillary and inguinal buttresses appear to be stronger than those of the remaining parts of the bridge. The axillary buttress is moderately developed and contacts the carapace from the posterior half of peripheral 2 to the posterior end of peripheral 3, but does not contact costal 1 (Fig. 4B). The broken distal end of the right axillary buttress is preserved in situ in articulation with the carapace (Fig. 4B). An anterior and a posterior musk duct foramen are present on both hyoplastra and at least one musk duct foramen is present along the anterior portion of the hypoplastron. Mesoplastra are absent. The hypoplastra form the posterior half of the bridge and the relatively narrow base of the posterior lobe. Three pegs for the carapace attachment are preserved on the left side (Fig. 5A). The inguinal buttress terminates on the anterior third of peripheral 8. The distal end of the left inguinal buttress is found displaced on the visceral side of costal 5 (Fig. 4B). The distal portion generally resembles a free rib head in being flat, triangular, and by being ornamented with radiating striations.

The xiphiplastra form slightly more than half of the posterior lobe. An anal notch is absent (Fig. 5A). The dorsal side of the xiphiplastra shows a flat and oval articulation surface for the pubis.

Plastral Scales—There is one pair of gulars and one pair of extragulars. The extragulars are restricted to the epiplastron

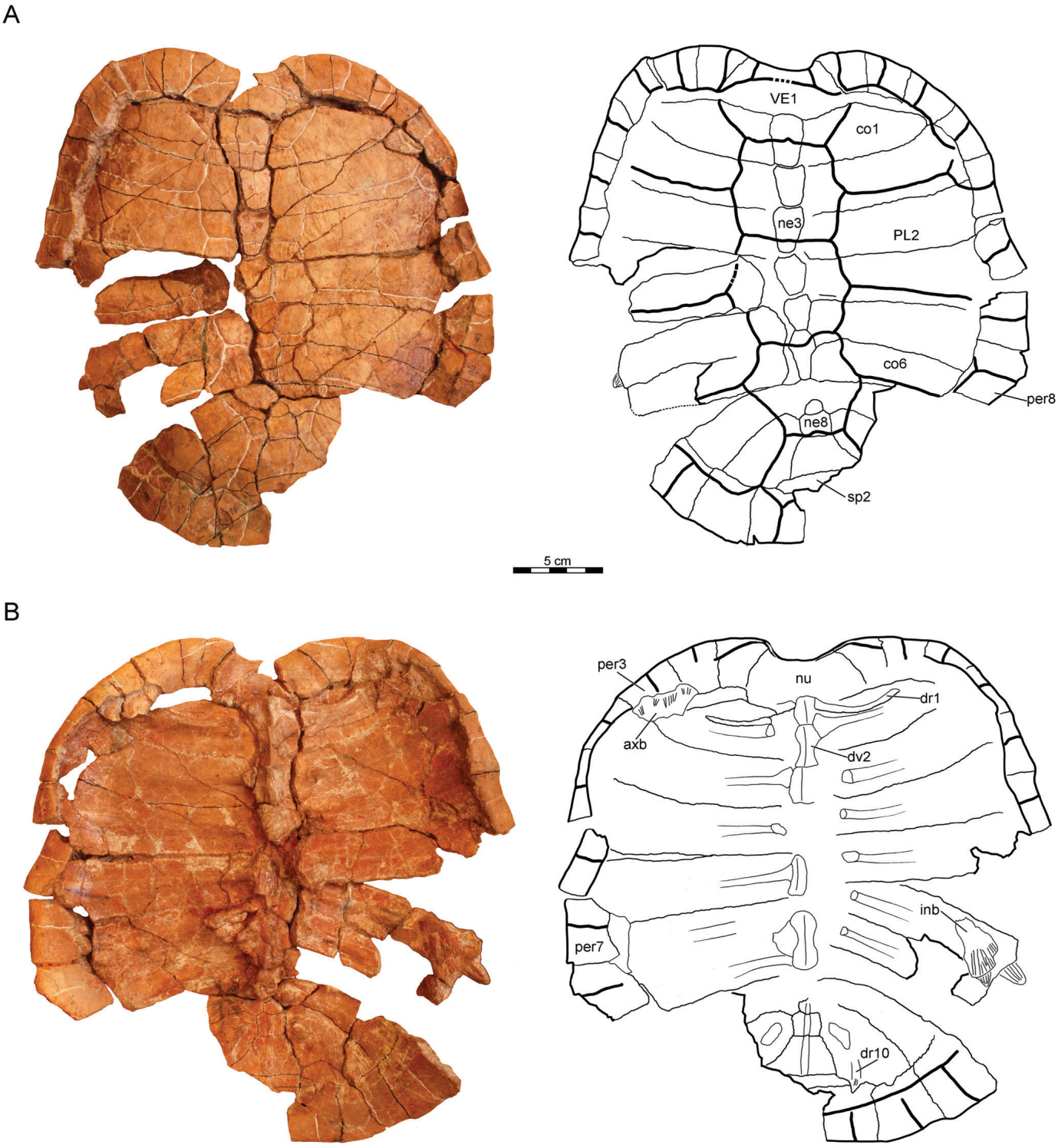

FIGURE 4. PIN 4636-4-1 (holotype), *Annemys levensis*, carapace, Late Jurassic, Shar Teg, Ulan Malgait beds, Govi Altai Aimag, Mongolia. **A**, photograph and line drawing in dorsal view; **B**, photograph and line drawing in ventral view. **Abbreviations**: **axb**, axillary buttress; **co**, costal; **dr**, dorsal rib; **dv**, dorsal vertebra; **inb**, inguinal buttress; **ne**, neural; **nu**, nuchal; **per**, peripheral; **PL**, pleural; **sp**, suprapygal; **VE**, vertebral.

and the left gular slightly extends onto the entoplastron. An asymmetric, aberrant scale and two short, aberrant blind sulci are present on the anterior region of the plastron. The midline sulcus is slightly sinusoidal and the humero-pectoral sulcus is positioned well posterior to the entoplastron. There are four pairs of inframarginals. They are relatively wide, restricted to the plastron, and do not extended on to the peripherals. The pectoral is slightly longer than the abdominal along the midline, but

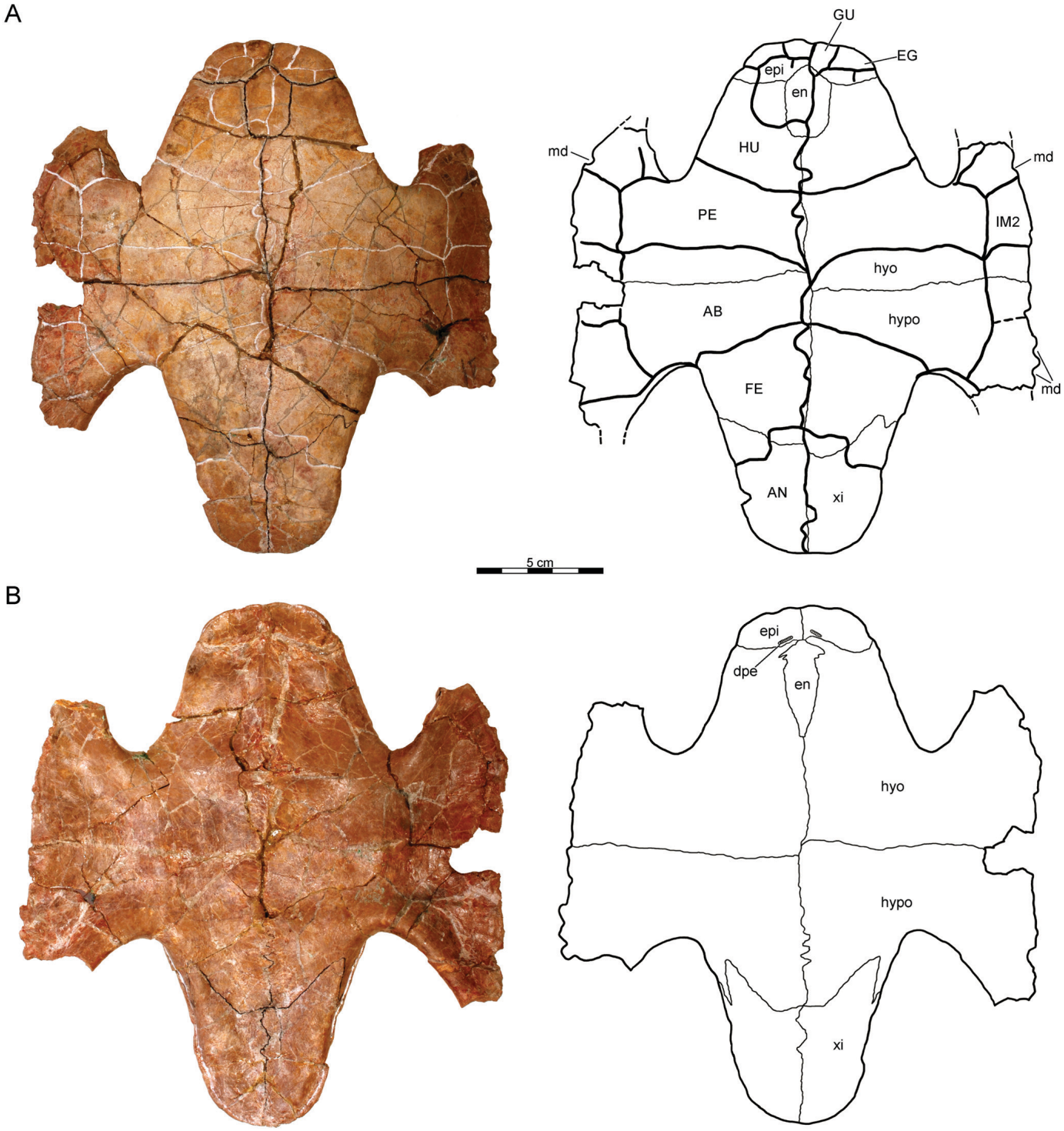

FIGURE 5. PIN 4636-4-1 (holotype), *Annemys levensis*, plastron, Late Jurassic, Shar Teg, Ulan Malgait beds, Govi Altai Aimag, Mongolia. **A**, photograph and line drawing in ventral view; **B**, photograph and line drawing in dorsal view. **Abbreviations**: **AB**, abdominal; **AN**, anal; **dpe**, dorsal process of epiplastron; **EG**, extragulars; **en**, entoplastron; **epi**, epiplastron; **FE**, femoral; **GU**, gular; **HU**, humeral; **hyo**, hyoplastron; **hypo**, hypoplastron; **IM**, inframarginal; **md**, musk duct foramen; **PE**, pectoral; **xi**, xiphiplastron.

significantly shorter than the abdominal laterally. The femoro-anal sulcus is omega-shaped, extends onto the hypoplastron, and covers about 60% of the length of the posterior lobe. The width of this extension makes up about 45% of the posterior lobe width at the base (Fig. 5A).

DESCRIPTION OF *ANNEMYS LATIENS*

Skull

The skull associated with the holotype of *Annemys latiens* (PIN 4636-5-2) is preserved in several fragments in poor condition and

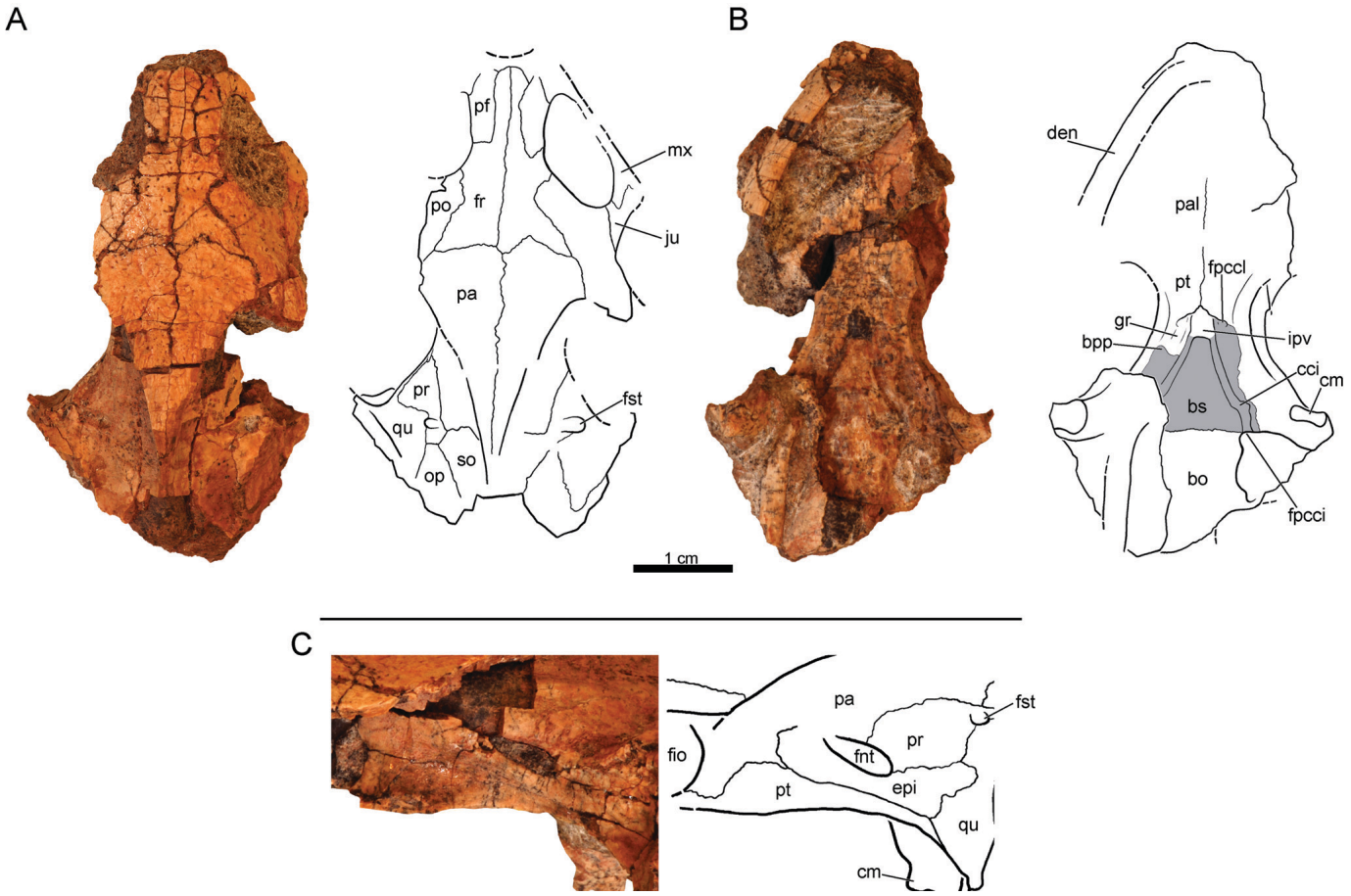

FIGURE 6. PIN 4636-6-1, *Annemys latiens*, skull, Late Jurassic, Shar Teg, Ulan Malgait beds, Govi Altai Aimag, Mongolia. **A**, photograph and line drawing in dorsal view; **B**, photograph and line drawing in ventral view; **C**, left trigeminal region in lateral view. **Abbreviations**: **bo**, basioccipital; **bpp**, basipterygoid process; **bs**, basisphenoid; **cci**, canalis caroticus internus; **cm**, condylus mandibularis; **den**, dentary; **epi**, epipterygoid; **fio**, foramen interorbitale; **fnt**, foramen nervi trigemini; **fpcci**, foramen posterius canalis carotici interni; **fpccl**, foramen posterius canalis carotici lateralis; **fr**, frontal; **fst**, foramen stapedio-temporale; **gr**, groove for palatine branch of carotid artery; **ipv**, interpterygoid vacuity; **ju**, jugal; **mx**, maxilla; **op**, opisthotic; **pa**, parietal; **pal**, palatine; **pf**, prefrontal; **po**, postorbital; **pr**, prootic; **pt**, pterygoid; **qu**, quadrate; **so**, supraoccipital. Gray color indicates eroded surfaces.

includes a partial left ramus of the lower jaw (not figured). The only informative part is the partial basicranium, which indicates that the skull could have been narrower than in *A. levensis*. The rostrum of the basisphenoid is anteriorly incomplete in this specimen, but it appears to be a flat structure. Dorsolaterally to the rostrum sits a pair of short and blunt processus clinoideus that appear to be damaged. The anterior opening of the canalis nervi abducentis is situated at the base of the processus clinoideus. The foramen anterior canalis carotici interni opens laterally to the sella turcica and its diameter is about half the size of the canalis cavernosus. The dorsum sellae slightly overhangs the sella turcica. What is preserved of the lower jaw is comparable to that of *A. levensis*.

PIN 4636-6-2 is an incomplete skull found associated with a partial *Annemys latiens* shell (Fig. 9; see below) that shows a number of distinct morphological characteristics that sharply differ from the skull of *A. levensis* (Fig. 6). The following cranial description focuses on the differences between the two species rather than repeating identical morphologies already described for *A. levensis* (see above).

PIN 4636-6-2 is missing the nasals and the premaxillae, the left maxilla, postorbital and jugal, the posterior end of the right postorbital, and the quadratojugals, squamosals, paroccipital processes, cava tympani, antra postoticum, exoccipitals, and the supraoccipital crest. The palate is largely obscured by matrix and the right dentary is still in articulation with the maxilla. The other dentary sits on the right side of the basicranial region. The ventral surface of the basisphenoid is extensively eroded revealing the canalis caroticus internus.

PIN 4636-6-2 strikingly differs from *Annemys levensis* in general proportions in being considerably more elongate and slender. This is best seen when the relative distance between the quadrate condyles are compared in the two skulls. This distance is approximately 30% less in PIN 4636-6-2 relative to *A. levensis*, even though the skulls have about the same anteroposterior length. Furthermore, the interorbital region of PIN 4636-6-2 is narrower and longer than that in *A. levensis*. The skull shape seen in the referred *A. latiens* skull is consistent with the narrow morphology seen in the holotype of this species (PIN 4636-5-2; see above). Cranial scales are not apparent.

Nasals—PIN 4636-6-2 lacks direct evidence for nasals, but a triangular space between the frontal and prefrontal is suggestive of the former presence of nasals (Fig. 6A). If this assertion were correct, the nasals would have been more trapezoidal shape in this specimen than in *A. levensis*.

Prefrontals—In PIN 4636-6-2, the prefrontals are fully separated from one another by the long anterior process of the frontals, unlike in *A. levensis* (Fig. 6A). This arrangement results in a more elongated shape for the prefrontals in *A. latiens* and slightly more extensive contributions of the prefrontals to the orbital rim relative to the frontals. The foramen interorbitale, the fossa orbitalis, and the fossa nasalis are completely obscured by matrix in this specimen.

Frontals—In PIN 4636-6-2, the anteromedial process of the frontal is longer, almost as long as the remaining parts of the bone and together with the more elongated prefrontal an extensive anteromedial process of the postorbital reduces the contribution of the frontals to the orbital margin relative to *A. levensis* (Fig. 6A). The long anteromedial process of the frontal in *A. latiens* probably also allowed a contact with the nasal, but this element is absent in the only available specimen. The interorbital space is narrower than in *A. levensis*.

Parietals—The parietals had a deep temporal emargination, but its precise extent cannot be clarified due to breakage. The inferior process of the parietal contributes to the dorsal margin of the trigeminal foramen (Fig. 6A).

Jugals—In PIN 4636-6-2, the jugal is present on the left side and its participation in the orbital margin is considerably reduced compared with *A. levensis* as a result of the expanded posterodorsal process of the maxilla (Fig. 6A).

Postorbital—In PIN 4636-6-2, the right postorbital is the least incomplete posteriorly. Both have considerably wider contacts (about twice) with the frontal compared with *A. levensis* thanks to the lateral constriction of the frontals caused by the anteromedial extension of the postorbitals. As a consequence of this, the frontal participation in the orbital margin is reduced in PIN 4636-6-2 relative to *A. levensis* (Fig. 6A).

Maxillae—The maxilla is incompletely preserved on the right side, although much of it is covered by the dentary (Fig. 6A). The maxilla has an expanded posterodorsal process that broadly contributes to the orbit and reduced the contribution of the jugal to the orbit relative to the condition seen in *A. levensis*. The triturating surface is narrow.

Pterygoids—A reduced interpterygoid vacuity is present at the anterior basisphenoid-pterygoid contact in *A. latiens*, similar to that of *A. levensis*. Just lateral to the remnant of the vacuity, still along the basisphenoid contact, there is a pair of incipient foramina, the foramen posterius canalis caroticus lateralis, that communicate with the interpterygoid vacuity and that likely held the palatal branch of the carotid artery (Fig. 6B). As in *A. levensis*, a narrow and shallow canal for the palatine branch of the carotid artery leads to this foramen that originated shortly after the fossa pterygoidea. It is possible that this foramen is present in the skull of *A. levensis*, but was obscured by poor preservation. The foramen posterius canalis carotici interni is not clearly discernable, but it was either formed by the pterygoid and the basisphenoid or solely by the pterygoid at the back of the skull.

Trigeminal Region—The foramen nervi trigemini is formed by the epipterygoid ventrally, the parietal anterodorsally, and the prootic posterodorsally (Fig. 6C). The epipterygoid is rod-like and the strong lip present in *A. levensis* is not apparent. The pterygoid contacts the quadrate posteriorly and it extends ventrally along the epipterygoid. The processus inferior parietalis of the parietal forms the posterior border of the foramen interorbitale and posteriorly it contacts the prootic. Unlike *A. levensis*, no posterior lamina of the parietal is apparent that would overlap the prootic just above the dorsal margin of the trigeminal foramen. There is no evidence of a laminar projection of the quadrate over the posterior half of the epipterygoid either. The pterygoid does not contribute to the posterior margin of the foramen, again unlike in *A. levensis*. These differences must be taken with caution because preservation and ambiguity with the interpretation of the *A. levensis* morphology make a clear comparison difficult.

Otic Region—Much of the cavum tympani and all of the antrum postoticum is missing. The incisura columella auris is slit-like. The quadrate bears with a modest processus trochlearis oticum in a form of a rugose surface (Fig. 6A). The contact of the opisthotic and the prootic hinders the quadrate from contacting the supraoccipital medially. The stapedial foramen opens on the dorsal face of the otic chamber and it is formed by the prootic and slightly by the quadrate. The supraoccipital contacts the opisthotic laterally, the parietal anteriorly, and the prootic anterolaterally.

Basisphenoid—The ventral surface of the basisphenoid is eroded and much of the floor of the canalis caroticus internus is missing. However, when complete, the canal most likely resembled the condition seen in *A. levensis* where only the posterior part of the canal is floored and the split for the palatine and cerebral branches of the carotid artery was not enclosed in bone. The paired basipterygoid process of the basisphenoid is tightly sutured to the corresponding 'pocket' of the pterygoid and it is horizontally oriented. Anteriorly, the basisphenoid terminates in a reduced interpterygoid vacuity that is clearly not the result of erosion. Laterally, the vacuity communicates with a pair of incipient foramen posterius canalis caroticus lateralis present along the basisphenoid-pterygoid contact. As best seen on the right side, a shallow groove leads to this foramen where the palatine branch must have extended. Our interpretation is that the palatine branch entered the skull via this foramen and that the vacuity already lost its function in transmitting the palatine branch at this evolutionary stage.

Shell

PIN 4636-5-1 (the holotype, not associated with the skull described above) is an incomplete shell lacking the right peripherals, the distal half of the right costals, both epiplastra, and parts of the bridge (Fig. 7). It resembles the shell of *A. levensis* in many respects and with the following description we intend to highlight the differences between the two species (most of them already reported in Sukhanov and Narmandakh, 2006).

Unlike in *A. levensis*, PIN 4636-5-1 lacks any ornamentation of the shell, but this might be a preservational artifact. The neural formula of the type specimen of *A. latiens* slightly differs from that of *A. levensis* in having a hexagonal neural 1, a quadrangular neural 2, and in being reduced to seven elements (Fig. 7A). Costal 7 sends a posterior process to contact the suprapygal hindering the midline contact of costals 8. Peripheral 1 is reduced and the nuchal excludes it from contacting costal 1. Vertebrals 2 and 3 are narrower in *A. latiens* and they are longer than wide. Marginals 4–8 overlap onto the costals, particularly marginal 5, as in *A. levensis*.

The plastron has a wider and shorter posterior lobe compared with that of *A. levensis* (Fig. 8). This is also evident from the difference in the relative proportions of the anal scale and the posterior lobe in the two species: in *A. levensis*, the anal scale does not reach the level of the transverse midline of the posterior lobe, whereas in *A. latiens* it extends to the midline (Fig. 8A). The axillary buttress may shortly contact the tip of costal 1 in addition to peripherals 2 and 3 (Fig 7B). In *A. levensis*, the contact with costal 1 is not apparent.

PIN 4636-6-1 is a partial shell preserving the plastron (posteriorly incomplete), the left peripherals 1–9, and the distal parts of costals 1–7 (Fig. 9). The PIN 4636-6-2 skull (see above; Fig. 6) is associated with this shell. We assign this shell (together with the skull) to *A. latiens* based on the presence of a wide posterior lobe and this attribute is confirmed by similarities in the skull. PIN 4636-6 may have a considerably wider entoplastron than all other *Annemys* specimens from Shar Teg, but preservation hinders an unambiguous determination of the original shape of this element.

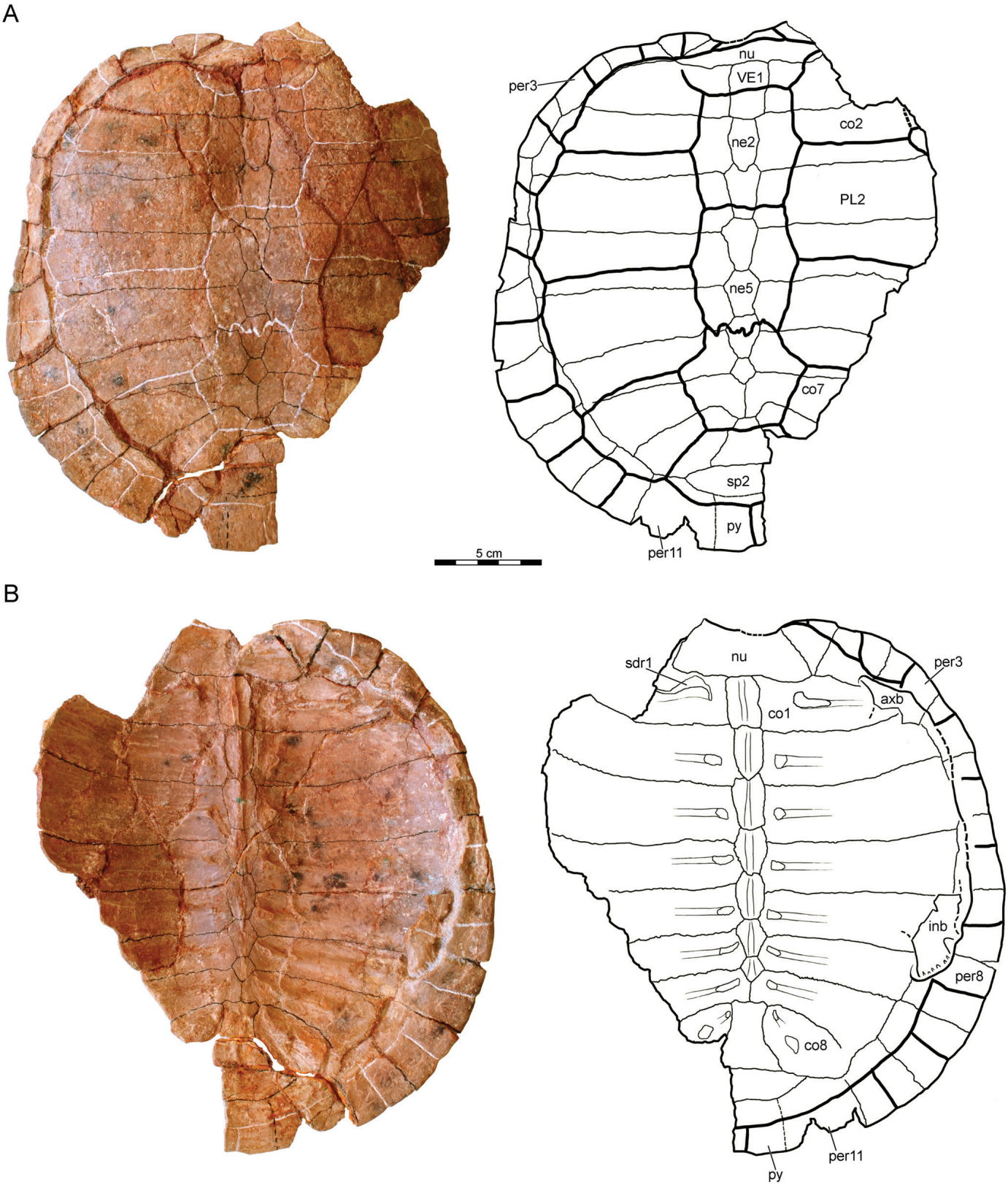

FIGURE 7. PIN 4636-5-1 (holotype), *Annemys latiens*, carapace, Late Jurassic, Shar Teg, Ulan Malgait beds, Govi Altai Aimag, Mongolia. **A**, photograph and line drawing in dorsal view; **B**, photograph and line drawing in ventral view. **Abbreviations**: **axb**, axillary buttress; **co**, costal; **inb**, inguinal buttress; **ne**, neural; **nu**, nuchal; **per**, peripheral; **PL**, pleural; **py**, pygal; **sdr**, scar for dorsal rib; **sp**, suprapygal; **VE**, vertebral.

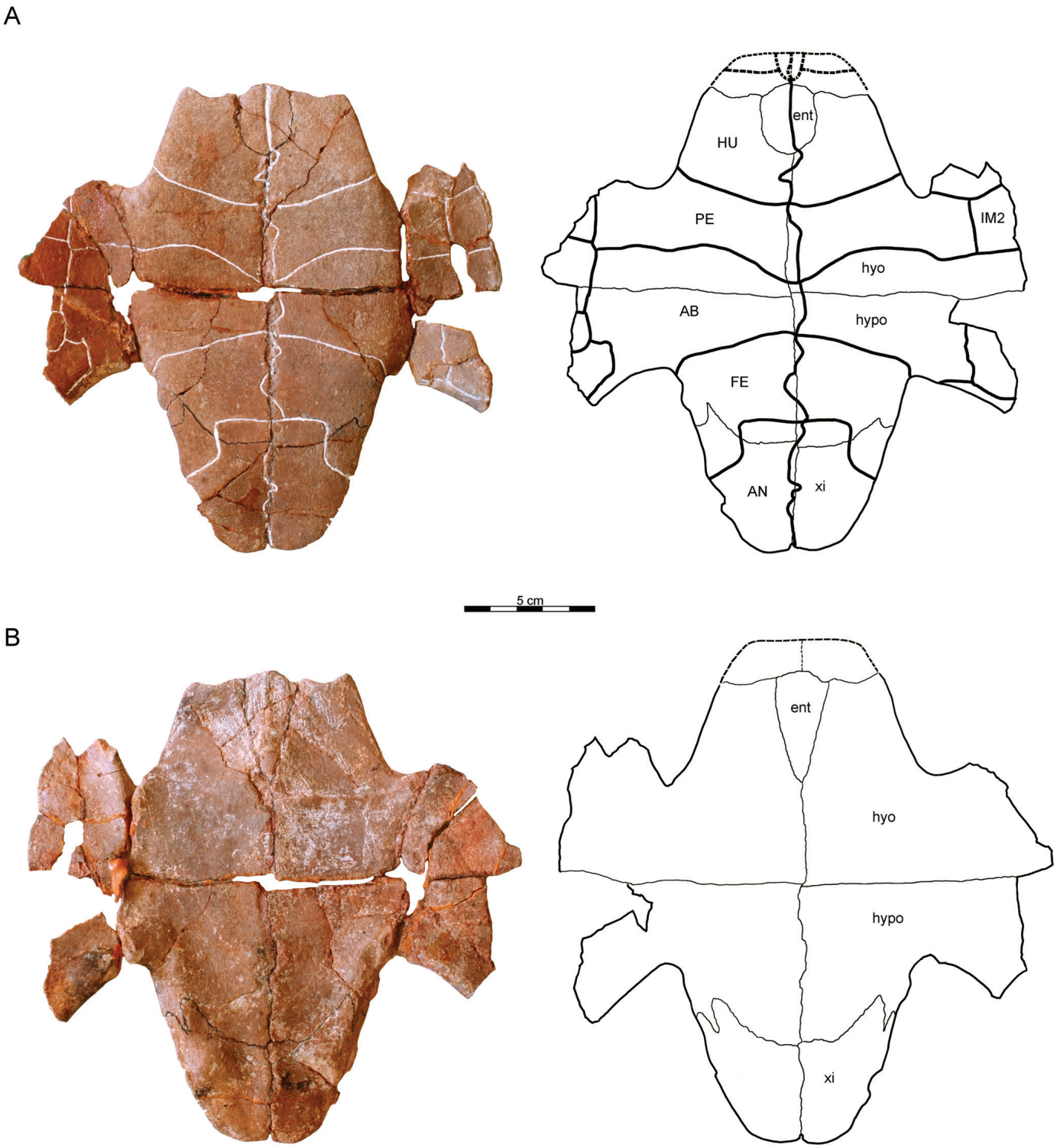

FIGURE 8. PIN 4636-5-1 (holotype), *Annemys latiens*, plastron, Late Jurassic, Shar Teg, Ulan Malgait beds, Govi Altai Aimag, Mongolia. **A**, photograph and line drawing in ventral view; **B**, photograph and line drawing in dorsal view. **Abbreviations**: **AB**, abdominal; **AN**, anal; **ent**, entoplastron; **FE**, femoral; **HU**, humeral; **hyo**, hyoplastron; **hypo**, hypoplastron; **IM**, inframarginals; **PE**, pectoral; **xi**, xiphiplastron.

PIN 4636-7 is a partial shell associated with a humerus (Figs. 10, 12C). It agrees with the morphology of the type specimen of *A. latiens* in having a hexagonal neural 1, a quadrangular neural 2, elongated vertebrals 2 and 3, marginals 4–8 overlapping onto costals (also likely present in the type of *A. levensis*), and a shorter, wider posterior plastral lobe (Fig. 10B). However, unlike the type of *A. latiens*, this specimen has a complete series of neurals preventing the midline contact of both costals 7 and 8. As a consequence, neural 7 is a regular hexagonal element with short sides facing anteriorly versus the pentagonal shape seen in the

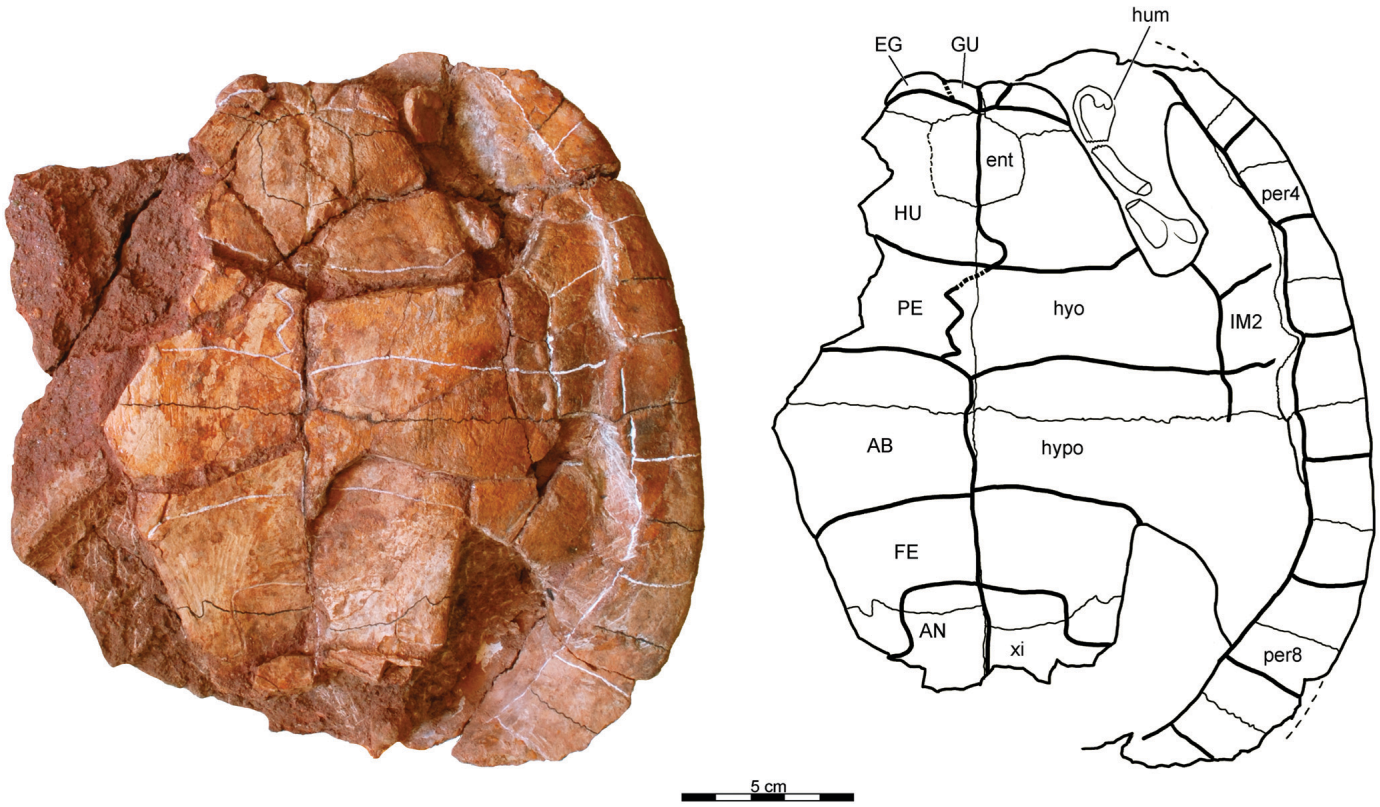

FIGURE 9. PIN 4636-6-2, *Annemys latiens*, plastron and incomplete carapace associated with the PIN 4636-6-2 skull, Late Jurassic, Shar Teg, Ulan Malgait beds, Govi Altai Aimag, Mongolia, photograph and line drawing of shell in ventral view. **Abbreviations**: **AB**, abdominal; **AN**, anal; **EG**, extragulars; **ent**, entoplastron; **FE**, femoral; **GU**, gular; **HU**, humeral; **hum**, humerus; **hyo**, hyoplastron; **hypo**, hypoplastron; **IM**, inframarginals; **PE**, pectoral; **per**, peripheral; **xi**, xiphiplastron.

holotype. Peripheral 1 has a wide contact with costal 1, unlike the holotype of *A. latiens*. A further difference is that in PIN 4636-7 the sulcus between vertebrals 3 and 4 crosses neural 5 instead of neural 6, but vertebrals 4 and 5 display an abnormal, asymmetric morphology and we therefore do not give this difference much weight (Fig. 10A). Plications of the vertebrals are more apparent in PIN 4636-7 than in the holotype of *A. latiens*.

DESCRIPTION OF *ANNEMYS* SP.

Hundreds of fragmentary turtle remains have been collected from the fossiliferous layers at Shar Teg, in particular isolated shell, girdle, and limb bones. Although some of these finds have been cataloged, the vast majority remains without numbers. Our study of the available material reveals that all fragments from Shar Teg originate from turtles of the same size class and that all fragments are consistent with the morphology seen in *Annemys levensis* and *A. latiens*, although species-level differences cannot be discerned. Although little is known about the morphology of coeval xinjiangchelyid turtles, and although the possibility must be acknowledged that some of these remains originate from other taxa, we herein refer all fragmentary material from Shar Teg to *Annemys* sp. and provide a description of the most important elements.

Peripherals

The peripherals (Fig. 11), particularly the bridge peripherals, are relatively thick compared with the small size of *Annemys levensis* and *A. latiens*. Peripheral 1 has a triangular outline and is rather thin and straight in cross-section. Its thickness, however, is 1.5 times greater posteriorly than anteriorly. Dorsally, its margin has an almost flat surface, whereas ventrally it is rounded. Some peripherals 1 are indistinctly guttered, but clear guttering is apparent in peripherals 2–7. The pleuromarginal sulcus passes close and parallel to the medial border of peripheral 1 and one specimen shows the sulcus coinciding with the peripheral 1/nuchal suture.

The posterior inner margin of the visceral side of peripheral 2 has a deep circular pit (or axillary fossa) for articulation with the anterior-most portion of the axillary buttress (Fig. 11A, B). This pit is partially confluent in some specimens with an additional, short, and finger-like scar that is situated at the sutural boundary between peripherals 2 and 3 and that serves as the insertion site for a peg of the hyoplastron (Fig. 11B): however, in other specimens these two structures are separated from one another (Fig. 11A). The position of the axillary fossa is variable ranging from the posterior fifth to the middle of peripheral 2, although it remains unclear whether these differences represent species characteristics. In cross-section, peripheral 2 has a subtriangular outline (Fig. 11A, B) and posteriorly it is two times thicker than anteriorly. The pleuromarginal sulcus passes slightly offset from the medial border of the plate and the intermarginal sulcus crosses the pleuralmarginal sulcus at the level of its anterior third.

Peripheral 3 (together with bridge peripherals 4–7) is elongated, 'C'-shaped in cross-section, and forms the anterior end of the bridge. The ventral plate of the medial rim bears two small pits that are aligned in a row for the reception of the pegs of the hyoplastron (Fig. 11C). The dorsomedial rim of peripherals 4–6

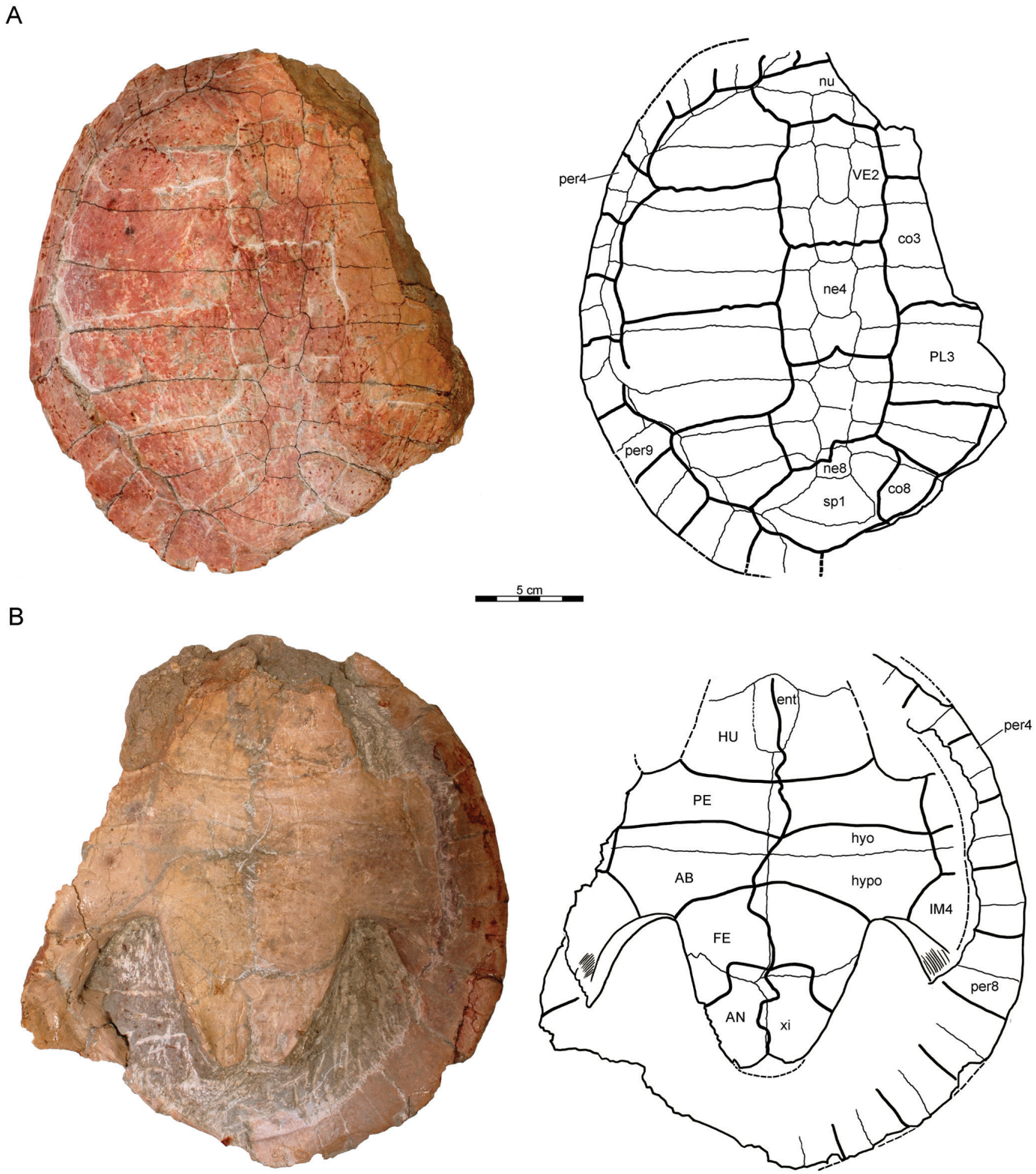

FIGURE 10. PIN 4636-7, *Annemys latiens*, shell, Late Jurassic, Shar Teg, Ulan Malgait beds, Govi Altai Aimag, Mongolia. **A**, photograph and line drawing of carapace in dorsal view; **B**, photograph and line drawing of plastron in ventral view. **Abbreviations**: **AB**, abdominal; **AN**, anal; **co**, costal; **ent**, entoplastron; **FE**, femoral; **HU**, humeral; **hyo**, hyoplastron; **hypo**, hypoplastron; **IM**, inframarginal; **ne**, neural; **nu**, nuchal; **PE**, pectoral; **per**, peripheral; **PL**, pleural; **sp**, suprapygal; **VE**, vertebral; **xi**, xiphiplastron.

(Fig. 11D–F) have a deep emargination where the corresponding convexity of the costal fits (Fig. 11D). These elements are more widely open than peripheral 3.

The medial edge of the ventral plate peripheral 7 (Fig. 11G, H) is perforated with a row of three shallow pits for the plastral pegs. Posteriorly, the pits are replaced by the anterior portion of the well-developed inguinal scar. Dorsal to and between the inguinal scar and the pits for the pegs, peripheral 7 received the free rib end of costal 5. Anteriorly, it is 'C'-shaped in cross-section, whereas posteriorly it is rather triangular and narrow.

Peripheral 8 is wider than long. The inguinal buttress terminates in a circular pit at the anterior inner corner (Fig. 11I). At the posterior inner corner, there is the pit for the insertion of the free rib of costal 6. In cross-section, peripheral 8 is half-moon-shaped (Fig. 11I).

Peripherals 9–11 are wide and flat, with gradually narrowing outline towards to lateral edge in cross-section. The free ribs insert anteriorly in peripheral 9, along the posterior half in 10 and approximately in the middle in 11.

Humerus

A humerus is associated with a shell that is referred to *Annemys latiens* (PIN 4636-7). The well-developed lateral process is placed at the same level as the humeral head and it is oriented ventrolaterally and therefore visible dorsally (Fig. 12C). A humeral shoulder is present. The medial process is slightly more reduced and rounded and the deltopectoral crest extends along the proximal fourth of the shaft. The humeral head is subspherical in dorsal view, with the anterior margin being narrower than the posterior. The shaft is relatively straight and more than twice long as wide. The ectepicondylar foramen is present in a form of a channel and not a fully open groove.

Femur

The femur has a subcircular femoral head and a slightly curved shaft (Fig. 12D). The femur is barely longer than the humerus. The trochanters are moderately developed. The proximal epiphysis has a similar width as the distal one. The trochanter minor faces anteriorly, the trochanter major faces dorsally, and the femoral head only slightly extends above the trochanters.

Scapula

The scapula lacks bony laminae between the dorsal process and the acromion, the glenoid and the acromion, and the glenoid and the dorsal process (Fig. 12B). A well-developed glenoid neck is present and the glenoid is sutured. The relative proportions of the scapular processes show that the acromion is more than half the length of the dorsal process and the angle between them is slightly more than 90°.

Pelvis

Apart from numerous isolated pelvic elements, an excellent complete pelvis comes from the Shar Teg locality (Fig. 12A). The pelvis is well ossified and it was ligamentously attached to the shell. The thyroid fenestrae are separated by a midline projection formed by the pubes and the ischia. The lateral pubic process is well developed, flat, and faces ventrolaterally, and the lateral ischial process is roughly as long as the metischial process. The posterior ilial process is almost perpendicular to the iliac neck in lateral view. The ilium has an elongated neck and a thelial process is absent. The acetabulum is not fused and lacks a posterior notch.

PHYLOGENETIC ANALYSIS

Methods

A maximum parsimony analysis was performed using TNT (Goloboff et al., 2008) based on the character-taxon matrix of Sterli and de la Fuente (2013), which in return is based on that of Joyce (2007), Sterli and de la Fuente (2011), and Sterli et al. (2013). The matrix was expanded by adding five taxa in particular: *Xinjiangchelys radiplicatoides*, *X. junggarensis* (sensu Brinkman et al., 2008), *Annemys levensis*, *A. latiens*, and *Basilochelys macrobios* Tong, Claude, Naksri, Suteethorn, Buffetaut, Khansubha, Wongko, and Yuangdetkla, 2009. The scorings of *X. radiplicatoides* are based on Brinkman et al. (2013), those of *X. junggarensis* on personal observation of IVPP material from Pingfengshan described in Peng and Brinkman (1993), those of *A. levensis* and *A. latiens* based on personal observation of PIN material, and those of *B. macrobios* based on Tong et al. (2009) and photographs obtained from H. Tong. We refrained from adding poorly known/described relevant taxa (e.g., *Anatolemys* spp., *Shartegemys laticentralis*, *Macrobaena mongolica*) to the matrix to minimize the risk of introducing mistakes.

We note that the scorings for *Xinjiangchelys latimarginalis* sensu Peng and Brinkman (1993) (= *X. junggarensis* sensu Brinkman et al., 2008) are likely based on a chimera. Brinkman and Wu (1999) used *X. latimarginalis* as a terminal taxon, but their scorings were based on material from two distantly placed localities: the shell characters were based on material from the Pingfengshan locality of the Junggar Basin, Xinjiang, China (Peng and Brinkman, 1993), whereas the skull characters were scored for material from Kyrgyzstan (Fergana Basin, Sarykamyshsay locality) after Kaznyshkin et al. (1990). However, Nessov (1995) separated the Fergana *X. latimarginalis* from the Junggar *X. latimarginalis* and included the former into a new species, *X. tianshanensis*. Joyce (2007) and all subsequent phylogenetic workers adopted the scorings of Brinkman and Wu (1999) for *X. latimarginalis*. For the present analyses, we considered *X. latimarginalis* synonymous with *X. junggarensis*, as suggested by Brinkman et al. (2008), and rescored this taxon based on Pingfengshan material only, as observed directly by W.G.J. and M.R. or described in Peng and Brinkman (1993). All skull characters for this taxon were therefore scored as '?' because no skull material is available from this locality.

The following scorings were changed relative to the matrix of Sterli and de la Fuente (2013; original scorings of Sterli and de la Fuente are in parenthesis): Epiplastron B: *Hangaiemys hoburensis*: 1 (?), *Sinemys lens* 1 (?); Pterygoid B: *Hangaiemys hoburensis* 1(2), *Dracochelys bicuspis* 1(2), *Pleurosternon bullockii* 1(2), *Kallokibotion bajazidi* 1(2), *Mongolochelys efremovi* 1(2), *Peligrochelys walshae* 1(2), *Chubutemys copelloi* 1(2) *Niolamia argentina* Ameghino, 1899?(2), *Eileanchelys waldmani* ?(2); Carapace D: *Hangaiemys hoburensis* 0(?), *Chengyuchelys baenoides* Young and Chow, 1953 (IVPP-V6507) 0(1); Carapace E: *Hangaiemys hoburensis* –(?); Vertebral A: *Siamochelys peninsularis* ?(1); Vertebral C: *Siamochelys peninsularis* ?(1); Anal A: *Siamochelys peninsularis* ?(0), *Chengyuchelys baenoides* ?(0); Entoplastron B: *Chengyuchelys baenoides* ?(1); Mesoplastron A: *Siamochelys peninsularis* 2(0); Hypoplastron A: *Chengyuchelys baenoides* ?(0); Xiphiplastrons A and B: *Chengyuchelys baenoides* ?(0); Dorsal Rib A: *Siamochelys peninsularis* ?(2); Plastral Scute B: *Siamochelys peninsularis* Tong, Buffetaut, and Suteethorn, 2002: 1(0).

The character Cervical Vertebrae A was omitted from the analysis because we found it difficult to replicate this character objectively and perceived a number of inconsistencies in the matrix. The character Diploid Number A was also omitted following the discussion in Joyce and Bell (2004) and Joyce (2007).

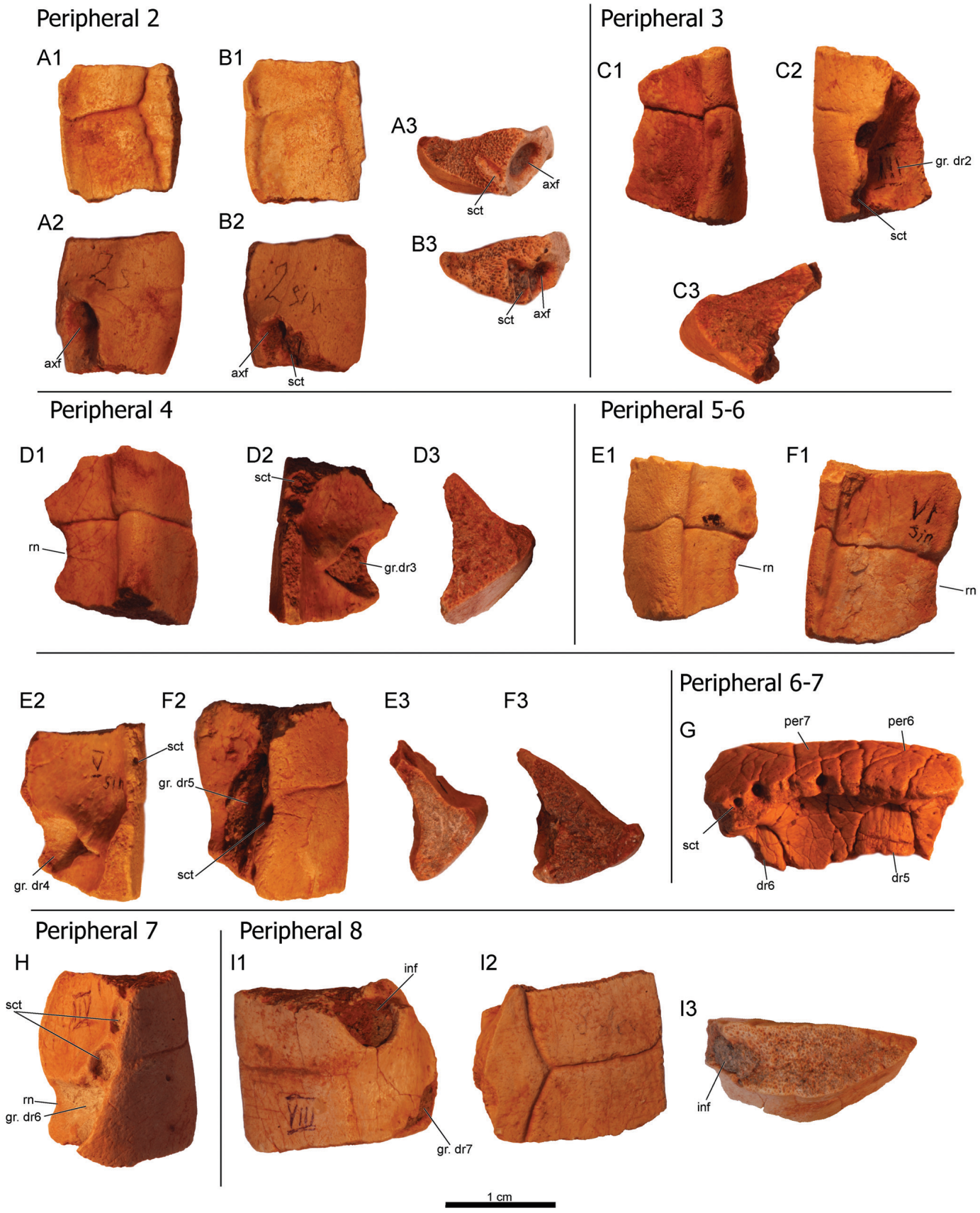
Peripheral 2
A1
B1
A3
axf
sct
A2
B2
B3
axf
axf
sct
sct
axf
Peripheral 3
C1
C2
gr. dr2
sct
C3
Peripheral 4
D1
D2
D3
sct
rn
gr.dr3
Peripheral 5-6
E1
F1
rn
rn
E2
F2
E3
F3
Peripheral 6-7
G
per7
per6
sct
gr. dr5
sct
gr. dr4
sct
dr6
dr5
Peripheral 7
H
sct
rn
gr. dr6
Peripheral 8
I1
inf
I2
I3
gr. dr7
inf
1 cm

The following characters were treated as ordered: 7 (Nasal A), 19 (Parietal H), 27 (Squamosal C), 40 (Maxilla D), 42 (Vomer A), 50 (Quadrate B+C), 52 (Antrum Postoticum A), 59 (Pterygoid B), 81 (Opisthotic C), 82 (Opisthotic D), 89 (Stapedial Artery B), 98 (Canalis Caroticum F), 120 (Carapace A), 121 (Carapace B), 130 (Peripheral A), 133 (Costal B), 138 (Supramarginal A), 158 (Hyoplastron B), 159 (Mesoplastron A), 161 (Hyoplastron B), 176 (Abdominal A), 213 (Cleithrum A), 214 (Scapula A), 232 (Manus B), and 233 (Manus C). *Sphenodon punctatus*, *Owenetta kitchingorum*, *Simosaurus gaillardoti*, and *Anthodon serrarius* were designated as outgroups following Sterli and de la Fuente (2013).

A preliminary analysis of this character-taxon matrix failed in that multiple runs consistently arrived at different results. We suspect that these difficulties are caused by a combination of rampant homoplasy, missing data, and the sheer size of the matrix. Given that this analysis is focused on the phylogenetic relationships and placement of xinjiangchelyid turtles, we decided to crop taxa not pertinent to these questions (e.g., most derived baenids, most meiolaniiforms) and a broad spectrum of taxa known from fragmentary material only (see Appendix 1 for a complete list). The resulting matrix consists of 237 characters for a total of 83 terminal taxa. The character-taxon matrix and the TNT file are provided as Supplementary Data.

The most parsimonious trees were found using two rounds of the heuristic search tree-bisection-reconnection (TBR), during which thousands of random addition sequences replicates were produced and 15 trees saved per replicate. The trees retained in the memory were exposed to a second round of TBR. The relationships of living cryptodiran taxa were manually constrained according to recent results of molecular phylogenetic studies (as suggested by Danilov and Parham, 2006, 2008), without assuming a priori, however, that Trionychia nests within Cryptodira (Krenz et al., 2005; Barley et al., 2010). The internal relationships of durocryptodires were constrained using the molecular topology of Barley et al. (2010) (i.e., (Emydidae (Geoemydidae + Testudinidae)) + (Chelonioidea (Chelydridae + Kinosternoidea)))). The complete list of taxa designated as floaters can be found in Appendix 2. By enforcing these constraints, TNT failed to find the most parsimonious trees (MPTs); therefore, the heuristic search was repeated until the MPTs were found 30 times during each replicate (using the command 'xmult = hits 30;'). After this, the trees retained in the memory were exposed to a second round of TBR. Strict consensus trees were calculated and rogue taxa were pruned a posteriori from the constrained analyses to achieve better resolution.

Results

The second round of TBR found 2916 trees (length = 867 steps) with a poorly resolved strict consensus topology. Nevertheless, an unresolved xinjiangchelyid clade composed of *Annemys levensis*, *A. latiens*, *Xinjiangchelys radiplicatoides*, and *X. junggarensis* was recovered, supported by a single unambiguous synapomorphy: presence of pronounced sinusoidal midline plastral sulcus (Plastral Scutes B). This clade has an unorthodox placement outside of crown group Testudines in a polytomy with baenids and pleurosternids (Fig. 13; see also Supplementary Data, Fig. S1, for complete consensus tree). When *X. junggarensis* is pruned (not shown), *A. levensis* is found as the sister taxon of *X. radiplicatoides* and *A. latiens*. Several wildcard taxa are identified, including *Yehguia tatsuensis*, *Basilochelys macrobios*, *Adocus beatus*, *Shachemys laosiana*, *Plesiochelys etalloni*, *Solnhofia parsonsi*, *Portlandemys mcdowelli*, *Santanachelys gaffneyi*, '*Thalassemys*' *moseri*, *Xinjiangchelys junggarensis*, *Siamochelys peninsularis*, *Chengyuchelys baenoides*, and *Judithemys sukhanovi*. When these taxa are pruned from the consensus cladogram (not shown), *Ordosemys leios*, *Dracochelys bicuspis*, *Sinemys lens*, and *Hangaiemys hoburensis* are placed at the stem of Testudines.

Following our proposed definitions, Xinjiangchelyidae consists of *A. levensis*, *A. latiens*, *X. radiplicatoides*, and *X. junggarensis*, whereas Sinemydidae only consists of *S. lens*. The name Macrobaenidae cannot be applied because it is not included in our analysis.

DISCUSSION

Phylogenetic Relationships of Xinjiangchelyidae

Our analysis clearly recovered a monophyletic clade that partially recreates the 'traditional' concept of Xinjiangchelyidae of some authors (e.g., Sukhanov, 2000) and to which the phylogenetic definition of the name Xinjiangchelyidae applies. The position of Xinjiangchelyidae outside of Testudines is, on the other hand, a rather unorthodox result (Fig. 13). Xinjiangchelyids are known to possess several primitive characters, including the presence of nasals, amphicoelous cervical vertebrae, chevrons, and dorsal process of epiplastron, yet previous analyses hypothesized a more derived position within Pancryptodira (Brinkman and Wu, 1999; Gaffney et al., 2007; Joyce, 2007; Danilov and Parham, 2008; Tong et al., 2009, 2012a; Anquetin, 2012) or near the base of crown Testudines (Sterli, 2010; Sterli and de la Fuente, 2011). The basal position in the present analysis is likely caused by numerous changes we undertook to the scoring of *Xinjiangchelys junggarensis*, *Siamochelys peninsularis*, and of *Annemys* from Shar Teg, which almost universally resulted in the recognition of primitive character states in these taxa (e.g., presence of interpterygoid vacuity, presence of basipterygoid process, open foramen jugulare posterius, long dorsal rib 1, position of the transverse process of the cervical in the middle of the centrum). Given that we are aware of similar adjustments to the scoring that will need to be undertaken for various sinemydids, macrobaenids, and plesiochelyids, we consider our results tentative pending a revision of the detailed morphology of the aforementioned taxa.

The results of our analysis are partially consistent with the only previous global analysis that included *Annemys levensis* (Anquetin, 2012), who scored this taxon on the basis of the preliminary reports by Sukhanov (2000) and Sukhanov and Narmandakh (2006). The analysis of Anquetin (2012) recovered Xinjiangchelyidae within Testudines and revealed that it consists of five taxa, including *Xinjiangchelys qiguensis*, *X. latimarginalis* sensu Peng and Brinkman, 1993 (= *X. junggarensis*), *X. tianshanensis*, *Annemys levensis*, and *Siamochelys peninsularis*. Although our analyses differs in the position of

← FIGURE 11. *Annemys* sp., peripherals, Late Jurassic, Shar Teg, Ulan Malgait beds, Govi Altai Aimag, Mongolia. **A**, PIN 4636-15, left peripheral 2, **A1**, dorsal view, **A2**, ventral view, **A3**, posterior view; **B**, PIN 4636-22, left peripheral 2, **B1**, dorsal view, **B2**, ventral view, **B3**, posterior view; **C**, PIN 4636-17, peripheral 3, **C1**, dorsal view, **C2**, ventral view, **C3**, anterior view; **D**, PIN 4636-23, right peripheral 4, **D1**, dorsal view, **D2**, ventral view, **D3**, posterior view; **E**, PIN 4636-18, left peripheral 5, **E1**, dorsal view, **E2**, ventral view, **E3**, anterior view; **F**, PIN 4636-19, left peripheral 6, **F1**, dorsal view, **F2**, ventral view, **F3**, anterior view; **G**, PIN 4636-16, right incomplete peripheral 6 and peripheral 7, ventral view; **H**, PIN 4636-20, left peripheral 7, ventral view; **I**, PIN 4636-21, left peripheral 8, **I1**, ventral view, **I2**, dorsal view, **I3**, anterior view. **Abbreviations**: **axf**, axillary fossa; **gr. dr**, groove for reception of tip of dorsal rib; **inf**, inguinal fossa; **per**, peripheral; **rn**, rib notch; **sct**, socket for plastral peg.

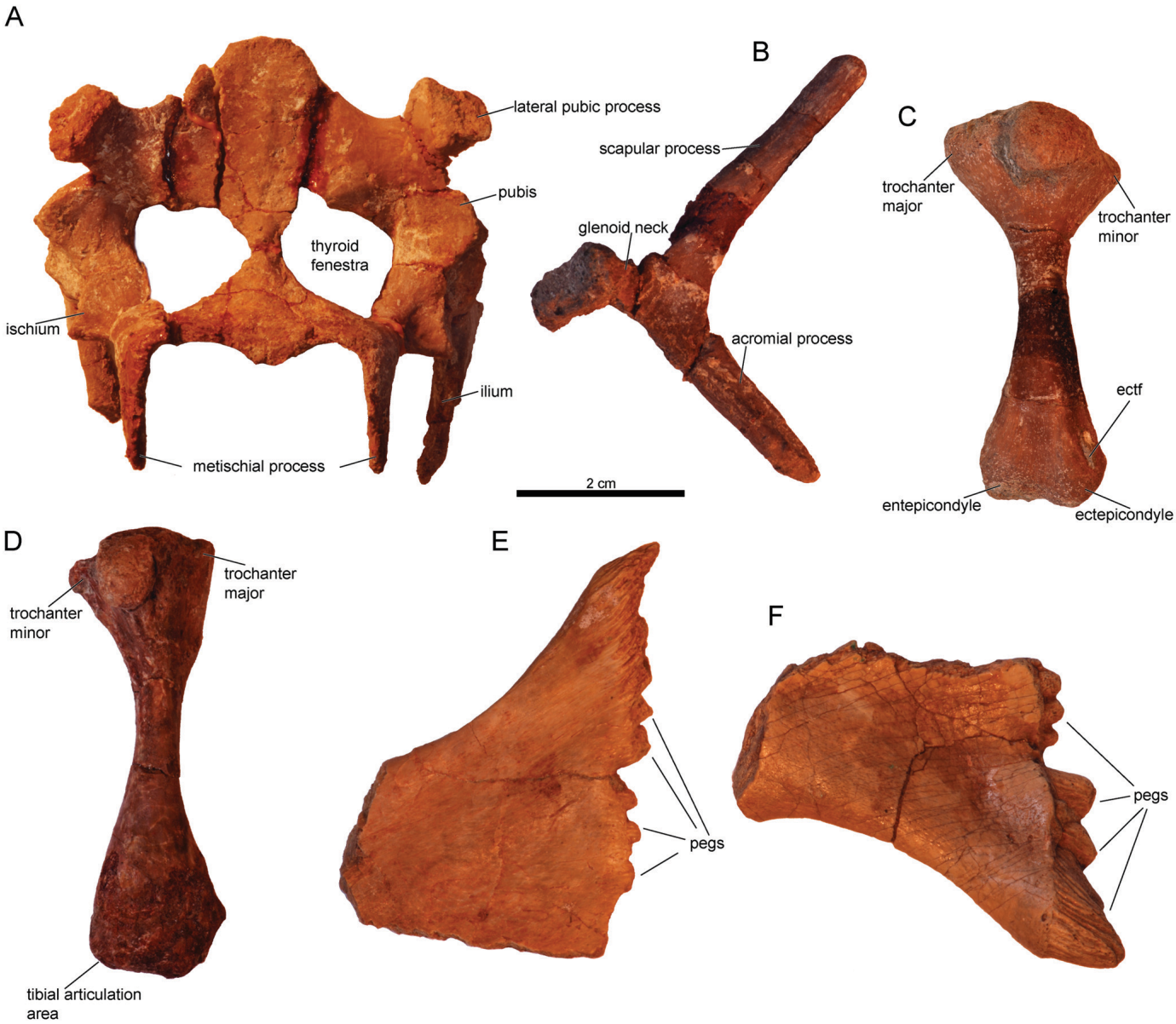

FIGURE 12. *Annemys* sp., appendicular elements, Late Jurassic, Shar Teg, Ulan Malgait beds, Govi Altai Aimag, Mongolia. **A**, PIN 4636-10, *Annemys* sp. pelvis in ventral view; **B**, PIN 4636-11, *Annemys* sp. right scapula in lateral view; **C**, PIN 4636-7, *A. latiens* right humerus in dorsal view; **D**, PIN 4636-12, right femur in dorsal view; **E**, PIN 4636-13, *Annemys* sp. left lateral part of hyoplastron with axillary buttress in ventral view; **F**, PIN 4636-14, *Annemys* sp. right lateral part of hypoplastron with inguinal buttress in dorsal view. **Abbreviation**: **ectf**, ectepicondylar foramen.

Xinjiangchelyidae and *Siamochelys peninsularis*, our study agrees with Anquetin (2012) in that *A. levensis* and *X. junggarensis* (= *X. latimarginalis*) are members of the group in question.

Presence of a Reduced Interpterygoid Vacuity in *Annemys*

One of the most interesting observations regarding the cranial morphology of *Annemys levensis* and *A. latiens* is the presence of a small gap between the pterygoid and the basisphenoid. In basal turtles, such as *Proganochelys quenstedti* Baur, 1887, *Kayentachelys aprix* Gaffney, Hutchison, Jenkins, and Meeker, 1987, and *Condorchelys antiqua* Sterli, 2008, the palatine artery entered the skull via a wide gap between the pterygoids, the interpterygoid vacuity. The vacuity is absent in all more derived fossil turtles and the palatine artery therefore entered the skull through a pair of distinct foramina, the foramina posterius canalis carotici lateralis (fpccl). *Annemys latiens* clearly displays an intermediate morphology by displaying both a pair of fpccl and remnants of the pterygoid vacuity. The corresponding region in *A. levensis* is somewhat damaged, but a pair of grooves that lead to the lateral edge of the gap and that evidently held the palatine arteries is indicative of the former presence of paired fpccl. Slit-like fpccl have otherwise been reported for *Xinjiangchelys radiplicatoides* (Brinkman et al., 2013), but this taxon shows no sign of a gap anterior to the basisphenoid and therefore represents the derived condition. The slit-like shape of the palatine foramina implies that the anterior contact of the basisphenoid with the pterygoid was at best poorly ossified in this xinjiangchelyid. An unossified area between the pterygoids coupled with fpccl is also present in *Annemys* sp. from Wucaiwan, Junggar Basin

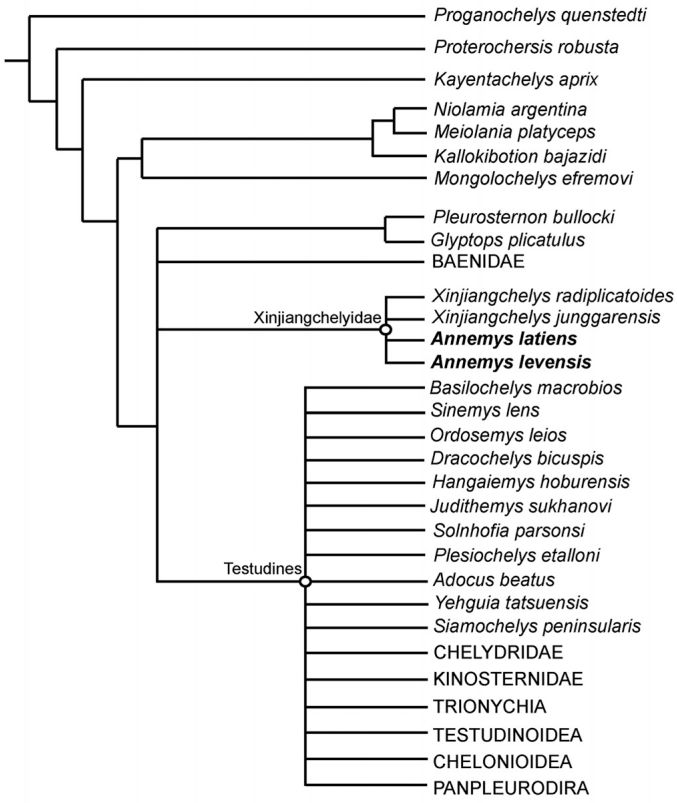

FIGURE 13. Simplified strict consensus tree of 2916 equally parsimonious trees (length = 867 steps) obtained after a maximum parsimony analysis of the modified taxon-character matrix of Sterli and de la Fuente (2013) including 83 taxa and 237 characters. The internal relationships of Durocryptodira is constrained after Barley et al. (2010): (Emydidae (Geoemydidae + Testudinidae)) + (Chelonioidea (Chelydridae + Kinosternoidea))). The inclusion of *Annemys latiens*, *A. levensis*, and *Xinjiangchelys radiplicatoides* into Xinjiangchelyidae is only supported by one character: presence of pronounced midline plastral sulcus (Plastral Scutes B). For complete consensus tree, see Supplementary Data, Figure S1.

(Brinkman et al., 2013), and is therefore consistent with the morphology of *A. latiens* and what is inferred for A. *levensis*. A larger sample of xinjiangchelyid skulls may eventually reveal that the gap between the pterygoids closes during ontogeny and abundant material from the Turpan Basin (Wings et al., 2012) is particularly promising (pers. observ. of material by M.R. and W.G.J.).

The palatine arteries probably entered via the fpccl in these taxa and the xinjiangchelyid condition may represent an evolutionary stage when the interpterygoid vacuity was not yet closed completely but already lost its function in carrying the palatine artery.

Taxonomy of *Annemys*

The taxa *Annemys levensis* and *A. latiens* were used informally in Sukhanov (2000) for material from the Upper Jurassic of Shar Teg, Mongolia, and the names were only made available following the rules of the International Commission on Zoological Nomenclature in a subsequent paper by Sukhanov and Narmandakh (2006). *Annemys latiens* is based on an almost complete shell (PIN 4635-5-1) associated with a poorly preserved lower jaw ramus and multiple skull fragments, of which the partial basicranium (PIN 4635-5-2) is the most informative. This damaged skull was not reported in Sukhanov (2000) or Sukhanov and Narmandakh (2006) and *A. latiens* was diagnosed relative to *A. levensis* on the basis of shell characters only (Sukhanov and Narmandakh, 2006). Another, previously unreported *A. latiens* skull-shell association from Shar Teg (PIN 4636-6) reveals distinct cranial differences relative to the skull of *A. levensis* (see above) and thereby supports the presence of two separate taxa at Shar Teg using cranial characters. The carapace (PIN 4636-6) of the associated skull is very incomplete, but its wide posterior plastral lobe is consistent with the morphology seen in the holotype of *A. latiens*. The small amount of information that we were able to extract from the badly preserved holotype skull of *A. latiens* (PIN 4636-5-2) agrees with PIN 4636-6-2 in being narrow and elongated, unlike *A. levensis* (see the description of PIN 4636-6-2 above). We tentatively also refer another shell (PIN 4636-7) to *A. latiens* based on the proportions of the posterior plastral lobe (see the description of this shell above). *Annemys levensis* is therefore only known from a single specimen, the type specimen (PIN 4636-4), which consists of an associated skull, lower jaw, shell, and some other appendicular elements. Additional material from Shar Teg may allow a better understanding of the intra- and interspecific variation in *Annemys* and at present it seems difficult to distinguish the two species on the basis of discrete shell characters. The lack of characters that allow distinguishing the postcranial of *A. levensis* and *A. latiens* forces us to refer all fragmentary remains to *Annemys* sp.

Matzke et al. (2004b) and Tong et al. (2012b) both synonymized *Annemys* with *Xinjiangchelys* because their phylogenetic analysis of 'xinjiangchelyids' revealed *A. levensis* and *A. latiens* to be situated within a clade formed by taxa typically attributed to *Xinjiangchelys*. However, neither analysis included any member of the 'sinemydid-macrobaenid' grade or other more advanced Pancryptodires but instead extensively sampled 'xinjiangchelyid' taxa—to an extent that it seems the authors a priori inferred that *Annemys* belong to the latter group. Our global analysis found *Annemys levensis* in a monophyletic clade with *X. latimarginalis* (sensu Peng and Brinkman, 1993), but the inclusion of more xinjiangchelyid taxa are required to test the monophyly of this group and the relationship of *Annemys* to *Xinjiangchelys* spp. Our analysis found no evidence for the exclusive monophyly of *Annemys* (Fig. 13), but we do not consider our analysis to be a highly rigorous test of the relationships of this taxon within xinjiangchelyids because our taxonomic sample is limited for this group. Until the phylogenetic relationships of xinjiangchelyid taxa have been resolved with greater assurance, we suggest keeping the name *Annemys*.

Brinkman et al. (2013) recently described and figured a skull with associated shell elements from the Upper Jurassic of the Junggar Basin (Wucaiwan area, Xinjiang, China) that they referred to *Annemys* sp. (also figured in Rabi et al., 2010:fig. 1g, h). As in A. *latiens* and A. *levensis*, this skull has an unossified gap anterior to the basisphenoid between the pterygoids; therefore, we agree that it is morphologically closer to *Annemys* spp. than to *Xinjiangchelys radiplicatoides*. We also agree that this skull is clearly different from that of *A. levensis* (see Brinkman et al., 2013, for a list of differences). The *Annemys* sp. skull is furthermore different from *A. latiens* in its proportions, by being less elongated and by having a distinctly more extensive frontal and jugal contribution to the orbit compared with *A. latiens*. We therefore suggest that this fossil represents a taxon different from both *A. levensis* and *A. latiens*, but likely closely related to them.

Paleoecology of *Annemys*

The overall shell morphology and the size of *A. latiens* and *A. levensis* are highly similar and these taxa are therefore only poorly diagnosed by the shells. On the other hand, the skulls of these two turtles are greatly different in the arrangement of the

dermal roofing elements and in their relative proportions: *A. latiens* has an elongated and narrow skull compared with the relatively broad skull of *A. levensis*.

Both species originate from a single larger horizon at Shar Teg (i.e., the Ulan Malgait beds); therefore, they may have been sympatric taxa, although no clear record exists of their co-occurrence in identical layers. However, whereas the absence of size difference may have allowed both taxa to share the same aquatic habitat, the distinct skull shapes suggest niche partitioning in terms of feeding strategies.

It is apparent from the depositional environment in which they were found that *Annemys latiens* and *A. levensis* were freshwater turtles. This conclusion is further supported by their overall anatomy: low, suboval shell, flat skull, and relatively straight humeral and femoral shafts. However, these two taxa were probably not as adapted to the aquatic realm as *Hangaiemys* (*Kirgizemys*) *hoburensis*, *Ordosemys leios*, or *Sinemys lens*, all of which exhibit more reduced shells. The flat, triangular skull with narrow and sharp triturating surfaces in *Annemys* spp. is consistent with a predatory lifestyle. In being elongated and flat, *A. latiens* had an even more streamlined skull compared with *A. levensis,* which may have been of great help while striking at small agile prey such as fish. Future collecting at Shar Teg should focus on finding the cervical vertebrae of *Annemys* in order to clarify whether they were short- or long-necked forms.

The Ecological Diversity of Xinjiangchelyidae during the Late Jurassic—Xinjiangchelyids have so far been mostly known from their shells, which are surprisingly uniform and conservative in their morphology, although size differences of some taxa with uncertain affinities are apparent (e.g., Matzke et al., 2005). However, new data (Brinkman et al., 2013, and this paper) indicate that the skull shape of xinjiangchelyids was more variable than their shells. At present, only a few xinjiangchelyids are known from their skulls, but these can nevertheless be clearly classified into three morphotypes. The first morphotype is represented by an inflated and relatively high skull shape with shallow upper temporal emargination, as seen in *Xinjiangchelys radiplicatoides* (Brinkman et al., 2013). The second is small, flat, and triangular with deeper temporal emargination, as seen in *Annemys levensis* and *Annemys* sp. from the Junggar Basin (Brinkman et al., 2013). The third is an elongated, narrow variant of the second type and seen in *A. latiens*. These morphotypes probably correspond to different feeding niches and strategies and indicate that by the Late Jurassic, the dominant turtle clade of Asia achieved only a moderate level of ecological diversity relative to what is present in later (e.g. Cretaceous) Pancryptodires, a group in which xinjiangchelyids are traditionally placed. However, it must be noted that the lack of skull material for most Jurassic Asian turtles may result in a significant underestimate of their actual ecological diversity.

Functional Aspects of the Trochlear System in *Annemys*—The skulls of *A. latiens* and *A. levensis* reveal that the processus trochlearis oticum is very poorly developed in these taxa and may not even qualify as a real process. The trochlear structure is best preserved in the skull of *A. levensis*. It consists of a rugose area on the anterodorsal wall of the otic chamber (Fig. 1A, B) and lacks the protrusion seen in many crown cryptodires (e.g., Gaffney, 1979; Joyce, 2007; Sterli and de la Fuente, 2010; Joyce and Sterli, 2012). It is likely that this surface held the cartilage that redirected the temporal musculature (the cartilago transiliens) over the otic capsule before reaching the coronoid process of the lower jaw (Schumacher, 1973). The undeveloped bony base of the synovial capsule suggests that the trochlear system of *Annemys* was not as advanced as in crown cryptodires. This would be consistent with the thickened laterally protruding lip of the epipterygoid present in *A. levensis* that could have served as a barrier that hindered the adductor musculature from crossing the path of the trigeminal nerve. The primitive trochlear system of *Annemys* spp. could result in lower bite performance relative to most crown cryptodires. This is probably correlated with the short supraoccipital process (at least present in *A. levensis*) that only allows for a reduced amount of muscle mass, but also does not require an advanced and well-developed trochlear system (Herrel et al., 2002; Sterli and de la Fuente, 2010).

CONCLUSIONS

Our thorough morphological revision of all available material from the Late Jurassic locality of Shar Teg, Mongolia, confirms the presence of two species of *Annemys*, *A. latiens* and *A. levensis*. Although both species exhibit highly similar shells, they clearly differ in the morphology of their skulls. In particular, whereas *A. levensis* has the relatively broad skull typical of generalist aquatic feeders, *A. latiens* has the elongate skull typical of piscivorous turtles. It is therefore likely that these two turtles shared the same habitat but pursued distinct feeding strategies. We expect future collecting at Shar Teg to produce higher quality postcranial material and anticipate that these two taxa will be distinguishable based on shell characters at some point in the future.

Our inclusion of *A. latiens, A. levensis*, *Xinjiangchelys junggarensis*, and *X. radiplicatoides* into a global analysis of turtle relationships united these taxa in a weakly supported clade and resulted in the hypothesis that xinjiangchelyid turtles are derived stem turtles. This unorthodox result is the result of a number of unambiguously primitive characters that are present in xinjiangchelyid turtles, such as well-developed basipterygoid processes and remnants of the interpterygoid vacuity. A basal position of Middle–Late Jurassic xinjiangchelyid turtles is furthermore consistent with the expected time of origin of crown-clade Testudines (Joyce et al., 2013). We are nevertheless aware of significant inconsistencies that exist in the character-taxon matrix we used that have arisen from recent insights into the morphology of various other Asian Mesozoic turtles. We therefore anticipate that our results are preliminary and will be adjusted by future changes to this dynamic character-taxon matrix.

ACKNOWLEDGMENTS

We thank E. Syromyatnikova for patiently assisting M.R. and W.G.J. during their stay at PIN. D. Brinkman, T. Lyson, and J. Parham are thanked for insightful discussions. J. Sterli, D. Brinkman, and an anonymous reviewer provided valuable comments that helped improve the quality of the manuscript. J. Sterli is particularly thanked for her assistance in using TNT. This research was supported by Deutsche Forschungsgemeinschaft (DFG) grant JO 928/2-1 to W.G.J. The participation of I.D. in this study was supported by DFG grant MA 1643/14-1 and the Russian Foundation for Basic Research (project 11-04-91331-NNIO). M.R. was also supported by the MTA Lendület Program Project No. 95104.

LITERATURE CITED

Ameghino, F. 1899. Sinopsis geológica paleontológica. Suplemento (adiciones y correcciones). Censo Nacional, La Plata:1–13.

Anquetin, J. 2012. Reassessment of the phylogenetic interrelationships of basal turtles (Testudinata). Journal of Systematic Paleontology 10:3–45.

Barley, A. J., P. Q. Spinks, R. C. Thomson, and H. B. Shaffer. 2010. Fourteen nuclear genes provide phylogenetic resolution for difficult nodes in the turtle tree of life. Molecular Phylogenetics and Evolution 55:1189–1194.

Batsch, A. J. G. C. 1788. Versuch einer Anleitung, zur Kenntniß und Geschichte der Thiere und Mineralien. Akademische Buchhandlung, Jena, 528 pp.

Baur, G. 1887. Osteologische Notizen über Reptilien (Fortsetzung II). Zoologischer Anzeiger 10:241–268.

Bohlin, B. 1953. Fossil reptiles from Mongolia and Kansu. Report from the scientific expedition to the north and western provinces of China under the leadership of Sven Hedin. The Sino-Swedish Expedition VI—Vertebrate Palaeontology 6:1–113.

Brinkman, D. B. 2001. New material of *Dracochelys* (Eucryptodira: Sinemydidae) from the Junggar Basin, Xinjiang, People's Republic of China. Canadian Journal of Earth Sciences 38:1645–1651.

Brinkman, D. B., and J.-H. Peng. 1993a. New material of *Sinemys* (Testudines, Sinemydidae) from the Early Cretaceous of China. Canadian Journal of Earth Sciences 30:2139–2152.

Brinkman, D. B., and J.-H. Peng. 1993b. *Ordosemys leios*, n. gen., n. sp., a new turtle from the Early Cretaceous of the Ordos Basin, Inner Mongolia. Canadian Journal of Earth Sciences 30:2128–2138.

Brinkman, D. B., and X.-C. Wu. 1999. The skull of *Ordosemys*, an Early Cretaceous turtle from Inner Mongolia, People's Republic of China, and the interrelationships of Eucryptodira (Chelonia, Cryptodira). Paludicola 2:134–147.

Brinkman, D. B., J.-L. Li, and X.-K. Ye. 2008. Order Testudines; pp. 35–102 in J.-L. Li, X.-C. Wu, and F.-C. Zhang (eds.), The Chinese Fossil Reptiles and Their Kin. Science Press, Beijing.

Brinkman, D. B., D. Eberth, J. Clark, X. Xing, and X.-C. Wu. 2013. Turtles from the Jurassic Shishugou Formation of the Junggar Basin, People's Republic of China, and the basicranial region of basal eucryptodires; pp. 147–172 in D. B. Brinkman, J. D. Gardner, and P. A. Holroyd (eds.), Morphology and Evolution of Turtles. Springer, Dordrecht.

Chkhikvadze, V. M. 1975. [Volume and systematic position of turtles of the suborder Amphichelydia Lydekker, 1899]. Soobscheniya AN Gruzinskoy SSRR 78:745–748. [Russian]

Chkhikvadze, V. M. 1977. [Fossil turtles of the family Sinemydidae. Izvestiya AN Gruzinskoy SSR]. Seriya Biologicheskaya 3:265–270. [Russian]

Chkhikvadze [Čkhikvadze], V. M. 1987. Sur la classification et les charactéres de certaines tortues fossiles d'Asie, rares et peu etudiees. Studia Geologica Salmaticensia, Studia Palaeocheloniologica 2:55–85.

Danilov, I. G., and J. F. Parham. 2006. A redescription of '*Plesiochelys tatsuensis*' from the Late Jurassic of China, with comments on the antiquity of the crown clade Cryptodira. Journal of Vertebrate Paleontology 26:573–580.

Danilov, I. G., and J. F. Parham. 2007. The type series of '*Sinemys*' *wuerhoensis*, a problematic turtle from the Lower Cretaceous of China, includes at least three taxa. Palaeontology 50:431–444.

Danilov, I. G., and J. F. Parham. 2008. A reassessment of some poorly known turtles from the Middle Jurassic of China, with comments on the antiquity of extant turtles. Journal of Vertebrate Paleontology 28:306–318.

Endo, R., and T. Shikama. 1942. Mesozoic reptilian fauna in the Jehol mountainland, Manchoukuo. Bulletin of Central National Museum of Manchoukuo 3:1–19.

Fang, Q.-R. 1987. A new species of Middle Jurassic turtle from Sichuan. Acta Herpetologica Sinica 6:65–9.

Gaffney, E. S. 1972. An illustrated glossary of turtle skull nomenclature. Amercian Museum Novitates 2486:1–33.

Gaffney, E. S. 1979. Comparative cranial morphology of Recent and fossil turtles. Bulletin of the American Museum of Natural History 164:69–376.

Gaffney, E. S. 1996. The postcranial morphology of *Meiolania platyceps* and a review of the Meiolaniidae. Bulletin of the American Museum of Natural History 229:1–166.

Gaffney, E. S., and X. Ye. 1992. *Dracochelys*, a new cryptodiran turtle from the Early Cretaceous of China. American Museum Novitates 3048:1–13.

Gaffney, E. S., J. H. Hutchison, F. A. Jenkins, and L. J. Meeker. 1987. Modern turtle origins: the oldest known cryptodire. Science 237:289–291.

Gaffney, E. S., L. Kool, D. B. Brinkman, T. H. Rich, and P. Vickers-Rich. 1998. *Otwayemys*, a new cryptodiran turtle from the Early Cretaceous of Australia. American Museum Novitates 3233:1–28.

Gaffney, E. S., T. H. Rich, P. Vickers-Rich, A. Constantine, R. Vacca, and L. Kool. 2007. *Chubutemys*, a new eucryptodiran turtle from the Early Cretaceous of Argentina, and the relationships of Meiolaniidae. American Museum Novitates 3599:1–35.

Goloboff, P. A., C. I. Mattoni, and A. S. Quinteros. 2008. TNT, a free program for phylogenetic analysis. Cladistics 24:774–786.

Gubin, Y. M., and S. M. Sinitza. 1996. Shar Teg: a unique Mesozoic locality of Asia. Museum of Northern Arizona Bulletin 60:311–318.

Herrel, A. J., C. O'Reilly, and A. M. Richmond. 2002. Evolution of bite performance in turtles. Journal of Evolutionary Biology 15:1083–1094.

Hirayama, R., D. B. Brinkman, and I. G. Danilov. 2000. Distribution and biogeography of non-marine Cretaceous turtles. Russian Journal of Herpetology 7:181–198.

Hutchison, J. H., and J. D. Archibald. 1986. Diversity of turtles across the Cretaceous/Tertiary Boundary in northeastern Montana. Palaeogeography, Palaeoclimatology, Palaeoecology 55:1–22.

Hutchison, J. H., and D. M. Bramble. 1981. Homology of the plastral sclaes of the Kinosternidae and related turtles. Herpetologica 37(2):73–85.

International Commission on Zoological Nomenclature. 1999. International Code of Zoological Nomenclature, Fourth Edition. International Trust for Zoological Nomenclature, London, 306 pp.

Joyce, W. G. 2007. Phylogenetic relationships of Mesozoic turtles. Bulletin of the Peabody Museum of Natural History 48:3–102.

Joyce, W. G., and C. J. Bell. 2004. A review of the comparative morphology of extant testudinoid turtles (Reptilia: Testudines). Asiatic Herpetological Research 10:53–109.

Joyce, W. G., and J. Sterli. 2012. Congruence, non-homology, and the phylogeny of basal turtles. Acta Zoologica 93:149–159.

Joyce, W. G., F. A. Jenkins, and T. Rowe. 2006. The presence of cleithra in the primitive turtle *Kayentachelys aprix*. Russian Journal of Herpetology 13, Supplement (Fossil Turtle Research 1):93–103.

Joyce, W. G., J. F. Parham, and J. A. Gauthier. 2004. Developing a protocol for the conversion of rank-based taxon names to phylogenetically defined clade names, as exemplified by turtles. Journal of Paleontology 78:989–1013.

Joyce, W. G., J. F. Parham, T. R. Lyson, R. C. M. Warnock, and P. C. J. Donoghue. 2013. A divergence dating analysis of turtles using fossil calibrations: an example of best practices. Journal of Paleontology 87:612–634.

Kaznyshkin, M. N., L. A. Nalbandyan, and L. A. Nessov. 1990. [Middle and Late Jurassic turtles of Fergana (Kirghiz SSR)]. Yezhegodnik Vsesoyuznogo Paleontologicheskogo Obshchestva [Annual of the All-union Palaeontological Society]] 33:185–204. [Russian]

Khosatzky L. I., and L. A. Nessov. 1979. [Large turtles of the Late Cretaceous of Middle Asia]. Trudy Zoologicheskogo Instituta AN SSSR 89:98–108. [Russian].

Klein, I. T. 1760. Klassification und kurze Geschichte der Vierfüßigen Thiere (translation by F. D. Behn). Jonas Schmidt, Lübeck, 381 pp.

Krenz, J. G., G. J. P. Naylor, H. B. Shaffer, and F. J. Janzen. 2005. Molecular phylogenetics and evolution of turtles. Molecular Phylogenetics and Evolution 37:178–191.

Maisch, M. A., A. Matzke, and G. Sun. 2003. A new sinemydid turtle (Reptilia: Testudines) from the Lower Cretaceous of the Junggar Basin (NW-China). Neues Jahrbuch für Geologie und Paläontologie, Monatshefte 2003(12):705–722.

Matzke, A. T., M. W. Maisch, H.-U. Pfretzschner, G. Sun, and H. Stöhr. 2004a. A new basal sinemydid turtle (Reptilia: Testudines) from the Lower Cretaceous Tugulu Group of the Junggar Basin (NW China). Neues Jahrbuch für Geologie und Paläontologie, Monatshefte 2004(3):151–167.

Matzke, A. T., M. W. Maisch, G. Sun, H.-U. Pfretzschner, and H. Stöhr. 2004b. A new xinjiangchelyid turtle (Testudines, Eucryptodira) from the Jurassic Qigu Formation of the southern Jungar Basin, Xinjiang, North-West China. Palaeontology 47:1267–1299.

Matzke, A. T., M. W. Maisch, G. Sun, H.-U. Pfretzschner, and H. Stöhr. 2005. A new Middle Jurassic xinjiangchelyid turtle (Testudines; Eucryptodira) from China (Xinjiang, Junggar Basin). Journal of Vertebrate Paleontology 25:63–70.

Nessov, L. A. 1995. On some Mesozoic turtles of the Fergana Depression (Kyrgyzstan) and Dzhungar Alatau Ridge (Kazakhstan). Russian Journal of Herpetology 2:134–141.

Nessov, L. A., and L. I. Khosatzky. 1973. [Early Cretaceous turtles from southeastern Fergana]; pp. 132–133 in Problems in Herpetology: Proceedings of the 3rd All-union Herpetological Conference, Leningrad, 1–3 February 1973. Zoological Institute of the Academy of Sciences USSR, Leningrad. [Russian]

Nessov, L. A., and L. I. Khosatzky. 1981. [Turtles of the Early Cretaceous of Transbaikalia]; pp. 74–78 in L. J. Borkin (ed.), [Herpetological Investigations in Siberia and the Far East]. Academy of Sciences of the USSR, Leningrad. [Russian]

Parham, J. F., and J. H. Hutchison. 2003. A new eucryptodiran turtle from the Late Cretaceous of North America (Dinosaur Provincial Park, Alberta, Canada). Journal of Vertebrate Paleontology 23:783–798.

Peng, G., Y. Ye, Y. Gao, C. Shu, and S. Jiang. 2005. Jurassic Dinosaur Faunas in Zigong. Zigong Dinosaur Museum, Zigong, 236 pp. [Chinese with English translation]

Peng, J.-H., and D. B. Brinkman. 1993. New material of *Xinjiangchelys* (Reptilia: Testudines) from the Late Jurassic Qigu Formation (Shishugou Group) of the Pingfengshan locality, Junggar Basin, Xinjiang. Canadian Journal of Earth Sciences 30:2013–2026.

Rabi, M., W. G. Joyce, and O. Wings. 2010. A review of the Mesozoic turtles of the Junggar Basin (Xinjiang, Northwest China) and the paleobiogeography of Jurassic to Early Cretaceous Asian Testudinates. Paleobiodiversity and Paleoenvironments 90:259–273.

Ryabinin, A. N. 1948. [Turtles from the Jurassic of Kara-Tau]. Trudy Paleontologiicheskogo Instituta AN SSSR 15:94–98. [Russian]

Schumacher, G. H. 1973. The head muscles and hyolaryngeal skeleton of turtles and crocodilians; pp. 101–199 in C. Gans and T. Parsons (eds.), Biology of the Reptilia, Volume 4. Academic Press, London and New York.

Sinitshenkova, N. D. 1995. New Late Mesozoic stoneflies from Shar Teg, Mongolia (Insecta: Perlida = Plecoptera). Paleontological Journal 29:93–104.

Sinitshenkova, N. D. 2002. New Late Mesozoic mayflies from the Shar Teg locality, Mongolia (Insecta, Ephemerida = Ephemeroptera). Paleontological Journal 36:43–48.

Sterli, J. 2008. A new, nearly complete stem turtle from the Jurassic of South America with implications for turtle evolution. Biology Letters 4:286–289.

Sterli, J. 2010. Phylogenetic relationships among extinct and extant turtles: the position of Pleurodira and the effects of the fossils on rooting crown-group turtles. Contributions to Zoology 79(3):93–106.

Sterli, J., and M. de la Fuente. 2010. Anatomy of *Condorchelys antiqua* Sterli, 2008, and the origin of the modern jaw closure mechanism in turtles. Journal of Vertebrate Paleontology 30:351–366.

Sterli, J., and M. de la Fuente. 2011. A new turtle from the La Colonia Formation (Campanian–Maastrichtian), Patagonia, Argentina, with remarks on the evolution of the vertebral column in turtles. Palaeontology 54:63–78.

Sterli, J., and M. de la Fuente. 2013. New evidence from the Palaeocene of Patagonia (Argentina) on the evolution and palaeobiogeography of meiolaniid-like turtles (Testudinata). Journal of Systematic Palaeontology 11:835–852.

Sterli, J., D. Pol., and M. Laurin. 2013. Incorporating phylogenetic uncertainty on phylogeny-based palaeontological dating and the timing of turtle diversification. Cladistics 29:233–246.

Sukhanov [Suhanov], V. B. 1964. Subclass Testudinata, Testudinates; pp. 354–438 in A. K. Rožděstvenskij and L. P. Tatarinov (eds.), [Fundamentals of Paleontology; Amphibians, Reptiles and Birds]. Nauka, Moscow. [Russian]

Sukhanov, V. B. 2000. Mesozoic turtles of Middle and Central Asia; pp. 309–367 in M. J. Benton, M. A. Shishkin, D. M. Unwin, and E. N. Kurochkin (eds.), The Age of Dinosaurs in Russia and Mongolia. Cambridge University Press, Cambridge, U.K.

Sukhanov, V. B., and P. Narmandakh. 1974. [New Early Cretaceous turtle from the continental deposits of the Northern Gobi]; pp. 192–220 in Mesozoic and Cenozoic Faunas and Bistratigraphy of Mongolia. The Joint Soviet-Mongolian Paleontological Expedition, Transactions, 1. Nauka Publishers, Moscow. [Russian]

Sukhanov, V. B., and P. Narmandakh. 2006. New taxa of Mesozoic turtles from Mongolia. Fossil Turtle Research 1:119–127.

Tatarinov, L. P. 1959. [A new turtle of the family Baenidae from the Lower Eocene of Mongolia]. Paleontologicheskiy Zhurnal 1:100–113. [Russian]

Tong, H., and D. Brinkman. 2013. A new species of *Sinemys* (Testudines: Cryptodira: Sinemydidae) from the Early Cretaceous of Inner Mongolia, China. Palaeobiodiversity and Palaeoenvironments 93:355–366.

Tong, H., E. Buffetaut, and V. Suteethorn. 2002. Middle Jurassic turtles from southern Thailand. Geological Magazine, 139:687–697.

Tong, H., S.-A. Ji, and Q. Ji. 2004. *Ordosemys* (Testudines: Cryptodira) from the Yixian Formation of Liaoning Province, northeastern China: new specimens and systematic revision. American Museum Novitates 3438:1–20.

Tong, H., I. G. Danilov, Y. Ye, H. Ouyang, and G. Peng. 2012a. Middle Jurassic turtles from Sichuan Basin, China: a review. Geological Magazine 149:675–695.

Tong, H., I. G. Danilov, Y. Ye, H. Ouyang, G. Peng, and K. Li. 2012b. A revision of xinjiangchelyid turtles from the Late Jurassic of Sichuan Basin, China. Annales de Paléontologie 98:73–114.

Tong, H., J. Claude, W. Naksri, V. Suteethorn, E. Buffetaut, S. Khansubha, K. Wongko, and P. Yuangdetkla. 2009. *Basilochelys macrobios* n. gen. and n. sp., a large cryptodiran turtle from the Phu Kradung Formation (latest Jurassic–earliest Cretaceous) of the Khorat Plateau, NE Thailand. Geological Society of London Special Publications 315:153–173.

Watabe, M., K. Tsogtbaatar, L. Uranbileg, and L. Gereltsetseg. 2004. Report on the Japan-Mongolia Joint Paleontological Expedition to the Gobi desert, 2002. Hayashibara Museum of Natural Sciences Research Bulletin 2:97–122.

Wiman, C. 1930. Fossile Schildkröten aus China. Paleontologia Sinica, Series C 6:1–56.

Wings, O., M. Rabi, J. W. Schneider, L. Schwermann, G. Sun, C.-F. Zhou, and W. G. Joyce. 2012. An enormous Jurassic turtle bone bed from the Turpan basin of Xinjiang, China. Naturwissenschaften 99:925–935.

Ye, X. 1963. Fossil turtles of China. Palaeontologica Sinica, Series C 150:1–113.

Ye, X. 1982. Middle Jurassic turtles from Sichuan, SW China. Vertebrata PalAsiatica 20:282–290.

Ye, X. 1986. A Jurassic turtle from Junggar, Xinjiang. Vertebrata PalAsiatica 24:171–181.

Ye, Y. 1999. A new genus of Sinemydidae from the Late Jurassic of Neijiang, Sichuan. Vertebrata PalAsiatica 37:81–87.

Young, C.-C., and M.-C. Chow. 1953. New fossil reptiles from Szechuan, China. Acta Scientia Sinica 2:216–229.

Zhou, C.-F. 2010a. A new eucryptodiran turtle from the Early Cretaceous Jiufotang Formation of western Liaoning, China. Zootaxa 2676:45–56.

Zhou, C.-F. 2010b. A second specimen of *Manchurochelys manchoukuoensis* Endo & Shikama, 1942 (Testudines: Eucryptodira) from the Early Cretaceous Yixian Formation of western Liaoning, China. Zootaxa 2534:57–66.

Submitted January 7, 2013; revisions received May 4, 2013; accepted May 16, 2013.
Handling editor: Juliana Sterli.

APPENDIX 1. List of taxa omitted from the matrix of Sterli and de la Fuente (2013).

Ninjemys oweni, Warkalania carinaminor, Patagoniaemys gasparinae, Otwayemys cunicularius, Prochelidella cerrobarcinae, Mychelys latisternum, Chelodina colliei, Yaminuchelys maior, Dinochelys whitei, Neurankylus eximius, Boremys pulchra, Baena arenosa, Chisternon undatum, Macroclemys schmidti, Protochelydra zangerli, Chelonidis gringorum, Stylemys nebraskensis, Echmatemys wyomingensis, Xenochelys formosa, Hoplochelys crassa, Plastomenus aff. thomassii, and *Anosteira ornata.*

APPENDIX 2. List of taxa designated as floaters after constraining the relationships of Durocryptodira in the phylogenetic analysis.

Siamochelys peninsularis, Basilochelys macrobios, Ordosemys leios, Dracochelys bicuspis, Judithemys sukhanovi, Hangaiemys hoburensis, Xinjiangchelys junggarensis, Xinjiangchelys radiplicatoides, Annemys latiens, Annemys levensis, Shachemys laosiana, Adocus beatus, Yehguia tatsuensis, Basilemys variolosa, Baptemys wyomingensis, all members of Trionychidae and Panpleurodira*, Toxochelys latiremis, Mesodermochelys undulatus, Plesiochelys etalloni, Santanachelys gaffneyi, Solnhofia parsonsi,* and *Portlandemys mcdowelli.*

NOTE ADDED AT PROOF

While this paper was in print, a modified version of the taxon-character matrix developed herein was published by the senior author and co-authors. The reference for this paper is:

Rabi, M., Zhou, C.-F., Wings, O., Sun, G., Joyce, W. G. 2013. A new xinjiangchelyid turtle from the Middle Jurassic of Xinjiang, China and the evolution of the basipterygoid process in Mesozoic Turtles. BMC Evolutionary Biology 13:203.

Publication #2

Rabi, M., Zhou, C.-F., Wings, O., Sun, G., Joyce, W.G. 2013. A new xinjiangchelyid Turtle from the Middle Jurassic of Xinjiang, China and the evolution of the basipterygoid process in Mesozoic Turtles. *BMC Evolutionary Biology*. 13 (203): 1–28.

Scientific ideas of candidate: 90 %

Data generation by candidate: 85 %

Analysis and Interpretation by candidate: 80 %

Paper writing by the candidate: 90 %

BMC
Evolutionary Biology

A new xinjiangchelyid turtle from the Middle Jurassic of Xinjiang, China and the evolution of the basipterygoid process in Mesozoic turtles

Rabi *et al.*

BioMed Central

Rabi *et al. BMC Evolutionary Biology* 2013, **13**:203
http://www.biomedcentral.com/1471-2148/13/203

Rabi et al. BMC Evolutionary Biology 2013, 13:203
http://www.biomedcentral.com/1471-2148/13/203

BMC Evolutionary Biology

RESEARCH ARTICLE Open Access

A new xinjiangchelyid turtle from the Middle Jurassic of Xinjiang, China and the evolution of the basipterygoid process in Mesozoic turtles

Márton Rabi[1,2*], Chang-Fu Zhou[3], Oliver Wings[4], Sun Ge[3] and Walter G Joyce[1,5]

Abstract

Background: Most turtles from the Middle and Late Jurassic of Asia are referred to the newly defined clade Xinjiangchelyidae, a group of mostly shell-based, generalized, small to mid-sized aquatic froms that are widely considered to represent the stem lineage of Cryptodira. Xinjiangchelyids provide us with great insights into the plesiomorphic anatomy of crown-cryptodires, the most diverse group of living turtles, and they are particularly relevant for understanding the origin and early divergence of the primary clades of extant turtles.

Results: Exceptionally complete new xinjiangchelyid material from the ?Qigu Formation of the Turpan Basin (Xinjiang Autonomous Province, China) provides new insights into the anatomy of this group and is assigned to *Xinjiangchelys wusu* n. sp. A phylogenetic analysis places *Xinjiangchelys wusu* n. sp. in a monophyletic polytomy with other xinjiangchelyids, including *Xinjiangchelys junggarensis*, *X. radiplicatoides*, *X. levensis* and *X. latiens*. However, the analysis supports the unorthodox, though tentative placement of xinjiangchelyids and sinemydids outside of crown-group Testudines. A particularly interesting new observation is that the skull of this xinjiangchelyid retains such primitive features as a reduced interpterygoid vacuity and basipterygoid processes.

Conclusions: The homology of basipterygoid processes is confidently demonstrated based on a comprehensive review of the basicranial anatomy of Mesozoic turtles and a new nomenclatural system is introduced for the carotid canal system of turtles. The loss of the basipterygoid process and the bony enclosure of the carotid circulation system occurred a number of times independently during turtle evolution suggesting that the reinforcement of the basicranial region was essential for developing a rigid skull, thus paralleling the evolution of other amniote groups with massive skulls.

Background

Most recent, morphology-based, phylogenetic studies of fossil and extant turtles agree that the Middle to Late Jurassic was a particularly important phase in the early diversification of crown group Testudines [1-6]. Xinjiangchelyidae is a clade of turtles that includes some of the most common taxa known from this time period in Asia and that is widely considered to represent the primitive morphology of the cryptodiran stem lineage [2-4,7-16]. The exact content of this clade is still an open question, however, as the anatomy and phylogenetic relationships of many candidate taxa are still poorly known.

A new species of xinjiangchelyid, *Xinjiangchelys wusu* n. sp., is described here on the basis of exceptionally well preserved skeletons that were found and recovered by the 2009 and 2011 Field Teams of the Sino-German Cooperation Project in the Upper Jurassic ?Qigu Formation of the Turpan Basin, Xinjiang Autonomous Province, China and that provide new insights into the morphology of xinjiangchelyids.

One anatomical region of special interest for turtle evolution is the basicranium. The basisphenoid of some paracryptodires and xinjiangchelyids, including *Xinjiangchelys wusu* n. sp., has previously been shown to exhibit a pair of lateral processes that were homologized with the basipterygoid process of basal amniotes

* Correspondence: iszkenderun@gmail.com
[1]Institut für Geowissenschaften, University of Tübingen, Hölderlinstraße 12, 72074, Tübingen, Germany
[2]Department of Paleontology & MTA–ELTE Lendület Dinosaur Research Group, Eötvös Loránd University, Budapest, Hungary
Full list of author information is available at the end of the article

BioMed Central

© 2013 Rabi et al.; licensee BioMed Central Ltd. This is an Open Access article distributed under the terms of the Creative Commons Attribution License (http://creativecommons.org/licenses/by/2.0), which permits unrestricted use, distribution, and reproduction in any medium, provided the original work is properly cited.

[15,17]. However, the homology of these structures is controversial in the literature [18-20] and a comprehensive assessment of this issue is still outstanding. We here identify similar basisphenoid processes in a broad range of extinct turtles and conclude that their presence has been overlooked in the Mesozoic turtle literature during the last forty years. We here furthermore provide compelling morphological evidence for the homology of the basisphenoid processes of xinjiangchelyids with the basipterygoid processes of basal turtles and basal amniotes and review the evolution of this structure in Mesozoic turtles. We finally present an internally consistent nomenclatural system that reflects recent insights into the morphology of the carotid canal system. To test the phylogenetic implications of our new insights, we analyzed an extensive sample of xinjiangchelyids in a global, cladistic framework of turtles. We obtained the unorthodox placement of this clade outside crown group Testudines, which may hint at a surprisingly extensive evolutionary history of the turtle stem lineage.

Methods

Geological settings

The "Turtle Cliff Fossil Site" yielded the new material described herein and is located within the Flaming Mountains about 26 km ENE of the city of Shanshan in the Turpan Basin, Xinjiang Autonomous Province, China (Figure 1). The Flaming Mountains consist of Triassic to Paleogene sediments that were uplifted during the Neogene [21-23]. Published reports on the geology and stratigraphy of the Flaming Mountains in particular and the Turpan Basin in general are rare (e.g., [24] and references therein) and many uncertainties therefore exist regarding the absolute age of formations and their correlation with similar units in other Central Asian basins. Jurassic clastic strata in the Flaming Mountains were preliminarily divided into the Early Jurassic Sangonghe Formation, the Middle Jurassic Xishanyao, Sanjianfang, Qiketai, and Qigu Formations (the latter was recently dated in the Junggar Basin with 164.6 Ma ± 1.4 Ma, [25]), and the Late Jurassic Karaza Formation [26]. Future

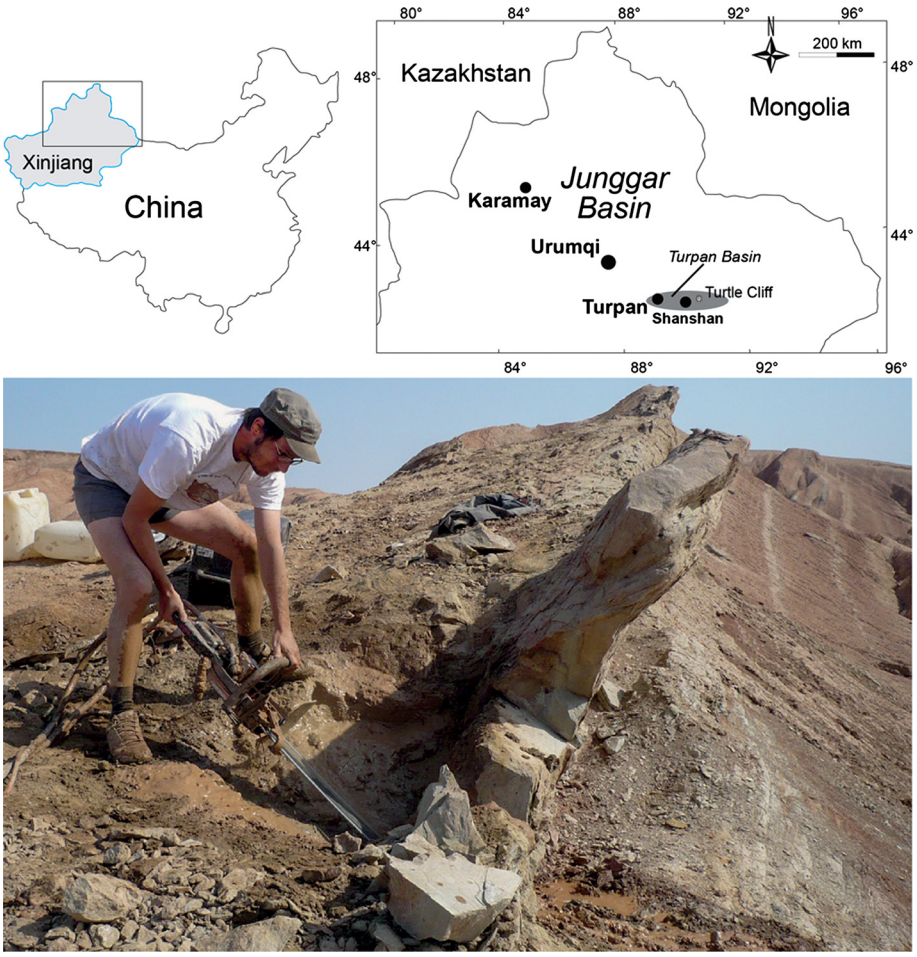

Figure 1 The geographic location of the "Turtle Cliff" site in the Turpan Basin of Xinjiang Autonomous Province, China (above) and a photograph of the cliff where the turtles were found and cut out with the help of a rock saw (below).

stratigraphic research needs to clarify whether Late Jurassic strata are indeed mostly absent in the area.

Piedmont-fluvial deposits dominate the upper parts of the Jurassic sequence [27,28]. Red-colored sediments, especially prominent in the Qigu Formation, indicate a reduction in the monsoonal circulation in Asia resulting in a paleoclimatic change from humid to seasonally dry during the late Middle and early Late Jurassic [24,25,28-31]. The total thickness of the supposed Qigu Formation is about 850 m in the area of the Turtle Cliff Fossil Site [31]. The formation is rich in vertebrate fossils, dominated by dinosaurs and turtles [28]. Finds of the latter include the spectacular turtle taphocoenosis at Mesa Chelonia [28] near the lower border of the formation and the herein introduced Turtle Cliff Fossil Site near the base of the upper third of the formation.

The Turtle Cliff Fossil Site is situated geographically 1 km to the ENE and stratigraphically 500 m above the Mesa Chelonia site [28]. Since no explicit justification has been given for the correlation of the strata supposedly belonging to the Qigu Formation in the Turpan Basin, the assignment of rocks units exposed in the Flaming Mountains to this formation is not transparent [28], but our preliminary classification places both sites within the Qigu Formation. The deposits that allegedly represent the Qigu Formation in the Turpan Basin are characterized by alternating coarse and fine-grained sediments that often contain unionid freshwater bivalves, reflecting changing depositional conditions typical of river systems [24,31]. Temporary subaerial exposure is indicated by paleosols [28].

The turtle skeletons at the Turtle Cliff Fossil Site were found on the top of a low hill in a steeply inclined (65°), fine-grained and strongly cemented sandstone layer rich in lithoclasts. Above and below the turtle-bearing sandstone horizon follows a succession of predominately red silt-and mudstones.

Material studied in this paper

Our description of *Xinjiangchelys wusu* n. sp. is based on a sandstone slab with at least 3 individuals (Figure 2) that were excavated during the 2011 joint field season of the University of Tübingen, Shenyang Normal University, and Jilin University, that was lead and carried out by all co-authors at the Turtle Cliff Fossil Site (see Geological Settings). The quarried fossils are currently housed at the Paleontology Museum of Liaoning (PMOL) at Shenyang Normal University, Shenyang, Liaoning but will eventually be integrated into the municipal museum of Shanshan, Xinjiang Autonomous Province that is currently under construction. All specimens have been assigned a combined PMOL-Sino-German Cooperation Project (SGP) number, which will be deposited with the specimens once the museum in Shanshan is operational. The detailed coordinates of the locality are archived at PMOL and will be disclosed to qualified researchers interested in studying the site.

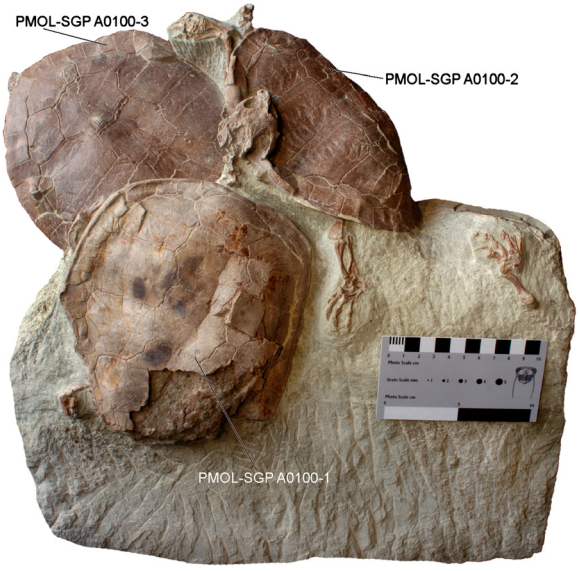

Figure 2 Type series of *Xinjiangchelys wusu* n. sp. from "Turtle Cliff", Turpan Basin of Xinjiang Autonomous Province, China, ?Qigu Formation, Middle Jurassic.

Specimen PMOL-SGP A0100-1 was discovered with the carapace exposed in dorsal view in 2009 below a small cliff and was cut out of the hard sandstone ledge in a block with an ICS diamond chain rock saw in 2011. Subsequent preparation revealed that the slab contained two more individuals with PMOL-SGP A0100-2 cut in half through the long axis during excavation. The slab in total includes PMOL-SGP A0100-3: shell with carapace partially exposed, femora, skull and lower jaw; PMOL-SGP A0100-2: shell (plastron not exposed), partial neck, left foot and left hand and PMOL-SGP A0100-1: posteriorly incomplete carapace, neck, crushed skull with articulated mandible, left and right hand and incomplete left posterior limb.

The anatomy of fossil taxa was reviewed mostly based on personal observations of published material and with the help of photographs. The following fossil taxa were studied first hand: *Allopleuron hoffmanni* (Gray, 1831) [32] (NHMUK R42913); *Chubutemys copelloi* Gaffney et al., 2007 [10] (MPEF-PV1236); *Dracochelys bicuspis* Gaffney and Ye, 1992 [33] (IVPP V4075); *Hangaiemys hoburensis* Sukhanov and Narmandakh, 1974 [34] (PIN 3334-4, PIN 3334-34, PIN 3334-35, PIN 3334-36, PIN 3334-37); *Heckerochelys romani* Sukhanov, 2006 [35] (PIN 4561-2 and PIN 4719-34); *Hoyasemys jimenezi* Pérez-García et al., 2012 [36] (MCCM-LH-84); *Helochelydra nopcsai* Lapparent de Broin and Murelaga, 1999 [37] (IWCMS 1998.21); *Judithemys sukhanovi* Parham and Hutchison, 2003 [9]

(TMP 87.2.1); *Kallokibotion bajazidi* Nopcsa, 1923 [38] (NHMUK R4921 and NHMUK R4925); *Kayentachelys aprix* Gaffney et al., 1987 [39] (MNA V1558, MCZ 8917); *Macrobaena mongolica* Tatarinov, 1959 [40] (PIN 533-4); *Manchurochelys manchoukuoensis* Endo and Shikama, 1942 [41] (PMOL AR00008); *Meiolania platyceps* Owen, 1886 [42] (NHMUK R682); *Mongolemys elegans* Khosatzky and Mlynarski, 1971 [43] (five uncatalogued skulls at the collections of PIN); *Mongolochelys efremovi* Khozatsky, 1997 [44] (PIN 552-459 and two uncatalogued skulls); *Naomichelys speciosa* Hay, 1908 [45] (FMNH PR 273); *Niolamia argentina* Ameghino 1899 [46] *Notoemys laticentralis* Cattoi and Freiberg, 1961 [47] (cast of MOZP 2487); *Odontochelys semitestacea* Li et al., 2008 [48] (IVPP V13240); *Ordosemys leios* Brinkman and Peng, 1993 [49] (IVPP V9534-1); *Peligrochelys walshae* Sterli and de la Fuente, In press [16] (MACN PV CH 2017, MACN PV CH 2017); *Portlandemys mcdowelli* Gaffney, 1975 [50] (NHMUK R2914, NHMUK R3163, NHMUK R3164); *Proganochelys quenstedti* Baur, 1887 [51] (SMNS 16980); *Rhinochelys elegans* Lydekker, 1889 [52] (NHMUK R27); *Sandownia harrisi* Meylan et al., 2000 [53] (MIWG 3480); *Sinemys gamera* Brinkman and Peng, 1993 [54] (IVPP V9532-11); *Sinemys brevispinus* Tong and Brinkman, In press [55] (IVPP V9538-1); *Solnhofia parsonsi* Gaffney, 1975 [56] (TM 4023); *Toxochelys latiremis* Cope, 1873 [57] (NHMUK R4530 and NHMUK R3902); *Xinjiangchelys* (*Annemys*) *levensis* Sukhanov and Narmandakh, 2006 [58] (PIN 4636-4-2, [59]); *Xinjiangchelys* (*Annemys*) *latiens* Sukhanov and Narmandakh, 2006 (PIN 4636-6-2, [59]); and *Xinjiangchelys radiplicatoides* Brinkman et al., 2013 [15] (IVPP V18104).

The following taxa were studied on the basis of photographs: *Adocus lineolatus* Cope, 1874 [60] (CCM 60-15); *Basilochelys macrobios* Tong et al., 2009 [61] (MD 8-2); *Bouliachelys suteri* Kear and Lee, 2006 [62] (SAM P41106); *Meiolania platyceps* AM F: 18671; *Plesiochelys etalloni* Pictet and Humbert, 1857 [63] (MH 435); *Pleurosternon bullockii* Owen 1842 [64] (UMZC T1041).

Osteological terminology

The cranial nomenclature presented by Gaffney [65,66] has been highly influential, because all anatomical systems of the cranium were clearly described and illustrated in these publications and because a broad audience was thereby enabled to apply these names consistently to the skulls of fossil and recent turtles. Only in the last few years have some shortcomings become apparent, however, particularly in regards to the nomenclature of the carotid system and we herein seek to rectify this situation by providing an internally consistent nomenclatural system for this anatomical region (Figure 3).

The internal carotid artery of most turtles, like most amniotes, splits into a cerebral and a palatine (lateral) branch. Although these structures are interrelated, they can be thought of as three different vessels, which are herein terms the internal carotid artery, the cerebral artery, and the palatine artery. New insights into the cranial anatomy of basal turtles [15,20,67] has revealed that these three blood vessels can enter the skull through three non-homologous foramina and that they can also exit the skull through three non-homologous foramina, for a total of six non-homologous foramina. The nomenclatural system of Gaffney [65,66] proved to be confusing, because it only provides three names for these six foramina (i.e., foramen *anterior* [italics added for emphasis] canalis carotici interni, foramen *posterior* canalis carotici interni, and foramen caroticum laterale) and because these names were defined as applying to inappropriate portions of the carotid system. For instance, the foramen *anterior* canalis carotici interni was defined as applying to the exit of the cerebral artery, not to the exit of the internal carotid artery, whereas the foramen posterior canalis *carotici interni* could either be the entry of the internal carotid artery or of the cerebral artery [65,66]. An addition oddity of this nomenclatural system that makes it difficult for neophytes to learn that the palatine artery is situated in the "lateral canal," not the palatine canal. Incidentally, the use of the "-ior" suffix

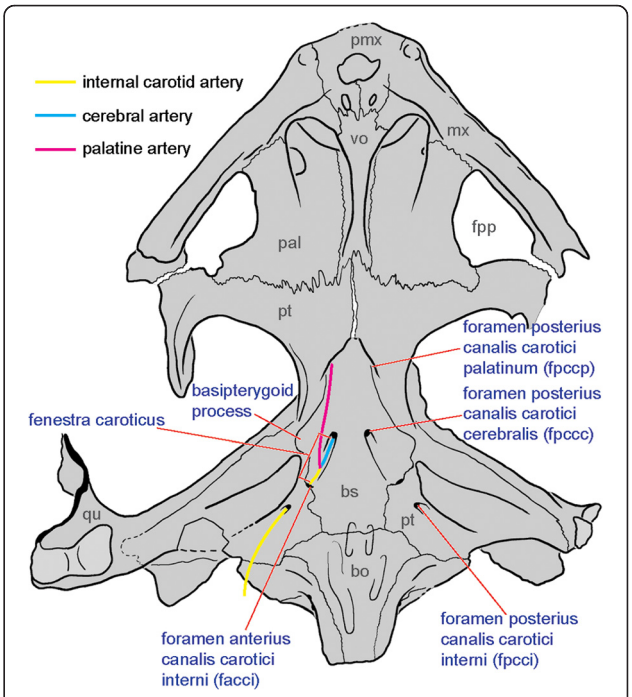

Figure 3 Proposed internally consistent nomenclature for the osseous portion of the carotid circulation system of turtles as exemplified on the skull of *Dracochelys bicuspis* (IVPP V4075). Abbreviations: **bo**: basioccipital, **bs**: basisphenoid, **fpp**: foramen palatinum posterius, **mx**: maxilla, **pal**: palatine, **pmx**: premaxilla, **pt**: pterygoid, **qu**: quadrate, **vo**: vomer.

(as in *anterior* and *posterior*) is not appropriate, given that the "-ius" suffix is the proper neuter singular ending in Latin.

Sterli et al. [20] were the first to realize these deficiencies in the nomenclatural system of Gaffney [65,66] and proposed new terms, but these new terms are not sufficient to name all six potential foramina and they break with tradition set by Gaffney [65,66] in their grammatical construction. These inconsistencies were partially addressed recently [15] but some parts of the system still remain unnamed and the palatine artery is still defined as sitting in the lateral canal.

We herein propose a new nomenclatural system that attempts to follow the grammatical precedence set forth by Gaffney [65,66], but that breaks tradition by providing names for all potential foramina and by renaming the lateral canal the palatine canal. This nomenclatural system consists of a total of 10 new terms (Figure 3):

Canalis caroticus internus

The bony canal that holds any portion of the internal carotid artery, absent, among others, in basal turtles and paracryptodires.

Foramen posterius canalis carotici interni (fpcci)

The posterior entry of the internal carotid artery, absent, among others, in basal turtles and paracryptodires.

Foramen anterius canalis carotici interni (facci)

The anterior exit of the internal carotid artery, only present in turtles with a fenestra caroticus.

Canalis caroticus cerebralis

The bony canal that holds any portion of the cerebral artery, present in all turtles.

Foramen posterius canalis carotici cerebralis (fpccc)

The posterior entry of the cerebral artery, not developed in turtles where the split of the internal carotid artery into the cerebral and palatine branches is covered by bone.

Foramen anterius canalis carotici cerebralis (faccc)

The anterior exit of the cerebral artery, present in all turtles, typically located near the dorsum sellae.

Canalis caroticus palatinum

The bony canal that holds any portion of the palatine artery, generally absent in turtles with an open interpterygoid vacuity.

Foramen posterius canalis carotici palatinum (fpccp)

The posterior entry of the palatine artery, generally developed in turtles with a closed interpterygoid vacuity, but not in those where the split of the internal carotid artery into the cerebral and palatine branches is covered by bone.

Foramen anterius canalis carotici palatinum (faccp)

The anterior exit of the palatine artery, generally present in turtles with a close interpterygoid vacuity.

Fenestra caroticus (fca)

A figurative bony window into the otherwise closed carotid system, which exposes the split of the internal carotid artery into the cerebral and palatine branches. The window is posteriorly defined by the foramen anterius canalis carotici interni and anteriorly defined by the foramen posterius canalis carotici cerebralis and the foramen posterius canalis carotici palatinum or the interpterygoid vacuity.

Phylogenetic analysis

A phylogenetic analysis was performed using TNT [68,69] using a modified version of a previous character/taxon matrix [16], which in return is based on earlier studies [3,5,59,70] [Additional file 1]. Part of the changes are reported in an in press paper by Rabi et al. [59] and these are repeated below for the sake of clarity. Five taxa were added to the matrix [16], including *Xinjiangchelys radiplicatoides*, *X. junggarensis* (sensu Brinkman et al. 2008 [71]), *X.* (*Annemys*) *levensis*, *X.* (*Annemys*) *latiens*, and *Basilochelys macrobios*. The scorings of *X. radiplicatoides* are primarily based on the literature [15], those of *X. junggarensis* (=*X. latimarginalis* [72]) on personal observation of IVPP material from Pingfengshan [72], those of *X.* (*Annemys*) *levensis*, and *X.* (*Annemys*) *latiens* based on personal observation of PIN material, and those of *B. macrobios* based on the literature [60] and photographs obtained from H. Tong. The following scorings were changed relative to the original matrix [16] (the earlier scorings are in parenthesis): Epiplastron B: *Hangaiemys hoburensis*: 1 (?), *Sinemys lens* Wiman, 1930 [73] 1 (?); Pterygoid B: *H. hoburensis* 1 (2), *Dracochelys bicuspis* 1 (2), *Pleurosternon bullockii* 1 (2), *Kallokibotion bajazidi* 1 (2), *Mongolochelys efremovi* 1 (2), *Chubutemys copelloi* 1 (2), *Eileanchelys waldmani* Anquetin, 2009 [74] ? (2); Carapace D: *H. hoburensis* 0 (?), *Chengyuchelys baenoides* Young and Chow, 1953 [75] (IVPP-V6507) 0 (1); Carapace E: *H. hoburensis*-(?); Vertebral A: *Siamochelys peninsularis* Tong et al., 2002 [76] ? (1); Vertebral C: *S. peninsularis* ? (1); Anal A: *S. peninsularis* ? (0), *Ch. baenoides* ? (0); Entoplastron B: *Ch. baenoides* ? (1); Mesoplastron A: *S. peninsularis* 2 (0); Hypoplastron A: *Ch. baenoides* ? (0); Xiphiplastron A-B: *Ch. baenoides* ? (0); Dorsal Rib A: *S. peninsularis* ? (2); Plastral Scute B: *S. peninsularis* 1 (0).

Further modifications relative to Rabi et al. in press [59] include the addition of *Xinjiangchelys wusu* to the

matrix and changing of the following scorings: Supraoccipital A: *X.* (*Annemys*) *levensis* 1 (0); *X. radiplicatoides* ? (0); *X.* (*Annemys*) *latiens* ? (0); Pterygoid B: *Sphenodon punctatus* 0 (2), *Anthodon serrarius* 1 (2), *Peligrochelys walshae* 2 (1), *Niolamia argentina* 2 (?); Dentary A: *X.* (*Annemys*) *levensis* 0 (1); *X. junggarensis* ? (1).

The character Cervical Vertebrae A was omitted from the analysis because we found it difficult to replicate this character objectively and perceived a number of inconsistencies in the matrix [59]. The character Diploid Number A was also omitted following previous studies [3,59,77].

The following characters were treated as ordered: 7 (Nasal A), 19 (Parietal H), 27 (Squamosal C), 40 (Maxilla D), 42 (Vomer A), 50 (Quadrate B + C), 52 (Antrum Postoticum A), 59 (Pterygoid B), 81 (Opisthotic C), 82 (Opisthotic D), 89 (Stapedial Artery B), 98 (Canalis Caroticum F), 120 (Carapace A), 121 (Carapace B), 130 (Peripheral A), 133 (Costal B), 138 (Supramarginal A), 158 (Hyoplastron B), 159 (Mesoplastron A), 161 (Hyoplastron B), 176 (Abdominal A), 213 (Cleithrum A), 214 (Scapula A), 232 (Manus B), 233 (Manus C). *Sphenodon punctatus, Owenetta kitchingorum, Simosaurus gaillardoti* and *Anthodon serrarius* were designated as outgroups [16,59]. Although, there is growing evidence for a turtle-archosaur clade among molecular studies, morphological analyses still suggest lepidosaurian or parareptilian affinities for turtles at the moment. As it turns out, however, the choice of outgroup is irrelevant, as all outgroups reveal that the presence of teeth and the lack of a complete shell should be considered primitive for turtles and that the partially shelled, toothed taxon *Odontochelys semitestacea* is therefore sister to all turtles. The fusion of the basicranium discussed in our paper occurs far deeper within the turtle tree and is therefore not influenced by the choice of outgroups, but rather by the arrangement of basal turtles.

Given that this analysis is focused on the phylogenetic relationships and placement of xinjiangchelyid turtles, we decided to crop taxa not pertinent to these questions (e.g., most derived baenids, most meiolaniforms) and a broad spectrum of taxa known from fragmentary material only (see Appendix A for a complete list) in order to reduce the size of the matrix [59]. The resulting matrix consists of 237 characters for a total of 84 terminal taxa. The character-taxon matrix and the tnt. file are found under [Additional files 1, and 2], respectively.

The relationships of living cryptodiran taxa were manually constrained according to recent results of molecular phylogenetic studies (following previous studies [1,2,59]), without assuming a priori, however, that Trionychia nests within Cryptodira [78,79]. The internal relationships of durocryptodires were constrained using a molecular topology [79] (i.e., (Emydidae (Geoemydidae + Testudinidae)) + (Chelonioidea (Chelydridae + Kinosternoidea))). The complete list of taxa designated as floaters can be found in Appendix B. A first run of heuristic search tree-bisection-reconnection, using thousands of random addition sequence replicates and 10 trees saved per replicate, failed to find all the most parsimonious trees (MPT) and therefore the heuristic search was repeated until the MPTs were found 30 times during each replicate (using the command "xmult = hits 30;"). The trees retained in the memory were exposed to a second round of tree-bisection-reconnection.

Systematic paleontology

TESTUDINATA Klein, 1760 [80]

TESTUDINES Batsch, 1788 [81]

XINJIANGCHELYIDAE Nessov in Kaznyshkin et al., 1990 [7] (sensu Rabi et al., In press [59])

Remark

We follow the phylogenetic definition of Xinjiangchelyidae used in Rabi et al. (In press [59]) where Xinjiangchelyidae is defined as the most inclusive clade containing *Xinjiangchelys junggarensis* Ye, 1986 [82], but not *Sinemys lens*, *Macrobaena mongolica*, or any species of Recent turtle.

Xinjiangchelys Ye, 1986 [82]

Remark: A number of genera other than *Xinjiangchelys* have been referred to Xinjiangchelyidae in recent years, including *Chengyuchelys* Young and Chow, 1953 [75]; *Tienfuchelys* Young and Chow, 1953 [75]; *Annemys* Sukhanov and Narmandakh, 2006 [58]; *Shartegemys*, Sukhanov and Narmandakh, 2006 [58]; *Yanduchelys* Peng et al. 2005 [83]; *Protoxinjiangchelys* Tong et al. 2012 [13] ([8,13-15,58,71]). The majority of these genera are sufficiently diagnosed relative to *Xinjiangchelys*, but there is no up-dated diagnosis available for *Xinjiangchelys*. This taxon has therefore been rendered a waste-backed taxon defined by what it is *not*. To avoid further complications we suggest using a more inclusive definition for *Xinjiangchelys* that includes all species of Xinjiangchelyidae (sensu Rabi et al., In press [59]) until the phylogenetic relationships of the included taxa can be determined more confidently.

Xinjiangchelys wusu sp. nov.

(Figure 2, Figures 4, 5, 6, 7, and 8)

urn:lsid:zoobank.org:pub:2BCCC095-7622-4 F27-8 F80-6199F24690B5

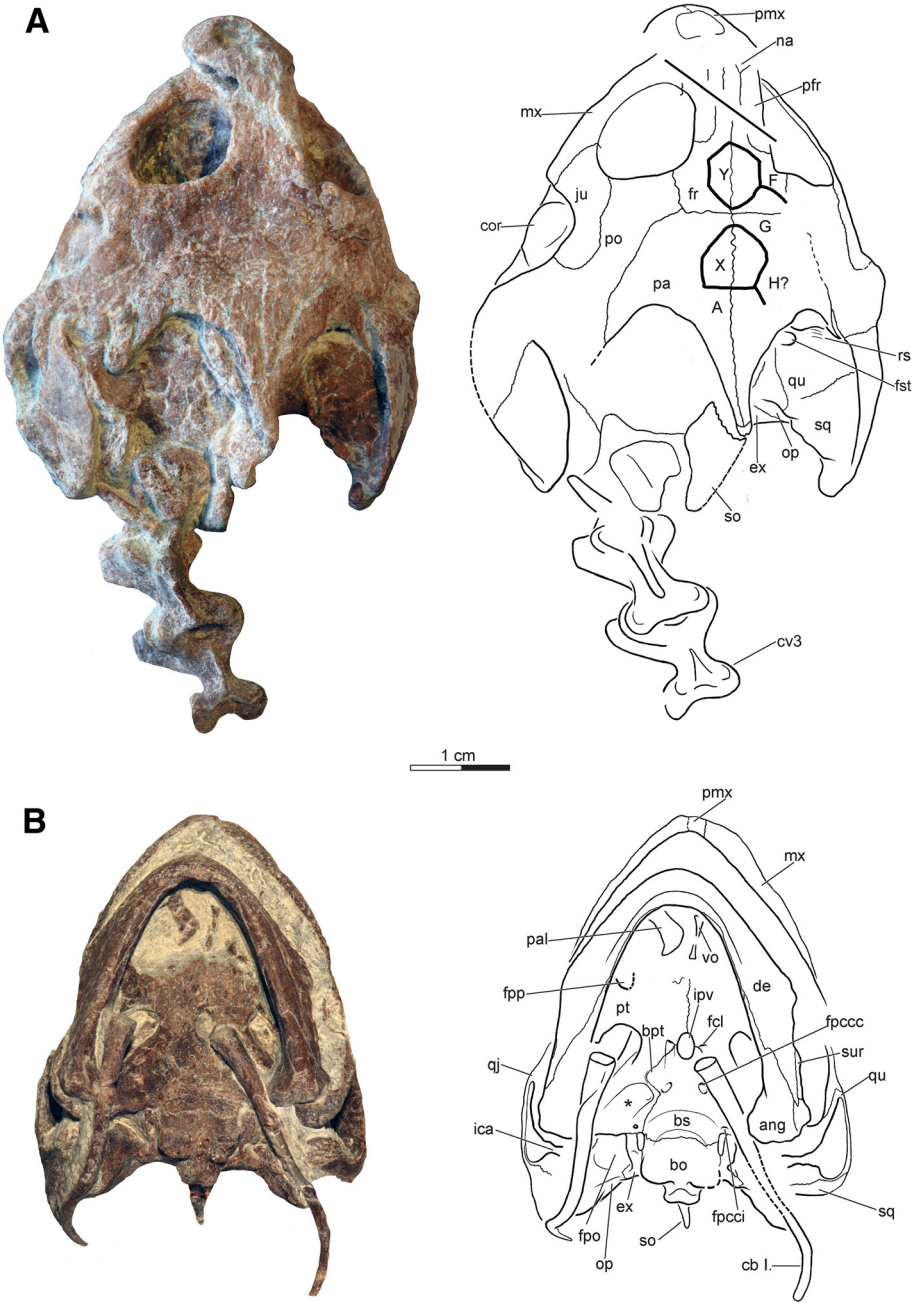

Figure 4 Skulls and partial neck of *Xinjiangchelys wusu*, Middle Jurassic, ?Qigu Formation, "Turtle Cliff", Shanshan area, Turpan Basin, Xinjiang Autonomous Province, China. A, PMOL-SGP A0100-1 (holotype), photograph and line drawing of skull and anterior cervical vertebrae in dorsal view; **B**, PMOL-SGP A0100-3, photograph and line drawing of skull, mandible and hyoid apparatus in ventral view. Abbreviations: **ang**: angular, **bo**: basioccipital, **bpt**: basipterygoid process, **bs**: basisphenoid, **cb I.**: cornu branchiale I, **cor**: coronoid, **cv**: cervical vertebra, **de**: dentary, **ex**: exoccipital, **fcl**: foramen caroticum laterale, **fpccc**: foramen posterius canalis carotici cerebralis, **fpcci**: foramen posterius canalis carotici interni, **fpo**: fenestra postotica, **fpp**: foramen palatinum posterius, **fr**: frontal, **fst**: foramen stapedio-temporale, **ica**: incisura columella auris, **ipv**: interpterygoid vacuity, **ju**: jugal, **mx**: maxilla, **na**: nasal, **op**: opisthotic, **pa**: parietal, **pal**: palatine, **pfr**: prefrontal, **pmx**: premaxilla, **po**: postorbital, **pt**: pterygoid, **qj**: quadratojugal, **qu**: quadrate, **rs**: rugose surface of processus trochlearis oticum, **so**: supraoccipital, **sq**: squamosal, **sur**: surangular, **vo**: vomer, * refers to fossa pterygoidea. A, X, G, H, Y refer to scales after Sterli and de la Fuente [16].

Holotype
PMOL-SGP A0100-1, a partial skeleton, including the skull exposed in dorsal view (Figures 2, 4, 6 and 8B).

Referred material
PMOL-SGP A0100-3, partial skeleton (Figures 2, 4, 5 and 7,); PMOL-SGP A0100-2, partial skeleton without skull, plastron not exposed (Figures 2, 6 and 7A, C-D).

Locality and horizon
Turtle Cliff Fossil Locality (see Geological Settings), Shanshan, Turpan Basin, Xinjiang Autonomous Province, People's Republic of China (Figure 1); ?Qigu Formation, Upper Jurassic.

Etymology
wusu refers to a small town in Xinjiang Autonomous Province.

Diagnosis
A species of *Xinjiangchelys*; skull differing from *X.* (*Annemys*) *levensis* in the prefrontals being fully separated by the frontals; from *X.* (*Annemys*) *latiens* by the broader skull and the extensive jugal and frontal contribution to the orbit, from *X. radiplicatoides* by the flattened skull and the presence of a remnant of the interpterygoid vacuity. Shell differing from *X. chowi* Matzke et al. [84] *X. qiguensis* Matzke et al., [85] *X. tianshanensis* Kaznyshkin et al. [7] and *X. junggarensis* (sensu Brinkman et al. 2008 [70]) by the narrow vertebral scales.

Description
Skull

Preservation The skull of PMOL-SGP A0100-1 is exposed only in dorsal and lateral views, whereas its palatal side is covered by the carapace of PMOL-SGP A0100-2 (Figure 2). It is dorsoventrally crushed and the preorbital region is slightly shifted from its original position. The skull of PMOL-SGP A0100-3, on the other hand, is exposed in ventral view and in articulation with the hyoids and the mandible (Figures 4B and 5).

Scales Some of the cranial scales are traceable in PMOL-SGP A0100-1, but most of them are not apparent (Figure 4A). Using a recently suggested nomenclatural system [16] we identify the unpaired scale Y on the posterior half of the frontal posteriorly bordered by the paired scale F. Scale G is bordered by the unpaired parietal scale X posteriorly. Scale A is another unpaired scale of the parietal found posteriorly to scale X. Scale H may have also been present laterally to scale X. The skull roof is otherwise decorated with fine grooves and very shallow pits that do not show a clear pattern.

Nasals The nasals are very poorly preserved but their sutures with the frontal and the prefrontal are partially traceable on the right side of PMOL-SGP A0100-1 (Figure 4A). They are reduced, posteriorly tapering elements that are partially separated by the anterior frontal process. The nasals contribute to the formation of the external nares.

Prefrontals The dorsal plate of the prefrontals is elongate and medially separated from its counterpart by the anterior frontal process (Figure 4A). The prefrontal contacts the nasal anteriorly and the maxilla ventrally. The descending process of the prefrontal has a wide contact with the palatines within the fossa orbitalis. Its contact with the vomer is not visible, but given the large size of the prefrontal pillars it was very likely present. The frontal forms the anterior half of the dorsal margin of the orbit.

Frontals The frontals form an anterior process that is wedged between the prefrontals (Figure 4A). The posterior half of the dorsal margin of the orbit is formed by the frontals. The orbit has a subcircular outline and faces dorsolaterally.

Parietals The dorsal plate of the parietals exhibits a relatively deep temporal emargination that reaches beyond the level of the anterior border of the cavum tympani (Figure 4A). The parietal meets the frontal anteriorly and has a long contact with the postorbital. Even though the parietals are slightly shifted from their original position in PMOL-SGP A0100-1, their posterolateral tips also touched the squamosal, as seen on the right side. Dorsoventral crushing obscures the structures of the processus inferior parietalis.

Jugal The jugal area is compressed and its entire lateral surface is exposed in dorsal view in PMOL-SGP A0100-1 and it is also partially visible in PMOL-SGP A0100-3 (Figures 4A and 5B). It sends a long posterior process along the postorbital but it is unclear whether it meets the quadratojugal. The skull exhibits a moderate cheek emargination that exposes the coronoid process of the mandible. Anteriorly, the jugal forms the posterolateral margin of the orbit and contacts the maxilla. It is unclear whether the ventral plate of the jugal contacts the posterior end of the triturating surface and/or the anterolateral tip of the external pterygoid process.

Quadratojugal The quadratojugal is a reduced, flat element that is best preserved in PMOL-SGP A0100-3,

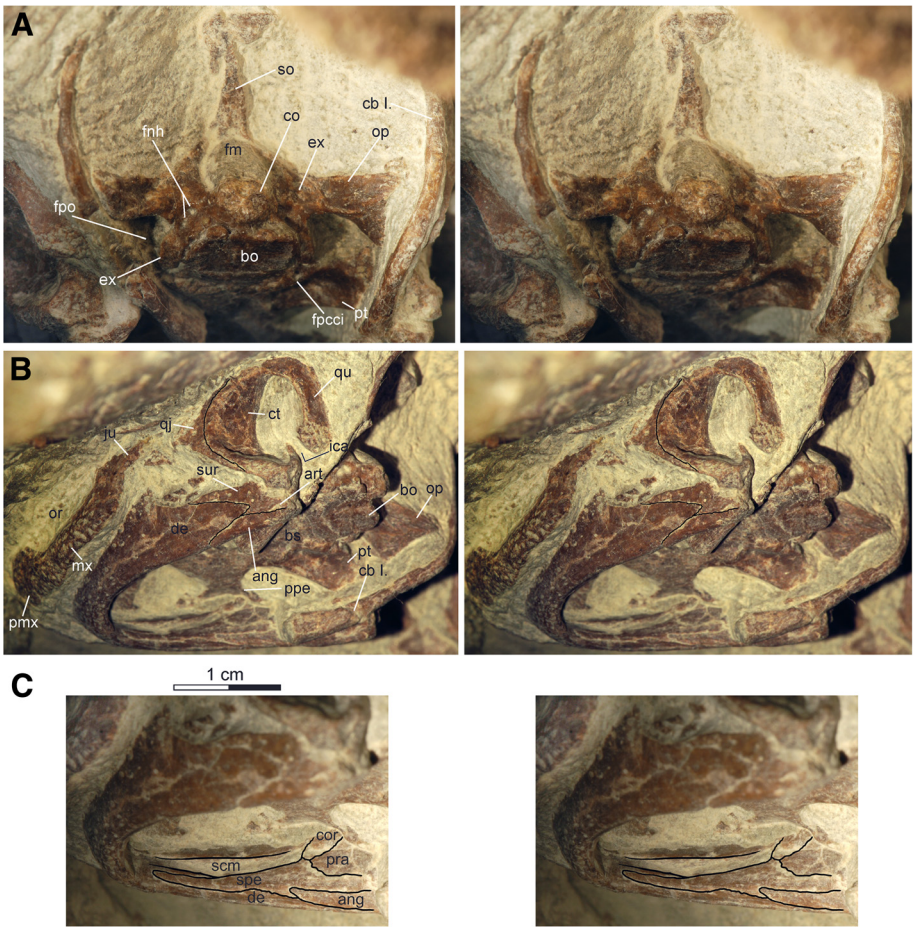

Figure 5 PMOL-SGP A0100-3, skull, mandible and hyoid apparatus of *Xinjiangchelys wusu*, Middle Jurassic, ?Qigu Formation, "Turtle Cliff", Shanshan area, Turpan Basin, Xinjiang Autonomous Province, China. **A**, occipital view of skull; **B**, left ventrolateral view of skull and mandible; **C**, medial view of right ramus of mandible. Abbreviations: **ang**: angular, **art**: articular, **bo**: basioccipital, **bs**: basisphenoid, **cb I.**: cornu branchiale I., **co**: condylus occipitalis, **cor**: coronoid, **ct**: cavum tympani, **de**: dentary, **ex**: exoccipital, **fm**: foramen magnum; **fnh**: foramen nervi hypoglossi, **fpcci**: foramen posterius canalis carotici interni, **fpo**: fenestra postotica, **ica**: incisura columella auris, **ju**: jugal, **mx**: maxilla, **op**: opisthotic, **or**: orbit, pmx: premaxilla, **ppe**: processus pterygoideus externus, **pra**: prearticular, **pt**: pterygoid, **qj**: quadratojugal, **qu**: quadrate, **scm**: sulcus cartilaginis Meckelii, **so**: supraoccipital, **spe**: splenial, **sur**: surangular.

though not fully exposed (Figure 5B). It has no clear contact with the jugal anteriorly but this is all but certain. Dorsally, it meets the postorbital and posteriorly it borders the cavum tympani. Its lower rim of the skull is emarginated, which gives the quadratojugal a subtriangular outline. The quadratojugal sends a pair of narrow and tapering processes along the dorsal and the ventral margins of the cavum tympani, respectively. The dorsal one of these processes is wedged between the postorbital and the quadrate and appears not to reach the squamosal. The ventral one terminates slightly before the level of the condylus mandibularis.

Squamosal The squamosal is better preserved on the right side of PMOL-SGP A0100-1, the left one being compressed and the lateral plate being exposed when the skull is viewed dorsally (Figure 4). The lateral surface of the squamosal is smooth and there is no squamosal horn. The squamosal has a very short point-like contact with the parietal along the anterior margin of the upper temporal emargination. There is no contribution to the formation of the anterior opening of the antrum postoticum as seen in PMOL-SGP A0100-3. Medially, the squamosal contacts the quadrate and may even have a short contact with the opisthotic within the upper temporal fossa. The contact of the ventral portion with the opisthotic and the quadrate is not exposed in either specimen.

Postorbital The postorbitals are long elements; they form the posterodorsal margin of the orbit and also contribute to the rim of the upper temporal emargination (Figure 4A). The postorbital has an anteroventral contact with the jugal, a posteroventral contact with the

quadratojugal, a long lateral contact with the parietal, and also meets the squamosal posteriorly.

Premaxilla The premaxillary region is shifted anteriorly from the original position and damaged in PMOL-SGP A0100-1 (Figure 4). The premaxilla forms the ventral margin of the external nares and contacts the other premaxilla medially and the maxilla posterolaterally. The external nares are undivided. Only little of the ventral aspect of the premaxillary region is exposed but it is apparent that there is no premaxillary hook.

Maxilla The maxilla forms the ventral margin of the orbit, sends a dorsal process to contact the descending pillar of the prefrontal, and contacts the premaxilla anteriorly and the jugal posteriorly (Figures 4 and 5B). The triturating surface is only partially exposed but it is apparently narrow and straight with a sharp and low labial ridge.

Vomer A single, slightly damaged and displaced, elegant vomer is present in PMOL-SGP A0100-3 exposed in dorsal view (Figure 4B). Its outline is very similar to that of *Xinjiangchelys levensis*.

Palatine The right palatine is preserved incompletely and shifted from the original position in PMOL-SGP A0100-3 (Figure 4B). It shows an extensive free lateral margin that is indicative of a large foramen palatinum posterius.

Quadrate Apart from the region of the cavum tympani, the right quadrate of PMOL-SGP A0100-1 is in good condition whereas the left otic region is badly fragmented and compressed (Figures 4 and 5B). In PMOL-SGP A0100-3 the region of the cavum tympani is exposed in lateral view. The cavum tympani is anteriorly bordered by the quadratojugal and by the squamosal dorsally and posteriorly. The incisura columella auris is an open but tight notch and there is no precolumellar fossa. The antrum postoticum is well developed and its opening is formed entirely by the quadrate, although the squamosal comes very close to the lateral rim. The quadrate contacts within the upper temporal fossa the squamosal posterolaterally and the opisthotic medially, but its medial contact with the prootic is obscured. Together with the prootic it forms a large foramen stapedio-temporale. The quadrate forms a poorly developed processus trochlearis oticum that is composed of a rugose area.

Epipterygoid The epipterygoids are not exposed in either specimen.

Pterygoid The pterygoids are almost intact in PMOL-SGP A0100-3 except for their anteriormost edges (Figures 4B and 5A-B). The pterygoid has a long posterior process reaching as far as the back of the skull and terminating slightly anterior to the basioccipital-basisphenoid suture. The pterygoid covers the cranioquadrate space and contacts the posterolateral corner of the basisphenoid but not the basioccipital. The pterygoid has a short dorsal contact with the exoccipital, but this contact is not part of the skull surface. The foramen posterius canalis carotici interni opens at the back of the skull within the ventral surface of the pterygoid. The quadrate ramus of the pterygoid bears a well-developed, oval-shaped pterygoid fossa. The processus pterygoideus externus is present and it is characterized by a posteriorly extending horizontal plate and a dorsoventrally thickened vertical plate. A characteristic feature of the pterygoid is a large oval opening just anterior to the basisphenoid and posterior to the region where the pterygoids meet one another along the midline. This opening has intact margins, is clearly not a result of erosion or any other taphonomic processes, but is distinct from the foramen posterius canalis carotici palatinum. We interpret this structure as the remnant of the interpterygoid vacuity. Anterolaterally, the pterygoid bears a margin that is indicative of a large foramen palatinum posterius.

Supraoccipital Much of the crista supraoccipitalis is displaced and preserved in fragments in PMOL-SGP A0100-1 (Figures 4 and 5A). The supraoccipital provides only a small contribution to the skull roof where it contacts the parietals. The ventral plate of the supraoccipital contacts the opisthotic laterally and forms the dorsal margin of the foramen magnum. The crista supraoccipitalis extended apparently only slightly beyond the posterior tip of the squamosals. In PMOL-SGP A0100-3 the supraoccipital crest is intact as exposed in ventral view and does not protrude much beyond the level of the occipital condyle.

Exoccipitals The exoccipitals are preserved on both sides in PMOL-SGP A0100-3 (Figures 4 and 5A). They form the ventrolateral wall of the foramen magnum. A pair of foramen nervi hypoglossi pierce each elements but the formed foramen jugulare posterius is not distinct from the fenestra postotica (Figure 5A). Laterally, the exoccipitals contact the opisthotic and have a ventromedial contact with the basioccipital. Anteroventrally, the exoccipital has a short contact with the posteriormost tip of the pterygoid, but this contact does not contribute to the smooth, palatal surface of the skull. A suboval, unossified area excludes the exoccipital from anteromedially contacting the basisphenoid.

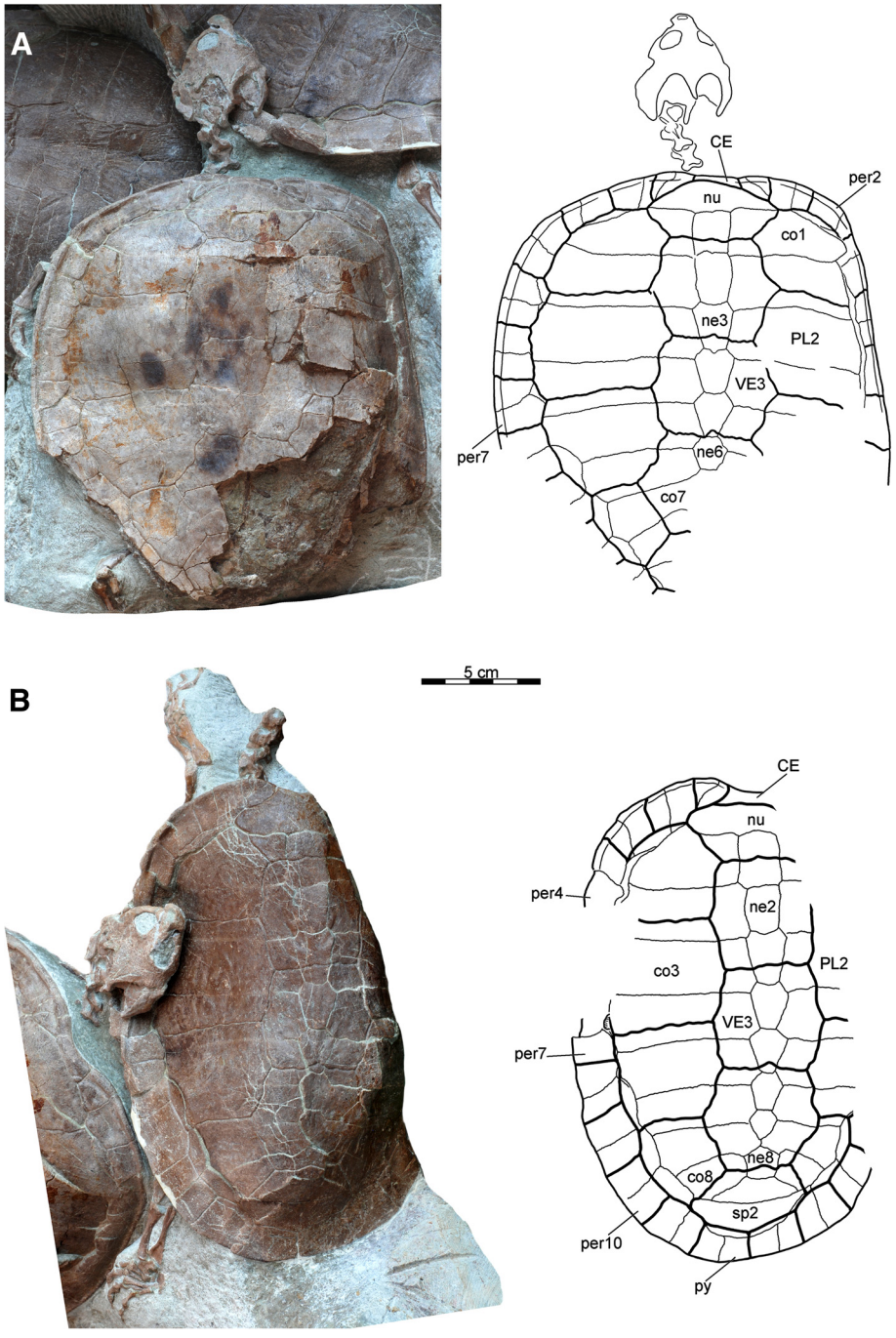

Figure 6 Carapaces of *Xinjiangchelys wusu*, Middle Jurassic, ?Qigu Formation, "Turtle Cliff", Shanshan area, Turpan Basin, Xinjiang Autonomous Province, China. **A**, PMOL-SGP A0100-1 (holotype), photograph and line drawing; **B**, PMOL-SGP A0100-2, photograph and line drawing. Abbreviations: **CE**: cervical scute, **co**: costal, **ne**: neural, **nu**: nuchal, **per**: peripheral, **PL**: pleural, **VE**: vertebral, **py**: pygal, **sp**: suprapygal.

Basioccipital The basioccipital has a pair of basioccipital tubera with rounded posterior edges that extends as a roof over the foramen nervi hypoglossi when the skull is viewed ventrally (Figures 4B and 5A-B). The neck of the basioccipital condyle is short and lacks paired ridges or grooves. The basioccipital has no contact with the pterygoid and the processus interfenestralis of the opisthotic is therefore visible in ventral view. Anteriorly, the basioccipital meets the basisphenoid via a transverse suture. A shallow concavity extends on the ventral surface of the basioccipital that barely protrudes onto the basisphenoid.

Prootic The prootic is barely exposed on the right side of the skull of PMOL-SGP A0100-1 (not visible in dorsal view due to crushing). The skull roof in this specimen is deformed and thereby obscures the dorsomedial third of the ear capsule. On the left side, the ear capsule is so crushed that the structures cannot be identified with confidence. The prootic contributes to the large foramen stapedio-temporale together with the quadrate and maybe even with the opisthotic. There seem to be no prootic contribution to the processus trochlearis oticum (i.e. the rugose surface on the anterodorsal portion of the quadrate) by the prootic.

Opisthotic The opisthotic is exposed in both skulls (Figures 4 and 5A-B). The supraoccipital has a thin lateral lamina that partially covers the opisthotic within the upper temporal fossa. The opisthotic has a long lateral contact with the quadrate, may have a short contact with the squamosal, and ventrolaterally contacts the exoccipital. The dorsal portion of the opisthotic has a sutured contact with the quadrate whereas its contact with the squamosal is covered by matrix. The opisthotic forms a pillar-like processus interfenestralis that is visible in ventral view.

Basisphenoid The basisphenoid is preserved in good condition in PMOL-SGP A0100-3 (Figures 4B and 5B). It contacts the basioccipital along a straight suture posteriorly and is surrounded by the pterygoid rami laterally. The ventral surface is smooth and paired pits are therefore absent. The basisphenoid has a marked basipterygoid process in a form of a triangular, flat, horizontal plate that is sutured to and fits into a slightly-raised "pocket" of the pterygoid (Figure 4B). The foramen posterius canalis carotici interni is limited to the pterygoid but at least the anterior half of the floored canalis carotici interni extends along the pterygoid-basisphenoid suture. More anteriorly the carotid artery was exposed in a relatively deep and short, anteromedially directed sulcus, the fenestra caroticus, in the basisphenoid in which the split of the cerebral and palatine arteries was located. The cerebral branch diverged anteromedially and reentered the skull via the foramen posterius canalis carotici cerebralis at the medialmost corner of the fenestra. After exiting the fenestra, the palatine branch extended anteriorly in a shallow groove and entered the skull via the foramen posterius canalis carotici palatinum, which is situated on the basisphenoid-pterygoid contact just lateral to the residual interpterygoid vacuity. Since the latter foramen is clearly present, we infer that the palatine branch entered the skull here and not via the interpterygoid vacuity. The reduced condition of the interpterygoid vacuity in PMOL-SGP A0100-3 could represent a transitional state between a fully formed interpterygoid vacuity as seen in basal turtles [19,35,86,87] and a completely closed one as seen in numerous crown-group turtles [3].

Mandible

The elegant and shallow mandible is preserved in articulation in PMOL-SGP A0100-3 (Figure 4B and 5B-C) and PMOL-SGP A0100-1 (Figure 4A), the former exposing the left coronoid region and the lateral plate of the dentary whereas the latter exposing the entire ventral and lateral aspects.

The dentary is characterized by a narrow triturating surface and a fused symphysis but neither the dentary ridges nor the anterodorsal tip of the symphyseal region are exposed. Laterally, the dentary extends posteriorly to meet the angular and the surangular whereas its contact with the articular is uncertain.

The coronoid is rather low and a long. An anteriorly tapering splenial is present that extends below the Meckelian canal along the dentary and approaches the symphysis. The splenial sends a posterior process between the angular and the prearticular, whereas the angular sends a similarly long anterior process into the splenial ventral to this projection. At the anteroventral tip of the angular process there is a triple junction with the dentary and the splenial. The processus retroarticularis is short. The splenial has a short dorsal contact with the coronoid.

Hyoid apparatus

Both cornu branchiale I are preserved almost in situ in PMOL-SGP A0100-3 (Figures 4B and 5A-B), the right one being slightly crushed and incomplete. There is no evidence of an ossified corpus hyoidis or cornu branchiale II and these structures were therefore likely cartilaginous. The cornu branchiale I is a single, elegant element that can be divided into an anterior horizontal half and a posterior vertical half. It tapers posteriorly and terminates in a narrow, whip-like structure. When the skull is viewed from laterally, the border of the vertical and the horizontal portion is roughly at the level of the posterior rim of the cavum tympani.

Shell

Carapace The carapace is present in all three specimens (Figures 3, 6 and 7A). PMOL-SGP A0100-1 and PMOL-SGP A0100-2 cover the anterior third of the carapace of PMOL-SGP A0100-3. PMOL-SGP A0100-1 has a posteriorly incomplete and slightly anterodorsally compressed carapace whereas PMOL-SGP A0100-2 is considerably deformed along its long axis and its right lateral third is missing due to damage that occurred during recovery of

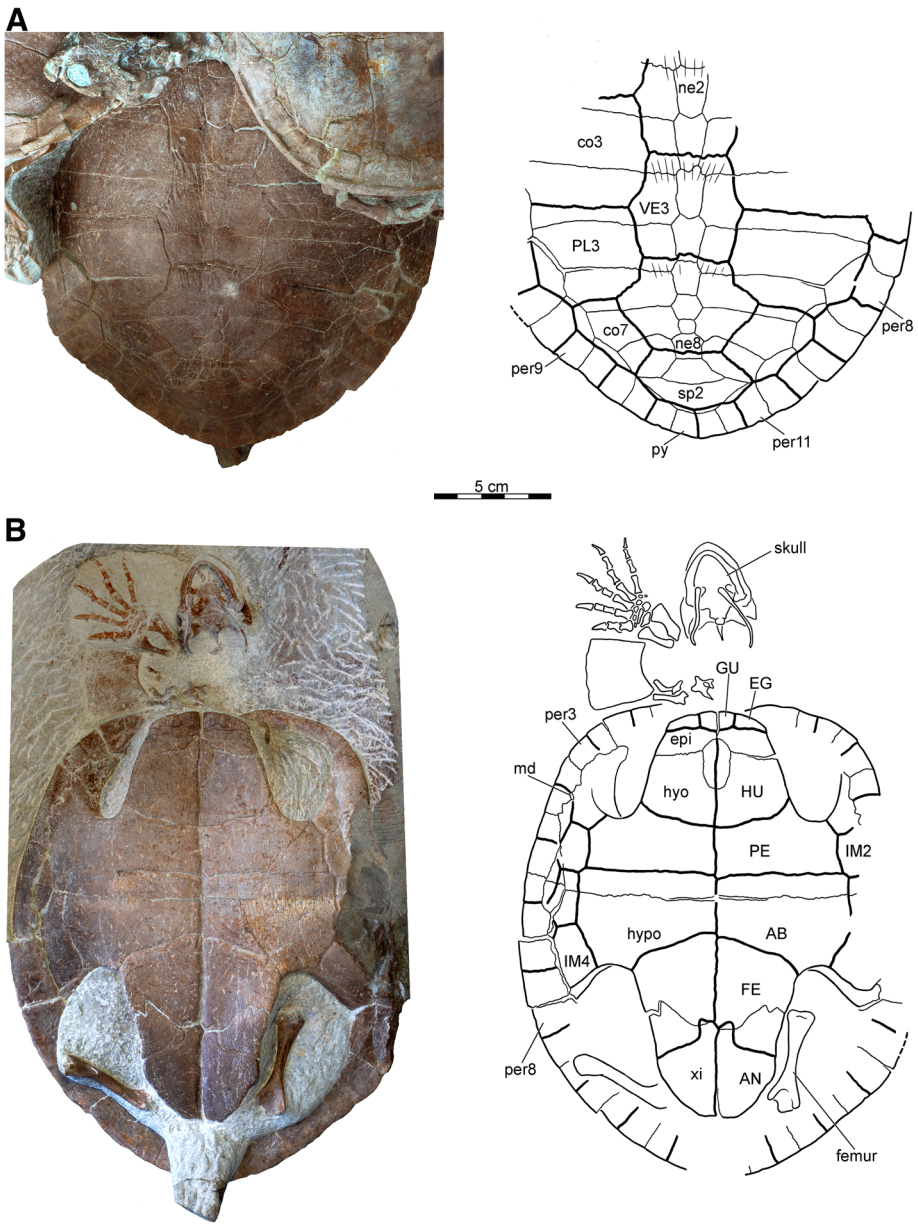

Figure 7 PMOL-SGP A0100-3 *Xinjiangchelys wusu* shell, Middle Jurassic, ?Qigu Formation, "Turtle Cliff", Shanshan area, Turpan Basin, Xinjiang Autonomous Province, China. A, photograph and line drawing of posterior two third of carapace; **B**, photograph and line drawing of plastron. The right forelimb in 'B' does not belong to PMOL-SGP A0100-3 but to PMOL-SGP A0100-1. Abbreviations: **AB**: abdominal, **AN**: anal, **co**: costal, **EG**: extra gular, **epi**: epiplastron, **FE**: femoral, **GU:** gular, **HU**: humeral, **hyo**: hyoplastron, **hypo**: hypoplastron, **IM**: inframarginal, **md**: musk duct foramen, **ne**: neural, **per**: peripheral, **PE**: pectoral, **PL**: pleural, **py**: pygal, **sp**: suprapygal, **VE**: vertebral, **xi**: xiphiplastron.

the block (see Materials and Methods). PMOL-SGP A0100-3 is not deformed; the exposed portion preserves the original outline of the carapace suggesting a relatively wide shell.

Carapacial bones The nuchal is a trapezoidal element and more than twice as wide than long (Figure 6). The nuchal emargination is minor in PMOL-SGP A0100-1 but appears to be slightly deeper in PMOL-SGP A0100-2. This emargination extends onto peripheral 1 in both specimens.

There are eight pairs of costal bones, all of which have firm contacts with the peripherals and lack costal fontanelles. The reduction of neural 7 in PMOL-SGP A0100-2 allows for a short, medial contact of costals 7, which contrasts the morphology of PMOL-SGP A0100-3, where a subdivided neural 7 does not allow for this

contact (Figures 6B and 7A). This region is not preserved in PMOL-SGP A0100-1.

Costal 1 tapers laterally and is subequal in anteroposterior length with the more posterior costals. The figure of PMOL-SGP A0100-2 (Figure 6B) hints at a seemingly longer costal 1, but this is an optical illusion resulting from distortion. Costal 2 has a slightly concave anterolateral outline and sends a wide rectangular posterolateral process into the posterior half of peripheral 4, as is best seen on the left side of PMOL-SGP A0100-1 (Figure 6A), but also visible on the right side and in PMOL-SGP A0100-2 (Figure 6B). Costal 3 is the mediolaterally widest element and has straight and parallel anterior and posterior sides. Costal 4 is slightly concave anteriorly and convex posteriorly and has strongly concave contacts with peripheral 6 and 7. Costal 5 is slightly convex anteriorly and posteriorly. It has a short, oblique contact with peripheral 7 and a strongly concave contact with peripheral 8. PMOL-SGP A0100-3 is different in that costal 5 barely touches peripheral 7 (Figure 7A). The contact of costal 6 with peripheral 8 projects more laterally relative to its contact with peripheral 9. Costal 7 has an oblique and straight anterior border and a concave posterior border. Costal 8 is narrow and slightly convex anteriorly and posteriorly.

The neural series is complete and consists of eight elements, including a subdivided neural 7 in PMOL-SGP A0100-3 (Figure 7A). In PMOL-SGP A0100-2 the series is interrupted by the short contact of costals 7 (Figure 6B). In PMOL-SGP A0100-1, this region is incomplete. Most neurals are hexagonal, coffin-shaped elements with the short sides facing anterolaterally. Neural 1 of PMOL-SGP A0100-1 and 3 is quadrangular whereas it is hexagonal with short sides facing posterolaterally in PMOL-SGP A0100-2 the quadrangular element being neural 2 instead. In PMOL-SGP A0100-3 neural 7 is subdivided into a larger, regular, hexagonal element and a small, square element and neural 8 is hexagonal. In PMOL-SGP A0100-2 both neurals 7 and 8 are pentagonal and do not contact one another, thereby allowing for a medial contact of costals 7.

There are two suprapygals, the anterior one is trapezoidal has no contacts with the peripherals and considerably wider and shorter in PMOL-SGP A0100-2 than in PMOL-SGP A0100-3 (Figures 6B and 7A). Suprapygal 2 is a wide element that contacts costal 8 and peripheral 11.

There are 11 pairs of peripherals (Figures 6 and 7). A distinct gutter extends from the lateral corner of the nuchal to peripheral 7 along the lateral margin of the carapace. Peripheral 1 contacts costal 1 and is larger on the right side than on the left in PMOL-SGP A0100-1 (Figure 6A). Peripheral 2-6 are narrow elements whereas 7-11 are considerably expanded laterally. Peripheral 8 is the widest peripheral element and has a strong medial projection into costal 5 in all specimens.

Carapacial scales There are five vertebrals and a single wide cervical (Figures 6 and 7B). Vertebral 1 is wider than long and barely touches peripheral 1. The proportions of vertebrals 2-4 vary somewhat among the specimens, but all are narrower than most pleurals. PMOL-SGP A0100-1 has the relatively widest vertebrals of all. Vertebral 2 is slightly longer than wide in PMOL-SGP A0100-3 (as reconstructed) and PMOL-SGP A0100-2 whereas in PMOL-SGP A0100-1 it is markedly wider than long. Vertebral 3 is slightly wider than long in PMOL-SGP A0100-3 and PMOL-SGP A0100-3-3 and slightly longer than wide in PMOL-SGP A0100-2. Vertebral 4 is considerably wider than long in PMOL-SGP A0100-3 and PMOL-SGP A0100-3-3 and this is less distinct in PMOL-SGP A0100-2. The vertebral 3-4 sulcus has anterior projection at the midline that extends onto the posterior portion of neural 5 in all specimens. Vertebral 5 is wider than long, contacts peripherals 11 laterally, and does not prolong onto the suprapygal (as preserved in PMOL-SGP A0100-1 and PMOL-SGP A0100-3).

The pleurals are all wider than long except for pleural 4 that is longer than wide (Figures 6 and 7A).

The marginals are either restricted to the peripherals or their borders coincide with the costo-peripheral contacts or, as in the case of marginals 5 and 7, they slightly lap onto the costals. Marginal 11 indistinctly prolongs onto the costals on the left sides of all specimens (right side not preserved in PMOL-SGP A0100-1).

Plastron The plastron is only exposed in PMOL-SGP A0100-3 (Figure 7B). In this specimen the plastron is preserved in perfect condition except for minor damage in the right bridge area. The dorsal aspect of the plastron is not visible. The plastron is characterized by complete ossification (i.e., no fontanelles) and compact, sutural contacts. Scale sulci are clearly developed. The anterior lobe is about 40% wider than long, shorter than the posterior lobe, and has a slightly rounded anterior margin. Mesoplastra are absent. The posterior lobe is posteriorly tapering, slightly wider at its base than long, and lacks an anal notch. At least one musk duct foramen is present between peripheral 4 and the hyoplastron.

Plastral bones The epiplastron is trapezoidal, shows a roughly transverse suture with the hyoplastron, an anteromedially directed contact with the entoplastron, and a sagittal contact with the other epiplastron (Figure 7B). The entoplastron is oval-shaped, about twice as long as wide, and only partially separates the epiplastra. The buttress of the hyoplastron is relatively low and it terminates on the anterior half of peripheral 2. The contact of the plastron with the carapace is tight

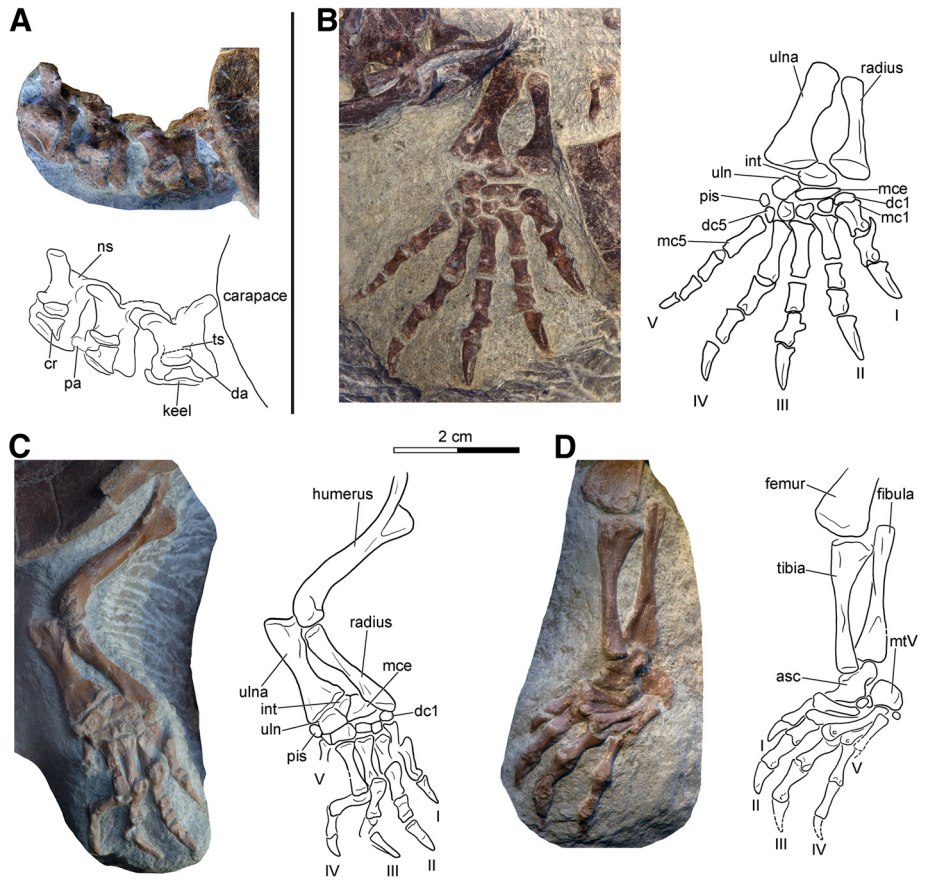

Figure 8 Neck and appendicular elements of *Xinjiangchelys wusu*, Middle Jurassic, ?Qigu Formation, "Turtle Cliff", Shanshan area, Turpan Basin, Xinjiang Autonomous Province, China. A, PMOL-SGP A0100-2, photograph and line drawing of articulated cervical vertebrae III-V in lateral view; **B**, PMOL-SGP A0100-1, photograph and line drawing of right distal fore limb; **C**, PMOL-SGP A0100-2, photograph and line drawing of left fore limb; **D**, PMOL-SGP A0100-2, photograph and line drawing of left hind limb. Abbreviations: **asc**: fused astragalocalcaneum, **cr**: cervical rib, **da**: diapophysis, **dc**: distal carpal, **int**: intermedium, **mc**: metacarpal, **mce**: medial central, **mt**: metatarsal, **ns**: neural spine, **pa**: parapophysis, **pis**: pisiform, **ts**: transverse process, **uln**: ulnare.

but we interpret it as being ligamentous rather than sutured owing for the presence of plastral pegs. However, we note that our meaning of ligamentous contact is probably different from the concept of earlier studies [13,14]. The edges of the bridge peripherals slightly overlap the margin of the bridge of the plastron. Peripherals 3, 4, and the anterior third of peripheral 5 contact the plastron via well-developed pegs. Further posteriorly, the contact between the plastron and the carapace transfers into a smooth-edged contact until the posterior third of peripheral 6. Just medial to this edge the plastron is notched at the contact of the hyo- and the hypoplastron, but this space is filled up with two elements (on one side) that appear to be aberrant extra ossifications that meet the hyo- and the hypoplastron along finely serrated edges. The anterior edge of these elements is partially fused with the hyoplastron. More posteriorly, the hypoplastron contacts the peripherals via pegs with the inguinal buttress terminating on the anterior third of peripheral 8. The xiphiplastra are well developed and they have a fork-like contact with the posterolateral portion of the hypoplastron in ventral view. Interfingering interplastral sutures are absent.

Plastral scales One pair of gulars and one pair of extragulars are present. The gulars do not extend onto the entoplastron and the extragulars have a transverse contact with the humeral scales. The midline sulcus of the plastron is straight instead of sinusoidal. The pectoral scale is shorter than the abdominal. The femoral/anal sulcus is omega-shaped and the anals barely extend near the midline onto the hypoplastron. Four pairs of inframarginals are present, of which the third covers the hyo/hypoplastral suture (Figure 7B).

Appendicular skeleton

The articulated distal half of the right fore limb of PMOL-SGP A0100-1 is exposed in antipalmar view next to the skull of PMOL-SGP A0100-3 (Figures 7B and 8B). The left distal fore limb of this individual is less complete and preserved tucked on the other side of the slab next to the carapace (Figure 6A). The articulated left fore and hind limbs of PMOL-SGP A0100-2 (Figure 6B) are preserved in palmar and antipalmar view, respectively (Figures 8C-D). Only the left ulna, radius, an associated phalanx, the distal end of the right humerus, and both femora are exposed in specimen PMOL-SGP A0100-3 (Figure 7B). An additional, isolated left hind limb is present on the slab that likely belongs to a fourth specimen (Figure 3).

Humerus The humerus has a slightly curved shaft with a suboval cross-section (Figure 8C). The lateral process is slightly better developed than the medial process and both processes are situated at the same level relative to one and another along the proximal part of the humerus. The ectepicondylar foramen is closed.

Radius and ulna The radius is elegant and narrow and has a straight and relatively flat shaft in cross-section (Figures 8B-C). Its proximal epiphysis is subcircular in cross-section whereas its distal epiphysis is expanded and more compressed. The articulation surface for the medial centrale extends along the distal margin of the epiphysis as in *Podocnemis expansa* [19]. The medial edge of the distal epiphysis lacks a medial projection that is otherwise present in *Macrochelys temminckii*. The lateral ridge below the proximal epiphysis, presumably for the attachment of the radio-ulnar ligament [19], is reduced. The ulna is flattened and more robust than the radius. The medial margin of the shaft is more curved than the lateral one. The ridge for the bicipital tendon attachment is reduced and the olecranon is poorly developed. The medial process of the proximal epiphysis is situated slightly below the level of the olecranon as in *M. temminckii* but unlike in *P. expansa*. The relative proportions of the proximal and distal epiphyses more resemble *M. temminckii* in having similar width (the distal being slightly wider).

Manus The relatively elongate and narrow phalanges of the manus suggest intermediate aquatic adaptation [88]. The phalangeal formula is 2-3-3-3-3 (Figures 8B-C). The unguals are clawed, narrow, and pointed, and decrease in size from the digit I to V. The distal articulation surfaces of the proximal phalanges exhibit posteriorly projecting flanges that underlap the proximal epiphysis of the preceding metacarpals. The first metacarpal is the shortest and the most robust. The lateral overlapping of the metacarpals with one another is present but not marked. The distal carpals are ovoid and that of the first digit is slightly wider than those of the remaining digits. There is a small pisiform and the medial centrale is tightly connected with the lateral centrale. The intermedium is not elongate proximodistally, the ulnare is flat and deep, and the radiale bears little if any articulation with the radius.

Femur The femur has a slightly curved shaft (Figures 7B and 8D). The trochanter minor faces anteriorly, the trochanter major faces dorsally, and the femoral head only slightly extends above the trochanters. The trochanters are moderately developed. The proximal epiphysis has a similar width as the distal one.

Tibia and fibula The tibia has a wide proximal epiphysis (Figure 8D) than *Podocnemis expansa* or *Macrochelys temminckii*. The ridge for the patellar tendon attachment is placed close to the midline of the shaft as in *M. temminckii* and unlike in *P. expansa* where it is shifted laterally. The fibula is straight and has a more expanded and more compressed distal epiphysis than its proximal one. Proximally, the shaft lacks a medial flange, unlike in *Podocnemis expansa*.

Pes The hooked fifth metatarsal is a large, blocky element (Figure 8D). The astragalus is fused with the calcaneum. The pedal formula is 2-3-3-3-? and digits 1-4 were clawed, whereas digit 5 is incompletely preserved. The first metatarsal is more robust than the others.

Vertebral column

Four cervicals are preserved in PMOL-SGP A0100-2, three in PMOL-SGP A0100-1, and PMOL-SGP A0100-3 exhibits one cervical vertebra and two anterior caudals (Figures 4A, 6 and 8A).

In PMOL-SGP A0100-2 three cervicals are well exposed in lateral and dorsal views that could represent any series of cervicals between 2 to 6 (Figure 8A). In PMOL-SGP A0100-1 cervicals 2 and 3 are exposed in dorsal view (Figure 4A). The centra are amphicoelous and more than twice as long than high (excluding the ventral keel and including the dorsal spine). A low ventral keel extends along the entire midline of the centra. The transverse processes are compressed, relatively robust, with parallel anterior and posterior sides, and exhibit clear diapophyses. The transverse process does not extend much laterally and is slightly longer than wide. The posterior third of the transverse process extends beyond the middle of the centrum whereas its anterior two-thirds extend anteriorly to the middle of the centrum, terminating well before the anterior end of the centrum. The cervicals have well-developed bifurcated

ribs. The dorsal articulation of the ribs with the transverse processes is not preserved and elements therefore must have shifted, but the anterior contact with the parapophysis is still preserved. The parapophyses are situated at the anteroventral margin of the centrum and is best developed in the second cervical preserved in PMOL-SGP A0100-2 (probably cervical 3 or 4). The neural arch is longer and more than twice as high as the centrum (centrum including the transverse process but excluding the ventral keel and the arch including the zygapophyses but excluding the dorsal spine). The postzygapophyses are only slightly separated and unite in a common low stem. The anterodorsal surface of the postzygapophysis is convex whereas the posterodorsal is concave with a groove extending anteromedially. The neural spines are damaged and their full height is therefore unknown, except for the most anterior preserved cervical in PMOL-SGP A0100-2. Cervical 2 has a long neural spine extending all along the dorsal surface of the arch whereas cervical 3 has a shorter spine (PMOL-SGP A0100-1). The anteriormost cervical in PMOL-SGP A0100-2 has a low but long spine, the following is higher, and the third has a short and high process. The prezygapophyses are a little higher than the postzygapophyses (except for the third preserved in PMOL-SGP A0100-2) and slightly extend beyond the level of the anterior edge of the centrum in lateral view.

Results and discussion

Taxonomic comments

Following the phylogenetic definition of Rabi et al. [59], *Xinjiangchelys wusu* is assigned to Xinjiangchelyidae because it is recovered in a monophyletic group together with *Xinjiangchelys junggarensis* (Figure 9). Other members of Xinjiangchelyidae include *X. radiplicatoides*, *X.* (*Annemys*) *latiens* and *X.* (*Annemys*) *levensis* and this clade is only supported by one unambiguous synapomorphy (Anal A:1, extension of anal scale onto hypoplastron).

Among taxa traditionally referred to Xinjiangchelyidae, the morphology of *X. wusu* is most similar to that of *X.* (*Annemys*) *levensis*, *Xinjiangchelys* (*Annemys*) *latiens* and *X. radiplicatoides*, however, a number of differences justify its recognition as a separate taxon. In contrast to *X. levensis*, the prefrontals do not meet in the midline in *X. wusu*, the basioccipital tubera are better developed, there are two foramina nervi hypoglossi instead of three, the vertebral 3-4 sulcus extends onto neural 5 not neural 6, and the midline plastral sulcus is straight instead of sinusoidal. *Xinjiangchelys* (*Annemys*) *latiens* has a proportionally more elongated skull, reduced frontal and jugal contribution to the orbit and sinusoidal midline plastral sulcus, whereas *X. radiplicatoides* has a more inflated skull, a slit-like interpterygoid vacuity instead of a round opening with very indistinct foramen caroticus palatinum, a strongly plicated carapace, and a sinusoidal midline plastral sulcus.

Since the interrelationships of xinjiangchelyids are unresolved in the consensus tree and pruning the rouge taxon *Xinjiangchelys junggarensis* reveals that *Annemys* (i.e., *X. levensis* and *X. latiens*) is paraphyletic (*levensis* forms the sister taxon of a *latiens*, *X. wusu* and *X. radiplicatoides* trichotomy), we suggest referring *wusu* and all other species to the genus *Xinjiangchelys* Ye 1986 [82] as this taxon has priority over *Annemys* Sukhanov and Narmandakh 2006 [58].

Recently, abundant remains of xinjiangchelyids were reported from the Mesa Chelonia turtle bone bed, which is stratigraphically situated 500 m below and spatially located 1 km away from the Turtle Cliff site [28]. These Mesa Chelonia turtles are represented by several partial skeletons and were all referred to an indeterminate species of *Annemys* [28]. The Mesa Chelonia form is very similar to *X. wusu* but a few differences are present and therefore we consider it a separate taxon. *Xinjiangchelys wusu* is about 15% larger, the foramen posterius canalis carotici interni is located along the posterior surface of the pterygoid, not in a notch at the back of the skull, the vertebral 3-4 sulcus extends onto neural 5 (extends onto neural 6 in eleven specimens out of twelve in the Mesa Chelonia form) and the plastral pegs are visible even when the plastron is articulated with the carapace, whereas the pegs are mostly covered by the peripheral ring in the fully ossified specimens of the Mesa Chelonia forms. A further difference might be that *X. wusu* lacks any types of fontanelles in the carapace or the plastron whereas they are present in more than half of the specimens from Mesa Chelonia that appear to be adult-sized individuals.

Another closely related form, mostly known by the skull, has been reported from the Junggar Basin [15] and was referred to *Annemys* sp. The foramen posterius canalis carotici interni of this skull is located in a notch between the basisphenoid and the pterygoid (unlike *X. wusu*) and the lateral plate of the jugal lacks a posterodorsal process extending ventral to the postorbital [15]. On the other hand, the skull from the Junggar Basin is very similar to the Mesa Chelonia form and we tentatively refer them to the same, yet unnamed taxon.

The homology of the basipterygoid process in Mesozoic turtles

Basal tetrapods and basal amniotes have no sutural relationship between their basicranium and the palatoquadrate region [89]. Instead, the basicranium articulates anteriorly

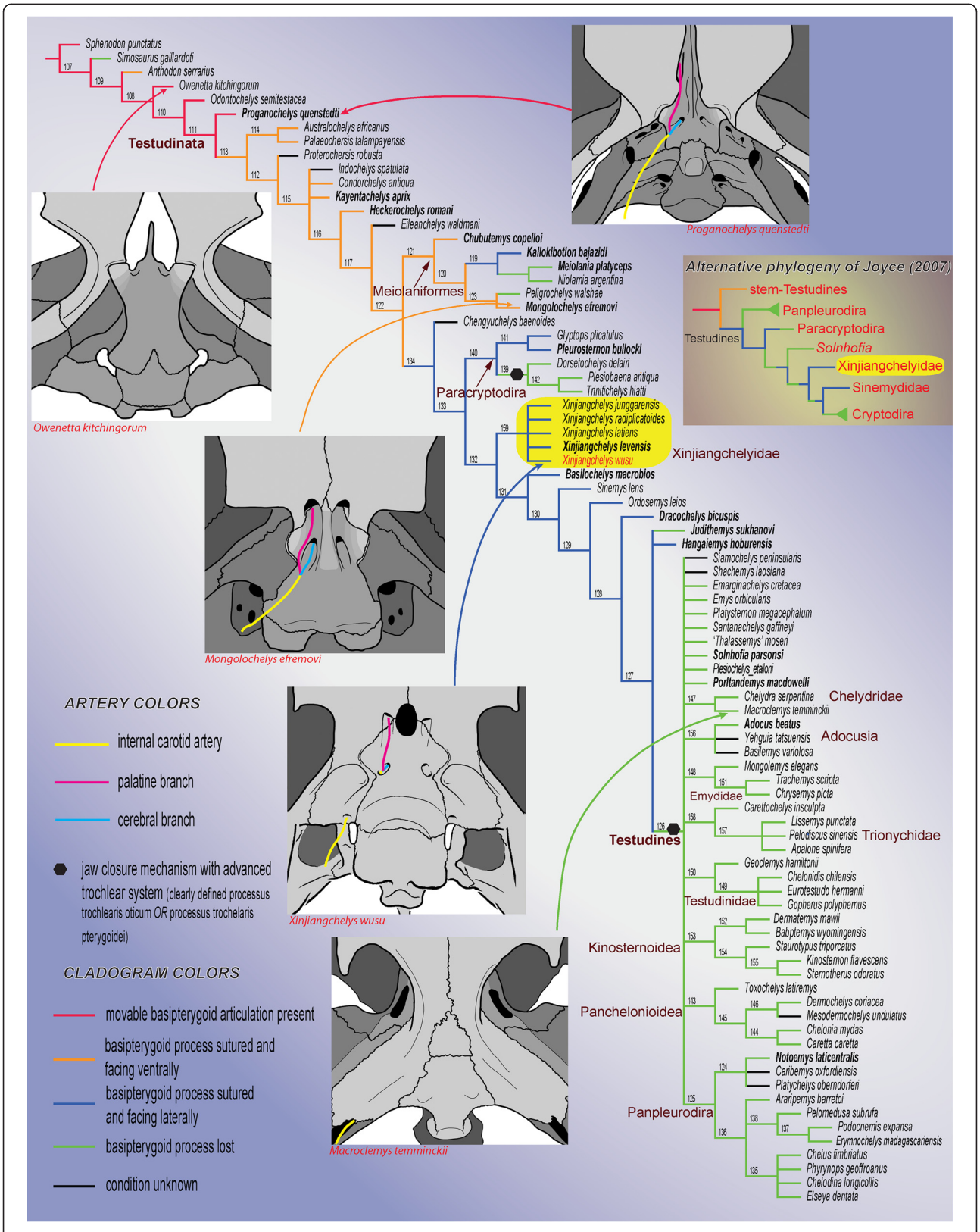

Figure 9 (See legend on next page.)

(See figure on previous page.)
Figure 9 Hypothetical relationships of the major clades of turtles and the evolution of the basipterygoid process and the carotid artery circulation system. The cladogram is the strict consensus tree of 9261 trees of 870 steps obtained after a parsimony analysis of 237 morphological characters and 84 extinct and extant turtle taxa. The relationships of Durocryptodira [1] were constrained after the molecular phylogeny of Barley et al. [79]. Note the unorthodox position of Xinjiangchelyidae outside of Testudines. The more traditional phylogenetic placement of Xinjiangchelyidae [3] is presented on the right for comparison. Taxa in bold are figured in Figures 10, 11, 12. Numbers correspond to nodes.

with the pterygoid via the basipterygoid process of the basisphenoid (also termed the basitrabecular process) and posteriorly with the quadrate and the squamosal via the paroccipital process of the opisthotic. A basipterygoid process has been identified in a number of basal turtles and proto-turtles (Figures 10A-C), including *Odontochelys semitestacea* [48], *Proganochelys quenstedti* [19], *Palaeochersis talampayensis* Rougier et al., 1995 [90,91] *Australochelys africanus* Gaffney et al., 1994 [92,93], *Kayentachelys aprix* [86,94], *Heckerochelys romani* [35], and *Condorchelys antiqua* Sterli, 2008 [87,95]. Among this group of taxa, the more primitive ones, such as *O. semitestacea* and *Pr. quenstedti*, retain a movable basipterygoid articulation in the form of a ventrolaterally directed, blunt basipterygoid process that articulates with the corresponding facet in the pterygoid (Figure 10A). All more derived basal turtles with an unambiguous basipterygoid process are interpreted as having a fused articulation [18,20,35,66,86,87,93,94] whereas all more advanced stem-testudine taxa and all crown turtles are universally considered to have lost their basipterygoid process completely (e.g., [66]). Some derived taxa have nevertheless been hypothesized to retain a reduced basipterygoid process, but the homology of this structure has been a controversial issue.

The presence of a basipterygoid process was first reported in the Late Jurassic turtle *Mesochelys durlstonensis* Evans and Kemp, 1975 [17], a taxon that was subsequently synonymized with *Pleurosternon bullockii* [96]. A similar structure was noticed by Gaffney (1979) [18] in *Glyptops plicatulus* Cope 1877 [97] and he concluded that it is not homologous with the unambiguous basipterygoid process of basal turtles based on topological considerations, a concept subsequently confirmed by Sterli et al. [20]. More recently, Brinkman et al. [15] identified a paired process of the basisphenoid similar to that seen in *Pleurosternon bullockii* (Figure 11H) in a broad selection of Jurassic and Early Cretaceous Asian eucryptodires and interpreted it as being homologous with the basipterygoid process of the earliest turtles, thereby contradicting the homology assessment of Gaffney [18] and Sterli et al. [20].

According to the homology concept of Gaffney [18] and Sterli et al. [20], the paired lateral processes of the basisphenoid that fit into corresponding pockets in the pterygoids in *G. plicatulus* and *Pl. bullockii* cannot be interpreted as the basipterygoid process because: a) they are placed posterior to the dorsum sellae and therefore have different topological relationships compared to the true basipterygoid processes seen in captorhinomorphs (e.g., the purported basal amniote condition) and b) because the processes in question do not ascend, as in basal turtles, but are instead aligned in the same horizontal plane as the pterygoids. Indeed, the basipterygoid process of captorhinomorphs is situated anterior to the dorsum sellae, the foramen posterius canalis carotici cerebralis [15], and the foramen nervi abducentis, whereas in *G. plicatulus* and *Pl. bullockii* the process in question is found posteriorly to these structures ([18], figure 23, note that the foramen posterius canalis carotici cerebralis is labeled foramen posterius canalis carotici interni). However, as already noted by others [15], when the condition seen in *Pr. quenstedti* (Figure 10A; unknown for Gaffney [18]) is compared to that of captorhinomorphs, it is evident that the dorsum sellae is in a derived position similar to that seen in *G. plicatulus* and *Pl. bullockii* (Figure 11H) in that it extends more anteriorly over the foramen anterius canalis carotici cerebralis ([19], figures 42-44). This anterior movement of the dorsum sellae likely resulted in the anterior migration of the foramen nervi abducentis and the foramen posterius caroticus cerebralis (the latter being erroneously named the foramen posterius canalis carotici interni in previous studies [17,18] for *G. plicatulus*, *Pl. bullockii*, and *Captorhinus* sp., as recently demonstrated [20,67]). The apparent morphocline shows that the basipterygoid process of *Pr. quenstedti,* whose homology relative to captorhinomorphs had never been questioned (e.g., [19]), is derived relative to the basal amniote condition and that it is in the same relative position as that seen in basal paracryptodires, except that in *G. plicatulus* and *Pl. bullockii* the cerebral foramen is positioned slightly more to the anterior. In addition, there is no reason to consider the foramina of the carotid circulation system to be stable landmarks that cannot shift from their position during evolution: in *K. aprix* the cerebral foramen is positioned just posteriorly to the basipterygoid process (Figure 10B) whereas in *H. romani* it is placed close to the anterior termination of the process (Figure 10C).

Sterli et al. [20] furthermore argued that the basisphenoid process of *G. plicatulus* and *Pl. bullockii* is not homologous with the basipterygoid process of basal amniotes, because it is directed laterally and found in the same plane as the pterygoid, unlike in *Pr.*

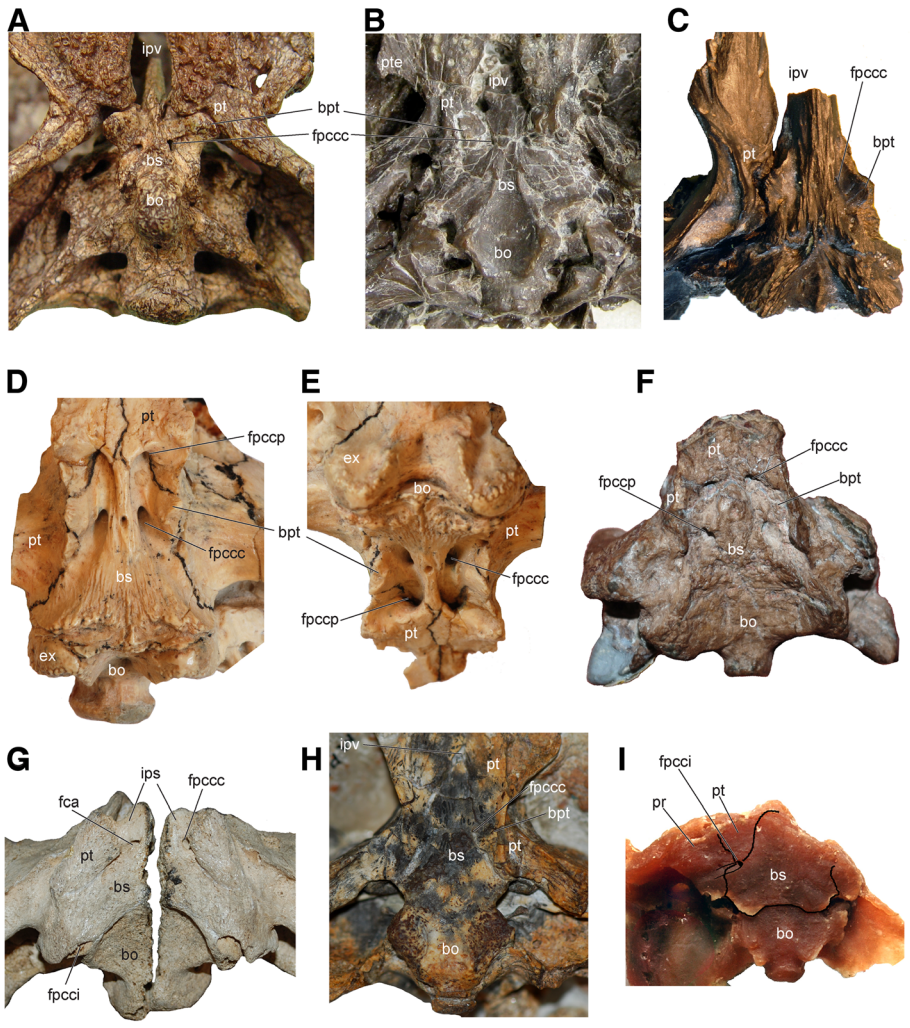

Figure 10 Braincase and palatoquadrate of select basal turtles and a pan-pleurodire showing the presence or absence of a basipterygoid process. A, *Proganochelys quenstedti* (SMNS 16980); **B**, *Kayentachelys aprix* (MCZ 8917); **C**, *Heckerochelys romani* (PIN 4561–2); **D-E**, *Mongolochelys efremovi* (PIN, uncatalogued) in ventral and oblique posterior view; **F**, *Kallokibotion bajazidi* (NHMUK R4925); **G**, *Meiolania platyceps* (NHMUK R682); **H**, *Chubutemys copelloi* (MPEF-PV1236); **I**, *Notoemys laticentralis* (cast of MOZP 2487). Abbreviations: **bo**: basioccipital, **bpt**: basipterygoid process, **bs**: basisphenoid, **ex**: exoccipital, **fca**: fenestra caroticus, **fpccc**: foramen posterius canalis carotici cerebralis, **fpcci**: foramen posterius canalis carotici interni, **fpccp**: foramen posterius canalis carotici palatinum, **ips**: intrapterygoid slit, **ipv**: interpterygoid vacuity, **pr**: prootic, **pt**: pterygoid, **pte**: processus pterygoideus externus.

quenstedti, where the basipterygoid process is directed ventrolaterally and situated ventral to the pterygoid. However, not all basal turtles have their basipterygoid process projecting ventrally. In *H. romani* the basipterygoid process is clearly present [35] but it projects laterally with a very minor ventral component and it is in the same plane as the pterygoid (Figure 10C). Thus, this taxon demonstrates that there was a phase in the evolution of the basicranium when the basipterygoid articulation was already sutured and was in the same level as the rest of the palate. The morphology of the basipterygoid in *H. romani* is close to that of xinjiangchelyids and "sinemydids/macrobaenids" (Figures 11A-E). A flat, triangular process projects laterally and slightly ventrally in these taxa to fit into the corresponding pit of the pterygoid in the same plane. There is no basis for interpreting this process as a neomorphic structure and given the identical topological position and the highly comparable shape the lateral basisphenoid process in basal paracryptodires (Figure 11H), xinjiangchelyids and "sinemydids/macrobaenids" can be confidently interpreted as being homologous with the basipterygoid process of basal turtles and basal amniotes.

The basipterygoid process in Mesozoic turtles

Since the basipterygoid process is generally interpreted to be a primitive character absent in derived turtles, many

published descriptions of Mesozoic turtle skulls fail to report and illustrate the basipterygoid process. This is especially true for various Jurassic and Early Cretaceous Asian forms (i.e., xinjiangchelyids, sinemydids, and macrobaenids, Figure 11A-E). In addition to the taxa listed in a previous study [15] we further identified a laterally facing basipterygoid process in *Kallokibotion bajazidi* (Figure 10F), *Dracochelys bicuspis* (Figure 11F), *Manchurochelys manchoukuoensis*, *Sinemys brevispinus* (as also reported elsewhere [55]), *Ordosemys leios*, *Xinjiangchelys levensis* (Figure 11B), and *Xinjiangchelys latiens*, the alleged stem-adocusian *Basilochelys macrobios* (Figure 11F) and the basal eucryptodire *Hoyasemys jimenezi* (Figure 12A). In *Sandownia harrisi* the basipterygoid process is reduced and only visible in the floor of an opening formed by the pterygoids (i.e., the fenestra caroticus, Figure 12B). A similar morphology may be present in the macrobaenids *Judithemys sukhanovi* (Figure 11C) and *Macrobaena mongolica* and in the adocid *Adocus lineolatus* (Figure 12C) but the corresponding opening is so tight that the basipterygoid process (if any) is not visible. Consequently, we suggest scoring these taxa, including *S. harrisi*, as lacking the basipterygoid process, since the ventral surface of the basicranium lacks this structure. Various early marine turtles, including *Solnhofia parsonsi* (Figure 12D), *Portlandemys mcdowelli* (Figure 12E), *Plesiochelys etalloni*, and the early protostegid *Bouliachelys suteri* (Figure 12F) also lack basipterygoid processes. All other members of Testudines, including *Mongolemys elegans* lack a basipterygoid process as well.

The basipterygoid process is present and ventrolaterally directed in several representatives of the Meiolaniformes, a recently recognized Mesozoic to Pleistocene clade of basal turtles [16], including *Mongolochelys efremovi* (Figures 10D-E) and *Chubutemys copelloi* (Figure 10H). Another putative member of this clade, *Kallokibotion bajazidi* (Figure 10F) also retains the downward facing basipterygoid process (contrary to a previous report [98]). On the other hand, in *Meiolania platyceps* it is not the basisphenoid that extends ventrally to contact the pterygoid but rather it is the pterygoid that sends a process dorsally to contact the basisphenoid and to form the lateral wall of the intrapterygoid-slit ([99], figure 58). This is apparent since the suture between the basisphenoid and the pterygoid extends inside the fenestra caroticus, indicating that the basipterygoid process is lost (Figure 10G). A similar morphology can be observed in the Eocene meiolaniid *Niolamia argentina* as well. In the solemydid *Helochelydra nopcsai* the basipterygoid process is clearly absent given the complete loss of basisphenoid exposure whereas the condition in *Naomichelys speciosa* is clearly more derived than in more basal turtles (e.g. *Kayentachelys aprix*, Figure 10B) but a clear interpretation is difficult at the moment.

The oldest known panpleurodire skull is that of *Notoemys laticentralis* (Figure 10I) from the Late Jurassic of Argentina. The basisphenoid of this species shows a very reduced lateral protrusion just anterior to the foramen posterius canalis carotici interni ([100], Figure 2B; [101], pl. 1C). Since the split of the cerebral and palatine branches of the carotid artery is always situating ventral to the basipterygoid process in turtles known to retain this structure, we do not consider the protrusion of *Notoemys laticentralis* to be homologous with the basipterygoid process, given that it is situated dorsal to the split of the arterial branches, not ventral. The same rationale is applied for the interpretation of a lateral protrusion in the basisphenoid of several chelids and in *Araripemys barretoi* Price, 1973 [102-104].

Given that this structure has been notoriously overlooked in many Mesozoic taxa, we suggest that future workers should always explicitly note the presence or absence of the basipterygoid process while describing and/or scoring extinct turtles and also illustrate the basisphenoid accordingly. We suggest using the term "basipterygoid process" or "processus basipterygoideus" instead of "basitrabecular process" since the latter is less widely used in the fossil turtle literature. The term "fused basipterygoid articulation" [66] is not very precise since the basipterygoid process and the pterygoid are never fused per se, but rather connected by a suture.

The evolution of the basipterygoid process in turtles

In the basal most known Triassic turtles and proto-turtles, such as *Proganochelys quenstedti* and *Odontochelys semitestacea*, the basipterygoid process is a robust and relatively thick structure that is directed ventrolaterally to articulate with a facet in the pterygoid. The pterygoid of these turtles is situated ventrally to the plane of the basisphenoid (Figure 10A). In spite of the presence of a kinetic joint in these taxa, their skull was not kinetic in the sense of others Holliday and Witmer [105]. In more derived turtles, such as *Palaeochersis talampayensis* and *Australochelys africanus*, the basipterygoid process is still prominent and faces ventrolaterally, but the articulation with the ventrally positioned pterygoid is transformed into a sutural contact. The Early and Middle Jurassic turtles *Kayentachelys aprix* (Figure 10B) and *Condorchelys antiqua* together with Cretaceous *Mongolochelys efremovi*, *Kallokibotion bajazidi* and *Chubutemys copelloi* (Figures 10D-F,G) represent a more advanced phase in that the process is more reduced and compressed, but the basisphenoid is still situated dorsal to the pterygoid. The next phase is exemplified by *Heckerochelys romani* (Figure 10C), and various members of Xinjiangchelyidae, Sinemydidae, and Macrobaenidae (Figures 11A-E) where the process is compressed and mainly laterally oriented and the basisphenoid is aligned with the pterygoid.

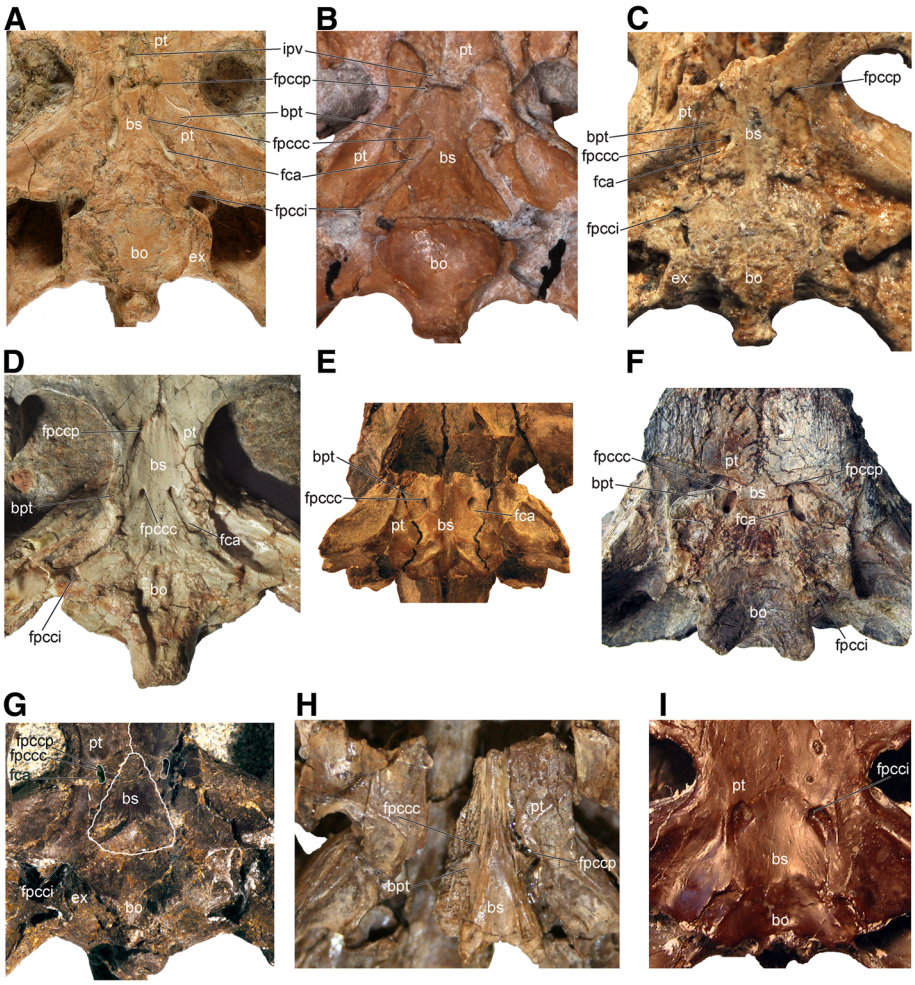

Figure 11 Braincase and palatoquadrate of select Asian and North American Mesozoic turtles. A, "*Annemys*" sp. from Turpan Basin, Mesa Chelonia, (SGP 2009/18, see [28]); **B**, *Xinjiangchelys levensis* (PIN 4636-4-2); **C**, *Sinemys gamera* (IVPP V9532-11); **D**, *Dracochelys bicuspis* (IVPP V4075); **E**, *Hangaiemys hoburensis* (PIN 3334-36); **F**, *Basilochelys macrobios* (MD8-2); **G**, *Judithemys sukhanovi* (TMP 87.2.1); **H**, *Pleurosternon bullockii* (UMZC 1041); **I**, *Eubaena cephalica* (MRF 571). Abbreviations: **bo**: basioccipital, **bpt**: basipterygoid process, **bs**: basisphenoid, **ex**: exoccipital, **fca**: fenestra caroticus, **fpccc**: foramen posterius canalis carotici cerebralis, **fpcci**: foramen posterius canalis carotici interni, **fpccp**: foramen posterius canalis carotici palatinum, **ipv**: interpterygoid vacuity, **pt**: pterygoid. *Judithemys sukhanovi* (G) has a reduced fenestra caroticus (fca, highlighted in green). The fpccp and the fpccc in this species are situated close to one another inside the fenestra caroticus and are therefore not visible in ventral view.

According to our phylogenetic hypothesis, the complete reduction and reorientation of the basipterygoid process happened independently in a number of turtle clades. The basipterygoid process was lost once within paracryptodires since basal members, such as *Glyptops plicatulus* and *Pleurosternon bullockii* (Figure 11H), still retain a process, whereas it is absent in *Compsemys victa* and all baenids (Figure 11I) [106-109]. The basipterygoid process is furthermore lost in derived members of Meiolaniformes (i.e., *Niolamia argentina*, *Peligrochelys walshae* and *Meiolania platyceps*, Figure 10G). At least one more independent loss occurred within crown Testudines (i.e., along the stem of Pleurodira and Cryptodira) as indicated by the presence of the basipterygoid process in most xinjiangchelyids, sinemydids, and *Hangaiemys hoburensis*. Furthermore, the basal position of *Judithemys sukhanovi* implies an additional independent loss in this species.

Considering the more traditional phylogenetic hypotheses that place Xinjiangchelyids on the stem of Cryptodira (e.g. [3]), these either infer two additional independent losses of the basipterygoid process (in Panpleurodires and early marine turtles including *Solnhofia parsonsi*) or alternatively (and perhaps less likely) the basipterygoid process was reacquired in basal paracryptodires (pleurosternids), xinjiangchelyids and sinemydids (Figure 9). Since our results themselves demonstrate that the loss of the basipterygoid process is quite homoplastic in turtles, two additional losses do not render considerably lower support for the traditional phylogenetic hypothesis [3] relative to the hypothesis presented here.

The reduction of the basipterygoid process in paracryptodires and crown-group Testudines was associated with the expansion of the parasphenoid ventral to the basisphenoid that eventually resulted in the complete enclosure of the arteries of the carotid circulation system in bone [20]. In the case of Cryptodires the pterygoid was involved as well [15,66]. In all groups the synchronous loss of the basipterygoid process led to the final reinforcement of the basicranial region [19,87].

The multiple parallel losses of the basipterygoid process suggest that several clades of turtles gained an advantage by reinforcing the contact between the basicranium and the palatoquadrate. Interestingly, the loss of the basipterygoid process is often associated with another derived trait, the presence of a well-developed trochlear system. Many pancryptodires, including all crown-group members, and all pleurodires have an advanced jaw closure mechanism where the jaw adductor muscle is redirected by the otic trochlea in the former and the pterygoid trochlea in the latter, in both cases acting like a pulley system [65]. As already pointed out previously [94,110], many basal taxa do not possess, or do not clearly possess the advanced otic trochlear process found in most crown-group cryptodires. Our review of taxa that retain a basipterygoid process, including basal turtles, most meiolaniforms, xinjiangchelyids, sinemydids, and macrobaenids reveals that these taxa possess poorly developed otic trochlea (if any) in form of a rugose surface or a low ridge that only barely protrudes anteriorly, unlike in taxa where the basipterygoid process is absent, including plesiochelyids, eurysternids, baenids, and most crown-group cryptodires, where the otic trochlea is robust and protrudes significantly (Figure 9). The condition in pleurodires is also consistent with this correlation as they have an advanced trochlear process formed by the pterygoid and the basipterygoid process is absent even in the earliest known extinct species, *Notoemys laticentralis* (Figures 9 and 10I) [101].

The loss of the basipterygoid process and the enclosure of the carotid circulation system in bone probably results in a reinforced connection between the basicranium and the palatoquadrate and therefore in a more rigid skull. As previous works pointed out [66,87,111] the development of advanced jaw closure mechanisms during turtle evolution likely required a more rigid skull that is compliant with higher bite performance and the loss of the basipterygoid process in association with the formation of an advanced trochlear system is therefore consistent with this pattern. In this regard the evolution of turtles parallels other amniote groups with rigid skulls including, therapsids, sauropterygians, and crocodyliformes which also lost their basipterygoid processes and enclosed the carotid system during the reinforcement of the basicranium [89].

Phylogenetic implications

The phylogenetic analysis found 9261 most parsimonious trees (length = 870) and most cryptodire clades were only partially recovered in the strict consensus relative to the molecular based topology we used as a constraint. This might be due to character conflict caused by the extinct taxa designated as floaters (see Appendix B for a list of taxa) and urges a thorough review of all scorings of the matrix in the future.

The results of our analysis conflict with previous studies regarding the position of Xinjiangchelyidae (i.e., the clade of all turtles more closely related to *Xinjiangchelys junggarensis* than to any extant turtle), a group that is otherwise commonly hypothesized to be pancryptodiran [1-4,8-11,16,61,70,72], by placing it outside of crown group Testudines (Figure 9). On the other hand they are consistent with the results of the most recent analysis of turtle phylogeny [59]. Xinjiangchelyids indeed possess a number of primitive characters, including the presence of a reduced interpterygoid vacuity and a basipterygoid process, the absence of a bony canal for the split of the cerebral and palatine branches, the presence of dorsal processes of epiplastron, long first dorsal ribs, and amphicoelous cervicals. We identify two characters that are responsible for the basal position of Xinjiangchelyidae in our cladogram. In contrast to our current and earlier analysis [59], the presence of a basipterygoid process was previously scored as unknown whereas the first dorsal rib was scored as short for *Xinjiangchelys junggarensis* (formerly *X. latimarginalis*), the only xinjiangchelyid in the original matrix [16]. However, as we demonstrated above and in accordance with a recent study [15], a basipterygoid process is present in the basicranium of *X. radiplicatoides*, *X. wusu*, *X. levensis* and *X. latiens*. The first dorsal rib of *X. latimarginalis* was previously identified as short [72] (reaching about half way to the axillary buttress), but revision of the specimen in question (IVPP V9537-1) reveals that the rib was long. In fact, the rib is incompletely preserved, but the corresponding scar extends along the entire anterior edge of the second dorsal rib. A long first dorsal rib is furthermore present in *X. levensis* (unknown for *X. latiens* and *X. wusu*) and a long scar is described and figured for *X. radiplicatoides* [15]. We therefore scored *X. junggarensis*, *X. radiplicatoides* and *X. levensis* as having a long first dorsal rib.

It was previously unknown that the junction of the palatine and cerebral branches of the carotid artery was not floored in xinjiangchelyids (see also [59]), but this can not be responsible for their basal position since sinemydids had been scored with this primitive condition [16], but were placed on the stem of crown Cryptodira.

On the other hand, we realized that the original matrix [16] contains a good number of inconsistently scored characters and fixing these errors would likely

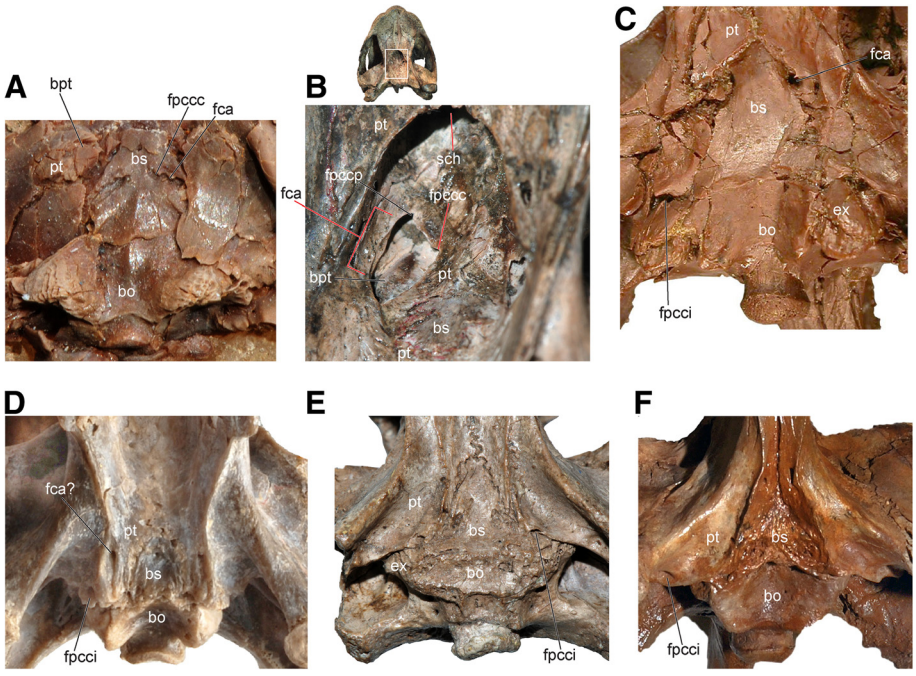

Figure 12 Braincase and palatoquadrate of select Mesozoic turtles. A, *Hoyasemys jimenezi* MCCM-LH-84; **B**, *Sandownia harrisi* (MIWG 3480); **C**, *Adocus* sp. (CCM 60-15); **D**, *Solnhofia parsonsi* (TM 4023); **E**, *Portlandemys mcdowelli* (NHMUK R2914); **F**, *Bouliachelys suteri* (SAM P41106). Abbreviations: **bo**: basioccipital, **bpt**: basipterygoid process, **bs**: basisphenoid, **ex**: exoccipital, **fca**: fenestra caroticus, **fpccc**: foramen posterius canalis carotici cerebralis, **fpcci**: foramen posterius canalis carotici interni, **fpccp**: foramen posterius canalis carotici palatinum, **pt**: pterygoid, **sch**: secondary choana. *Sandownia harrisi* (B) appears to retain a small basipterygoid process inside the fenestra caroticus, but given that is not exposed on the palatal surface of the skull and not visible in ventral view we suggest reflecting this difference in the scoring of this taxon in the future. *Adocus lineolatus* (C) has a reduced fenestra caroticus (fca). The fpccp and the fpccc in this species are situated close to one another deep inside the fenestra caroticus and therefore they are not visible in ventral view.

alter the current results (see also [59]). A comprehensive revision and expansion of this matrix is therefore in progress as part of a larger scale project (including WGJ, MR and J. Sterli).

Relationships of Cretaceous "Eucryptodires"

The Cretaceous "eucryptodires" of Asia and North America, including *Sinemys lens*, *Ordosemys leios*, *Dracochelys bicuspis*, *Hangaiemys hoburensis*, and *Judithemys sukhanovi* are often collectively referred to as "sinemydids/macrobaenids" in the literature ([12] and references therein) reflecting the likely paraphyletic nature of the group (see Rabi et al. [59] for a phylogenetic definition of these clades). All previous works, however, agree that these taxa are placed somewhere along the stem of crown Cryptodira or that parts nest within it. Our cladogram here preliminarily places all of these turtles outside of Testudines in a paraphyletic grade more derived than Xinjiangchelyidae, but more basal than crown Testudines (Figure 9).

Previous analyses also acknowledged the presence of long first dorsal rib in *O. leios* and *D. bicuspis* but ignored the presence of a basipterygoid process in these taxa (see above), a condition that pulled them to a more basal position, together with *Hangaiemys hoburensis*, another taxon with a basipterygoid process but with short first dorsal rib. Interestingly, *Judithemys sukhanovi* lacks a basipterygoid process, but is found just outside of crown Testudines in a polytomy with *H. hoburensis*, which possess this process.

Some previous published analyses have actually found that some of these taxa do form a clade [3,4,16] but due to changes we introduced in their scorings, we cannot recover such groups rendering further support to the paraphyletic nature of "sinemydids/macrobaenids".

Relationships of early marine turtles

Most previous analyses that included various Late Jurassic marine European taxa (e.g., *Plesiochelys solodurensis*, *Portlandemys mcdowelli*, "*Thalassemys*" *moseri* Bräm 1965 [112]) and the Early Cretaceous South American *Santanachelys gaffneyi* variously united them into clades and/or paraphyletic grades somewhere along the stem of crown Cryptodira in a more basal position than xinjiangchelyids [3,4,10,61,70,113,114]. A recent exception is the analysis we modified in our study [16] and

which found a (*Ples. solodurensis* + *Port. mcdowelli*) clade sister
to Testudines and a (*Sol. parsonsi* (*Sant. gaffneyi* + "*T.*" *moseri*)) clade in a polytomy with members of "sinemydids/macrobaenids" on the stem of Cryptodira. We found these taxa in an even more derived position as part of the crown group Testudines (Figure 9). One of the reasons for the more derived position of these taxa is likely the recognition of the basipterygoid process in xinjiangchelyids and "sinemydids/macrobaenids" that is clearly lost in all the European taxa (Figures 10D-E) and *Santanachelys gaffneyi*. Again, these results must be viewed with caution given the necessity of a comprehensive revision of the current matrix (see above).

Relationships of Basilochelys macrobios

Basilochelys macrobios from the Latest Jurassic/Earliest Cretaceous of Thailand has been hypothesized to represent an early crown group Cryptodire closely related to or nesting within Trionychia [61,115]. The position of *Basilochelys macrobios* in crown-group Cryptodira is not supported by our analyses and this taxon is recovered instead in the next less inclusive node to Xinjiangchelyidae outside of crown Testudines (Figure 9). *Basilochelys macrobios* has a sculptured shell surface that is reminiscent of certain nanhsiungchelyids [61] but there has been no attempt to homologize it with the sculpturing of trionychians and therefore we scored the type of sculpturing (Carapace E) as unknown. However, the scoring of the presence of "trionychian-type" sculpture (Carapace E-2) does not alter the position of *B. macrobios*. A trionychian-like sculpturing is also present in *Yehguia tatsuensis* and *Siamochelys peninsularis* ([1], MR, WGJ pers. obs.) but no matter how we score this character it does not influence the position of these three taxa. Based on detailed photographs we are confident that *B. macrobios* possesses a sutured basipterygoid process (Figure 11F; contrary what has been previously reported [61]) and this is clearly the reason for its relatively basal position in our analysis. *Y. tatsuensis* is recovered as part of Testudines in the Adocusia clade which is consistent with earlier hypotheses [1,16]. On the other hand, the placement of *S. peninsularis* in the crown group of turtles contrasts previous results [4,16].

Conclusions

The discovery of *Xinjiangchelys wusu* from the Late Jurassic of the Turpan Basin, Xinjiang, China adds to the known diversity of xinjiangchelyid turtles and provides the first step in the direction of understanding the biogeographical relationships of the Turpan Basin tetrapod faunas with roughly coeval faunas, especially those of the adjacent Junggar Basin (e.g. [12]).

Xinjiangchelyids have been mostly known on the basis of shells but these new findings together with recently described material from the Junggar Basin provides new insights into the anatomy of the rest of the skeleton.

The study of *X. wusu* made clear the necessity for reviewing the basicranial morphology of Mesozoic turtles, which revealed that the basipterygoid process has been overlooked in a broad range of extinct taxa. The repeated independent loss of the basipterygoid process together with the enclosure of the carotid circulation system in bone during turtle evolution argues for strong selective pressures to reinforce the basicranial region and to develop a more rigid skull. Testing the phylogenetic implications of these novel anatomical data in a global context resulted in the unorthodox basal placement of xinjiangchelyids, sinemydids, and macrobaenids. This topology needs further testing since it would infer unexpected reversals in Pan-Pleurodires, including the reacquisition of a "reduced" mesoplastron and the reorganization of the entry of the carotid artery into the skull among others and therefore a thorough revision of the matrix is of primary importance. Nevertheless, this analysis, together with an earlier study [16], raises the issue that certain widely recognized Pan-Cryptodiran synapomorphies [91], including the complete flooring of the cranioquadrate space by the pterygoid and the presence of at least a poorly developed otic trochlea, might be symplesiomorphies of Testudines.

Appendix A

List of omitted taxa from the matrix of Sterli and de la Fuente (In press)

Ninjemys oweni, *Warkalania carinaminor*, *Patagoniaemys gasparinae*, *Otwayemys cunicularius*, *Prochelidella cerrobarcinae*, *Myuchelys latisternum*, *Chelodina colliei*, *Yaminuechelys maior*, *Dinochelys whitei*, *Neurankylus eximius*, *Boremys pulchra*, *Baena arenosa*, *Chisternon undatum*, *Macrochelys schmidti*, *Protochelydra zangerli*, *Chelonoidis gringorum*, *Stylemys nebraskensis*, *Echmatemys wyomingensis*, *Xenochelys formosa*, *Hoplochelys crassa*, *Plastomenus aff. thomassii*, *Anosteira ornata*.

Appendix B

List of taxa designated as floaters after constraining the relationships of Durocryptodira in the phylogenetic analysis

Siamochelys peninsularis, *Basilochelys macrobios*, *Ordosemys leios*, *Dracochelys bicuspis*, *Judithemys sukhanovi*, *Hangaiemys hoburensis*, *Xinjiangchelys junggarensis*, *Xinjiangchelys radiplicatoides*, *Xinjiangchelys wusu, X.* (*Annemys*) *latiens*, *X.* (*Annemys*) *levensis*, *Shachemys laosiana*, *Adocus beatus*, *Yehguia tatsuensis*, *Basilemys variolosa*, *Baptemys wyomingensis*, *Mongolemys elegans*, all members of Trionychidae and Panpleurodira, *Carettochelys insculpta*, *Toxochelys latiremis*, *Mesodermochelys undulatus*, *Plesiochelys etalloni*, *Santanachelys gaffneyi*, *Solnhofia parsonsi* and *Portlandemys mcdowelli*.

Additional files

Additional file 1: Contains the taxon-character matrix used in the phylogenetic analysis in nexus.

Additional file 2: Corresponds to the character-taxon matrix exported into a tnt. format file that can be analyzed with the TNT phylogenetic software.

Abbreviations

AM: Australian Museum, Sydney, Australia; **CCM**: Carter County Museum, Montana USA; **FMNH**: Field Museum of Natural History, Chicago, USA; **IVPP**: Institute of Vertebrate Paleontology and Paleoanthropology, Beijing, China; **IWCMS**: Dinosaur Isle Museum, see MIWG; **MACN**: Museo Argentino de Ciencias Naturales "Bernardino Rivadavia", Buenos Aires, Argentina; **MCCM**: Museo de las Ciencias de Castilla–La Mancha, Cuenca, Spain; **MCZ**: Museum of Comparative Zoology, Harvard University, Cambridge, USA; **MD**: Sirindhorn Museum, Phu Kum Khao, Sahatsakhan, Kalasin Province, Thailand; **MH**: Naturhistorisches Museum, Basel, Switzerland; **MIWG**: Museum of Isle of Wight Geology, Sandown, United Kingdom; **MNA**: Museum of Northern Arizona, Flagstaff, USA; **MOZP**: Museo "Prof. Dr. Juan A. Olsacher", Zapala, Argentina; **MPEF**: Museo Paleontológico Egidio Feruglio, Trelew, Argentina; **MRF**: Marmarth Research Foundation, Marmarth, North Dakota, USA; **NHMUK**: Natural History Museum of London, United Kingdom; **PIN**: Paleontological Institute, Russian Academy of Sciences, Moscow, Russia; **PMOL**: Paleontological Museum of Liaoning, Shenyang Normal University, Shenyang, China; **SAM**: South Australian Museum, Adelaide, Australia; **SGP**: Sino-German Cooperation Project; **SMNS**: Staatliches Museum für Naturkunde, Stuttgart, Germany; **UMZC**: University Museum of Zoology, Cambridge, United Kingdom; **TM**: Teylers Museum, Haarlem, The Netherlands; **TMP**: Royal Tyrrell Museum of Palaeontology, Drumheller, Canada.

Competing interests

The authors declare that they have no competing interests.

Authors' contributions

WGJ initiated study and raised funds. SG obtained permits for fieldwork and MR, OW, CFZ, and WGJ participated in fieldwork. MR, CFZ, and WGJ gathered data, illustrated specimens, and performed analyses. MR wrote primary draft of manuscript. All authors read and approved manuscript.

Acknowledgements

We would like to thank Leonie Schwermann for discovering this site. For collaboration and organization of the fieldwork, we are deeply indebted to Hans-Ulrich Pfretzschner (Tübingen) and to personnel from the Geological Survey No. 1 and the Geological Surveying Institution in Urumqi, and the Jilin University in Changchun, especially Du Qing. Sincere thanks goes to Verena Régent for preparation. The following people kindly provided access to fossil specimens under their care: Vladimir Sukhanov (PIN), Xu Xing, Liu Jun, Corwin Sullivan (IVPP), Bert Sliggers and Wouter Meyboom (TM), Sandra Chapman (NHMUK), Eduardo Ruigómez (MPEF), Donald Brinkman and James Gardner (TMP), Peter Makovicky, Bill Simpson (FMNH), Jesús Madero and Adán Perez García (MCCM), and Rainer Schoch (SMNS). Benjamin P. Kear (University of Uppsala), Juliana Sterli (CONICET), Igor Danilov (ZIN), and Haiyan Tong (IVPP) provided photographs of specimens and useful comments. MR would like to thank the MTA-ELTE Lendület Dinosaur Research Group for support and Juliana Sterli for her valuable assistance with the TNT software. The Willi Hennig Society is thanked for providing free access to the program TNT. The 2009 field season, including OW, were funded by a grant to Hans-Ulrich Pfretzschner (PF 219/21) of the Deutsche Forschungsgemeinschaft (DFG). The 2011 field season, including MR, was funded by DFG grant to WGJ (JO 928/2). This project was also funded by SYNTHESYS grant GB-TAF-1882 to M. Rabi. We are grateful for Juliana Sterli and Massimo Delfino for their constructive reviews.

Author details

[1]Institut für Geowissenschaften, University of Tübingen, Hölderlinstraße 12, 72074, Tübingen, Germany. [2]Department of Paleontology & MTA–ELTE Lendület Dinosaur Research Group, Eötvös Loránd University, Budapest, Hungary. [3]Paleontological Institute, Shenyang Normal University, 253 North Huanghe Street, Shenyang 110034, China. [4]Niedersächsisches Landesmuseum Hannover, 5 Willy-Brandt-Allee, Hannover 530169, Germany. [5]Yale Peabody Museum of Natural History, 170 Whitney Avenue, New Haven, Connecticut 06511, USA.

Received: 12 June 2013 Accepted: 16 September 2013
Published: 22 September 2013

References

1. Danilov IG, Parham JF: **A redescription of '*Plesiochelys tatsuensis*' from the late jurassic of China, with comments on the antiquity of the crown clade Cryptodira.** *J Vertebr Paleontol* 2006, **26:**573–580.
2. Danilov IG, Parham JF: **A reassessment of some poorly known turtles from the middle jurassic of China, with comments on the antiquity of extant turtles.** *J Vertebr Paleontol* 2008, **28:**306–318.
3. Joyce WG: **Phylogenetic relationships of Mesozoic turtles.** *Bull Peabody Mus Nat Hist* 2007, **48:**3–102.
4. Anquetin J: **Reassessment of the phylogenetic interrelationships of basal turtles (Testudinata).** *J Syst Palaeontol* 2012, **10:**3–45.
5. Sterli J, Pol D, Laurin M: **Incorporating phylogenetic uncertainty on phylogeny-based palaeontological dating and the timing of turtle diversification.** *Cladistics*. In press, doi: 10.1111/j.1096-0031.2012.00425.x.
6. Joyce WG, Parham JF, Lyson TR, Warnock RCM, Donoghue PCJ: **Fossil calibrations for molecular rate studies of turtle evolution: an example of best practice.** *J Paleontol* 2013, **87:**612–634.
7. Kaznyshkin MN, Nalbandyan LA, Nessov LA: **Middle and late jurassic turtles of Fergana (Kirghiz SSR) [in Russian].** *Yezhegodnik Vsesoyuznogo Paleontologicheskogo Obshchestva (Annu All-union Palaeontol Soc)* 1990, **33:**185–204.
8. Sukhanov VB: **Mesozoic turtles of Middle and Central Asia**. In *The age of dinosaurs in Russia and Mongolia*. Edited by Benton MJ, Shishkin MA, Unwin DM, Kurochkin EN. Cambridge: Cambridge University Press; 2000:309–367.
9. Parham JF, Hutchison JH: **A new eucryptodiran turtle from the late cretaceous of North America (Dinosaur Provincial Park, Alberta, Canada).** *J Vertebr Paleontol* 2003, **23:**783–798.
10. Gaffney ES, Rich TH, Vickers-Rich P, Constantine A, Vacca R, Kool L: ***Chubutemys*, a new eucryptodiran turtle from the early cretaceous of Argentina, and the relationships of Meiolaniidae.** *Am Mus Novit* 2007, **3599:**1–35.
11. Brinkman DB, Wu XC: **The skull of *Ordosemys*, an early cretaceous turtle from Inner Mongolia, People's Republic of China, and the interrelationships of Eucryptodira (Chelonia, Cryptodira).** *Paludicola* 1999, **2:**134–147.
12. Rabi M, Joyce WG, Wings O: **A review of the Mesozoic turtles of the Junggar Basin (Xinjiang, Northwest China) and the paleobiogeography of Jurassic to early cretaceous Asian Testudinates.** *Paleobiodiv Paleoenv* 2010, **90:**259–273.
13. Tong H, Danilov IG, Ye Y, Ouyang H, Peng G: **Middle jurassic turtles from Sichuan Basin, China: a review.** *Geol Mag* 2012, **149:**675–695.
14. Tong H, Danilov IG, Ye Y, Ouyang H, Peng G, Li K: **A revision of xinjiangchelyid turtles from the late jurassic of Sichuan Basin, China.** *Ann Paleontol* 2012, **98:**73–114.
15. Brinkman DB, Eberth D, Clark J, Xing X, Wu XC: **Turtles from the Jurassic Shishugou formation of the Junggar Basin, People's Republic of China, and the basicranial region of basal eucryptodires**. In *Morphology and evolution of turtles*. Edited by Brinkman DB, Gardner JD, Holroyd PA. Dordrecht: Springer; 2013:147–172.
16. Sterli J, de la Fuente MS: **New evidence from the Palaeocene of Patagonia (Argentina) on the evolution and palaeobiogeography of meiolaniid-like turtles (Testudinata).** *J Syst Paleontol*. In press.
17. Evans J, Kemp TS: **The cranial morphology of a new lower cretaceous turtle from southern England.** *Palaeontol* 1975, **18:**25–40.
18. Gaffney ES: **The jurassic turtles of North America.** *Bull Am Mus Nat Hist* 1979, **162:**91–136.
19. Gaffney ES: **The comparative osteology of the triassic turtle *Proganochelys*.** *Bull Am Mus Nat Hist* 1990, **194:**1–263.
20. Sterli J, Müller J, Anquetin J, Hilger A: **The parabasisphenoid complex in Mesozoic turtles and the evolution of the testudinate basicranium.** *Can J Earth Sci* 2010, **47:**1337–1346.
21. Zhao XJ: **Mesozoic vertebrate-bearing beds and stratigraphy of northern Xinjiang.** *Mem Inst Vert Paleontol Paleoanthropol* 1980, **16:**1–120 [in Chinese].
22. Dong ZM: *Dinosaurian faunas of China.* Beijing: China Ocean Press; 1992:188.

23. Wings O, Schellhorn R, Mallison H, Thuy B, WuW SG: **The first dinosaur tracksite from Xinjiang, NW China (Middle Jurassic Sanjianfang Formation, Turpan Basin)—a preliminary report.** *Global Geol* 2007, **10:**113–129.
24. Shao L, Stattegger K, Li W, Haupt BJ: **Depositional style and subsidence history of the Turpan Basin (NW China).** *Sed Geol* 1999, **128:**155–169.
25. Wang SE, Gao LZ: **SHRIMP U-Pb dating of zircons from tuff of jurassic Qigu formation in Junggar Basin, Xinjiang.** *Geol Bull China* 2012, **31:**503–509.
26. Dong ZM: **Vertebrates of the Turpan Basin, the Xinjiang Uygur autonomous Region, China**. In *Sino-Japanese silk road dinosaur expedition.* Edited by Dong ZM. Beijing: China Ocean Press; 1997:96–101.
27. Liu LY, Di SX: **Characteristics of middle jurassic sedimentation and reservoir pore evolution in Turpan depression [in Chinese with English abstract].** *Oil Gas Geol* 1997, **3:**247–260.
28. Wings O, Rabi M, Schneider JW, Schwermann L, Sun G, Zhou CF, Joyce WG: **An enormous Jurassic turtle bone bed from the Turpan basin of Xinjiang, China.** *Naturwissenschaften* 2012, **99:**925–935.
29. Hendrix MS, Graham SA, Carroll AR, Sobel ER, McKnight CL, Schulein BJ, Wang Z: **Sedimentary record and climatic implications of recurrent deformation in the Tian Shan; evidence from Mesozoic strata of the north Tarim, south Junggar, and Turpan basins, Northwest China.** *Geol Soc Am Bull* 1992, **104:**53–79.
30. Eberth DA, Brinkman DB, Chen P, Yuan F, Wu S, Li G, Cheng X: **Sequence stratigraphy, paleoclimate patterns, and vertebrate fossil preservations in jurassic-cretaceous strata of the Junggar Basin, Xinjiang autonomous region, People's Republic of China.** *Can J Earth Sci* 2001, **38:**1627–1644.
31. Schwermann L: *Der Mittlere bis Obere Jura östlich von Shanshan im zentralen Turpan-Becken, Uigurisches Autonomes Gebiet Xinjiang (NW China).* University of Bonn, Bonn: Unpublished Diplom Mapping Thesis; 2010.
32. Gray JE: *Synopsis reptilium, Part 1: tortoises.* London: Crocodiles and Enaliosaurians; 1831:85.
33. Gaffney ES, Ye X: ***Dracochelys*, a new cryptodiran turtle from the early cretaceous of China.** *Am Mus Novit* 1992, **3048:**1–13.
34. Sukhanov VB, Narmandakh P: **A new early cretaceous turtle from the continental deposits of the Northern Gobi.** *Trans Joint Soviet-Mongolian Paleontol Exped* 1974, **1:**192–220 [in Russian].
35. Sukhanov VB: **An archaic turtle, *Heckerochelys romani* gen. et sp. nov., from the middle jurassic of Moscow region, Russia**. In *Fossil turtle research.* 1st edition. Edited by Danilov IG, Parham JF. St. Petersburg: Zoological Institute, Russian Academy of Sciences; 2006:112–118.
36. Pérez-García A, de la Fuente MS, Ortega F: **A new freshwater basal eucryptodiran turtle from the early cretaceous of Spain.** *Acta Paleontol Pol* 2012, **57:**285–298.
37. Lapparent de Broin F, Murelega X: **Turtles from the upper cretaceous of Laño (Iberian peninsula).** *Estud Mus Cienc Nat Alava* 1999, **14:**135–211.
38. Nopcsa F: **On the geological importance of the primitive reptilian fauna of the uppermost Cretaceous; with a description of a new tortoise (*Kallokibotion*).** *J Geol Soc London* 1923, **79:**100–116.
39. Gaffney ES, Hutchison JH, Jenkins FA Jr, Meeker LJ: **Modern turtle origins: the oldest known cryptodire.** *Science* 1987, **237:**289–291.
40. Tatarinov LP: **A new turtle of the family Baenidae from the lower Eocene of Mongolia.** *Paleontologicheskiy Zhurnal* 1959, **1:**100–113 [in Russian].
41. Endo R, Shikama T: **Mesozoic reptilian fauna in the Jehol mountainland, Manchoukuo.** *Bull Centr Nat Mus Manchoukuo* 1942, **3:**1–19.
42. Owen R: **Description of some fossil remains of two species of a Megalanian genus (*Meiolania*) from "Lord Howe's Island".** *Philos T Roy Soc B* 1886, **179:**181–191.
43. Khosatzky LI, Młynarski M: **Chelonians from the upper cretaceous of Gobi desert, Mongolia.** *Palaeontol Pol* 1971, **25:**131–144.
44. Khozatsky LI: **Large turtles from the late cretaceous of Mongolia.** *Russ J Herpetol* 1997, **4:**148–154.
45. Hay OP: **The fossil turtles of North America.** *Pub Carnegie Inst Washington* 1908, **75:**1–568.
46. Ameghino F: **Sinopsis geológica-paleontológica: suplemento (adiciones y correcciones).** *La Plata, Julio de* 1899, **1899:**1–13.
47. Cattoi N, Freiberg MA: **Nuevo hallazgo de Chelonia extinguidos en la Republica Argentina.** *Physis* 1961, **22:**202.
48. Li C, Wu XC, Rieppel O, Wang LT, Zhao J: **Ancestral turtle from the late triassic of southwestern China.** *Nature* 2008, **456:**497–501.
49. Brinkman DB, Peng JH: ***Ordosemys leios*, n.gen., n.sp., a new turtle from the early cretaceous of the Ordos Basin, Inner Mongolia.** *Can J Earth Sci* 1993, **30:**2128–2138.
50. Gaffney ES: **A taxonomic revision of the jurassic turtles *Portlandemys* and *Plesiochelys*.** *Am Mus Novit* 1975, **2574:**1–19.
51. Baur G: **Osteologische Notizen über Reptilien (Fortsetzung II).** *Zool Anz* 1887, **10:**241–268.
52. Lydekker RA: **On remains of Eocene and Mesozoic Chelonia and a tooth of (?) Ornithopsis.** *J Geol Soc London* 1889, **45:**227–246.
53. Meylan PA, Moody RTJ, Walker CA, Chapman SD: ***Sandownia harrisi*, a highly derived trionychoid turtle (Testudines: Cryptodira) from the early cretaceous of the Isle of Wight, England.** *J Vert Paleontol* 2000, **20:**522–532.
54. Brinkman DB, Peng JH: **New material of *Sinemys* (Testudines, Sinemydidae) from the early cretaceous of China.** *Can J Earth Sci* 1993, **30:**2139–2152.
55. Tong H, Brinkman D: *A new species of Sinemys (Testudines: Cryptodira: Sinemydidae) from the early cretaceous of Inner Mongolia.* China: Palaeobiodiversity and Palaeoenvironments. In press.
56. Gaffney ES: ***Solnhofia parsoni*, a new cryptodiran turtle from the late jurassic of Europe.** *Am Mus Novit* 1975, **2576:**1–25.
57. Cope ED: **Description of *Toxochelys latiremis*.** *Proc Acad Nat Sci Philadelphia*, **1873:**10.
58. Sukhanov VB, Narmandakh P: **New taxa of Mesozoic turtles from Mongolia**. In *Fossil turtle research.* 1st edition. Edited by Danilov IG, Parham JF. St. Petersburg: Zoological Institute, Russian Academy of Sciences; 2006:119–127.
59. Rabi M, Sukhanov VB, Egorova VN, Danilov I, Joyce WG: **Osteology, relationships, and ecology of *Annemys* (Testudines, Eucryptodira) from the late jurassic of Shar Teg, Mongolia and phylogenetic definitions for Xinjiangchelyidae, Sinemydidae, and Macrobaenidae.** *J Vertebr Paleontol*. In press.
60. Cope ED: **Description of *Adocus lineolatus*.** *Bull US Geol and Geogr Surv Terrs* 1874, **1**(2):30.
61. Tong H, Claude J, Naksri W, Suteethorn V, Buffetaut E, Khansubha S, Wongko K, Yuangdetkla P: ***Basilochelys macrobios* n. gen. and n. sp., a large cryptodiran turtle from the Phu Kradung formation (latest Jurassic–earliest Cretaceous) of the Khorat Plateau, NE Thailand.** *Geol Soc London Spec Pub* 2009, **315:**153–173.
62. Kear BP, Lee MSY: **A primitive protostegid from Australia and early sea turtle evolution.** *Biol Lett* 2006, **2:**116–119.
63. Pictet FJ, Humbert A: **Description d'une emyde nouvelle (*Emys etalloni*) du terrain jurassique supérieur des environs de Saint-Claude.** *Mat Paléontol Suisse* 1857, **1:**1–10.
64. Owen R: **Report on British fossil reptiles:Part II.** *Rep Brit Assoc Adv Sci* 1842, **11:**60–204.
65. Gaffney ES: **An illustrated glossary of turtle skull nomenclature.** *Am Mus Novit* 1972, **2486:**1–33.
66. Gaffney ES: **Comparative cranial morphology of recent and fossil turtles.** *Bull Am Mus Nat Hist* 1979, **164:**69–376.
67. Müller J, Sterli J, Anquetin J: **Carotid circulation in amniotes and its implications for turtle relationships.** *N Jb Geol Paläont (Abh)* 2011, **261:**289–297.
68. Goloboff PA, Mattoni CI, Quinteros AS: **TNT, a free program for phylogenetic analysis.** *Cladistics* 2008, **24:**774–786.
69. Goloboff PA, Farris J, Nixon K: *TNT: tree search using new technology, vers. 1.1.* Willy Hennig Society Edition; 2008. Program and documentation available at http://www.zmuc.dk/public/phylogeny/tnt.
70. Sterli J, de la Fuente MS: **A new turtle from the La Colonia formation (Campanian–Maastrichtian), Patagonia, Argentina, with remarks on the evolution of the vertebral column in turtles.** *Paleontology* 2011, **54:**63–78.
71. Brinkman DB, Li JL, Ye XK: **Order Testudines**. In *The Chinese fossil reptiles and their kin.* Edited by Li JL, Wu XC, Zhang FC. Beijing: Science Press; 2008:35–102.
72. Peng JH, Brinkman DB: **New material of Xinjiangchelys (Reptilia: Testudines) from the late jurassic Qigu formation (Shishugou Group) of the Pingfengshan locality, Junggar Basin, Xinjiang.** *Can J Earth Sci* 1993, **30:**2013–2026.
73. Wiman C: **Fossile Schildkröten aus China.** *Paleontol Sin C* 1930, **6:**1–56.
74. Anquetin J, Barrett PM, Jones MEH, Moore-Fay S, Evans S: **A new stem turtle from the middle jurassic of Scotland: new insights into the evolution and palaeoecology of basal turtles.** *Proc R Soc B* 2009, **276:**879–886.
75. Young CC, Chow MC: **New fossil reptiles from Szechuan, China.** *Acta Sci Sin* 1953, **2:**216–229.

76. Tong H, Buffetaut E, Suteethorn V: **Middle jurassic turtles from southern Thailand.** *Geol Mag* 2002, **139:**687–697.
77. Joyce WG, Bell CJ: **A review of the comparative morphology of extant testudinoid turtles (Reptilia: Testudines).** *Asiat Herpetol Res* 2004, **10:**53–109.
78. Krenz JG, Naylor GJP, Shaffer HB, Janzen FJ: **Molecular phylogenetics and evolution of turtles.** *Mol Phylogenet Evol* 2005, **37:**178–191.
79. Barley AJ, Spinks PQ, Thomson RC, Shaffer HB: **Fourteen nuclear genes provide phylogenetic resolution for difficult nodes in the turtle tree of life.** *Mol Phylogenet Evol* 2010, **55:**1189–1194.
80. Klein IT: *Klassification und kurze Geschichte der vierfüßigen Thiere (translated by F. D. Behn).* Lübeck: Jonas Schmidt; 1760.
81. Batsch AJGC: *Versuch einer Anleitung, zur Kenntniß und Geschichte der Thiere und Mineralien.* Jena: Akademische Buchhandlung; 1788:528.
82. Ye X: **A jurassic turtle from Junggar, Xinjiang.** *Vert PalAsiat* 1986, **24:**171–181.
83. Peng GY, Ye Y, Gao CS, Jiang S: *Jurassic dinosaur faunas in Zigong.* Zigong: Zigong Dinosaur Museum; 2005:236 [in Chinese with English translation].
84. Matzke AT, Maisch MW, Sun G, Pfretzschner HU, Stöhr H: **A new xinjiangchelyid turtle (Testudines, Eucryptodira) from the jurassic Qigu formation of the southern Jungar Basin, Xinjiang, North-West China.** *Palaeontology* 2004, **47:**1267–1299.
85. Matzke AT, Maisch MW, Sun G, Pfretzschner HU, Stöhr H: **A new middle Jurassic xinjiangchelyid turtle (Testudines; Eucryptodira) from China (Xinjiang, Junggar Basin).** *J Vertebr Paleontol* 2005, **25:**63–70.
86. Sterli J, Joyce WG: **The cranial anatomy of the early jurassic turtle *Kayentachelys aprix*.** *Acta Palaeontol Pol* 2007, **52:**675–694.
87. Sterli J, de la Fuente MS: **Anatomy of *Condorchelys antiqua* Sterli, 2008, and the origin of the modern jaw closure mechanism in turtles.** *J Vertebr Paleontol* 2010, **30:**351–366.
88. Joyce WG, Gauthier JA: **Paleoecology of triassic stem turtles sheds new light on turtle origins.** *Proc R Soc B* 2004, **271:**1–5.
89. Romer AS: *Osteology of reptiles.* Chicago: University of Chicago Press; 1956:772.
90. Rougier GW, de la Fuente MS, Arcucci AB: **Late triassic turtles from South America.** *Science* 1995, **268:**855–858.
91. Sterli J, de la Fuente MS, Rougier GW: **Anatomy and relationships of *Palaeochersis talampayensis*, a late triassic turtle from Argentina.** *Palaeontogr Abt A* 2007, **281:**1–61.
92. Gaffney ES, Kitching JW: **The most ancient African turtle.** *Nature* 1994, **369:**55–58.
93. Gaffney ES, Kitching JW: **The morphology and relationships of *Australochelys*, an early jurassic turtle from South Africa.** *Am Mus Novit* 1995, **3130:**1–29.
94. Gaffney ES, Jenkins FA Jr: **The cranial morphology of *Kayentachelys*, an early jurassic cryptodire, and the early history of turtles.** *Acta Zool-Stockholm* 2010, **91:**335–368.
95. Sterli J: **A new, nearly complete stem turtle from the jurassic of South America with implications for turtle evolution.** *Biol Lett* 2008, **4:**286–289.
96. Gaffney ES, Meylan PA: **A phylogeny of turtles**. In *The phylogeny and classification of the tetrapods, Volume 35A*, Amphibians, Reptiles, Birds. Systematics Association Special Volume. 1st edition. Edited by Benton MJ. Oxford: Clarendon Press; 1988:157–219.
97. Cope ED: **On reptilian remains from the Dakota beds of Colorado.** *Proc Amer Phil Soc* 1877, **17:**193–196.
98. Gaffney ES, Meylan PA: **The Transylvanian turtle *Kallokibotion*, a primitive cryptodire of cretaceous age.** *Am Mus Novit* 1992, **3040:**1–37.
99. Gaffney ES: **The cranial morphology of the extinct horned turtle *Meiolania platyceps*, from the Pleistocene of Lord Howe Island, Australia.** *Bull Am Mus Nat Hist* 1983, **175:**361–480.
100. Fernandez MS, de la Fuente M: **Redescription and phylogenetic position of *Notoemys*: the oldest Gondwanian pleurodiran turtle.** *N Jb Geol und Paläont Abh* 1994, **193:**81–105.
101. Lapparent de Broin F, de la Fuente MS, Fernandez MS: ***Notoemys laticentralis* (Chelonii, Pleurodira), late jurassic of Argentina: new examination of the anatomical structures and comparisons.** *Rev Paléobiol* 2007, **26:**99–136.
102. Price LI: **Quelônio Amphichelydia no Cretáceo Inferior do Nordeste do Brasil.** *Rev Brasil Geociênc* 1973, **3:**84–95.
103. Gaffney ES: **The side-necked turtle family Chelidae: a theory of relationships using shared derived characters.** *Am Mus Novit* 1977, **2620:**1–28.
104. Gaffney ES, Tong H, Meylan PA: **Evolution of the side-necked turtles: the families Bothremydidae, Euraxemydidae, and Araripemydidae.** *Bull Am Mus Nat Hist* 2006, **300:**1–698.
105. Holliday CM, Witmer LM: **Cranial kinesis in dinosaurs: intracranial joints, protractor muscles and their significance for cranial evolution and function in diapsids.** *J Vertebr Paleontol* 2008, **28:**1073–1088.
106. Lyson TR, Joyce WG: **A new species of *Palatobaena* (Testudines: Baenidae) and a maximum parsimony and Bayesian phylogenetic analysis of Baenidae.** *J Paleontol* 2009, **83:**457–470.
107. Lyson TR, Joyce WG: **A revision of *Plesiobaena* (Testudines: Baenidae) and an assessment of baenid ecology across the K/T boundary.** *J Paleontol* 2009, **83:**833–853.
108. Lyson TR, Joyce WG: **A new baenid turtle from the late cretaceous (Maastrichtian) hell creek formation of North Dakota and a preliminary taxonomic revision of cretaceous baenidae.** *J Vert Paleontol* 2010, **30:**394–402.
109. Lyson TR, Joyce WG: **Cranial anatomy and phylogenetic placement of the enigmatic turtle *Compsemys victa*.** *J Paleontol* 2011, **85:**789–801.
110. Joyce WG, Sterli J: **Congruence, non-homology, and the phylogeny of basal turtles.** *Acta Zool-Stockholm* 2012, **93:**149–159.
111. Herrel AJ, O'Reilly C, Richmond AM: **Evolution of bite performance in turtles.** *J Evolution Biol* 2002, **15:**1083–1094.
112. Bräm H: **Die Schildkröten aus dem oberen Jura (Malm) der Gegend von Solothurn.** *Schweiz Paläont Abh* 1965, **83:**1–190.
113. Hirayama R, Brinkman DB, Danilov IG: **Distribution and biogeography of non-marine Cretaceous turtles.** *Russ J Herpetol* 2000, **7:**181–198.
114. Sterli J: **Phylogenetic relationships among extinct and extant turtles: the position of Pleurodira and the effects of the fossils on rooting crown-group turtles.** *Contrib Zool* 2010, **79:**93–106.
115. Lourenço JM, Claude J, Galtier N, Chiari Y: **Dating cryptodiran nodes: origin and diversification of the turtle superfamily Testudinoidea.** *Mol Phylogenet Evol* 2012, **62:**496–07.

doi:10.1186/1471-2148-13-203
Cite this article as: Rabi *et al.*: A new xinjiangchelyid turtle from the Middle Jurassic of Xinjiang, China and the evolution of the basipterygoid process in Mesozoic turtles. *BMC Evolutionary Biology* 2013 **13**:203.

Submit your next manuscript to BioMed Central and take full advantage of:

- **Convenient online submission**
- **Thorough peer review**
- **No space constraints or color figure charges**
- **Immediate publication on acceptance**
- **Inclusion in PubMed, CAS, Scopus and Google Scholar**
- **Research which is freely available for redistribution**

Submit your manuscript at
www.biomedcentral.com/submit

BioMed Central

Publication #3

Zhou, C.-F†., **Rabi, M†.** & Joyce, W.G. 2014. A new specimen of *Manchurochelys manchoukuoensis* from the Early Cretaceous Jehol Biota of Chifeng, Inner Mongolia, China and the phylogeny of Cretaceous basal eucryptodiran turtles. *BMC Evolutionary Biology*. 14 (77): 1–16.

† = equal contributors

Scientific ideas of candidate: 60 %

Data generation by candidate: 50 %

Analysis and Interpretation by candidate: 80 %

Paper writing by the candidate: 60 %

Zhou et al. BMC Evolutionary Biology 2014, 14:77
http://www.biomedcentral.com/1471-2148/14/77

BMC Evolutionary Biology

RESEARCH ARTICLE Open Access

A new specimen of *Manchurochelys manchoukuoensis* from the Early Cretaceous Jehol Biota of Chifeng, Inner Mongolia, China and the phylogeny of Cretaceous basal eucryptodiran turtles

Chang-Fu Zhou[1*†], Márton Rabi[2,3†] and Walter G Joyce[4]

Abstract

Background: *Manchurochelys manchoukuoensis* is an emblematic turtle from the Cretaceous Yixian Formation of Liaoning, China, a geological rock unit that is famous for yielding perfectly preserved skeletons of fossil vertebrates, including that of feathered dinosaurs. *Manchurochelys manchoukuoensis* was one of the first vertebrates described from this fauna, also known as the Jehol Biota. The holotype was lost during World War II and only one additional specimen has been described since. *Manchurochelys manchoukuoensis* is a critical taxon for unraveling the phylogenetic relationships of Cretaceous pancryptodires from Asia, a group that is considered to be of key importance for the origin of crown-group hidden-neck turtles (Cryptodira).

Results: A new specimen of *Manchurochelys manchoukuoensis* is described here from the Jiufotang Formation of Qilinshan, Chifeng, Inner Mongolia, China. This is the third specimen described and expands the range of this taxon from the Yixian Formation of the Fuxin-Yixian Basin in Liaoning to the Jiufotang Formation of the Chifeng-Yuanbaoshan Basin. A possible temporal extension of the range is less certain. The new finding adds to our understanding of the morphology of this taxon and invites a thorough revision of the phylogeny of Macrobaenidae, Sinemydidae, and closely allied forms.

Conclusions: Our comprehensive phylogenetic analyses of Cretaceous Asian pancryptodires yielded two main competing hypotheses: in the first these taxa form a paraphyletic grade, whereas in the second they form a monophyletic clade. The inclusion of problematic tree changing taxa, such as Panpleurodires (stem + crown side-neck turtles) has a major influence on the phylogenetic relationships of Sinemydidae and closely allied forms. *Manchurochelys manchoukuoensis* nests within Sinemydidae together with *Sinemys* spp. and *Dracochelys bicuspis* in the majority of our analyses.

Background

To date, three turtle taxa have been recognized in the Early Cretaceous Jehol Biota of western Liaoning and adjacent areas: *Manchurochelys manchoukuoensis* Endo and Shikama 1942 [1]; *Ordosemys liaoxiensis* (Ji 1995) [2,3]; and *Liaochelys jianchangensis* Zhou 2010 [4]. Of these, *M. manchoukuoensis* is notable because it was one of the first tetrapod fossils to be described from the Jehol Biota, together with the choristodere *Manchurosuchus splendens* and the lizard *Yabeinosaurus tenuis*. Unfortunately, the holotype, a partial shell, appears to have been lost during World War II [5]. Our knowledge regarding the anatomy of this species was nevertheless recently expanded by the referral of a second specimen, which consists of a nearly complete skeleton [5], but much remains to be learned about this taxon, in particular in regards to its skeletal anatomy, phylogenetic relationships, and its geographic and temporal distribution.

In the present paper, a new partial skeleton of *M. manchoukuoensis* is described from a new site in the Jiufotang Formation of Qilinshan, Chifeng, Inner Mongolia (Figure 1). In addition to expanding the geographical distribution of *M. manchoukuoensis* to Inner Mongolia, this specimen is interesting because it allows a reassessment of the

* Correspondence: zhoucf528@163.com
† Equal contributors
[1]Paleontological Institute, Shenyang Normal University, 253 North Huanghe Street, Shenyang, Liaoning 110034, People's Republic of China
Full list of author information is available at the end of the article

BioMed Central

© 2014 Zhou et al.; licensee BioMed Central Ltd. This is an Open Access article distributed under the terms of the Creative Commons Attribution License (http://creativecommons.org/licenses/by/2.0), which permits unrestricted use, distribution, and reproduction in any medium, provided the original work is properly credited. The Creative Commons Public Domain Dedication waiver (http://creativecommons.org/publicdomain/zero/1.0/) applies to the data made available in this article, unless otherwise stated.

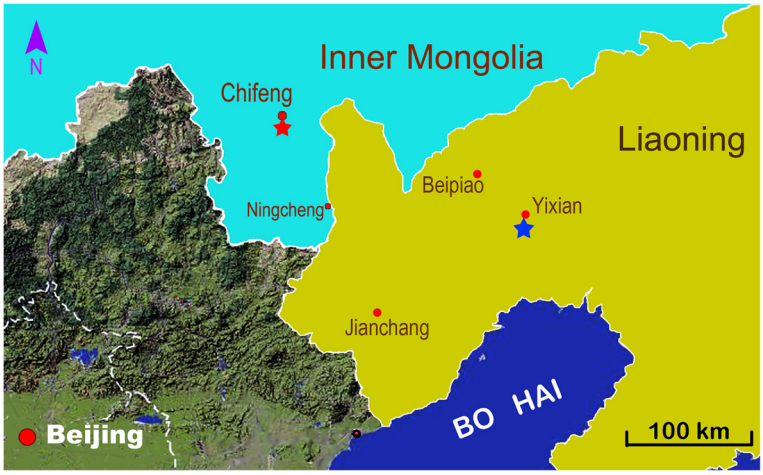

Figure 1 Map showing the known localities of *Manchurochelys manchoukuoensis*, in Qilinshan (=Heishangou; marked by a red asterisk; E118°50′46.4″, N42°08′33.3″), Chifeng City, Inner Mongolia; and in Yixian (marked by a blue asterisk), Jinzhou City, Liaoning Province.

morphology and phylogenetic relationships of this enigmatic species.

Asian Cretaceous basal eucryptodires, such as *M. manchoukuoensis*, are widely recognized as a critical group for resolving the early evolution of pancryptodires [6-20], a clade that represents about 75% of extant turtle diversity. There currently is no consensus on the phylogenetic arrangement of Cretaceous pancryptodires, but most workers historically distinguished two primary groups with doubtful monophyly: Sinemydidae and Macrobaenidae [6,8-10,21-26]. There historically also was little agreement on the content of these taxa, but recent phylogenetic definitions provided some level of nomenclatural stability [27]. In particular, Sinemydidae is now defined as referring to the most inclusive clade containing *Sinemys lens* but not *Xinjiangchelys junggarensis, Macrobaena mongolica*, or any species of recent turtle, whereas Macrobaenidae is defined as referring to the most inclusive clade containing *Macrobaena mongolica* but not *Xinjiangchelys junggarensis*, *Sinemys lens*, or any species of Recent turtle. A summary of the taxonomic history of these groups is provided in Rabi et al. [19,27].

There have been numerous attempts to resolve the phylogeny and position of Macrobaenidae and Sinemydidae, but these either suffered from low taxon sampling and/or lack of specific characters and/or use of literature based data rather than actual observations on fossil specimens [4,5,11,12,14,17,18,20,28-36]. Here, we considerably improve upon previous analyses by rescoring taxa based on our own observations of specimens, by adding six new taxa and new characters, and by testing for tree changing and wildcard taxa.

Methods

The fossil described herein is housed in the Paleontological Museum of Liaoning (= Liaoning Paleontological Museum, PMOL), Shenyang Normal University, with the number PMOL-AR00180. The specimen was obtained in two blocks that were subsequently glued together during the preparation process at PMOL. The surrounding sediment was then removed to expose the skeleton in dorsal and ventral views.

The following fossil taxa were studied first hand for comparative purposes and for the phylogenetic analysis: *Dracochelys bicuspis* Gaffney and Ye, 1992 [8] (IVPP V4075 holotype); *Kirgizemys* (= *Hangaiemys*) *hoburensis* (Sukhanov and Narmandakh, 1974) [6,15] (PIN 3334-4, PIN 3334-1, PIN 3334-5, PIN 3334-16, PIN 3334-34, PIN 3334-35, PIN 3334-36, PIN 3334-37); *Judithemys sukhanovi* Parham and Hutchison, 2003 [14] (TMP 87.2.1 holotype); *Liaochelys jianchangensis* Zhou, 2010 [4] (PMOL-AR00140 holotype, PMOL-AR00160); *Manchurochelys manchoukuoensis* Endo and Shikama, 1942 [1] (PMOL AR00008); *Ordosemys leios* [10] (IVPP V9534-1 holotype, and material listed in Brinkman and Peng 1993 [10]); *Sinemys gamera* Brinkman and Peng 1993 [9] (IVPP V9532-1 holotype, IVPP V9532-11 and the material listed in Brinkman and Peng 1993 [9]); *Sinemys brevispinus* Tong and Brinkman, 2013 [37] (IVPP V9538-1 holotype); Wiman, 1930 [38] (IVPP V8755, IVPP V9533-1).

The cranial carotid circulation nomenclature follows Rabi et al. [36] and taxonomic nomenclature follows the phylogenetic definitions of Rabi et al. [27].

Phylogenetic analysis

Four separate phylogenetic analyses were run in order to test the relationships of Cretaceous basal eucryptodires from Asia and North America. All analyses used a modified version of the latest global turtle character-taxon matrix by Rabi et al. [36], which in turn is based on Rabi et al. [27], Sterli and de la Fuente [20,23], Sterli [30], and Joyce [18]. In

addition to the taxa sampled in Rabi et al. [36], the matrix includes *Liaochelys jianchangensis*, *Changmachelys bohlini* Brinkman et al., 2013 [35], *Sinemys gamera*, *Sinemys lens*, *Sinemys brevispinus*, and the skull of *Ordosemys* sp. [12]. The taxon *Ordosemys leios* is only considered to consist of material described in Brinkman and Peng [10]. *Manchurochelys manchoukuoensis* was scored on the basis of three specimens: the specimen described herein (PMOL-AR00180), the one described by Zhou [5]; PMOL-AR00008), and the lost holotype [1]. Several scorings were changed for *Kirgizemys hoburensis*, *Sinemys lens*, *Dracochelys bicuspis*, and *Ordosemys leios*, among others, based on personal observations of the relevant material (see Appendix 1 for list of changes).

The following characters were treated as ordered: 7 (Nasal A), 19 (Parietal H), 27 (Squamosal C), 40 (Maxilla D), 42 (Vomer A), 50 (Quadrate B + C), 52 (Antrum Postoticum A), 59 (Pterygoid B), 81 (Opisthotic C), 82 (Opisthotic D), 89 (Stapedial Artery B), 98 (Canalis Caroticum F), 120 (Carapace A), 121 (Carapace B), 130 (Peripheral A), 133 (Costal B), 138 (Supramarginal A), 158 (Hyoplastron B), 159 (Mesoplastron A), 161 (Hyoplastron B), 176 (Abdominal A), 213 (Cleithrum A), 214 (Scapula A), 232 (Manus B), 233 (Manus C). *Sphenodon punctatus*, *Owenetta kitchingorum*, *Simosaurus gaillardoti*, and *Anthodon serrarius* were designated as outgroups.

In each analysis we omitted the following characters: Maxilla B, Basioccipital B, Pterygoid M, and Cervical Vertebra D and K. Maxilla B was omitted because we cannot reproduce the meaning or scoring of this character as provided by Sterli and de la Fuente [20]. As scored, this character does not show any variation within Cretaceous basal eucryptodires and we therefore do not expect any impact from its omission.

Basioccipital B is omitted for similar reasons: the definition of a deep, C-shaped concavity on the basioccipital is quite vague since almost all turtles with basioccipital tubera have some sort of C-shaped concavity, but were scored as absent by Sterli and de la Fuente.

Pterygoid M is omitted because, unlike as stated [20], the derived state of this character (basisphenoid and pterygoid in different levels) is present in many basal taxa (actually being the ancestral state for turtles, e.g. *Proganochelys quenstedti*) and therefore the character should be rescored in the future.

Cervical D is omitted once again because we cannot reproduce the meaning of 'triangular diapophysis' and because the current distribution of this character does not help us either (scored as present for panpleurodires, *Chubutemys copelloi*, *Glyptops plicatulus* and baenids).

Finally, Cervical vertebra K is omitted because we find it redundant with Cervical Vertebra B (both characters pertain to the depth of the ventral keel on posterior cervicals).

The taxon-character matrix, the TNT file and strict consensus trees are deposited on the website of the journal as Additional files 1, 2 and 3 and in TreeBase (Study Accession URL: http://purl.org/phylo/treebase/phylows/study/TB2:S15457).

Analysis A

For this analysis, a simple heuristic search was performed in TNT [39,40] using the tree-bisection-reconnection swapping algorithm with thousands of random addition sequence replicates and 10 trees saved per replicate. Wildcard taxa were removed following the search to improve resolution within the strict consensus tree.

Analysis B

The protocol from 'Analysis A' was repeated, but this time the relationship of the major crown-cryptodire clades (not only Durocryptodira as in Rabi et al. [36]) were constrained following the current molecular consensus [41]: (Trionychia (Emydidae (Geoemydidae + Testudinidae)) + (Chelonioidea (Chelydridae + Kinosternoidea)))). The internal relationships of these clades were left unconstrained and *Platysternon megacephalum* was considered a stem-emydid. Heuristic searches were repeated until the most parsimonious trees (MPT) were found 30 times during each replicate (using the command "xmult = hits 30").

Analysis C

The protocol from 'Analysis B' was repeated, but nine new characters that are thought to be relevant for the interrelationships of Cretaceous basal eucryptodires were added (see Appendix 2 for character definitions). Heuristic searches were repeated until the most parsimonious trees (MPT) were found 30 times during each replicate.

Analysis D

This analysis differs from 'C' in that *Basilochelys macrobios* and most pan-pleurodires except for *Podocnemis expansa* and *Pelomedusa subrufa* were excluded a priori before running the heuristic search. This experimental approach is justified by the work of Rabi et al. [27,36] in which the position of pan-pleurodires proved to be problematic in that xinjiangchelyids, sinemydids, and other, widely recognized Mesozoic stem-cryptodires were unorthodoxly placed outside of Testudines and in that Cryptodira was not found to be monophyletic relative to Pleurodira. As such, we were interested in testing how the removal of most pan-pleurodires affects tree topology, especially in the case of Mesozoic basal eucryptodires. The search was again repeated until the most parsimonious trees (MPT) were found 30 times during each replicate.

Systematic Paleontology

TESTUDINATA Klein [42]
TESTUDINES Batsch [43]
PANCRYPTODIRA Joyce, Parham, and Gauthier [44]
Manchurochelys manchoukuoensis Endo and Shikama [1] (Figures 2 and 3)

Referred specimen

PMOL-AR00180 (Figures 2 and 3), a partial articulated skeleton, including the skull, the first six cervical vertebrae, the anterior part of the carapace, two fragmentary scapulae, and a proximal end of the right humerus.

Locality and Horizons

The fossil is from a site near Qilinshan (Heishangou), Chifeng City, Inner Mongolia (E118°50′46.4″, N42°08′33.3″; Figure 1); the Early Cretaceous Jiufotang Formation [45]. Given the novelty of this site, detailed information is not yet available regarding its precise age or accompanying fauna.

Revised Diagnosis

Manchurochelys manchoukuoensis is diagnosed as a primitive pancryptodire by the presence of a low domed shell and a ligamentous connection between the plastron and carapace. It is distinguished from other basal pancryptodires by the following unique combination of characters: prefrontals contact one another along the midline, postorbital-squamosal contact absent, parietal and squamosal separated, crista supraoccipitalis relatively long, foramen palatinum posterius large, nuchal emargination shallow, cervical scale present, vertebral scales 2-4 longer than wide, first vertebral wider than nuchal, preneural absent, eight neurals present, peripheral 1 - costal contact present, costal 3 with parallel anterior and posterior sides, process or spine on peripheral 7 absent, two suprapygals present of which the posterior one is much larger than the anterior one, pygal present, central and posterior fontanelles absent, posterior lobe of plastron long and narrow.

Description

Skull

The skull is exposed in dorsal and ventral views (Figures 2 and 3). The cranial elements can be readily distinguished from one another although some cracks are present due to diagenetic compression. The skull is slightly elongated and similar in its proportions to the skull of PMOL-AR00008. The skull roof is ornamented with a rugose surface and there are no apparent cranial scale sulci.

Dermal roofing elements The nasals are not preserved, but were likely present by comparison to PMOL-AR00008. The dorsal plate of the right prefrontal is preserved, but its left counterpart is missing completely. The descending process cannot be observed on either side. Anteriorly, the right prefrontal is partially hidden by the right maxilla and the anterior contacts of the prefrontal with the adjacent elements are therefore uncertain. It seems that the prefrontals contact one another along the midline in PMOL-AR00180. In the description of PMOL-AR00008, the prefrontals were interpreted as being separated due to the anterior processes of the frontals [5]. However, a revision of this specimen reveals that the component of the frontal process that was actually exposed in the skull roof is short and did not separate the prefrontals completely.

Much of the frontal is well exposed except for the anterior process, which is only partially preserved on the left side. The anterior process is slender and a notch on its lateral side indicates an insertion for the prefrontal. Posterior to the notch, the frontal provides a small contribution to the dorsal rim of the orbit that is greater than that of PMOL-AR00008 [5]. More posteriorly, the frontal has a slightly curved suture that contacts the postorbital laterally. The frontal reaches its greatest width at the straight, posterior suture with the parietal.

The parietals are well exposed in dorsal view, forming an irregular pentagon in outline. They contact each other along their entire length, except for their distal ends, which are separated by the supraoccipital. On the skull surface the parietal contacts the frontal anteriorly, the postorbital laterally, and the supraoccipital posteriorly. Posterolaterally, the parietal contributes to the upper temporal emargination. As in *Sinemys* spp. the upper temporal emargination is well developed and the processus trochlearis oticum is therefore fully exposed in dorsal view. The deepest portion of the upper temporal emargination coincides with the parietal-postorbital suture. This condition is similar to that present in *Sinemys* spp. and *M. manchoukuoensis*, but contrast that present in *Ordosemys* spp., *Kirgizemys hoburensis*, and *Liaochelys jianchangensis*, where the parietal frames the deepest part of the upper temporal emargination by a distinct posterolateral process. The long and narrow processes of the parietals that surround the supraoccipital posteriorly are longer than those of PMOL-AR00008 ([5]: Figure 3ab), but this might be a preservational difference. The parietal has an additional lateral contact with the prootic within the upper temporal fossa.

The right jugal is preserved along the posteroventral corner of the fossa orbitalis. It has a long and slender anterior process that forms the ventral rim of the orbit together with the maxilla. Dorsally, the jugal has a curved sutural contact with the postorbital. Other, potential posterior contacts of the jugal with other elements are uncertain due to compression.

The presence of the quadratojugals is uncertain due to compression in the temporal area.

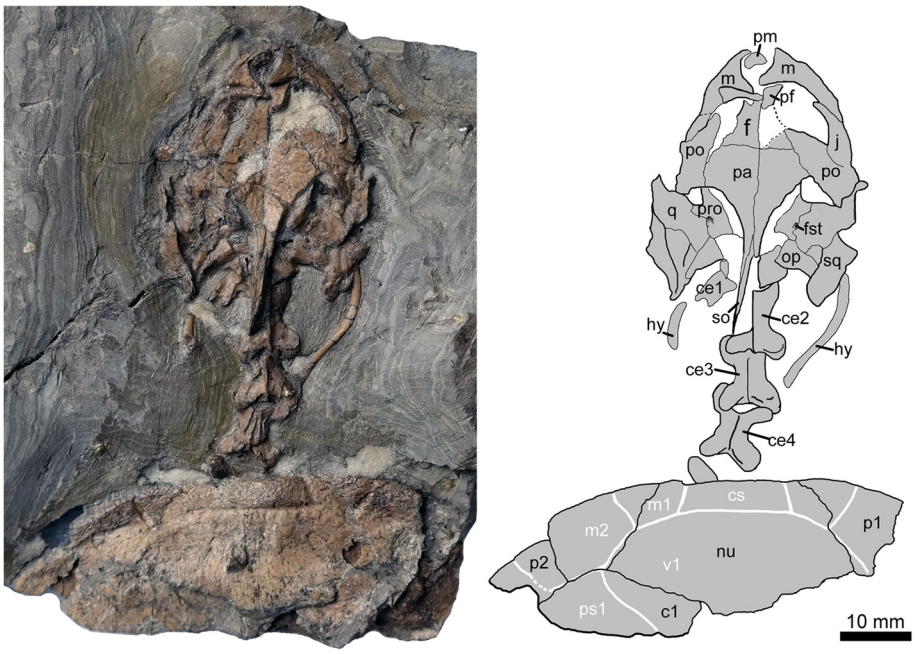

Figure 2 New material of *Manchurochelys manchoukuoensis* (PMOL-AR00180) in dorsal view, from the Early Cretaceous Jiufotang Formation of Qilinshan, Chifeng, Inner Mongolia, China. Abbreviations: c1, costal Plate 1; **cs,** cervical scale; **ce1-4**, cervical vertebrae 1-4; **f,** frontal; **fst,** foramen stapedio-temporale; **hy,** hyoid; **m,** maxilla; **m1-2,** marginal scales 1–2; **nu,** nuchal; **op,** opisthotic; **p1-2,** peripheral Plates 1–2; **pa,** parietal; **pf**, prefrontal; **pm,** premaxilla; **po,** postorbital; **pro,** prootic; **ps1,** pleural scale 1; **q,** quadrate; **so,** supraoccipital; **sq,** squamosal; **v1,** vertebral scale 1.

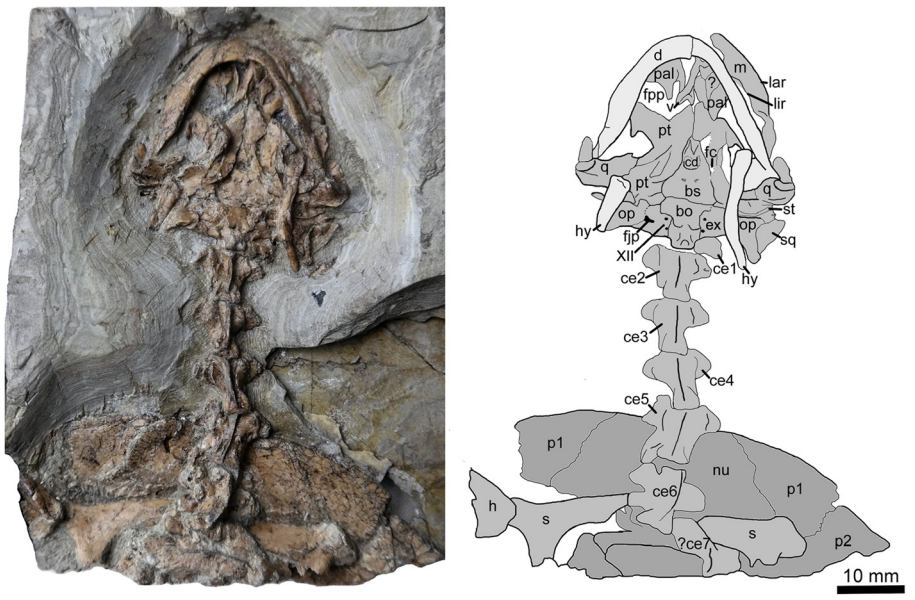

Figure 3 New material of *Manchurochelys manchoukuoensis* (PMOL-AR00180) in ventral view, from the Early Cretaceous Jiufotang Formation of Qilinshan, Chifeng, Inner Mongolia, China. Abbreviations: bo, basioccipital; **bs,** basisphenoid; **cd,** central depression of basisphenoid (maybe taphonomic); **ce1-7,** cervical vertebrae 1-7; **d,** dentary; **ex,** exoccipital; **fc**, fenestra caroticus; **fjp,** foramen jugulare posterius; **h,** humerus; **hy,** hyoid; **lar,** labial ridge of the triturating surface in maxilla; **lir,** lingual ridge of the triturating surface in maxilla; **m,** maxilla; **nu,** nuchal; **op,** opisthotic; **p1-2,** peripheral Plates 1-2; **pal,** palatine; **pt,** pterygoid; **q,** quadrate; **s,** scapula; **sq,** squamosal; **st,** stapes; **XII,** foramina of cranial nerve XII.

The squamosal is positioned at the posterolateral corner of the skull. A posteromedially directed low crest extends along the dorsal plate of the squamosal that frames the lateral aspects of the upper temporal emargination. The squamosal crest is short relative to the elongated crista supraoccipitalis and therefore similar to PMOL-AR00008. The posteriormost tip of the squamosal is pinched and directed posterolaterally, as in *K. hoburensis* and PMOL-AR00008. Medial to the crest, the squamosal contacts the quadrate anteriorly and the opisthotic posteromedially. The left squamosal is exposed in ventral view and reveals the anteromedial contacts with the quadrate and the opisthotic.

The right postorbital is preserved in articulation, whereas the left one is slightly offset from its original position. Anteriorly, the postorbital forms the posterior rim of the fossa orbitalis and contacts the frontal and parietal medially and the jugal laterally. The postorbital is the largest element in the temporal region and helps framing the deep upper temporal emargination together with the parietal.

Palatal elements A slender and laminar fragment between the two maxillae is presumed to be the premaxilla.

The maxilla is the largest element of the snout. The vertical (prefrontal) process contacts the prefrontal dorsally and forms the lateral rim of the apertura narium externa and the anterior rim of the fossa orbitalis. The maxilla contacts the jugal posterodorsally. The horizontal (palatine) plate of the maxilla forms the triturating surface. The triturating surface consists of a longitudinal depression bordered by the labial ridge and a single lingual ridge. Both ridges are comparable in height along their anterior third, but the lingual ridge is distinctly higher than the labial one along its posterior third. The medial contact of the maxilla with the palatine is obscured in ventral view by the mandibles.

The vomer, an unpaired and elongate bone, is slightly displaced from its original position. Its contact with the adjacent elements is uncertain. The vomer is dumbbell-shaped with bilaterally expanded anterior and posterior ends and a keeled main body. The expanded ends are notched, the posterior notch being slightly less developed than the anterior one. These expansions coincide with Y-shaped divergences of the ventral, keel-like ridge of the main body. The posterior notch possibly received the anterior processes of the pterygoids.

The palatines are partially exposed in ventral view and slightly displaced from their original positions. The palatine is a flat plate that encloses the foramen palatinum posterius together with the maxilla and the pterygoid. The exact outline of the foramen palatinum posterius is unclear, but it was apparently large, as in *D. bicuspis* and *Sinemys* spp., which is different from the moderately sized condition seen in *Ordosemys* spp. and *Kirgizemys dmitrievi*. Posteromedially, the palatine has a broad and rounded edge to contact the vomer and the pterygoid.

Palatoquadrate elements The quadrate is well exposed in dorsal and ventral view. It forms the wall of the cavum tympani. Within the temporal fossa, the quadrate has a broad sutural contact with the prootic medially and the squamosal posteriorly. Together with smaller contribution from the prootic, the quadrate forms a thickening at the anterior wall of the otic capsule, the processus trochlearis oticum. The trochlear process is poorly developed and therefore does not protrude significantly into the lower temporal fossa. The quadrate portion of the processus trochlearis oticum is sculptured along the prootic-quadrate suture by several small grooves and ridges, but it is unclear if these ridges had a particular function. In ventral view, the condylus mandibularis are well preserved on both sides of the skull except for a slight lateral twisting caused by compression. The articular surface is a concave facet. Posterior to the condylus mandibularis, a well-developed crest is apparent that runs parallel to the incisura columella auris. In many derived turtles, this crest contacts the posteroventral process of the quadrate to enclose the incisura columella auris. In PMOL-AR00180, however, such a contact is absent. However, this does not logically imply that the incisura was completely open posteriorly, since *Sinemys gamera* has a comparable morphology in ventral view but nevertheless exhibits a closed incisura in lateral view.

The pterygoid is a major element in ventral view. Anteriorly, the pterygoid has a short palatal process that is subtriangular and pointed rostrally. The pterygoids contact one another along their anterior thirds. More posteriorly, the pterygoids are separated from one another by the basisphenoid. Laterally, the pterygoid forms a horizontal plate with a concave posterior margin and a small, recurving processus pterygoideus externus. At the posterior margin of the skull, the pterygoid appears to have a contact with the basioccipital and exoccipital. The foramen posterius canalis carotici interni is not visible.

Braincase elements The supraoccipital crest is notably elongated when compared to *Ordosemys liaoxiensis* or *Liaochelys jianchangensis* and reaches beyond the posterior tip of the squamosals, as in PMOL-AR00008. In lateral view, the crista supraoccipitalis has a slightly convex dorsal outline and a maximum height of approximately 3 mm. It contacts the parietals anterolaterally and the opisthotic and exoccipital laterally.

The exoccipitals are well exposed ventrally and are pierced by a pair of foramina nervi hypoglossi. More laterally, together with the opisthotic, the exoccipital encloses a large foramen, the foramen jugulare posterius,

which is consistent with the condition seen in *Sinemys gamera*. The exoccipital has an anterior contact with the pterygoid. Medially, the exoccipital contacts the basioccipital and contributes to the condylus occipitalis.

The basioccipital forms the floor of the braincase together with the basisphenoid anteriorly and the exoccipitals posterolaterally. Anterolaterally, the basioccipital has a contact with the pterygoid. More posteriorly, the paired, horizontally oriented tubera basioccipitale are well developed and separated from one another by a deep midline depression. The distal portion of the basioccipital forms the ventral portion of the condylus occipitalis.

The prootic forms the processus trochlearis oticum together with the quadrate. The foramen stapediotemporale is primarily enclosed by the prootic, but there is also a small contribution from the quadrate.

The opisthotic contacts the prootic anteriorly, the quadrate and squamosal laterally, and the supraoccipital and exoccipital medially. Posteriorly it encloses the foramen jugulare posterius together with the exoccipital.

The basisphenoid is pointed anteriorly and broadened posteriorly and therefore has a triangular outline. Anteriorly, it is wedged between the pterygoids. In comparison to closely related taxa, the basisphenoid appears to be greatly elongated, but this may be a result of damage to the pterygoids. Posteriorly, the basisphenoid contacts the basioccipital along a straight transverse suture and with the latter forms a smooth and flat braincase floor. The basisphenoid is sculptured by a round median depression, which may be a taphonomic artifact. The fenestra caroticus (sensu [36]) opens along the pterygoid-basisphenoid suture, anteriorly to the basisphenoid pits. Anteriorly, the fenestra ends in the foramen posterius canalis carotici cerebralis. The basipterygoid process of the basisphenoid and the foramen posterius canalis carotici palatinum are not visible, probably due to the displacement of the pterygoids.

The left columella auris (stapes) is well preserved with the basis columellae (footplate) and columella. As in modern turtles, the columella auris has a well-expanded basis columellae and a rod-like delicate columella. Medially, the basis columellae remains in situ and fits well into the fenestra ovalis, but this is partially obscured from ventral view by the hyoid bone. Laterally, the columella is well exposed between the fenestra ovalis and the quadrate, with a length of approximately 5.5 mm. The columella is broken at its middle point, and the distal part is offset slightly. However, its terminal end still remains within the incisura columella auris. The terminal end of the columella is slightly expanded.

Mandible

The mandibles are exposed in ventral view and form a gentle V-shaped outline. They are occluding with the skull. The left mandible appears to be nearly straight, while the right one appears to be convex, but this is likely a taphonomic artifact. Medially, the rami meet at a short, fused symphysis.

The hyoids consist at least of a pair of cornu branchiale I, of which the left one is incomplete distally. The cornu branchiale I is slender, elongated, and curved with a slightly expanded proximal end. Its length is approximately 22 mm. We now interpret the hyoid element preserved in PMOL-AR00008 as the cornu branchiale II because of its greater thickness and its greatly expanded distal end. This indicates that *Manchurochelys manchoukuoensis* probably possessed two pairs of ossified cornu branchiale even though these two pairs are not preserved in the available specimens.

Shell

Only the anterior part of the carapace is preserved, including the nuchal plate, first costal plates, first peripherals, left second peripheral, and a fragment of the left third peripheral (Figure 2). The shell appears to be low and is slightly sculptured by numerous tiny pits and grooves.

There is a shallow nuchal emargination, as in PMOL-AR00008 and *Liaochelys jianchangensis* but quite different from *Sinemys lens* and *Dracochelys bicuspis* where a deeper emargination is present. The nuchal is a massive element with a trapezoidal shape that contacts the first peripherals laterally and the first costal plates posteriorly. It is distinctly anteroposteriorly longer than that of *Sinemys brevispinus* (the morphology is not entirely clear in *S. lens*). The first costal plate shows a broad contact with the subtriangular first peripheral, as in PMOL-AR00008 and *Sinemys* spp., but unlike *Dracochelys bicuspis* where the first peripheral is triangular and does not contact the costal (Figures 2 and 3).

The sulci of the scales are clearly impressed on the carapace, including the cervical scale, the first vertebral scale, the anterior three marginal scales, and the first pleural scale. The cervical scale is present, as in PMOL-AR00008, but absent in *Sinemys lens* and *Dracochelys bicuspis*. It is small and sub-trapezoidal, with a maximum width of 15 mm and a minimum length of 4 mm. The first vertebral scale is hexagonal and distinctly wider than long. It contacts the cervical anteriorly, the first two marginals anterolaterally, and the first pleural posterolaterally. The first pleural is partially preserved on the left side. The anterior two marginal scales are identified on the right side, while the anterior three scales are present on the left side. The first marginal is much smaller than the second one.

Vertebral column

The cervical series is well preserved in articulation between the skull and shell, but only the six anterior

cervicals can be identified with confidence. The articulation prohibits observing the development and orientation of the articular surfaces of the centra, and it is not possible to recognize cervical ribs along the cervical series. However, the centra are formed and the presence of a biconvex centrum can be excluded.

The atlas is displaced from its original position. The atlas neural arch is positioned against the supraoccipital and the left exoccipital and is slightly hidden by the latter anteriorly. The arch is clearly shorter than the axis. As in most crown cryptodires, the neural arch is a flat lamina. It is expanded dorsally to bear a broad medial contact with its counterpart. The neural arch bifurcates posteriorly with a short lateral spine and a medial process. The lateral spine is positioned slightly beyond the medial process. Medially, the spine conjoins the process along a semicircular notch. The medial process is broad for articulating with the prezygapophysis of the axis.

The axis is well preserved below the crista supraoccipitalis in articulation with the succeeding cervicals. As in crown turtles, the prezygapophyses of the axis face dorsolaterally, whereas the prezygapophyses of the following cervicals face dorsomedially. The axis is a large element with a length of 10 mm and a width of 8 mm, comparable to the following cervicals. In dorsal view, the axis is dumbbell-shaped due to the lateral expansion of the prezygapophyses and postzygapophyses. The prezygapophysis extends more anteriorly than laterally, thereby forming a dorsolaterally facing articular surface. In contrast, the postzygapophyses are expanded more laterally than posteriorly, thereby forming the maximum width of the axis. Between the postzygapophyses, there is a posterior notch with a gentle curvature. The neural spine is developed with a height of 1 mm, beyond the posterior notch. In ventral view, a well-developed keel is present along the entire length of the centrum. The keel is reduced posteriorly and disappears at the posterior margin of the centrum. The transverse processes are well developed, forming a maximum width of 10 mm. As in crown cryptodires, the transverse process is positioned along the anterior half of the centrum. Posteriorly, the centrum is compressed bilaterally.

The remaining cervicals are similar to each other in morphology. The third and fourth cervicals are well exposed in dorsal view. They are similar to the axis in general morphology except for the dorsomedially-facing prezygapophyses. The prezygapophyses are divergent laterally and comparable to the postzygapophyses in extent. The right prezygapophysis of the fourth cervical is flat and faces dorsally and medially. The anterior notch between the prezygapophyses is comparable to the posterior one between the postzygapophyses. This condition is different from PMOL-AR00008, in which the anterior notch has an angle of 120 degrees, and the posterior notch is anterior to the middle point of the neural arch with an angle of 70 degrees [5]. The neural spine is present on the whole length of the neural arch, different from *M. manchoukuoensis*, in which the neural spine is limited to the anterior half of the neural arch [5].

In ventral view, the third and fourth cervicals are comparable in size to the axis, while the fifth and sixth cervicals appear to be prolonged. The transverse process is positioned at the anterior portion of the centrum. Along the cervical series, the transverse process increases posteriorly in size. The posterior end of the centrum broadens posteriorly along the cervical series. The ventral keel is well developed along the whole length of the centrum. Posteriorly, the keel increases in depth along the cervical series.

Pectoral girdle

The scapulae are partially preserved on both sides in ventral view. The scapula is triradiate with a dorsally directed scapular process, a ventrally directed acromial process, and a laterally directed glenoid process. The scapular process is long and slender, but its distal end is hidden by the cervical series on both sides. The scapular process gradually expands proximally and forms a gentle curve with the acromial process. The scapular process is set at an angle of 87 degree relative to the acromial process. Most of the acromial process is broken on both sides. Its remains are slightly longer than the glenoid process on the right side and confluent proximally to the glenoid process and scapular process. In contrast, the glenoid process is stout and bears a laterally facing glenoid fossa. On the right side, the glenoid fossa is occupied by the humeral head. The left glenoid fossa is exposed with a concave facet. However, the precise configuration of the glenoid fossa is uncertain because the coracoid portion is missing.

Humerus

The proximal head of the humerus is partially preserved on the right side in articulation with the glenoid fossa. The lateral process is identifiable as a ventrally directed crest. Medially, there is a distinct intertubercular fossa between the lateral and medial processes. The medial process is expanded posteriorly and is larger than the lateral process.

Results

Phylogenetic Analysis

None of the four phylogenetic analyses placed xinjiangchelyids, sinemydids, or other Cretaceous basal eucryptodires within Testudines, the crown-group of turtles. However, the relationships of Cretaceous forms vary among three of the analyses. All four analyses agree in that all Cretaceous

taxa are consistently placed in a derived position relative to Xinjiangchelyidae.

Analysis A (220 equally parsimonious trees, tree length = 887): This analysis with no topological constraint and no new characters resulted in a largely paraphyletic arrangement of basal eucryptodires with a basally placed Sinemydidae (sensu [27]) that is only composed of *Sinemys* spp., an (*Ordosemys leios* + *Liaochelys jianchangensis*) clade and a successively more derived clade including *Judithemys sukhanovi*, *Kirgizemys hoburensis* and *Changmachelys bohlini* (the latter group roughly corresponds to the traditional circumscription of Macrobaenidae). *Manchurochelys manchoukuoensis* is found in the next less inclusive node to Sinemydidae. *Dracochelys bicuspis* occupies the most derived position among these taxa. The skull of *Ordosemys* sp. proved to be a wildcard taxon (Figure 4; Additional file 3).

Analysis B (136 equally parsimonious trees, tree length = 909): The constrained analysis obtained poor resolution for Cretaceous basal eucryptodires, similarly to the recent results of Rabi et al. [36]. However, a monophyletic Sinemydidae composed only of *Sinemys* spp. as well as a *Judithemys sukhanovi* – *Kirgizemys hoburensis* - *Changmachelys bohlini* clade was again recovered. Removal of wildcard taxa, including *Ordosemys* sp. and *Basilochelys macrobios* does not improve resolution (Additional file 3).

Analysis C (151 equally parsimonious trees, tree length = 925): Inclusion of new characters into the constrained analysis further decreases resolution. However, after pruning several Cretaceous taxa, a monophyletic Sinemydidae was obtained including *Sinemys* spp., *Manchurochelys manchoukuoensis*, and *Dracochelys bicuspis*. Removal of the constraint results in the basal placement of *M. manchoukuoensis* within Sinemydidae and in a (*Liaochelys jianchangensis* + *Ordosemys leios*) clade that in turn forms a polytomy with other Cretaceous basal eucryptodires (Additional file 3).

Analysis D (143 equally parsimonious trees, tree length = 819): When most pleurodires and *Basilochelys macrobios* are *a priori* excluded from the analysis a monophyletic Sinemydidae (sensu [27]) is recovered containing all Cretaceous forms. *Manchurochelys manchoukuoensis* is sister to a (*Dracochelys bicuspis* + *Sinemys* spp.) clade and combined they are sister to an (*Ordosemys leios* + *Liaochelys jianchangensis*) clade. *Judithemys sukhanovi* + *Kirgizemys hoburensis* are the most basal sinemydids in the context of this analysis. *Ordosemys* sp. and *Changmachelys bohlini* turned to be acting as wildcards and the inclusion of any of them sinks the *J. sukhanovi* + *K. hoburensis* clade into a polytomy. Another notable feature of these results that *Xinjiangchelys* (= *Annemys*) *levensis* is no longer recovered as a xinjiangchelyid but in the next less inclusive node to them (Figure 5). Exclusion of new characters does not influence tree topology but decrease bootstrap support for the *Sinemys* spp. clade by 47%. Other changes in support are insignificant. A search without constraints results in a basal polytomy of Cretaceous basal eucryptodires with *Manchurochelys manchoukuoensis* placed as sister to *Sinemys* spp. when most other Cretaceous target taxa are pruned (Additional file 3).

Discussion

Taxonomic comments

PMOL-AR00180 is assigned to *Manchurochelys manchoukuoensis* because no major differences are apparent in the proportions and contacts in the skull and the shell with those of the holotype [1] or the referred specimen PMOL-AR00008 [5]. A striking similarity of PMOL-AR00180 with PMOL-AR00008 is the presence of a long supraoccipital crest that extends markedly more posteriorly than in *Liaochelys jianchangensis*, *Ordosemys liaoxiensis*, *Kirgizemys hoburensis*, and *Sinemys lens* (unknown for other species of *Sinemys*). Although differences appear to be present, at first sight, between the neck of PMOL-AR00008 and PMOL-AR00180, particularly in the degree of separation of the postzygapophyses, these are only because different sections of the neck are exposed in the two specimens. As in modern cryptodires, the postzygapophyses of the anterior cervicals in *M. manchoukuoensis* (as well as in *Sinemys brevispinus*, *Kirgizemys hoburensis*) are more fused than the posterior ones. In addition, the foramen posterius canalis carotici cerebralis was illustrated in the pterygoid in PMOL-AR00008 (labeled as foramen basisphenoidale [5]) but a revision of the specimen reveals that the position of this foramen is unclear and preservation makes comparison difficult with PMOL-AR00180 where it is on the pterygoid-basisphenoid suture.

With the discovery of the new specimen, the number of described *M. manchoukuoensis* fossils has increased to three. Two of these originate from the Yixian Formation of Liaoning Province (including the lost holotype [1,5]) whereas PMOL-AR00180 was recovered from the Jiufotang Formation of Inner Mongolia. Both formations are considered to be Lower Cretaceous, with the Yixian being Barremian to Upper Aptian (129-122 Ma) and the younger Jiufotang Formation being Aptian to Upper Albian (122-110 Ma) in age. Thus, the range of *M. manchoukuoensis* is extended geographically and, less unequivocally, temporally by the new fossil from Chifeng. However, given this difference in geography and perhaps in age it is not excluded that more complete findings may reveal distinct morphological features not preserved in the specimen from Chifeng and arguing for a separate species of *Manchurochelys*.

Relationships of Cretaceous basal eucryptodire turtles

A broad range of phylogenetic hypotheses of Cretaceous basal eucryptodires has been proposed over the course

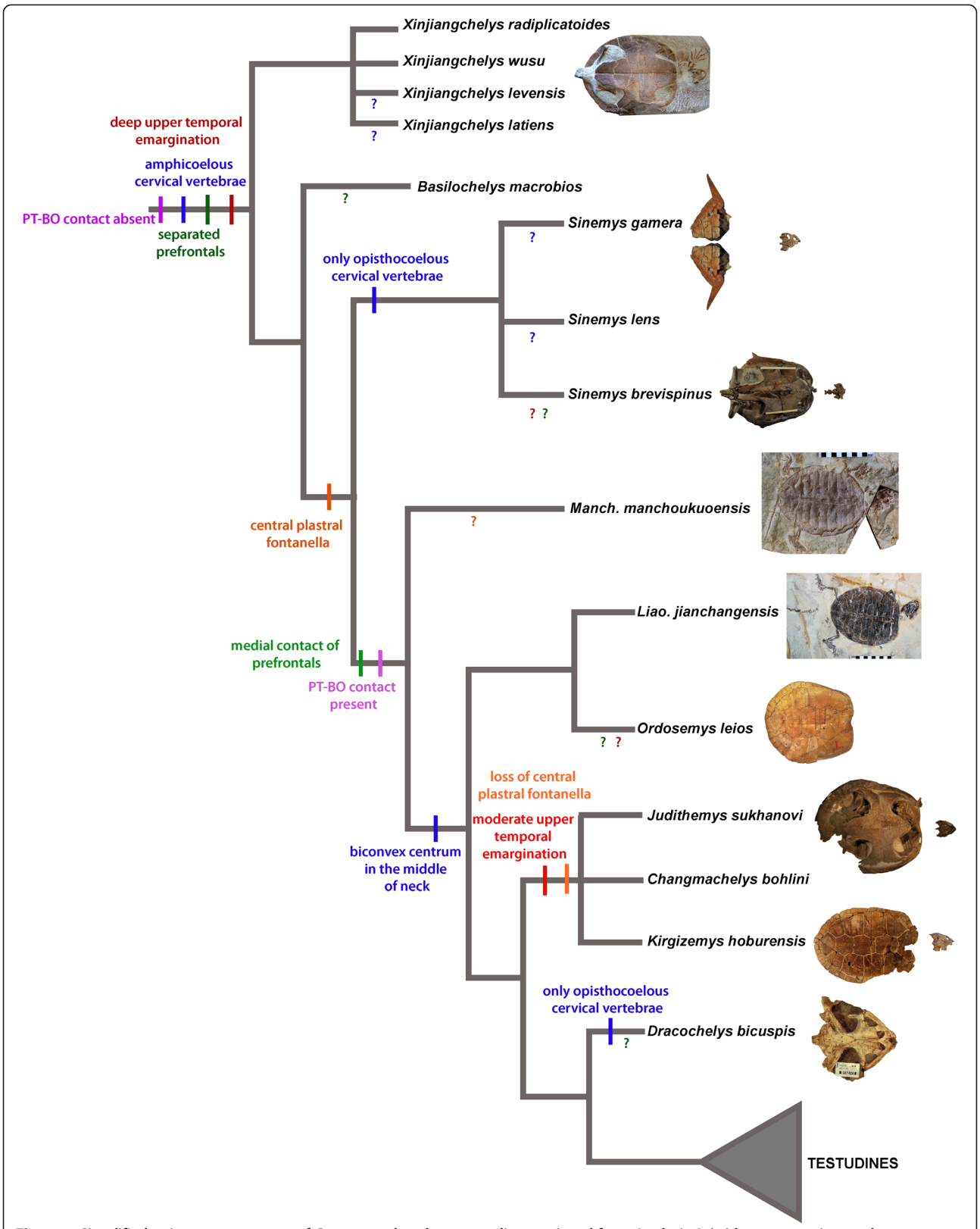

Figure 4 Simplified strict consensus tree of Cretaceous basal eucryptodires retrieved from Analysis A (with no constraints and no new characters added) showing a paraphyletic arrangement for the taxa in question. The inferred evolution of selected characters varying among these taxa is shown on the tree. Ambiguous character states for a given taxon are indicated with '?' in a color that is corresponding to the color of that character. An alternative topology with *Changmachelys bohlini* not pruned from the strict consensus is shown in a box at the upper right corner.

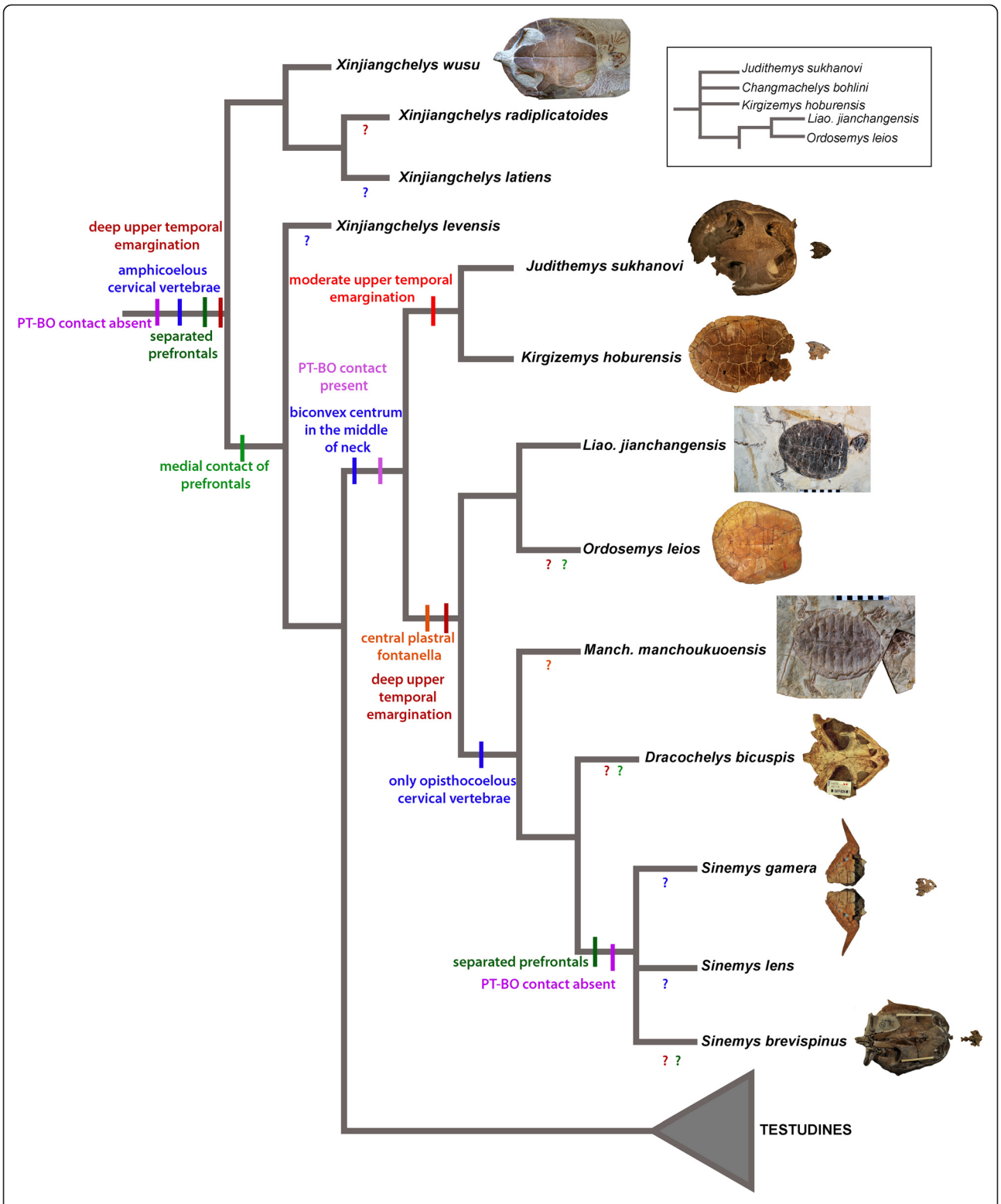

Figure 5 Simplified strict consensus tree of Cretaceous basal eucryptodires retrieved from Analysis D. In this analysis most pan-pleurodires and *Basilochelys macrobios* was a priori removed, nine new characters were added and the relationships of cryptodires were constrained according to molecular phylogenetic results. The inferred evolution of selected characters varying among these taxa is shown on the tree. Ambiguous character states for a given taxon are indicated with '?' in a color that is corresponding to the color of that character.

of the last decade. Some studies consider these turtles to be a predominantly monophyletic clade [18,30,31,33] whereas others interpret them as being a predominantly paraphyletic assemblage [4,5,12,17,28,29,32,36]. Two analyses [20,34] obtained a monophyletic Sinemydidae to the exclusion of *Judithemys sukhanovi* and *Kirgizemys hoburensis*. A more crown-ward position for *J. sukhanovi* and *K. hoburensis* has been suggested in other studies as well [4,5,14,17,29,32,35]. All of these analyses build either on Gaffney [11] or Joyce [18]. The studies expanding the matrix of Gaffney [11] are problematic in assuming monophyly for many higher groups of turtles and for using a small number of characters only (max. 45), but they have the advantage of including many Cretaceous basal eucryptodiran taxa. The matrices expanding the work of Joyce [18] are improved in using single species as terminals and a large number of characters, but they are limited in taxon sampling, at least for the group in question. Other downsides of all of these analyses are the dominantly literature-based character scorings and the lack of specific, phylogenetically relevant characters for sinemydids, macrobaenids, and closely allied taxa.

We sought progress relative to previous analysis by significantly expanding the sample of Cretaceous basal eucryptodires, by utilizing a large, global matrix, by correcting several errors that are apparent in the scorings of previous matrices, through the addition of new characters relevant to this group, and by directly studying all relevant specimens. Therefore, our new analysis is the most comprehensive and the most exhaustive attempt to resolve the phylogeny of Cretaceous basal eucryptodires to date.

The results of our unconstrained phylogenetic analysis (Analysis A, Figure 4) agree in its primary aspects with the "paraphyletic hypothesis" of earlier global studies. However, the molecular backbone constraint of crown-cryptodire clades (Analysis B) collapses most of the nodes containing Cretaceous basal eucryptodires. Addition of new morphological characters places *Manchurochelys manchoukuoensis* and *Dracochelys bicuspis* within Sinemydidae together with *Sinemys* spp. while leaving other taxa largely unresolved. Interestingly, *a priori* exclusion of most panpleurodires and *Basilochelys macrobios* (Analysis D, Figure 5), results in the monophyly of all Cretaceous basal eucryptodires.

Conclusions

The question remains unanswered whether the monophyletic or the paraphyletic hypothesis of basal eucryptodires is a better estimate of the phylogeny of sinemydid and macrobaenid turtles. From a parsimony point of view, the monophyletic arrangement is better supported since it requires five (or at least four, as two characters seem to be correlated) steps less than the paraphyletic topology as optimized within this part of the consensus trees of analysis A and D. However, most of these differences in the number of steps correspond either to the loss of traits, retention of juvenile characters (i.e. plastral fontanelles), or the acquisitions of highly variable and homoplastic characters (i.e. number of neurals). When only the acquisitions of more complex characters are taken into account, the differences are far less obvious and the monophyletic hypothesis appears to have less support. In this case, the monophyletic hypothesis requires a reversal to separated prefrontals (from medially contacting prefrontals) and the absence of pterygoid-basioccipital (and exoccipital) contact. On the other hand, the paraphyletic hypothesis requires that opisthocoely in the neck evolved twice within this group (Figures 4 and 5). In summary, until the position of panpleurodires relative to basal eucryptodires is instable, the phylogeny of sinemydids and macrobaenids remains ambiguous as well.

There are some other noteworthy results of the present contribution. The Mongolian *Kirgizemys hoburensis* and the North American *Judithemys sukhanovi* form a clade in all of our analyses (in agreement with some previous works; [17,29,34]) and the Chinese *Changmachelys bohlini* is part of the same clade in three of the analyses, though their exact relationships are unresolved. In addition, *Liaochelys jianchangensis* is found as the sister taxon of *Ordosemys leios* in three of the analyses. As for the target taxon of this work, *Manchurochelys manchoukuoensis* is placed within Sinemydidae (sensu [27]) together with *Sinemys* spp. and *Dracochelys bicuspis* in the majority of the analyses or alternatively, it is more derived than Sinemydidae and retained some typical characters of this group.

Appendix 1

Changes to the taxon-character matrix of Rabi et al. [36]

Taxa added:

Changmachelys bohlini, *Manchurochelys manchoukuoensis*, *Liaochelys jianchangensis*, *Sinemys brevispinus*, *Sinemys gamera*, *Ordosemys* sp. skull [12]. Unlike in all previous analyses, *Ordosemys leios* is here treated separately from the *Ordosemys* sp. skull because they likely represent different species [12]. Most skull character scorings were therefore removed from *Ordosemys leios*, except for a few that could be deduced with the help of the skull fragments associated with the holotype.

Characters omitted from this study:

Maxilla B, Pterygoid M, Basioccipital B, Cervical Vertebra D, Cervical vertebra K (see explanation in 'Methods').

Characters modified in this study:

Pterygoid I. Vertical flange on processus pterygoideus externus: (0) absent; (1) present all along the process; (2) reduced.
New definition: Vertical flange of processus pterygoideus externus: (0) absent, (1) present.
The character of Sterli and de la Fuente [20] pertains to the vertical flange on the processus pterygoideus externus. This character is modified and completely rescored here because the definition of state 2 (reduced) is not clear and the original scorings of [20] do not help us to understand it either. For instance, *Emys orbicularis* and trionychids are scored as reduced in [20], whereas *Carettochelys insculpta* is not. In our opinion *Emys orbicularis* has a fully developed vertical flange, whereas *C. insculpta* and trionychids all have a reduced, barely thickened vertical component. Moreover, *Proganochelys quenstedti* and *Palaeochersis talampayensis* are scored 1 (vertical flange present almost all along the lateral process) but cheloniid sea turtle were scored as not having a vertical flange despite the clear presence of such a flange (which is more developed than in *P. quenstedti* and *Pal. talampayensis*). To assure better reproducibility we modify this character to contain only two states: vertical flange of processus pterygoideus externus: (0) absent or (1) present. Under the new definition *P. quenstedti*, *Kayentachelys aprix* and other basal turtles, including Meiolaniiformes, are scored as absent (0). And contrary to the previous scoring, we code *Carettochelys insculpta* and *Anosteira ornata* as present (1) because we see no difference from the trionychid condition.
Cervical Vertebra I. Sterli and de la Fuente [20] accidentally used "posteroventrally" not "anteroventrally" for the direction of the postzygapophyses of the 8th cervical. *Caretta caretta* and *Chelonia mydas* is changed from 0 to 1 because they clearly show posteroventrally directing postzygapophyses.

Character rescored in this study:

Pterygoid L. Processus pterygoideus externus: (0) like in *Proganochelys quenstedti*; (1) like in testudinoids; (2) like in *Kayentachelys aprix*. This character pertains to the outline of the processus pterygoideus externus. In state 0 the processus is reduced, in state 1 it is better developed whereas in state 2 it is posteriorly recurved. The character is completely rescored because Sterli and de la Fuente [20] accidentally scored testudinoids with state 2.
Changes to the character scorings of Rabi et al. [36] (for justification see the corresponding character in the taxon-character matrix (Additional file 1).

Prefrontal A: *Dracochelys bicuspis*: 1—›?
Prefrontal D: *Dracochelys bicuspis*: 1—›?
Prefrontal E: *Dracochelys bicuspis*: 1—›?
Parietal A: *Dracochelys bicuspis*: 1—›?
Parietal G: *Dracochelys bicuspis:* ?—›1 ; *Kirgizemys hoburensis:* ?—›1
Parietal H: *Dracochelys bicuspis:* 2—›?; *Ordosemys* sp. skull: 2—›1
Jugal A: *Dracochelys bicuspis:* 1—›?; *Ordosemys* sp. skull: ?—›1
Quadratojugal A: *Sinemys lens*: 0—›?
Premaxilla A: *Xinjiangchelys wusu*, *Xinjiangchelys* (= *Annemys*) *levensis*, *Xinjiangchelys radiplicatoides*: 0—›1
Premaxilla E: *Ordosemys* sp. skull: ?—›0
Maxilla A: *Ordosemys* sp. skull: ?—›0
Maxilla B: *Kirgizemys hoburensis*: 1—›0
Maxilla C: *Ordosemys* sp. skull: ?—› –
Maxilla D: *Ordosemys* sp. skull: ?—›0; *Kirgizemys hoburensis*: ?—›0
Quadrate D: *Sinemys lens*: 0—›?
Quadrate F: *Sinemys lens*: 2—›?
Quadrate H: *Sinemys lens*: 1—›0
Epipterygoid A: *Kirgizemys hoburensis*: ?—›1
Pterygoid D: *Kirgizemys hoburensis*: 1—›0/1
Pterygoid G: *Kirgizemys hoburensis*: 1—›0
Pterygoid J: *Judithemys sukhanovi*: ?—›1
Supraoccipital A: *Dracochelys bicuspis*: 1—›?
Basioccipital A: *Kirgizemys hoburensis*: 1—›0
Basisphenoid A: *Kirgizemys hoburensis*: ?—›0
Basisphenoid B: *Dracochelys bicuspis*: ?—›0
Basisphenoid E: *Kirgizemys hoburensis*: ?—›0
Hyomandibular Nerve A: *Xinjiangchelys radiplicatoides*: 1—›0
Foramen Jugulare Posterius A: *Judithemys sukhanovi*: ?—›1; *Kirgizemys hoburensis*: ?—›0
Foramen Nervi Hypoglossi: *Xinjiangchelys wusu*: 2—›0; *Xinjiangchelys radiplicatoides*: 2—›0
Fenestra Perilymphatica A: *Sinemys lens*: 0—›?
Cranial Scutes A: *Judithemys sukhanovi*: 1—›?
Dentary A: *Kirgizemys hoburensis*: ?—›0
Carapace D: *Judithemys sukhanovi*: ?—›0
Nuchal C: *Kirgizemys hoburensis*: ?—›0
Neural B: *Kirgizemys hoburensis*: ?—›1
Cervical A: *Dracochelys bicuspis*: ?—›1
Marginal A: *Kirgizemys hoburensis*: ?—›0
Entoplastron D: *Dracochelys bicuspis*: ?—›0
Entoplastron F: *Kirgizemys hoburensis*: 0—›1
Epiplastron A: *Sinemys lens*: – —›0
Cervical Rib A: *Kirgizemys hoburensis*: ?—›0
Cervical Vertebra B: *Kirgizemys hoburensis*: 0—›1
Cervical Vertebra C: *Kirgizemys hoburensis*: ?—›1; *Judithemys sukhanovi*: ?—›1
Cervical Vertebra G: *Sinemys lens*: 0—›?
Cervical Vertebra H: *Kirgizemys hoburensis*: ?—›1

Cervical Vertebra I: *Kirgizemys hoburensis*: ?—›1; *Judithemys sukhanovi*: 0—›0&1
Caudal B: *Kirgizemys hoburensis*: ?—›1
Pectoral Girdle A: *Kirgizemys hoburensis*: ?—›1
Cleithrum A: *Kirgizemys hoburensis*: ?—›2; *Judithemys sukhanovi*: ?—›2
Scapula A: *Kirgizemys hoburensis*: ?—›2
Humerus C: *Kirgizemys hoburensis*: ?—›0
Humerus D: *Kirgizemys hoburensis*: ?—›0
Humerus E: *Kirgizemys hoburensis*: ?—›1
Illium A: *Kirgizemys hoburensis*: ?—›1
Pes A: *Dracochelys bicuspis*: – —›0

Appendix 2

Definitions of new morphological characters:

Posterior Plastral Fontanelle: posterior plastral fontanelle between the xiphiplastra and/or the hypoplastra: (0) absent in adult stage; (1): retained in adult stage.
Neural Number: number of neurals (0) less than 9 elements; (1) nine elements.
Plastron Lobe: posterior lobe of plastron (0) relatively wide and short; (1) posterior lobe of plastron elongated and narrow coupled with widely spaced plastral buttresses. *Comment:* This character is included to capture the characteristic proportions of the posterior lobe of *Manchurochelys manchoukuoensis*, *Sinemys lens* and *Sinemys brevispinus* (unknown for *S. gamera*). In these taxa the posterior lobe is not simply just long and narrow with subparallel lateral sides but the base of the hyo- and hypoplastral buttresses are also placed wide apart resulting in an extensive central part of the plastron. Both these criteria have to be fulfilled in the derived state.
Shape of Costal 3: costal 3 (0) tapering towards the lateral side of the shell or with parallel anterior and posterior borders; (1) costal 3 broadens towards the lateral side of the shell. *Comment:* this character is shared by *Dracochelys bicuspis* and *Liaochelys jianchangensis* (especially marked in the latter).
Costal Rib: (0) distal portion of costal ribs not visible within the costal; (1) distal portion of costal rib visible on the surface of the costal.
Comment: In *Liaochelys jianchangensis* and *Dracochelys bicuspis* the rib portion of the costal is visible distally within the costal element. This is not to be confused with the presence of free rib heads in taxa with peripheral fontanelles which is a much more widespread character. With this character the rib has to be visible on the surface of the costals.
Carapacial Sutures: (0) carapacial elements finely sutured or the contact is smooth; (1) carapacial sutures strongly serrated in adult stage.
Comment: This character is shared by *Liaochelys jianchangensis* and *Dracochelys bicuspis* whereas other Cretaceous pancryptodires have smooth contacts between the elements of the carapace.
First Vertebral: (0) vertebral 1 does not enter anterior margin of carapace; (1) enters anterior margin.
Comment: the derived state is present in *Dracochelys bicuspis* (based on [37]), *Sinemys* spp. (unknown in *Sinemys gamera*) and curiously also in the aberrant pleurodire, *Araripemys barretoi* Price [46].
Peripheral Gutter: (0) peripheral gutter absent or only anteriorly developed; (1) peripheral gutter extensively developed along anterior and bridge peripherals. *Comment:* extensive gutter along the anterior two-thirds of the peripheral ring is characteristic for a number of Mesozoic pancryptodires [47,48] but has never been used in a phylogenetic analysis.
Costal Rib Distal End: (0) distal end of dorsal rib not visible or only within costo-peripheral fontanelles on the dorsal face of the carapace; (1) distal end of posterior dorsal ribs visible and surrounded by the peripheral. Comment: In sinemydids and a number of other related taxa the distal end of the posterior dorsal ribs are exposed in dorsal view within the peripherals even though these forms lack costo-peripheral fontanelles.

Additional files

Additional file 1: Taxon-character matrix in nexus format.
Additional file 2: Taxon-character matrix in tnt format.
Additional file 3: Strict consensus trees.

Abbreviations

IVPP: Institute of Vertebrate Paleontology and Paleoanthropology, Beijing, China; PIN: Paleontological Institute, Russian Academy of Sciences, Moscow, Russia; PMOL: Paleontological Museum of Liaoning, Shenyang Normal University, Shenyang, China; TMP: Royal Tyrrell Museum of Palaeontology, Drumheller, Canada.

Competing interests

The authors declare no competing interests.

Authors' contributions

CFZ initiated study, described and illustrated specimens. MR and WGJ collected data and MR performed analyses. MR, CFZ and WGJ wrote the manuscript. All authors read and approved the final manuscript.

Acknowledgements

The authors would like to thank the director of Paleontological Institute, Shenyang Normal University, Prof. Ge Sun for his encouragement. The following people kindly provided access to fossil specimens under their care: Vladimir Sukhanov (PIN), Xu Xing, Liu Jun, Corwin Sullivan (IVPP), Donald Brinkman and James Gardner (TMP). Juliana Sterli (CONICET), Igor Danilov, Elena Syromyatnikova (ZIN) and Haiyan Tong (IVPP) provided useful comments and assistance. MR would like to thank the MTA-ELTE Lendület Dinosaur Research Group grant for support. Insights from three anonymous reviewers and the editor, Diego Pol, greatly improved the quality of the manuscript. The Willi Hennig Society is thanked for providing free access to the program TNT. This project was in part funded by the Public Science and Technology Research Funds Projects of Land and Resources (No. 201311120), the National Natural Science Foundation of China (No. 40802007 and No.

41202014), the Program for Liaoning Excellent Talents in University (No. LJQ2011120), and Deutsche Forschungsgemeinschaft grant to WGJ (JO 928/2). We acknowledge support by Deutsche Forschungsgemeinschaft and Open Access Publishing Fund of Tübingen University.

Author details
[1]Paleontological Institute, Shenyang Normal University, 253 North Huanghe Street, Shenyang, Liaoning 110034, People's Republic of China. [2]Institut für Geowissenschaften, University of Tübingen, Hölderlinstraße 12, Tübingen 72074, Germany. [3]Department of Paleontology & MTA – ELTE Lendület Dinosaur Research Group, Eötvös Loránd University, Budapest, Hungary. [4]Department of Geosciences, University of Fribourg, Fribourg 1700, Switzerland.

Received: 21 January 2014 Accepted: 24 March 2014
Published: 5 April 2014

References

1. Endo R, Shikama R: **Mesozoic reptilian fauna in the Jehol Mountainland, Manchoukuo.** *Bull Centr Nat Mus Manchoukuo* 1942, **3:**1–20.
2. Ji S-A: **Reptiles.** In *Fauna and Stratigraphy of Jurassic-Cretaceous in Beijing and the Adjacent Areas.* Edited by Ren D, Lu L-W, Guo Z-G, Ji S-A. Beijing: Seismic Press; 1995:140–146.
3. Tong H, Ji S-A, Ji Q: ***Ordosemys* (Testudines: Cryptodira) from the Yixian Formation of Liaoning Province, northeastern China: new specimens and systematic revision.** *Am Mus Novit* 2004, **3438:**1–20.
4. Zhou C-F: **A new eucryptodiran turtle from the Early Cretaceous Jiufotang Formation of western Liaoning, China.** *Zootaxa* 2010, **2676:**45–56.
5. Zhou C-F: **A second specimen of *Manchurochelys manchoukuoensis* Endo & Shikama, 1942 (Testudines: Eucryptodira) from the Early Cretaceous Yixian Formation of western Liaoning, China.** *Zootaxa* 2010, **2534:**57–66.
6. Sukhanov VB, Narmandakh P: **A new Early Cretaceous turtle from the continental deposits of the Northern Gobi (in Russian). Mesozoic and Cenozoic Faunas and Biostratigraphy of Mongolia.** *Trans Joint Sov Mongolian Paleontol Expedition* 1974, **1:**192–220.
7. Nessov LA: **Data on late Mesozoic turtles from the USSR. Studia Geologica Salmaticensia.** *Stud Palaeocheloniol* 1984, **1:**215–223.
8. Gaffney ES, Ye X-K: ***Dracochelys*, a new cryptodiran turtle from the Early Cretaceous of China.** *Am Mus Novit* 1992, **3048:**1–13.
9. Brinkman DB, Peng J-H: **New material of *Sinemys* (Testudines, Sinemydidae) from the Early Cretaceous of China.** *Can J Earth Sci* 1993, **30:**2139–2152.
10. Brinkman DB, Peng J-H: ***Ordosemys leios*, n. gen., n. sp., a new turtle from the Early Cretaceous of the Ordos Basin, Inner Mongolia.** *Can J Earth Sci* 1993, **30:**2128–2138.
11. Gaffney ES: **The postcranial morphology of *Meiolania platyceps* and a review of the Meiolaniidae.** *Bull Am Mus Nat Hist* 1996, **229:**1–165.
12. Brinkman DB, Wu X-X: **The skull of *Ordosemys*, an Early Cretaceous turtle from Inner Mongolia, People's Republic of China, and the interrelationships of Eucryptodira (Chelonia, Cryptodira).** *Paludicola* 1999, **2:**134–147.
13. Sukhanov VB: **Mesozoic turtles of Middle and Central Asia.** In *The Age of Dinosaurs in Russia and Mongolia.* Edited by Benton MJ, Shishkin MA, Unwin DM, Kurochkin EN. Cambridge: Cambridge University Press; 2000:309–367.
14. Parham JF, Hutchison JH: **A new eucryptodiran turtle from the Late Cretaceous of North America (Dinosaur Provincial Park, Alberta, Canada).** *J Vertebr Paleontol* 2003, **23:**783–798.
15. Danilov IG, Averianov AO, Skutchas PP, Rezvyi AS: ***Kirgizemys* (Testudines, Macrobaenidae): new material from the Lower Cretaceous of Buryatia (Russia) and taxonomic revision.** *Fossil Turtle Res* 2006, **1:**46–62.
16. Sukhanov VB, Narmandakh P: **New taxa of Mesozoic turtles from Mongolia.** *Fossil Turtle Res* 2006, **1:**119–127.
17. Gaffney ES, Rich TH, Vickers-Rich P, Constantine A, Vacca P, Kool L: ***Chubutemys*, a new eucryptodiran turtle from the Early Cretaceous of Argentina, and the relationships of the Meiolaniidae.** *Am Mus Novit* 2007, **3599:**1–35.
18. Joyce WG: **Phylogenetic relationships of Mesozoic turtles.** *Bull Peabody Mus Nat Hist* 2007, **48:**3–102.
19. Rabi M, Joyce WG, Wings O: **A review of the Mesozoic turtles of the Junggar Basin (Xinjiang, Northwest China) and the paleobiogeography of Jurassic to early cretaceous Asian testudinates.** *Palaeobio Palaeoenv* 2010, **90:**259–273.
20. Sterli J, de la Fuente MS: **New evidence from the Palaeocene of Patagonia (Argentina) on the evolution and palaeobiogeography of meiolaniid-like turtles (Testudinata).** *J Syst Paleontol* 2013, **11:**835–852.
21. Ye X: **Fossil turtles of China.** *Palaeontol Sin* 1963, **150:**1–112.
22. Sukhanov VB: **Subclass Testudinata, Testudinates (In Russian).** In *Fundamentals of Palaeontology Amphibians, Reptiles and Birds.* Edited by Orlov JA. Moscow: Nauka; 1964:354–438.
23. Nessov LA, Khosatzky LI: **Early Cretaceous turtles from southeastern Fergana (in Russian).** In *Problems in herpetology: Proc 3rd All-union Herpetological Conf.* Leningrad: Zoological Institute of the Academy of Sciences USSR; 1973:132–133.
24. Chkhikvadze VM: **Fossil turtles of the family Sinemydidae (In Russian). Izvestiya AN Gruzinskoy SSR.** *Seriya Biologicheskaya* 1977, **3:**265–270.
25. Khosatzky LI, Nessov LA: **Large turtles of the Late Cretaceous of Middle Asia (in Russian).** *Trudy Zoologicheskogo Instituta AN SSSR* 1979, **89:**98–108.
26. Gaffney ES, Meylan PA: **A phylogeny of turtles.** In *The phylogeny and classification of the tetrapods, Volume 35A, Amphibians, Reptiles, Birds, Systematics Association Special Volume.* 1st edition. Edited by Benton MJ. Oxford: Clarendon Press; 1988:157–219.
27. Rabi M, Sukhanov VB, Egorova VN, Danilov I, Joyce WG: **Osteology, relationships, and ecology of *Annemys* (Testudines, Eucryptodira) from the Late Jurassic of Shar Teg, Mongolia and phylogenetic definitions for Xinjiangchelyidae, Sinemydidae, and Macrobaenidae.** *J Vertebr Paleontol*; 2014, **34:**327-352.
28. Danilov IG, Parham JF: **A redescription of '*Plesiochelys tatsuensis*' from the Late Jurassic of China, with comments on the antiquity of the crown clade Cryptodira.** *J Vertebr Paleontol* 2006, **26:**573–580.
29. Danilov IG, Parham JF: **A reassessment of some poorly known turtles from the Middle Jurassic of China, with comments on the antiquity of extant turtles.** *J Vertebr Paleontol* 2008, **28:**306–318.
30. Sterli J: **A new, nearly complete stem turtle from the Jurassic of South America with implications for turtle evolution.** *Biol Lett* 2008, **4:**286–289.
31. Sterli J: **Phylogenetic relationships among extinct and extant turtles: the position of Pleurodira and the effects of the fossils on rooting crown-group turtles.** *Contrib Zool* 2010, **79:**93–106.
32. Vandermark D, Tarduno JA, Brinkman DB, Cottrell RD, Mason S: **New Late Cretaceous macrobaenid turtle with Asian affinities from the High Canadian Arctic: dispersal via ice-free polar routes.** *Geology* 2009, **37:**183–186.
33. Sterli J, de la Fuente MS: **A new turtle from the La Colonia Formation (Campanian – Maastrichtian), Patagonia, Argentina, with remarks on the evolution of the vertebral column in turtles.** *Paleontology* 2011, **54:**63–78.
34. Anquetin J: **Reassessment of the phylogenetic interrelationships of basal turtles (Testudinata).** *J Syst Palaeontol* 2012, **10:**3–45.
35. Brinkman DB, Yuan C-X, Ji Q, Li D-Q, You H-L: **A new turtle from the Xiagou Formation (Early Cretaceous) of Changma Basin, Gansu Province, P. R. China.** *Palaeobio Palaeoenv* 2013, **93:**367–382.
36. Rabi M, Zhou C-F, Wings O, Sun G, Joyce WG: **A new xinjiangchelyid turtle from the Middle Jurassic of Xinjiang. China and the evolution of the basipterygoid process in Mesozoic turtles.** *BMC Evol Biol* 2013, **13:**203.
37. Tong H, Brinkman D: **A new species of *Sinemys* (Testudines: Cryptodira: Sinemydidae) from the Early Cretaceous of Inner Mongolia, China.** *Palaeobio Palaeoenv* 2013, **93:**355–366.
38. Wiman C: **Fossile Schildkröten aus China.** *Paleontol Sin C* 1930, **6:**1–56.
39. Goloboff PA, Mattoni CI, Quinteros AS: **TNT, a free program for phylogenetic analysis.** *Cladistics* 2008, **24:**774–786.
40. Goloboff PA, Farris J, Nixon K: *TNT: tree search using new technology, vers. 1.1*, Willy Hennig Society Edition; 2008. Program and documentation available at http://www.zmuc.dk/public/phylogeny/tnt.
41. Krenz JG, Naylor GJP, Shaffer HB, Janzen FJ: **Molecular phylogenetics and evolution of turtles.** *Mol Phylogenet Evol* 2005, **37:**178–191.
42. Klein IT: *Klassification und kurze Geschichte der vierfüßigen Thiere (translated by F. D. Behn).* Lübeck: Jonas Schmidt; 1760.
43. Batsch AJGC: *Versuch einer Anleitung, zur Kenntniß und Geschichte der Thiere und Mineralien.* Jena: Akademische Buchhandlung; 1788:528.
44. Joyce WG, Parham JF, Gauthier JA: **Developing a protocol for the conversion of rank -based taxon names to phylogenetically defined clade names, as exemplified by turtles.** *J Paleontol* 2004, **78:**989–1013.
45. Chang S-C, Zhang H, Renne PR, Fang Y: **High-precision 40Ar/39Ar age for the Jehol Biota.** *Palaeogeogr Palaeoclimatol Palaeoecol* 2009, **280:**94–104.

46. Meylan PA: **Skeletal morphology and relationships of the Early Cretaceous side-necked turtle, *Araripemys barretoi* (Testudines: Pelomedusoides: Araripemydidae), from the Santana Formation of Brazil.** *J Vertebr Paleontol* 1996, **16:**20–33.
47. Peng J-H, Brinkman DB: **New material of *Xinjiangchelys* (Reptilia: Testudines) from the Late Jurassic Qigu Formation (Shishugou Group) of the Pingfengshan locality, Junggar Basin, Xinjiang.** *Can J Earth Sci* 1993, **30:**2013–2026.
48. Danilov IG, Sukhanov VB: **A basal eucryptodiran turtle "*Sinemys*" *efremovi* (= *Wuguia efremovi*) from the Early Cretaceous of China.** *Acta Paleontol Pol* 2006, **51:**105–110.

doi:10.1186/1471-2148-14-77
Cite this article as: Zhou *et al.*: A new specimen of *Manchurochelys manchoukuoensis* from the Early Cretaceous Jehol Biota of Chifeng, Inner Mongolia, China and the phylogeny of Cretaceous basal eucryptodiran turtles. *BMC Evolutionary Biology* 2014 **14**:77.

Submit your next manuscript to BioMed Central and take full advantage of:

- **Convenient online submission**
- **Thorough peer review**
- **No space constraints or color figure charges**
- **Immediate publication on acceptance**
- **Inclusion in PubMed, CAS, Scopus and Google Scholar**
- **Research which is freely available for redistribution**

Submit your manuscript at
www.biomedcentral.com/submit

BioMed Central